Broder J. Merkel
Britta Planer-Friedrich

Edited by
Darrell Kirk Nordstrom

Groundwater Geochemistry

A Practical Guide to Modeling of Natural and Contaminated Aquatic Systems

Springer

Broder J. Merkel, Britta Planer-Friedrich

Edited by
Darrell Kirk Nordstrom

Groundwater Geochemistry

A Practical Guide to Modeling of Natural and Contaminated Aquatic Systems

Broder J. Merkel
Britta Planer-Friedrich

Edited by
Darrell Kirk Nordstrom

Groundwater Geochemistry

A Practical Guide to Modeling of Natural and Contaminated Aquatic Systems

With 76 Figures and a CD-ROM

Springer

Prof. Dr. Broder J. Merkel
Dr. Britta Planer-Friedrich
Department of Geology
Technische Universitaet
Bergakademie Freiberg
Gustav Zeuner Str. 12
09599 Freiberg
Germany

Dr. Darrell Kirk Nordstrom
U.S. Geological Survey
3215 Marine St., Suite E-127
Boulder, CO 80303
USA

E-mail: merkel@geo.tu-freiberg.de
b. planer-friedrich@geo.tu-freiberg.de
dkn@usgs.gov

This book has been translated and updated from the German version "Grundwasserchemie", ISBN 3-540-42836-4, published at Springer in 2002.

ISBN 3-540-24195-7 **Springer Berlin Heidelberg New York**

Library of Congress Control Number: 2004117858

Springer is a part of Springer Science+Business Media
springeronline.com

Printed in The Netherlands

Cover design: E. Kirchner, Heidelberg
Production: A. Oelschläger
Typesetting: Camera-ready by the Authors
Printing: Krips, Meppel
Binding: Litges+Dopf, Heppenheim
Printed on acid-free paper 30/2132/AO 5 4 3 2 1 0

Foreword

To understand hydrochemistry and to analyze natural as well as man-made impacts on aquatic systems, hydrogeochemical models have been used since the 1960's and more frequently in recent times.

Numerical groundwater flow, transport, and geochemical models are important tools besides classical deterministic and analytical approaches. Solving complex linear or non-linear systems of equations, commonly with hundreds of unknown parameters, is a routine task for a PC.

Modeling hydrogeochemical processes requires a detailed and accurate water analysis, as well as thermodynamic and kinetic data as input. Thermodynamic data, such as complex formation constants and solubility products, are often provided as data sets within the respective programs. However, the description of surface-controlled reactions (sorption, cation exchange, surface complexation) and kinetically controlled reactions requires additional input data.

Unlike groundwater flow and transport models, thermodynamic models, in principal, do not need any calibration. However, considering surface-controlled or kinetically controlled reaction models might be subject to calibration.

Typical problems for the application of geochemical models are:

- speciation
- determination of saturation indices
- adjustment of equilibria/disequilibria for minerals or gases
- mixing of different waters
- modeling the effects of temperature
- stoichiometric reactions (e.g. titration)
- reactions with solids, fluids, and gaseous phases (in open and closed systems)
- sorption (cation exchange, surface complexation)
- inverse modeling
- kinetically controlled reactions
- reactive transport

Hydrogeochemical models are dependent on the quality of the chemical analyses, the boundary conditions presumed by the program, theoretical concepts (e.g. calculation of activity coefficients) and the thermodynamic data. Therefore it is vital to check the results critically. For that, a basic knowledge about chemical and thermodynamic processes is required and will be outlined briefly in the following chapters on hydrogeochemical equilibrium (chapter 1.1), kinetics (chapter 1.2), and transport (chapter 1.3). Chapter 2 gives an overview on standard

hydrogeochemical programs, problems and possible sources of error for modeling, and a detailed introduction to run the program PHREEQC, which is used in this book. With the help of examples, practical modeling applications are addressed and specialized theoretical knowledge is extended. Chapter 4 presents the results for the exercises of chapter 3. This book does not aim to replace a textbook but rather attempts to be a practical guide for beginners at modeling.

Table of contents

1 Theoretical Background

1.1 Equilibrium reactions

1.1.1 Introduction

Chemical reactions determine occurrence, distribution, and behavior of aquatic species in water. The aquatic species is defined as organic and inorganic substances dissolved in water in contrast to colloids (1-1000 nm) and particles (> 1000 nm). This definition embraces free anions and cations sensu strictu as well as complexes (chapter 1.1.5.1). The term complex applies to negatively charged species such as OH^-, HCO_3^-, CO_3^{2-}, SO_4^{2-}, NO_3^-, PO_4^{3-}, positively charged species such as $ZnOH^+$, CaH_2PO4^+, $CaCl^+$, and zero charged species such as $CaCO_3^0$, $FeSO_4^0$ or $NaHCO_3^0$ as well as organic ligands. Table 1 provides a summary of relevant inorganic elements and examples of their dissolved species.

Table 1 Selected inorganic elements and examples of aquatic species

Elements	
Major elements (>5mg/L)	
Calcium (Ca)	Ca^{2+}, $CaCO_3^0$, $CaHCO_3^+$, $CaOH^+$, $CaSO_4^0$, $CaHSO_4^+$, $Ca(CH_3COO)_2^0$, $CaB(OH)_4^+$, $Ca(CH_3COO)^+$, $CaCl^+$, $CaCl_2^0$, CaF^+, $CaH_2PO_4^+$, $CaHPO_4^0$, $CaNO_3^+$, $CaP_2O_7^{2-}$, $CaPO_4^-$
Magnesium (Mg)	Mg^{2+}, $MgCO_3^0$, $MgHCO_3^+$, $MgOH^+$, $MgSO_4^0$, $MgHSO_4^+$
Sodium (Na)	Na^+, $NaCO_3^-$, $NaHCO_3^0$, $NaSO_4^-$, $NaHPO_4^-$, NaF^0
Potassium (K)	K^+ , KSO_4^-, $KHPO_4^-$
Carbon (C)	HCO_3^-, CO_3^{2-}, $CO_{2(g)}$, $CO_{2(aq)}$, $Me^{I}CO_3^-$, $Me^{I}HCO_3^0$, $Me^{II}CO_3^0$, $Me^{II}HCO_3^+$, $Me^{III}CO_3^+$
Sulfur (S)	SO_4^{2-}, $H_2S_{(g/aq)}$, HS^-, and metal sulfide complexes, $Me^{(2)}S0_4^0$, $Me^{(2)}HSO_4^+$ and further sulfate complexes with uni- or multi-valent metals
Chlorine (Cl)	Cl^-, $CaCl^+$, $CaCl_2^0$ and further chloro-complexes with uni- or multi-valent metals
Nitrogen (N)	NO_3^-, NO_2^-, $NO_{(g/aq)}$, $NO_{2(g/aq)}$, $N_2O_{(g/aq)}$, $NH_{3(g/aq)}$, $HNO_{2(g/aq)}$, NH_4^+, $Me^{II}NO_3^+$
Silicon (Si)	$H_4SiO_4^0$, $H_3SiO_4^-$, $H_2SiO_4^{2-}$, SiF_6^{2-}, $UO_2H_3SiO_4^+$
Minor elements (0,1-5 mg/L)	
Boron (B)	$B(OH)_3^0$, $BF_2(OH)_2^-$, BF_3OH^-, BF_4^-
Fluorine (F)	F^-, AgF^0, AlF^{2+}, AlF_2^+, AlF_3^0, AlF_4^-, AsO_3F^{2-}, $BF_2(OH)_2$, BF_3OH^-, BF_4^-, BaF^+, CaF^+, CuF^+, FeF^+, FeF^{2+}, FeF_2^+, $H_2F_2^0$, $H_2PO_3F^0$, $HAsO_3F^-$, HF^0, HF_2, HPO_3F^-, MgF^+, MnF^+, NaF^0, PO_3F^{2-}, PbF^+, PbF_2^0, $Sb(OH)_2F^0$, SiF_6^-, SnF^+, SnF_2^0, SnF_3^-, SrF^+, ThF^{3+}, ThF_2^{2+}, ThF_3^+,

	ThF_4^0, UF^{3+}, UF_2^{2+}, UF_3^+, UF_4^0, UF_5^-, UF_6^{2-}, UO_2F^+, $UO_2F_2^0$, $UO_2F_3^-$, $UO_2F_4^{2-}$, ZnF^+
Iron (Fe)	Fe^{2+}, Fe^{3+}, $Fe(OH)_3^-$, $FeSO4^0$, $FeH_2PO_4^+$, $Fe(OH)_2^0$, $FeHPO_4^0$, $Fe(HS)_2^0$, $Fe(HS)_3^-$, $FeOH^{2+}$, $FePO_4^+$, $FeSO_4^+$, $FeCl^{2+}$, $FeCl_2^+$, $FeCl_3^0$, $Fe(OH)_2^+$, $Fe(OH)_3^0$, $Fe(OH)_4^-$, $FeH_2PO_4^{2+}$, FeF^{2+}, FeF_2^+, FeF_3^0, $Fe(SO_4)_2^-$, $Fe_2(OH)_2^{4+}$, $Fe_3(OH)_4^{5+}$
Strontium (Sr)	Sr^{2+}, $SrCO_3^0$, $SrHCO_3^+$, $SrOH^+$, $SrSO_4^0$
Trace elements (<0,1 mg/L)	
Lithium (Li)	Li^+, $LiSO_4^-$, $LiOH^0$, $LiCl^0$, $LiCH_3COO^0$, $Li(CH_3COO)_2^-$
Beryllium	BeO_2^{2-}, $Be(CH_3COO)_2^0$, $BeCH_3COO^+$
Aluminum (Al)	Al^{3+}, $AlOH^{2+}$, $Al(OH)_2^+$, $Al(OH)_4^-$, AlF^{2+}, AlF_2^+, AlF_3^0, AlF_4, $AlSO_4^+$, $Al(SO_4)_2^-$, $Al(OH)_3^0$
Phosphor (P)	PO_4^{3-},HPO_4^{2-}, $H_2PO_4^-$, $H_3PO_4^0$, $MgPO_4^-$, $MgHPO_4^0$, $MgH_2PO_4^+$ (dito Ca, Fe^{II}), $NaHPO_4^-$, $KHPO_4^-$, $Fe^{III}H_2PO_4^{2+}$, $UHPO_4^{2+}$, $U(HPO_4)_2^0$, $U(HPO_4)_3^{2-}$, $U(HPO_4)_4^{4-}$, $UO_2HPO_4^0$, $UO_2(HPO_4)_2^{2-}$, $UO_2H_2PO_4^+$, $UO_2(H_2PO_4)_2^0$, $UO_2(H_2PO_4)_3^-$, $CrH_2PO_4^{2+}$, $CrO_3H_2PO_4^-$, $CrO_3HPO_4^{2-}$
Chromium (Cr)	Cr^{3+}, $Cr(OH)^{2+}$, $Cr(OH)_2^+$, $Cr(OH)_3^0$, $Cr(OH)_4^-$, CrO_2^-, $CrBr^{2+}$, $CrCl^{2+}$, $CrCl_2^+$, $CrOHCl_2^0$, CrF^{2+}, CrI^{2+}, $Cr(NH_3)_6^{3+}$, $Cr(NH_3)_5OH^{2+}$, $Cr(NH_3)_4(OH)_2^+$, $Cr(NH_3)_6Br^{2+}$, $CrNO_3^{2+}$, $CrH_2PO_4^{2+}$, $CrSO_4^+$, $CrOHSO_4^0$, $Cr_2(OH)_2(SO_4)_2^0$, CrO_4^{2-}, $HCrO_4^-$, $H_2CrO_4^0$, $Cr_2O_7^{2-}$, CrO_3Cl^-, $CrO_3H_2PO_4^-$, $CrO_3HPO_4^{2-}$, $CrO_3SO_4^{2-}$, $NaCrO_4^-$, $KCrO_4^-$
Manganese (Mn)	Mn^{2+}, $MnCl^+$, $MnCl_2^0$, $MnCl_3^-$, $MnOH^+$, $Mn(OH)_3^-$, MnF^+, $MnSO_4^0$, $Mn(NO_3)_2^0$, $MnHCO_3^+$
Cobalt (Co)	Co^{3+}, $Co(OH)_2^0$, $Co(OH)_4^-$, $Co_4(OH)_4^{4+}$,$Co_2(OH)_3^+$, $Co(CH_3COO)^+$, $Co(CH_3COO)_2^0$, $Co(CH_3COO)_3^-$, $CoCl^+$, $CoHS^+$, $Co(HS)_2^0$, $CoNO_3^+$,$CoBr_2^0$, CoI_2^0, $CoS_2O_3^0$, $CoSO_4^0$, $CoSeO_4^0$
Nickel (Ni)	Ni^{2+}, $Ni(CH_3COO)_2^0$, $Ni(CH_3COO)_3^-$, $Ni(NH_3)_2^{2+}$, $Ni(NH_3)_6^{2+}$, $Ni(NO_3)_2^0$, $Ni(OH)_2^0$, $Ni(OH)_3^-$, Ni_2OH^{3+}, $Ni_4(OH)_4^{4+}$, $NiBr^+$, $Ni(CH_3COO)^+$, $NiCl^+$, $NiHP_2O_7^-$, $NiNO_3^+$, $NiP_2O_7^{2-}$, $NiSO_4^0$, $NiSeO_4^0$
Silver (Ag)	Ag^+, $Ag(CH_3COO)_2^-$, $Ag(CO_3)_2^{2-}$, $Ag(CH_3COO)^0$, $AgCO_3^-$, $AgCl^0$, $AgCl_2^-$, $AgCl_3^{2-}$, $AgCl_4^{3-}$, AgF^0, $AgNO_3^0$
Copper (Cu)	Cu^+, $CuCl_2^-$, $CuCl_3^{2-}$, $Cu(S_4)_2^{3-}$, Cu^{2+}, $Cu(CH_3COO)^+$, $CuCO_3^0$, $Cu(CO_3)_2^{2-}$, $CuCl^+$, $CuCl_2^0$, $CuCl_3^-$, $CuCl_4^{2-}$, CuF^+, $CuOH^+$, $Cu(OH)_2^0$, $Cu(OH)_3^-$, $Cu(OH)_4^{2-}$, $Cu2(OH)_2^{2+}$, $CuSO_4^0$, $Cu(HS)_3^-$, $CuHCO_3^+$
Zinc (Zn)	Zn^{2+}, $ZnCl^+$, $ZnCl_2^0$, $ZnCl_3^-$, $ZnCl_4^{2-}$, ZnF^+, $ZnOH^+$, $Zn(OH)_2^0$, $Zn(OH)_3^-$, $Zn(OH)_4^{2-}$, $ZnOHCl^0$, $Zn(HS)_2^0$, $Zn(HS)_3^-$, $ZnSO_4^0$, $Zn(SO_4)_2^{2-}$, $ZnBr^+$, $ZnBr_2^0$, ZnI^+, ZnI_2^0, $ZnHCO_3^+$, $ZnCO3^0$, $Zn(CO_3)_2^{2-}$
Arsenic (As)	$H_3AsO_3^0$, $H_2AsO_3^-$, $HAsO_3^{2-}$, AsO_3^{3-}, $H_4AsO_3^+$, $H_2AsO_4^-$, $HAsO_4^{2-}$, AsO_4^{3-}, AsO_3F^{2-}, $HAsO_3F^-$
Selenium (Se)	Se^{2-}, HSe^-, H_2Se^0, $MnSe^0$, Ag_2Se^0, $AgOH(Se)_2^{4-}$, $HSeO_3^-$, SeO_3^{2-}, $H_2SeO_3^0$, $FeHSeO_3^{2+}$, $AgSeO_3^-$, $Ag(SeO_3)_2^{3-}$, $Cd(SeO_3)_2^{2-}$, SeO_4^{2-}, $HSeO_4^-$, $MnSeO_4^0$, $NiSeO_4^0$, $CdSeO_4^0$, $ZnSeO_4^0$, $Zn(SeO_4)_2^{2-}$
Bromine (Br)	Br^-, $ZnBr^+$, $ZnBr_2^0$, $CdBr^+$, $CdBr_2^0$,$PbBr^+$, $PbBr_2^0$, $NiBr^+$, $AgBr^0$, $AgBr_2^-$, $AgBr_3^{2-}$ (as well as Tl-, Hg- and Cr-complexes)
Molybdenum (Mo)	Mo^{6+}, $H_2MoO_4^0$, $HMoO_4^-$ and MoO_4^{2-}, $Mo(OH)_6^0$, $MoO(OH)_5^-$, MoO_2^{2+} , $MoO_2S_2^{2-}$, $MoOS_3^{2-}$
Cadmium (Cd)	Cd^{2+} , $CdCl^+$, $CdCl_2^0$, $CdCl_3^-$, CdF^+, CdF_2^0, $Cd(CO_3)_3^{4-}$, $CdOH^+$, $Cd(OH)_2^0$, $Cd(OH)_3^-$, $Cd(OH)_4^{2-}$, $Cd2OH^{3+}$, $CdOHCl^0$, $CdNO_3^+$, $CdSO_4^0$, $CdHS^+$, $Cd(HS)_2^0$, $Cd(HS)_3^-$, $Cd(HS)_4^2$, $CdBr^+$, $CdBr_2^0$, CdI^+,

	CdI_2^0, $CdHCO_3^+$, $CdCO_3^0$, $Cd(SO_4)_2^{2-}$
Antimony (Sb)	$Sb(OH)_3^0$, $HSbO_2^0$, $SbOF^0$, $Sb(OH)_2F^0$, SbO^+, SbO_2^-, $Sb(OH)_2^+$, $Sb_2S_4^{2-}$, $Sb(OH)_6^-$, SbO_3^-, SbO_2^+, $Sb(OH)_4^-$
Barium (Ba)	Ba^{2+}, $BaOH^+$, $BaCO3^0$, $BaHCO_3^+$, $BaNO_3^-$, BaF^-, $BaCl^+$, $BaSO_4^0$, $BaB(OH)_4^+$, $Ba(CH_3COO)_2^0$
Mercury (Hg)	Hg^{2+}, $Hg(OH)_2^0$, $HgBr^+$, $HgBr_2^0$, $HgBr_3^-$, $HgBr_4^{2-}$, $HgBrCl^0$, $HgBrI^0$, $HgBrI_3^{2-}$, $HgBr_2I_2^{2-}$, $HgBr_3I^{2-}$, $HgBrOH^0$, $HgCl^+$, $HgCl2^0$, $HgCl_3^-$, $HgCl_4^{2-}$, $HgClI^0$, $HgClOH^0$, HgF^+, HgI^+, HgI_2^0, HgI_3^-, HgI_4^{2-}, $HgNH_3^{2+}$, $Hg(NH_3)_2^{2+}$, $Hg(NH_3)_3^{2+}$, $Hg(NH_3)_4^{2+}$, $HgNO_3^+$, $Hg(NO_3)_2^0$, $HgOH^+$, $Hg(OH)_3^-$, HgS_2^{2-}, $Hg(HS)_2^0$, $HgSO_4^0$
Thallium (Tl)	Tl^+, $Tl(OH)_3^0$, $TlOH^0$, TlF^0, $TlCl^0$, $TlCl_2^-$, $TlBr^0$, $TlBr_2^-$, $TlBrCl^-$, TlI^0, TlI_2^-, $TlIBr^-$, $TlSO_4^-$, $TlNO_3^0$, $TlNO_2^0$, $TlHS^0$, $Tl2HS^+$, $Tl_2OH(HS)_3^{2-}$, $Tl_2(OH)_2(HS)_2^{2-}$, Tl^{3+}, $TlOH^{2+}$, $Tl(OH)_2^+$, $Tl(OH)_4^-$, $TlCl^{2+}$, $TlCl_2^+$, $TlCl_3^0$, $TlCl_4^-$, $TlBr^{2+}$, $TlBr_2^+$, $TlBr_3^0$, $TlBr_4^-$, TlI_4^-, $TlNO_3^{2+}$, $TlOHCl^+$
Lead (Pb)	Pb^{2+}, $PbCl^+$, $PbCl_2^0$, $PbCl_3^-$, $PbCl_4^{2-}$, $Pb(CO_3)_2^{2-}$, PbF^+, PbF_2^0, PbF_3^-, PbF_4^{2-}, $PbOH^+$, $Pb(OH)_2^0$, $Pb(OH)_3^-$, Pb_2OH^{3+}, $PbNO_3^+$, $PbSO_4^0$, $Pb(HS)_2^0$, $Pb(HS)_3^-$, $Pb3(OH)_4^{2+}$, $PbBr^+$, $PbBr_2^0$, PbI^+, PbI_2^0, $PbCO_3^0$, $Pb(OH)_4^{2-}$, $Pb(SO_4)_22^-$, $PbHCO_3^+$
Thorium (Th)	Th^{4+}, $Th(H_2PO_4)_2^{2+}$, $Th(HPO_4)_2^0$, $Th(HPO_4)_3^{2-}$, $Th(OH)_2^{2+}$, $Th(OH)^{3+}$, $Th(OH)_4^0$, $Th(SO_4)_2^0$, $Th(SO_4)_3^{2-}$, $Th(SO_4)_4^{4-}$, $Th_2(OH)_2^{6+}$, $Th_4(OH)_8^{8+}$, $Th_6(OH)_{15}^{9+}$, $ThCl^{3+}$, $ThCl_2^{2+}$, $ThCl_3^+$, $ThCl_4^0$, ThF^{3+}, ThF_2^{2+}, ThF_3^+, ThF_4^0, $ThH_2PO_4^{3+}$, $ThH_3PO_4^{4+}$, $ThHPO_4^{2+}$, $ThOH^{3+}$, $ThSO_4^{2+}$
Radium (Ra)	Ra^{2+}, $RaOH^+$, $RaCl^+$, $RaCO_3^0$, $RaHCO_3^+$, $RaSO_4^0$, $RaCH_3COO^+$
Uranium (U)	U^{4+}, UOH^{3+}, $U(OH)_2^{2+}$, $U(OH)_3^+$, $U(OH)_4^0$, $U(OH)_5^-$, $U6(OH)_{15}^{9+}$, UF^{3+}, UF_2^{2+}, F_3^+, UF_4^0, UF_5^-, UF_6^{2-}, UCl^{3+}, USO_4^{2+}, $U(SO_4)_2^0$, $UHPO_4^{2+}$, $U(HPO_4)_2^0$, $U(HPO_4)_3^{2-}$, $U(HPO4)_4^{4-}$, UO_2OH^+, $(UO_2)_2(OH)_2^{2+}$, $(UO_2)_3(OH)_5^+$, $UO_2CO_3^0$, $UO_2(CO_3)_2^{2-}$, $UO_2(CO_3)_3^{4-}$, UO_2^{2+}, UO_2F^+, $UO_2F_2^0$, $UO_2F_3^-$, $UO_2F_4^{2-}$, UO_2Cl^+, $UO_2SO_4^0$, $UO_2(SO_4)_2^{2-}$, $UO_2HPO_4^0$, $UO_2(HPO_4)_2^{2-}$, $UO_2H_2PO_4^+$, $UO_2(H_2PO_4)_2^0$, $UO_2(H_2PO_4)_3^-$, $UO_2H_3SiO_4^+$

Besides inorganic species there are a number of significant organic (Table 2) and biotic substances (Table 3) in water that are of great importance for water quality.

Table 2 Selected organic substances (plus-sign in brackets means that geogene formation in traces is possible, only the typical concentration range is indicated)

Substance	geogene	anthropogene	typical range of concentration
Humic matter	+	-	mg/L
aliphatic carbons: oil, fuel	+	+	mg/L
Phenols	+	+	mg/L
BTEX (benzene, toluene, ethylbenzene, xylene)	(+)	+	µg/L
PAHs (polycyclic aromatic hydrocarbons)	(+)	+	µg/L
PCBs (polychlorinated biphenyls)	-	+	µg/L

Substance	geogene	anthropogene	typical range of concentration
CFC´s (Chlorofluorocarbons)	-	+	ng/L
Dioxins, furans	(+)	+	pg/L
pesticides	(+)	+	ng/L
hormones	(+)	+	pg/L
pharmaceuticals	-	+	pg/L

Table 3 Organisms in groundwater

		size
Virus		10 - 1000 nm
Prokaryotes		
Bacteria		500 - 5.000 nm
Archaea (methaneogenous, extreme halophiles, extreme thermophiles)		100 - 15.000 nm
Eukaryotes		
Protozoa	(Foraminifera, Radiolaria, Dinoflagellata)	> 3 µm
Yeast	(anaerob)	~20 µm
Fungi	(aerob)	
Fish	(Brotulidae, Amblyopsidae, Astyanax Jordani, Caecobarbus Geertsi)	mm… cm

Interactions of the different species among themselves (chapter 1.1.5), with gases (chapter 1.1.3), and solid phases (minerals) (chapter 1.1.4.) as well as transport (chapter 1.3) and decay processes (biological decomposition, radioactive decay) are fundamental in determining the hydrogeochemical composition of ground and surface water.

Hydrogeochemical reactions involving only a single phase are called homogeneous, whereas heterogeneous reactions occur between two or more phases such as gas and water, water and solids, or gas and solids. In contrast to open systems, closed systems can only exchange energy, not constituents, with the environment.

Chemical reactions can be described by thermodynamics (chapter 1.1.2) and kinetics (chapter 1.2). Reactions expressed by the mass-action law (chapter 1.1.2.1), are thermodynamically reversible and independent of time. In contrast, kinetic processes are time dependent reactions. Thus, models that take into account kinetics can describe irreversible reactions such as decay processes that require finite amounts of time and cannot be reversed under a given set of conditions.

1.1.2 Thermodynamic fundamentals

1.1.2.1 Mass action law

In principle, any chemical equilibrium reaction can be described by the mass-action law.

$$aA + bB \leftrightarrow cC + dD \qquad \text{Eq. (1.)}$$

$$K = \frac{\{C\}^c \cdot \{D\}^d}{\{A\}^a \cdot \{B\}^b} \qquad \text{Eq. (2.)}$$

With a, b, c, d = number of moles of the reactants A, B, and the end products C, D, respectively for the given reaction, (1);
K = thermodynamic equilibrium or dissociation constant (general name)

In particular, the term K is defined in relation to the following types of reactions using the mass-action law:

- Dissolution/ Precipitation (chapter 1.1.4.1)
  K_S= solubility product constant
- Sorption (chapter 1.1.4.2)
  K_d=distribution coefficient
  K_x=selectivity coefficient
- Complex formation /destruction of complexes (chapter 1.1.5.1)
  K= complexation constant, stability constant
- Redox reaction (chapter 1.1.5.2)
  K= stability constant

If one reverses reactants and products in a reaction equation, then the solubility constant is K'=1/K. Hence it is important always to convey the reaction equation with the constant.

Furthermore, it must be clearly stated, if one deals with a conditional constant, being valid for one type of standard state, or with an infinite dilution constant, another type of standard state (i.e. T=25°C and ionic strength I=0). The latter might be calculated from the former. Standard temperature conditions can be calculated using the van't Hoff equation (Eq. 3), whereas the following equation (Eq. 4) can be applied to determine the effect of pressure:

$$\log(K_r) = \log(K_0) + \frac{H^0_r}{2.303 \cdot R} \cdot \frac{T_K - T_{K_0}}{T_K \cdot T_{K_0}} \qquad \text{Eq. (3.)}$$

with K_r = equilibrium constant at temperature
K_0 = equilibrium constant at standard temperature
T_K = temperature in degrees Kelvin
T_{K_0} = temperature in Kelvin, at which the standard enthalpy H^0_r was estimated
R = ideal gas constant (8.315 J/K mol)

$$\ln K(P) = \ln K(S) - \frac{\Delta V(T)}{T \cdot R \cdot \beta} \cdot \ln \frac{\sigma(P)}{\sigma(S)} \qquad \text{Eq. (4.)}$$

with K(P) equilibrium constant at pressure P
K(S) equilibrium constant at saturation vapor pressure

$\Delta V(T)$ = volume change of the dissociation reaction at temperature T and saturation water pressure S
ß =coefficient of the isothermal compressibility of water at T and P
σ (P) = density of water at pressure P
σ (S) = density of water at saturation water pressure conditions

Fig. 1 shows the dependence of calcite dissolution on different pressure and temperature conditions.

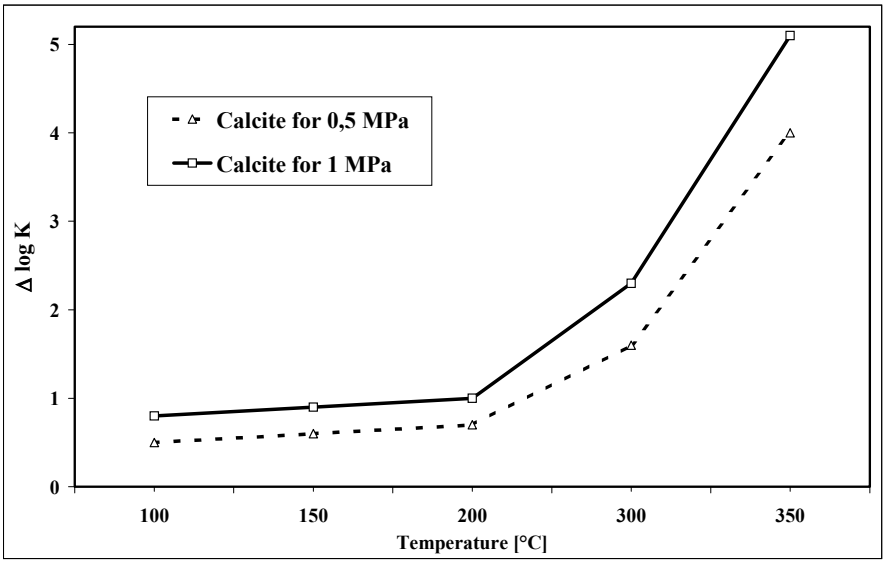

Fig. 1 Influence of pressure and temperature on the solubility of calcite (after Kharaka et al. 1988)

If a process consists of a series of subsequent reactions, as for instance the dissociation of H_2CO_3 to HCO_3^- and to CO_3^{2-}, then the stability (dissociation) constants are numbered in turn (e.g. K_1 and K_2).

1.1.2.2 Gibbs free energy

A system at constant temperature and pressure is at disequilibrium until all of its Gibbs free energy, G, is used up. In the equilibrium condition the Gibbs free energy equals zero.

The Gibbs free energy is a measure of the probability that a reaction occurs. It is composed of the enthalpy, H, and the entropy, S^0 (Eq. 5). The enthalpy can be described as the thermodynamic potential, which ensues H = U + p*V, where U is the internal energy, p is the pressure, and V is the volume. The entropy, according to classical definitions, is a measure of molecular order of a thermodynamic system and the irreversibility of a process, respectively.

$$G = H - S^0 \cdot T \qquad \text{Eq. (5.)}$$

with T = temperature in Kelvin

A positive value for G means that additional energy is required for the reaction to happen, and a negative value that the process happens spontaneously thereby releasing energy.

The change in free energy of a reaction is directly related to the change in energy of the activities of all reactants and products under standard conditions.

$$G = G^0 + R \cdot T \cdot \ln \frac{\{C\}^c \cdot \{D\}^d}{\{A\}^a \cdot \{B\}^b} \qquad \text{Eq. (6.)}$$

with R = ideal gas constant
G^0 = standard Gibbs free energy at 25°C and 100 kPa

G^0 equals G, if all reactants occur with unit activity, and thus the argument of the logarithm in Eq. 6 being 1 and consequently the logarithm becoming zero.

For equilibrium conditions it follows:

$$G = 0 \quad \text{and} \quad G^0 = -R \cdot T \cdot \ln K \qquad \text{Eq. (7.)}$$

Accordingly G provides a forecast of the direction in which the reaction aA + bB ↔ cC + dD proceeds. If G <0, the reaction to the right hand side will dominate, for G>0 it is the other way round.

1.1.2.3 Gibbs phase rule

The Gibbs phase rule states the number of the degrees of freedom that results from the number of components and phases, coexisting in a system.

$$F = C - P + 2 \qquad \text{Eq. (8.)}$$

with F = number of degrees of freedom
C = number of components
P = number of phases

The number 2 in the Eq. 8 arises from the two independent variables, pressure and temperature. Phases are limited, physically and chemically homogeneous, mechanically separable parts of a system. Components are defined as simple chemical entities or units that comprise the composition of a phase.

In a system, where the number of phases and the number of components are equal, there are two degrees of freedom, meaning that two variables can be varied independently (e.g. temperature and pressure). If the number of the degrees of freedom is zero, then temperature and pressure are constant and the system is invariant.

In a three-phase system including a solid and a liquid as well as a gas, the Gibbs phase rule is modified to:

$$F = C' - N - P + 2 \qquad \text{Eq. (9.)}$$

with F = number of the degrees of freedom
C′ = number of different chemical species
N = number of possible equilibrium reactions (species, charge balance, stoichiometric relations)-
P = number of phases

1.1.2.4 Activity

For the mass-action law, the quantities of substances are represented as activities, a_i, and not as concentrations, c_i, with respect to a species, i.

$$a_i = f_i \cdot c_i \qquad \text{Eq.(10.)}$$

In Eq. 10, the activity coefficient, f_i, is an ion-specific correction factor describing how interactions among charged ions influence each other. Since the activity coefficient is a non-linear function of ionic strength, the activity is a non–linear function of the concentration, too.

The activity decreases with increasing ionic strength up to 0.1 mol/kg and is always lower than the concentration, for the reason that the ions are charged and oppositely charged ions interact with each other to reduce the available charge. Thus the value of the activity coefficient is less than 1 (Fig. 2). Clearly, while increasing ion concentration, the higher the valence state, the stronger is the decrease in activity. In the ideal case of an infinitely dilute solution, where the interactions amongst the ions are close to zero, the activity coefficient is 1 and the activity equals the concentration.

Only mean activity coefficients can be experimentally determined for salts, not activity coefficients for single ions. The MacInnes Convention is one method for obtaining single ion activity coefficients and states that because of the similar size and mobility of the potassium and chloride ions:

$$f_i(K^+) = f_i(Cl^-) = f_{\pm}(KCl) \qquad \text{Eq.(11.)}$$

1.1.2.5 Ionic strength

The calculation of the ionic strength, the summation of the ionic forces, is one-half the sum of the product of the moles of the species involved, m_i, and their charge numbers z_i.

$$I = 0.5 \cdot \sum m_i \cdot z_i^2 \qquad \text{Eq.(12.)}$$

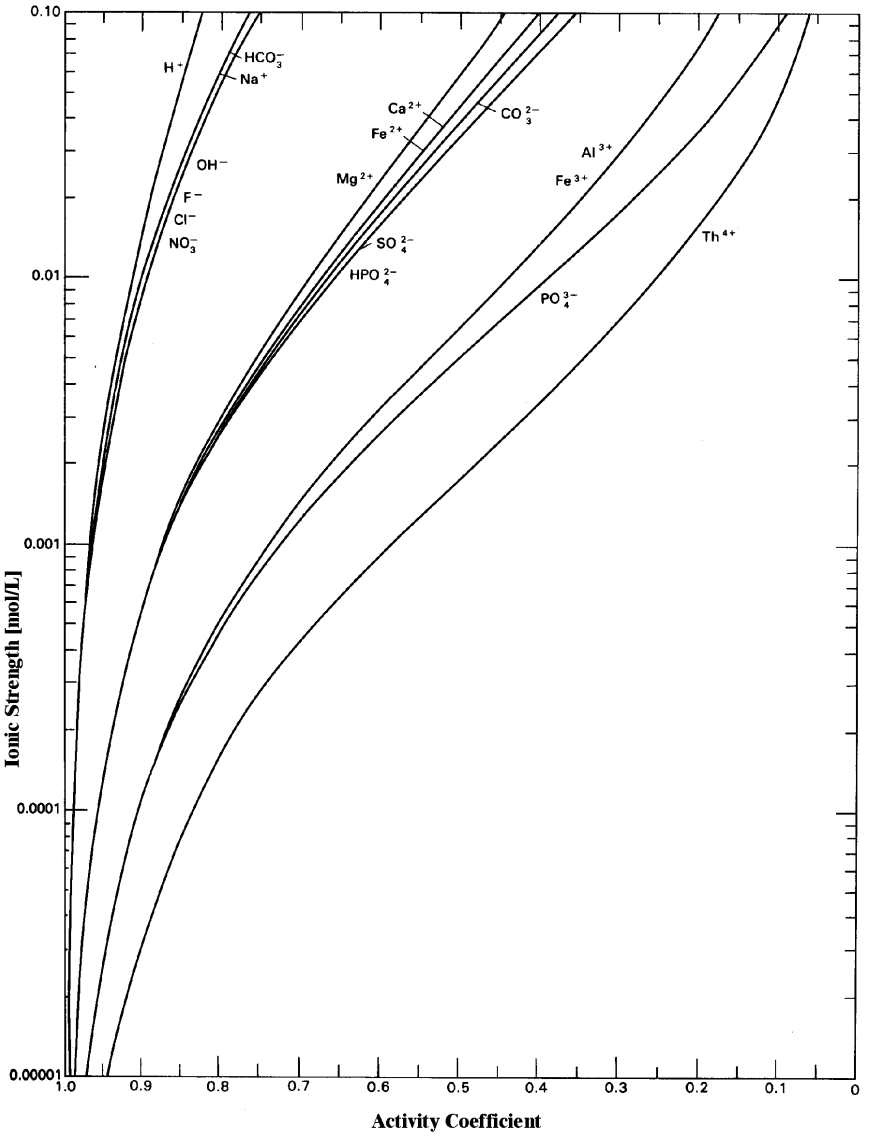

Fig. 2 Relation between ionic strength and activity coefficient in a range up to 0.1 mol/L (after Hem 1985)

1.1.2.6 Calculation of activity coefficient

1.1.2.6.1. Theory of ion dissociation

Given the ionic strength of the solution from the chemical analysis, the activity coefficient can be computed using several approximation equations. All of them are inferred from the DEBYE-HÜCKEL equation and differ in the range of the ionic strength they can be applied for.

DEBYE-HÜCKEL equation (Debye & Hückel 1923)

$$\log(f_i) = -A \cdot z_i^{\,2} \cdot \sqrt{I} \qquad I < 0.005 \text{ mol/kg} \qquad \text{Eq.(13.)}$$

extended DEBYE-HÜCKEL equation

$$\log(f_i) = \frac{-A \cdot z_i^{\,2} \cdot \sqrt{I}}{1 + B \cdot a_i \cdot \sqrt{I}} \qquad I < 0.1 \text{ mol/kg} \qquad \text{Eq.(14.)}$$

GÜNTELBERG equation (Güntelberg 1926)

$$\log(f_i) = -0.5 z_i^{\,2} \frac{\sqrt{I}}{1 + 1.4\sqrt{I}} \qquad I < 0.1 \text{ mol/kg} \qquad \text{Eq.(15.)}$$

DAVIES equation (Davies 1962, 1938)

$$\log(f_i) = -A \cdot z_i^{\,2} \left(\frac{\sqrt{I}}{1 + \sqrt{I}} - 0.3 \cdot I\right) \qquad I < 0.5 \text{ mol/kg} \qquad \text{Eq.(16.)}$$

"WATEQ" DEBYE-HÜCKEL equation (Truesdell & Jones 1974)

$$\log(f_i) = \frac{-A \cdot z_i^{\,2} \cdot \sqrt{I}}{1 + B \cdot a_i \cdot \sqrt{I}} + b_i \cdot I \qquad I < 1 \text{ mol/kg} \qquad \text{Eq.(17.)}$$

with f = activity coefficient
z = valence
I = ionic strength
a_i, b_i = ion- specific parameters (depend on the ion radius) (selected values see Table 4, complete overview in van Gaans (1989) and Kharaka et al. (1988))
A,B temperature dependent parameters, calculated from the following empirical equations (Eq. 18 to Eq. 21)

$$A = \frac{1.82483 \cdot 10^6 \cdot \sqrt{d}}{(\varepsilon \cdot T_K)^{3/2}} \qquad \text{Eq.(18.)}$$

$$B = \frac{50.2916 \cdot \sqrt{d}}{(\varepsilon \cdot T_K)^{1/2}} \qquad \text{Eq.(19.)}$$

$$d = 1 - \frac{(T_c - 3.9863)^2 \cdot (T_c + 288.9414)}{508929.2 \cdot (T_c + 68.12963)} + 0.011445 \cdot e^{-374.3 / T_c} \qquad \text{Eq.(20.)}$$

$$\varepsilon = 2727.586 + 0.6224107 \cdot T_K - 466.9151 \cdot \ln(T_K) - \frac{52000.87}{T_K} \qquad \text{Eq.(21.)}$$

with d = density (after Gildseth et al. 1972 for 0-100°)
ε = dielectric constant (after Nordstrom et al. 1990 for 0-100°C)
T_C = temperature in ° Celsius
T_K = temperature in Kelvin

For temperatures of about 25°C and water with a density of d: A = 0.51, B = 0.33. In some textbooks B is charted as $0.33 * 10^8$. For the use of the latter, a_i must be in cm, otherwise in Å (=10^{-8} cm).

Table 4 Ion-specific parameters a_i and b_i (after Parkhurst et al. 1980 and (*) Truesdell a. Jones 1974)

Ion	a_i [Å]	b_i [Å]
H^+	4.78	0.24
Li^+	4.76	0.20
Na^+ (*)	4.0	0.075
Na^+	4.32	0.06
K^+ (*)	3.5	0.015
K^+	3.71	0.01
Cs^+	1.81	0.01
Mg^{2+} (*)	5.5	0.20
Mg^{2+}	5,46	0.22
Ca^{2+} (*)	5.0	0.165
Ca^{2+}	4.86	0.15
Sr^{2+}	5.48	0.11
Ba^{2+}	4.55	0.09
Al^{3+}	6.65	0.19

Ion	a_i [Å]	b_i [Å]
Mn^{2+}	7.04	0.22
Fe^{2+}	5.08	0.16
Co^{2+}	6.17	0.22
Ni^{2+}	5.51	0.22
Zn^{2+}	4.87	0.24
Cd^{2+}	5.80	0.10
Pb^{2+}	4.80	0.01
OH^-	10.65	0.21
F^-	3.46	0.08
Cl^-	3.71	0.01
ClO_4^-	5.30	0.08
HCO_3^-, CO_3^{2-} (*)	5.40	0
SO_4^{2-} (*)	5.0	-0.04
SO_4^{2-}	5.31	-0.07

The valid range for the theory of dissociation does not exceed 1 mol/kg, some authors believe the upper limit should be at 0.7 mol/kg (sea water). Fig. 3 shows, that already at an ionic strength of > 0.3 mol/kg (H^+), the activity coefficient does not further decrease but increases, and eventually attains values of more than 1.

The second term in the DAVIES and extended DEBYE-HÜCKEL equations forces the activity coefficient to increase at high ionic strength. This is owed to the fact, that ion interactions are not only based on Coulomb forces any more, ion sizes change with the ionic strength, and ions with the same charge interact.

Moreover, with the increase in the ionic strength a larger fraction of water molecules is bound to ion hydration sleeves, whereby a strong reduction of the concentration of free water molecules occurs and therefore the activity or the activity coefficient, related to 1kg of free water molecules, increases correspondingly.

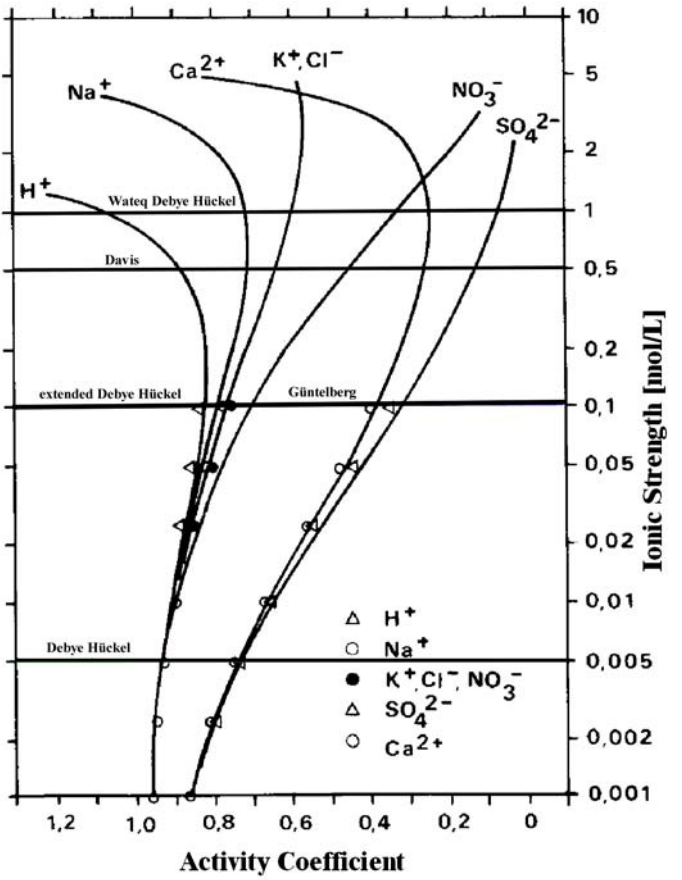

Fig. 3 Relation of ionic strength and activity coefficient in higher concentrated solutions, (up to I = 10mol/kg), valid range for the different theories of dissociation are indicated as lines (modified after Garrels and Christ 1965)

1.1.2.6.2. Theory of ion interaction

For higher ionic strength, e.g. highly saline waters; the PITZER equation can be used (Pitzer 1973). This semi-empirical model is based also on the DEBYE-HÜCKEL equation, but additionally integrates “virial” equations (vires = Latin for forces), that describe ion interactions (intermolecular forces). Compared with the ion dissociation theory the calculation is much more complicated and requires a

higher number of parameters that are often lacking for more complex solution species. Furthermore, a set of equilibrium constants (albeit minimal) for complexation reactions is still required.

In the following only a simple example of the PITZER equation is briefly described. For the complete calculations and the necessary data of detailed parameters and equations the reader is referred to the original literature (Pitzer 1973, Pitzer 1981, Whitfield 1975, Whitfield 1979, Silvester and Pitzer 1978, Harvie and Weare 1980, Gueddari et al. 1983, Pitzer 1991).

The calculation of the activity coefficient is separately done for positively (index i) and negatively (index j) charged species applying Eq. 22. In this example the calculation of the activity coefficients for cations is shown, which can be analogously done for anions just exchanging the corresponding indices.

$$\ln f_M = z_M^2 \cdot F + S1 + S2 + S3 + \left|z_M\right| \cdot S4 \qquad \text{Eq.(22.)}$$

with M = cation
z_M = valence state of cation M
F, S1-S4 = sums, calculated using Eqs. 23-30

$$S1 = \sum_{j=1}^{a} m_j (2 \cdot B_{Mj} + z \cdot C_{Mj}) \qquad \text{Eq.(23.)}$$

$$S2 = \sum_{i=1}^{c} m_i (2 \cdot \phi_{Mj} + \sum_{j=1}^{a} m_j \cdot P_{Mij}) \qquad \text{Eq.(24.)}$$

$$S3 = \sum_{j=1}^{a-1} \sum_{k=j+1}^{a} m_j^2 \cdot P_{Mjk} \qquad \text{Eq.(25.)}$$

$$S4 = \sum_{i=1}^{c} \sum_{j=1}^{a} m_i \cdot m_j \cdot c_{ij} \qquad \text{Eq.(26.)}$$

with B, C, Φ, P = species- specific parameters, which must be known for all combinations of the species
m = molarities [mol/L]
k = index
c = number of cations
a = number of anions

$$F = -\frac{2.303 \cdot A}{3.0} \left(\frac{\sqrt{I}}{1 + 1.2 \cdot \sqrt{I}} + \frac{2}{1.2} \cdot \ln(1 + 1.2 \cdot \sqrt{I})\right) + S5 + S6 + S7 \qquad \text{Eq.(27.)}$$

$$S5 = \sum_{i=1}^{c} \sum_{j=1}^{a} m_i \cdot m_j \cdot B'_{ij} \qquad \text{Eq.(28.)}$$

$$S6 = \sum_{i=1}^{c-1} \sum_{k=i+1}^{c} m_i^{\,2} \cdot \phi'_{ik} \qquad \text{Eq.(29.)}$$

$$S7 = \sum_{j=1}^{a-1} \sum_{l=j+1}^{a} m_j^{\,2} \cdot \phi'_{jl} \qquad \text{Eq.(30.)}$$

with A = DEBYE-HÜCKEL constant (Eq. 18)
B´, Φ´ = Virial coefficients, modified with regard to the ionic strength
k, l = indices

If the ionic strength exceeds 6 mol/L, the PITZER equation is no longer applicable though.

1.1.2.7 Theories of ion dissociation and ion interaction

Fig. 4 to Fig. 8 show the severe divergence for activity coefficients such as given here for calcium, chloride, sulfate, sodium and water ions, calculated with different equations. The activity coefficients were calculated applying Eq. 13 to Eq. 17 for the corresponding ion dissociation theories, whereas the values for the PITZER equations were gained using the program PHRQPITZ. The limit of validity of each theory is clearly shown.

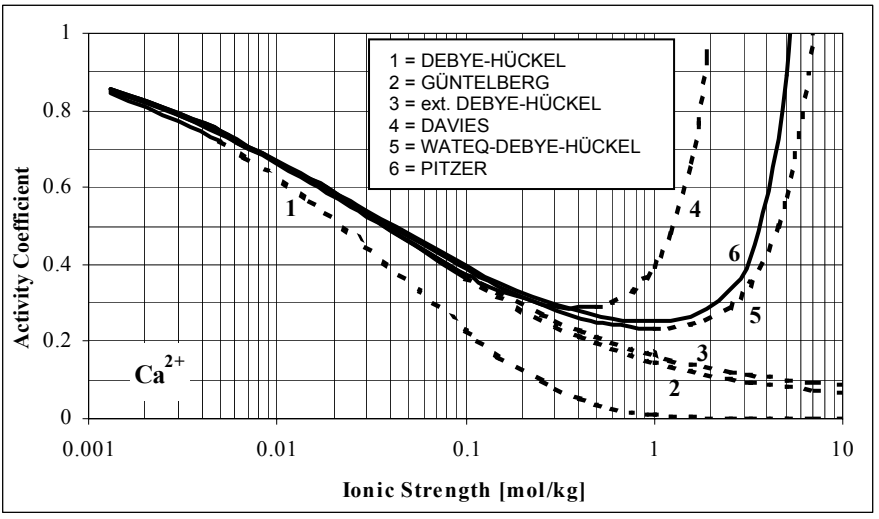

Fig. 4 Comparison of the activity coefficient of Ca^{2+} in relation to the ionic strength as calculated using a $CaCl_2$ solution (a_{Ca} = 4.86, b_{Ca} = 0.15 Table 4) and different theories of ion dissociation and the PITZER equation, dashed lines signify calculated values outside the validity range of the corresponding ion dissociation equation.

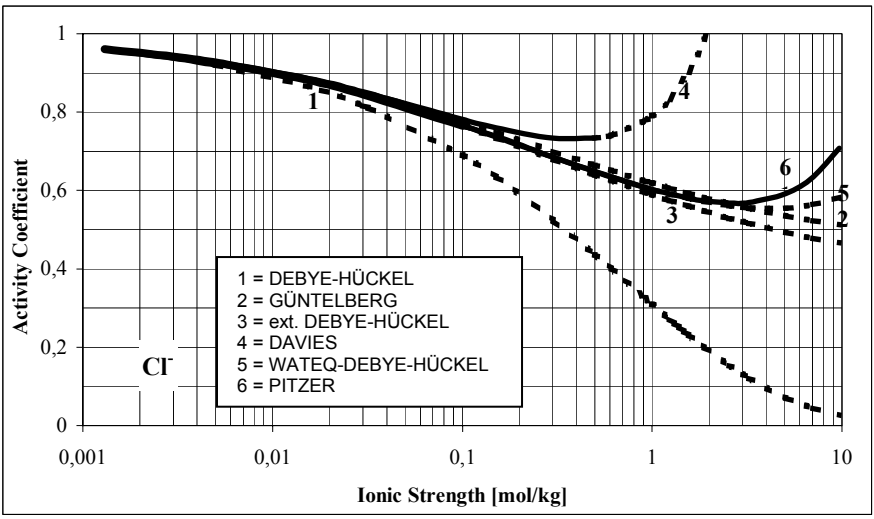

Fig. 5 Comparison of the activity coefficient of Cl^- in relation to the ionic strength as calculated using a $CaCl_2$ solution ($a_{Cl} = 3.71$, $b_{Cl} = 0.01$ Table 4) and different theories of ion dissociation and the PITZER equation, dashed lines signify calculated values outside the validity range of the corresponding ion dissociation equation.

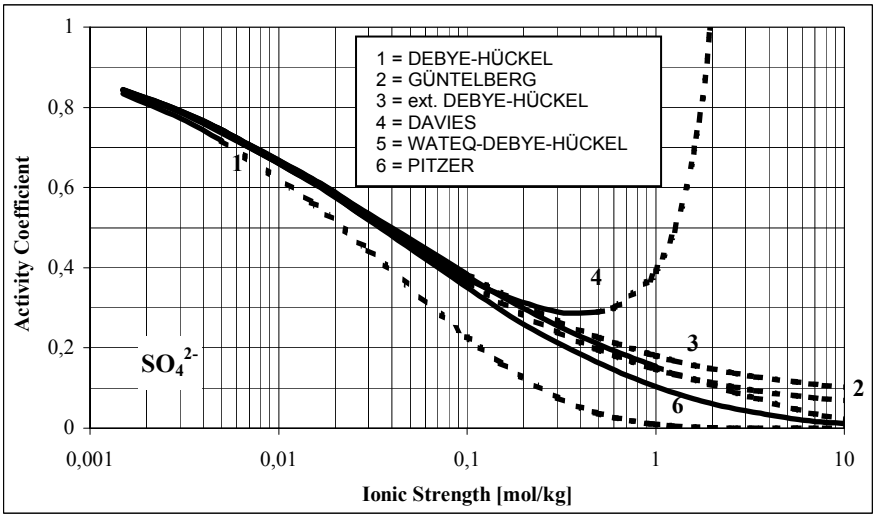

Fig. 6 Comparison of the activity coefficient of SO_4^{2-} in relation to the ionic strength as calculated using a $Na_2(SO_4)$ solution ($a_{SO4-2} = 5.31$, $b_{SO4-2} = -0.07$ Table 4) and different theories of ion dissociation and the PITZER equation, dashed lines signify calculated values outside the validity range of the corresponding ion dissociation equation.

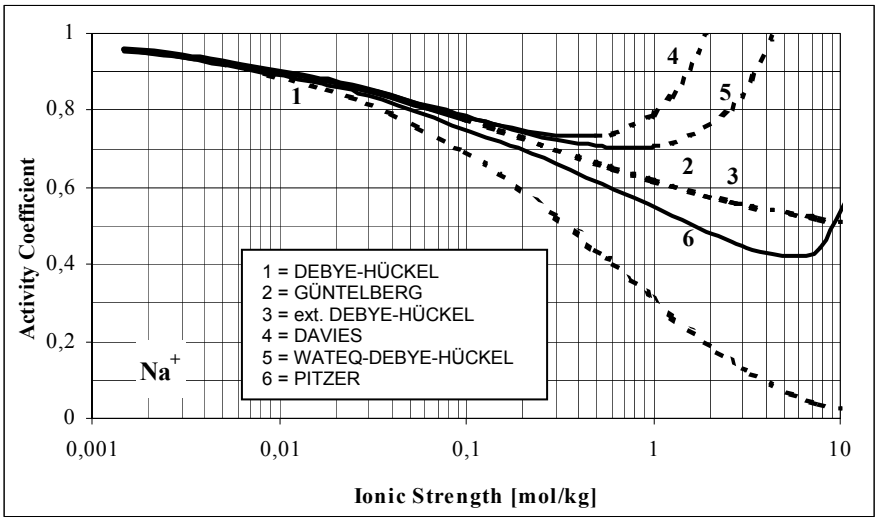

Fig. 7 Comparison of the activity coefficient of Na^+ in relation to the ionic strength as calculated using a $Na_2(SO_4)$ solution (a_{Na} = 4.32, b_{Na} = 0.06 Table 4) and different theories of ion dissociation and the PITZER equation, dashed lines signify calculated values outside the validity range of the corresponding ion dissociation equation.

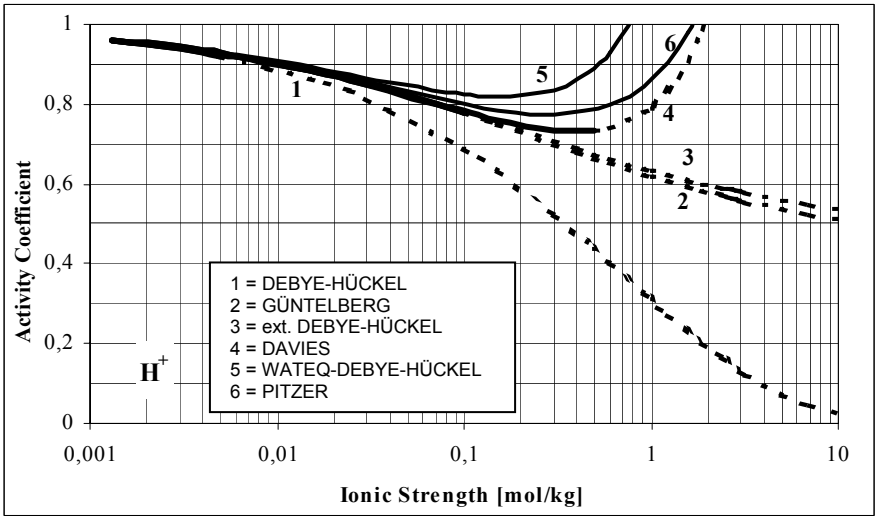

Fig. 8 Comparison of the activity coefficient of H^+ in relation to the ionic strength as calculated from the changing pH of a $CaCl_2$ solution (a_H = 4.78, b_H = 0.24 Table 4) using different theories of ion dissociation and the PITZER equation, dashed lines signify calculated values outside the validity range of the corresponding ion dissociation equation.

In particular, the strongly diverging graph of the simple DEBYE-HÜCKEL equation from the PITZER curve in the range exceeding 0.005 mol/kg (validity limit) is conspicuous. In contrast, the conformity of WATEQ-DEBYE-HÜCKEL and PITZER concerning the divalent calcium and sulfate ions is surprisingly good. Also for chloride the WATEQ-DEBYE-HÜCKEL and PITZER equation show a good agreement as far as 3 mol/kg. On contrary the activity coefficients for sodium and hydrogen ions clearly show strong discrepancies. There the validity range of 1 mol/kg for the WATEQ-DEBYE-HÜCKEL equation must be restricted, since significant differences already occur at ionic strength low as 0.1 mol/kg (one order of magnitude below the cited limit) in comparison to the PITZER equation. These examples demonstrate the flaws of the ion dissociation theory, which are especially grave for the mono-valent ions.

1.1.3 Interactions at the liquid-gaseous phase boundary

1.1.3.1 Henry-Law

Using the linear Henry's law the amount of gas dissolved in water can be calculated for a known temperature and partial pressure.

$$m_i = K_{Hi} \cdot p_i \qquad \text{Eq.(31.)}$$

m_i = molality of the gas [mol/kg]
K_{Hi} = Henry-constant of the gas i
p_i = partial pressure of the gas i[kPa]

Table 5 shows the Henry constants and the inferred amount of gas dissolved in water for different gases of the atmosphere. The partial pressures of N_2 and O_2 in the atmosphere at 25°C and 10^5Pa (1 bar), for example, are 78 kPa and 21 kPa respectively. These pressures correspond to concentrations of 14.00 mg/L for N_2 and 8.43 mg/L for O_2.

Table 5 Composition of the terrestrial atmosphere, Henry constants and calculated concentrations for equilibrium in water at 25°C, partial pressures of the atmosphere and ionic strength of 0 (after Alloway and Ayres 1996, Sigg and Stumm 1994, Umweltbundesamt 1988/89).

Gas	volume %	Henry constant K_H (25°C) in mol/ kg·kPa	Concentration in equilibrium	
N_2	78.1	$6.40 \cdot 10^{-6}$	0.50 mmol/L	14.0 mg/L
O_2	20.9	$1.26 \cdot 10^{-5}$	0.26 mmol/L	8.43 mg/L
Ar	0.943	$1.37 \cdot 10^{-5}$	12.9 mmol/L	0.515 mg/L
CO_2	0.028 ... 0.037	$3.39 \cdot 10^{-4}$	consecutive reactions	consecutive reactions
Ne	0.0018	$4.49 \cdot 10^{-6}$	8 nmol/L	0.16 mg/L
He	$0.51 \cdot 10^{-3}$	$3.76 \cdot 10^{-6}$	19 nmol/L	76 ng/L
CH_4	$1.7 \cdot 10^{-6}$	$1.29 \cdot 10^{-5}$	2.19 nmol/L	35 ng/L
N_2O	$0.304 \cdot 10^{-6}$	$2.57 \cdot 10^{-4}$	0.078 nmol/L	3.4 ng/L

Gas	volume %	Henry constant K_H (25°C) in mol/ kg·kPa	Concentration in equilibrium	
NO	---	$1.9 \cdot 10^{-5}$	consecutive reactions	consecutive reactions
NO_2	10 .... $22 \cdot 10^{-9}$	$1.0 \cdot 10^{-4}$	consecutive reactions	consecutive reactions
NH_3	$0.2\text{-}2 \cdot 10^{-9}$	0.57	consecutive reactions	consecutive reactions
SO_2	$10 \cdot 10^{-9}$ ... $19 \cdot 10^{-9}$	0.0125	consecutive reactions	consecutive reactions
O_3	$10 \cdot 10^{-9}$ ... $100 \cdot 10^{-9}$	$9.4 \cdot 10^{-5}$	0.094 ... 0.94 nmol/L	4.5 ... 45 ng/L

With decreasing temperature the gas solubility increases, such that at 0°C as compared to 25°C 1.6 times the amount of N_2 and 1.7 times the amount of O_2 can be dissolved (Table 6). Because of the linear dependency (Eq. 31) this also results in an increase of the Henry constants.

Table 6 Solubility of gases in water in mg/L under atmospheric pressure (Rösler and Lange 1975).

Temperature	0°C	5°C	10°C	15°C	20°C	25°C
N_2	22.88	20.25	18.09	16.37	15.10	14.00
O_2	14.46	12.68	11.24	10.10	9.18	8.43

Thus Henry's law is only directly applicable for gases, which subsequently do not react any further, as for example nitrogen, oxygen, or argon. For gases that react with water, the application of the Henry's law equation only works if ensuing reactions are taken into account. Although carbon dioxide just dissociates to an extent of 1% into HCO_3^- and CO_3^{2}, which is in turn dependent on the pH value, the subsequent complexation reactions result in a strongly increased solubility of CO_2 in water. Additionally, if protons are used up by the dissolution of a mineral phase (e.g. calcite), these consequent reactions cause increased solution of CO_2, which thus becomes far higher than that calculated by Henry's law.

1.1.4 Interactions at the liquid-solid phase boundary

1.1.4.1 Dissolution and precipitation

Dissolution and precipitation can be described with the help of the mass-action law as reversible and heterogeneous reactions. In general, the solubility of a mineral is defined as the mass of a mineral, which can be dissolved within a standard volume of the solvent.

1.1.4.1.1. Solubility product

The dissolution of a mineral AB into the components A and B occurs according to the mass-action law as follows:

$$AB \leftrightarrow A + B \qquad \text{Eq.(32.)}$$

$$K_{sp} = \frac{\{A\} \cdot \{B\}}{\{AB\}} \qquad \text{Eq.(33.)}$$

Because for a solid phase AB the activity is assumed to be constant at 1, the equilibrium constant of the mass-action law results in a solubility product constant (K_{sp}) or ion-activity product (IAP) as below:

$$K_{sp} = IAP = \{A\} \cdot \{B\} \qquad \text{Eq.(34.)}$$

Analytically determined analyses for A and B must be transformed into activities of the ions and that means complexing species must be accounted for.

The solubility product depends on the mineral, the solvent, the pressure or the partial pressure of certain gases, the temperature, pH, $E_{H,}$ and on the ions previously dissolved in the water and to what extent these have formed complexes amongst themselves. While partial pressure, pH, E_H, and complex stability are considered in the mass-action law, temperature and pressure have to be taken into account by additional factors.

Dependency of K_{SP} on the temperature

In contrast to the partial pressure, temperature rise does not generally contribute to the increase of the solubility. According to the principle of the smallest constraint (Le Chatelier), only endothermic dissolutions, i.e. reactions, which need additional heat, are favored (e.g. dissolution of silicates, aluminosilicates, oxides, etc.). Yet the dissolution of carbonates and sulfates is an exothermic reaction. Therefore the solubility of carbonates and sulfates is less favorable with increasing temperature.

Dependency of K_{SP} on the pressure

Up to a pressure prevailing at 500 m water depth (5 MPa) the pressure change has almost no influence on the solubility product. There is, however, a strong dependency on the partial pressure of particular gases.

Dependency of K_{SP} on the partial pressure

The increased rate of dissolution and precipitation in the upper layer of the soil is caused by the higher partial pressure of carbon dioxide in the soil (in the growth season about 10 to 100 times higher than in the atmosphere because of the biological and microbiological activity). Average carbon dioxide partial pressure under humid climate conditions in summer is at 3 to 5 kPa (3-5 vol%), whereas it amounts to up to 30 vol% in tropical climates and to up to 60 vol% in heaps or organically contaminated areas. Since the increased partial pressure of CO_2 is accompanied by a higher proton activity, those minerals are preferably dissolved for which the solubility depends on the pH value.

Dependency of K_{SP} on the pH value
Just a few ions like Na^+, K^+, NO_3^- or Cl^+ are soluble to the same extent across the whole range of pH values of normal groundwater. Mainly the dissolution of metals is strongly pH dependent. While precipitating as hydroxides, oxides, and salt under basic conditions, they dissolve and are mobile as free cations under acid conditions. Aluminum is soluble under acid as well as under basic conditions. It precipitates as hydroxide or clay mineral in the pH range of 5 to 8.

Dependency of K_{SP} on the E_H value
For those elements that occur in different oxidation states, the solubility not only depends on the pH but on the redox chemistry too. For example, the solubility of uranium as U^{4+} is almost insoluble at moderate pH values, but U^{6+} is readily soluble. Iron behaves completely different: at pH > 3, the oxidized form, Fe^{3+}, is only soluble to a very small extent; however, Fe^{2+} is readily soluble.

Dependency of K_{SP} on complex stability
In general, the formation of complexes increases the solubility, while the dissociation of complexes decreases it.

The extent to which elements are soluble and thus more mobile is indicated in Table 7. There, the relative enrichment of the elements compared to river water is depicted in a periodic system. Substances, which are readily soluble and thus highly mobile are enriched in seawater, whereas less mobile and less soluble substances are depleted.

1.1.4.1.2. Saturation index

The logarithm of the quotient of the ion activity product (IAP) and solubility product constant (K_{SP}) is called the saturation index (SI). The IAP is calculated from activities that are calculated from analytically determined concentrations by considering the ionic strength, the temperature, and complex formation. The solubility product is derived in a similar manner as the IAP but using equilibrium solubility data corrected to the appropriate water temperature.

$$SI = \log \frac{IAP}{K_{SP}} \qquad \text{Eq.(35.)}$$

The saturation index SI indicates, if a solution is in equilibrium with a solid phase or if under-saturated and super-saturated in relation to a solid phase respectively. A value of 1 signifies a ten-fold supersaturation, a value of -2 a hundred-fold undersaturation in relation to a certain mineral phase. In practice, equilibrium can be assumed for a range of -0.2 to 0.2. If the determined SI value is below -0.2 the solution is understood to be undersaturated in relation to the corresponding mineral, if SI exceeds +0.2 the water is assumed to be supersaturated with respect to this mineral.

Table 7 Periodic system depicting the relative enrichment (ratio > 1) of the elements in sea water as compared to river water; elements enriched in sea water (mobile elements) are shaded (after Faure 1991, Merkel and Sperling 1996, 1998)

H ---																	He
Li 56.7	Be 0.02										B 450	C ---	N ---	O ---	F 1300		Ne
Na 1714	Mg 315										Al 0.016	Si 0.43	P 3.6	S 243	Cl 2500		Ar
K 173	Ca 27.5	Sc 0.17		Ti 0.32	V 1.3	Cr 0.2	Mn 0.04	Fe 0.0015	Co 0.02	Ni 1.7	Cu 0.04	Zn 0.02	Ga 0.2	Ge 1	As 0.85	Se 2.2	Br 3350	Kr
Rb 120	Sr 109	Y 0.18		Zr ---	Nb ---	Mo 18.3	Tc ---	Ru ---	Rh ---	Pd ---	Ag 0.009	Cd 8.0	In ---	Sn 0.013	Sb 2.1	Te ---	I 8.0	Xe
Cs 14.5	Ba 0.7	Lu 0.22		Hf ---	Ta ---	W 3.3	Re ---	Os ---	Ir ---	Pt ---	Au 2.5	Hg 0.14	Tl ---	Pb 0.002	Bi ---	Po ---	At ---	Rn
Fr ---	Ra ---																
"---" no data or no consistent data in the literature																	
La 0.094	Ce 0.044	Pr 0.14		Nd 0.11	Pm ---	Sm 0.10	Eu 0.10	Gd 0.11	Tb 0.14	Dy 0.15	Ho 0.20	Er 0.22	Tm 0.21	Yb 0.25			
Ac ---	Th 0.0006	Pa ---		U 2.7	Np ---	Pu ---	Am ---	Cm ---	Bk ---	Cf ---	Es ---	Fm ---	Md ---	No ---			

1.1.4.1.3. Limiting mineral phases

Some elements in aquatic systems exist only at low concentrations (µg/L range) in spite of readily soluble minerals. This phenomenon is not always caused by a generally small distribution of the concerned element in the earth crust mineral as for instance with uranium. Possible limiting factors are the formation of new minerals, co-precipitation, incongruent solutions, and the formation of solid-solution minerals (i.e. mixed minerals).

Formation of new minerals

For example Ca^{2+}, in the presence of SO_4^{2-} or CO_3^{2} can be precipitated as gypsum or calcite, respectively. A limiting mineral phase for Ba^{2+} in the presence of sulfate is $BaSO_4$, or barite. If, for instance, a sulfate-containing groundwater is mixed with a $BaCl_2$-containing groundwater, barite becomes the limiting phase and is precipitated until the saturation index for barite attains the value of zero.

Co-precipitation

For elements like radium, arsenic, beryllium, thallium, molybdenum and many others, not only the low solubility of the related minerals but also the co-precipitation or adsorption with other minerals, plays an important role. For instance radium is co-precipitated with iron hydroxides and barium sulfate.

The mobility of radium is determined by redox-sensitive iron, which readily forms iron oxyhydroxides under oxidizing conditions and thus limits the concentrations of iron and radium because radium is effectively sorbed on iron oxyhydroxide. Redox-sensitive elements are elements that change their oxidation state by electron transfer depending on the relative oxidizing or reducing conditions of the aquatic environment (chapter 1.1.5.2.4 and 0). Thus radium behaves like a redox-sensitive element, even though it only occurs in the divalent form.

Incongruent solutions

Solution processes, in which one mineral is dissolving, while another mineral is inevitably precipitating, are called incongruent. Thus, if dolomite is added to water in equilibrium with calcite (SI = 0) then dolomite dissolves until equilibrium for dolomite is established. That leads consequently to an increase for the concentrations of Ca, Mg, and C in water, which in turn inevitably causes super-saturation with respect to calcite and thus precipitation of calcite.

Solid solutions

The examination of naturally occurring minerals shows, that pure mineral phases are rare. In particular they frequently contain trace elements as well as common elements. Classic examples of solid-solution minerals are dolomite or the calcite/rhodocrosite, calcite/strontianite, and calcite/otavite systems.

For these carbonates, the calculation of the saturation index gets more difficult. If, for instance, one considers the calcite/strontianite system, the solubility of both mineral phases is estimated by:

$$K_{calcite} = \frac{\{Ca^{2+}\} \cdot \{CO_3^{2-}\}}{\{CaCO_3\}_s} \qquad \text{Eq.(36.)}$$

and

$$K_{strontianite} = \frac{\{Sr^{2+}\} \cdot \{CO_3^{2-}\}}{\{SrCO_3\}_s} \qquad \text{Eq.(37.)}$$

Assuming a solid-solution mineral made up from a mixture of these two minerals, the conversion of the equations results in:

$$\frac{\{Sr^{2+}\}}{\{Ca^{2+}\}} = \frac{K_{strontianite} \cdot \{SrCO_3\}_s}{K_{calcite} \cdot \{CaCO_3\}_s} \qquad \text{Eq.(38.)}$$

That means that a certain activity ratio of Sr and Ca in aqueous solution is associated with a certain activity ratio in the minerals. If, analogously to the non-ideal behavior of the activity coefficient of the aquatic species, a specific correction factor $f_{calcite}$ and $f_{strontianite}$ for the activity is introduced, the following equation arises:

$$\frac{K_{strontianite} \cdot f_{strontianite}}{K_{calcite} \cdot f_{calcite}} = \frac{\{Sr\} \cdot X_{calcite}}{\{Ca\} \cdot X_{strontianite}} \qquad \text{Eq.(39.)}$$

where X is the molar proportion in the solid-solution mineral. In the simplest case, the ratio of both activity coefficients can be combined in order to obtain a distribution coefficient. The latter can be experimentally determined by semi-empirical approximation in the laboratory.

Using the solubility product constants for calcite and strontianite and assuming a calcium activity of 1.6 mmol/L, a distribution coefficient of 0.8 for strontium and 0.98 for calcite, and a ratio of 50:1 (=0.02) in the solid-solution mineral, the following equation gives the activity of strontium:

$$\begin{aligned}\{Sr\} &= \frac{K_{strontianite} \cdot f_{strontianite} \cdot X_{strontianite} \cdot \{Ca\}}{K_{calcite} \cdot f_{calcite} \cdot X_{calcite}} \\ &= \frac{10^{-9.271} \cdot 0.8 \cdot 0.02 \cdot 1.6 \cdot 10^{-3}}{10^{-8.48} \cdot 0.98} = 4.2 \cdot 10^{-6}\ \text{mol/l}\end{aligned} \qquad \text{Eq.(40.)}$$

If strontianite is assumed to be the limiting phase, significantly more strontium (activity approx. $2.4 \cdot 10^{-4}$ mol/L) could be dissolved compared to that of the solid-solution mineral phase.

This example shows a tendency with solid-solution minerals. There is a supersaturation or an equilibrium regarding the solid-solution minerals but an

undersaturation with respect to the pure mineral phases, i.e. the solid-solution mineral is formed but not one of the pure mineral phases. The prominence of this phenomenon depends upon the values of the activity coefficient of the solid-solution component.

For the calculation of solid-solution mineral behavior, two conceptual models may be used: the end-member model (arbitrary mixing of two or more phases) and the site-mixing model (substituting elements can replace certain elements only at certain sites within the crystal structure).

For some elements, limiting phases (pure minerals and solid-solution minerals) are irrelevant. Thus, there are no limiting mineral phases for Na or B under conditions prevailing in groundwater. Sorption on organic matter (humic and fulvic acids), on clay minerals or iron oxyhydroxides as well as cation exchange may be limiting factors instead of mineral formation. This issue will be addressed in the following.

1.1.4.2 Sorption

The term sorption combines matrix sorption and surface sorption. Matrix sorption can be described as the relatively unspecific exchange of constituents contained in water into the porous matrix of a rock ("absorption"). Surface sorption is understood to be the accretion of atoms or molecules of solutes, gases or vapor at a phase boundary ("adsorption"). In the following only surface sorption will be addressed more thoroughly.

Surface sorption may occur by physical binding forces (van de Waals forces, physisorption), by chemical bonding (Coulomb forces) or by hydrogen bonding (chemisorption). A complete saturation of all free bonds at the defined surface sites is possible involving specific lattice sites and/or functional groups (surface complexation, chapter 1.1.4.2.3). While physisorption is reversible in most cases, remobilization of constituents bound by chemisorption is difficult. Ion exchange is based on electrostatic interactions between differently charged molecules.

1.1.4.2.1. Hydrophobic /hydrophilic substances

Rocks may be hydrophobic or hydrophilic and this property is closely related to the extent of sorption. In contrast to hydrophilic materials, hydrophobic substances have no free valences or electrostatic charge available at their surfaces. Hence, neither hydrated water molecules nor dissolved species can be bound to the surface and in the extreme case, could largely prevent the wetting of the surface with aqueous solution.

1.1.4.2.2. Ion exchange

The ability of solid substances to exchange cations or anions with cation or anions in aqueous solution is called ion-exchange capacity. In natural systems anions are exchanged very rarely, in contrast to cations, which exchange more readily

forming a succession of decreasing intensity: $Ba^{2+} > Sr^{2+} > Ca^{2+} > Mg^{2+} > Be^{2+}$ and $Cs^{+} > K^{+} > Na^{+} > Li^{+}$. Generally, multivalent ions (Ca^{2+}) are more strongly bound than monovalent ions (Na^{+}), yet the selectivity decreases with increasing ionic strength (Stumm and Morgan, 1996). Large ions like Ra^{2+} or Cs^{+} as well as small ions like Li^{+} or Be^{2+} are merely exchanged to a lower extent. The H^{+}, having a high charge density and small diameter, is an exception and is preferentially absorbed.

Moreover, the strength of the binding depends on the respective sorbent, as Table 8 shows for some metals. The comparison of the relative binding strength is based on the pH, at which 50% of the metals are absorbed ($pH_{50\%}$). The lower this pH value, the stronger this distinct metal is bound to the sorbent, as for instance with Fe-oxides: Pb ($pH_{50\%}$ = 3.1) > Cu ($pH_{50\%}$ = 4.4) > Zn ($pH_{50\%}$ = 5.4) > Ni ($pH_{50\%}$ = 5.6) > Cd ($pH_{50\%}$ = 5.8) > Co ($pH_{50\%}$ = 6.0) > Mn ($pH_{50\%}$ = 7.8) (Scheffer and Schachtschabel 1982).

Table 8 Relative binding strength of metals on different sorbents (after Bunzl et al. 1976)

Substance	Relative binding strength
Clay minerals, zeolites	Cu>Pb>Ni>Zn>Hg>Cd
Fe, Mn-oxides and –hydroxides	Pb>Cr=Cu>Zn>Ni>Cd>Co>Mn
Organic matters (in general)	Pb>Cu>Ni>Co>Cd>Zn=Fe>Mn
Humic- and Fulvic acids	Pb>Cu=Zn=Fe
Peat	Cu>Pb>Zn>Cd
degraded peat	Cu>Cd>Zn>Pb>Mn

Corresponding to the respective sorbent, ion exchange capacity additionally depends on the pH value (Table 9).

Table 9 Cation exchange capacity at pH 7 and their dependency (after Langmuir 1997)

Substance	CEC (meq/100g)	pH dependency
Clay minerals		
Kaolinite	3-15	high
Illite and Chlorite	10-40	low
Smectite Montmorrilonite	80-150	rare or non existent
Vermiculite	100-150	negligible
Zeolites	100-400	negligible
Mn (IV) and Fe (III) Oxyhydroxides	100-740	high
Humic matter	100-500	high
synthetic cation exchangers	290-1020	low

Fig. 9 shows the pH-dependent sorption of metal cations; Fig. 10 the same for selected anions on iron hydroxide.

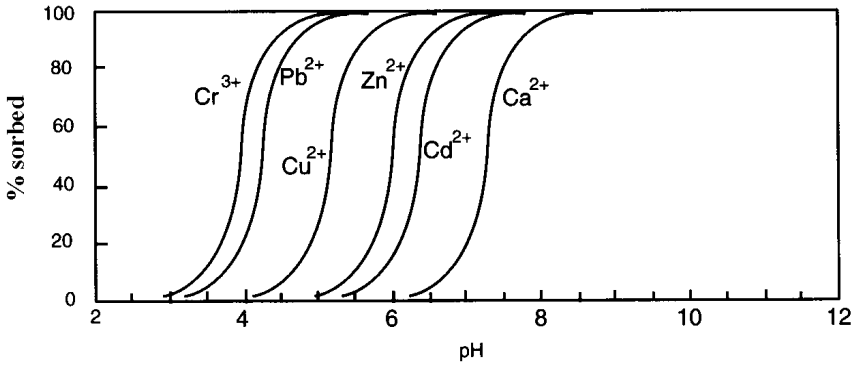

Fig. 9 pH-dependent sorption of metal cations on iron hydroxide (after Drever 1997)

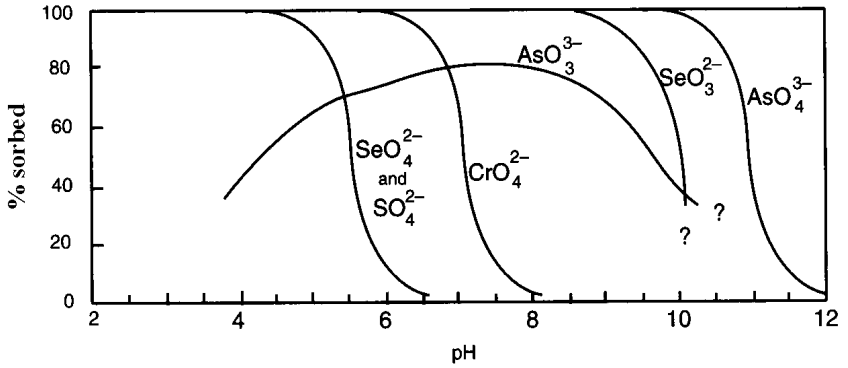

Fig. 10 pH-dependent sorption of anions on iron hydroxide (after Drever 1997)

Description of the ion exchange using the mass-action law

Assuming a complete reversibility of sorption, the ion exchange can be described through the mass-action law. The advantage of this approach is that virtually any number of species can interact at the surface of a mineral.

$$A^+ + B^+R^- \leftrightarrow A^+R^- + B^+$$

$$K_B^A = \frac{\{A^+R^-\}\cdot\{B^+\}}{\{A^+\}\cdot\{B^+R^-\}} = \frac{\{A^+R^-\}/\{A^+\}}{\{B^+R^-\}/\{B^+\}} \qquad \text{Eq.(41.)}$$

with A^+, B^+ monovalent ions
R= exchanger

K_x is the selectivity coefficient and is considered here as an equilibrium constant, even though, in contrast to complexation constants or dissociation constants, it depends not only on pressure, temperature and ionic strength, but also on the

respective solid phase with its specific properties of the inner and outer surfaces. Although to a lesser extent, it also depends on they way the reaction is written.

Thus, the exchange of sodium for calcium can be written as follows:

$$Na^+ + \frac{1}{2}CaX_2 \leftrightarrow NaX \cdot \frac{1}{2}Ca^{2+}$$

$$K_{Ca}^{Na} = \frac{\{NaX\} \cdot \{Ca^{2+}\}^{0.5}}{\{CaX_2\} \cdot \{Na^+\}} \qquad \text{Eq.(42.)}$$

This expression is called the Gaines-Thomas convention (Gaines and Thomas 1953). If using the molar concentration instead, it is identical to the Vanselow convention (Vanselow 1932). Gapon (1933) proposed the following form:

$$Na^+ + Ca\frac{1}{2}X \leftrightarrow NaX \cdot \frac{1}{2}Ca^{2+}$$

$$K_{Ca}^{Na} = \frac{\{NaX\} \cdot \{Ca^{2+}\}^{0.5}}{\{Ca\,\frac{1}{2}X\} \cdot \{Na^+\}} \qquad \text{Eq.(43.)}$$

Important ion exchanger

Important ion exchangers and sorbents are, as can be seen from the Table 8, clay minerals and zeolites (aluminous silicates), metal oxides (mainly iron and manganese oxides), and organic matter.

- Clay minerals consist of 1 to n sheets of Si-O tetrahedrons and of 1 to n layers of aluminum hydroxide octahedral sheets (gibbsite). Al very often replaces Si in the tetrahedral sheet as well as Mg does for Al in the octahedral sheet.
- As ion exchanger, zeolites play an important role in volcanic rocks and marine sediments.
- At the end of the weathering process, often iron and manganese oxides form. Manganese oxides usually form an octahedral arrangement resembling gibbsite. Hematite (Fe_2O_3) and goethite (FeOOH) also show a similar octahedral structure.
- Following Schnitzer (1986) 70 to 80% of organic matter is to be ascribed to humic substances. These are condensed polymers composed of aromatic and aliphatic components, which form through the decomposition of living cells of plants and animals by microorganisms. Humic substances are hydrophilic, of dark color and show molecular masses of some hundred to many thousands. They show widely differing functional groups being able to interact with metal ions. Humic substances (refractional organic acids) can be subdivided into humic and fulvic acids. Humic acids are soluble under alkaline conditions and precipitate under acid conditions. Fulvic acids are soluble under basic and acidic conditions.

Ion exchange or sorption can also occur on colloids, since colloids possess an electric surface charge, at which ions can be exchanged or sorptively bound. The proportion of colloids not caught in small pores preferentially utilizes larger pores, thus sometimes travelling faster than some of the water in groundwater (size-exclusion effect). That is why the colloid-bound contaminant transport is of such special importance.

Furthermore, there are synthetic ion exchangers, which are important for water desalination. They are composed of organic macromolecules. Their porous network, made up from hydrocarbon chains, may bind negatively charged groups (cation exchanger) or positively charged groups (anion exchanger). Cation exchangers are based mostly on sulfo-acidic groups with an organic leftover, anion exchangers are based on substituted ammonium groups with an organic remnant.

Surface charges

The cation-exchange capacity of clay minerals is in a range of 3 to 150 meq/100g (Table 9). These extremely high exchange capacities rely on two physical reasons:

- extremely large surface
- an electric charge of the surfaces

These electric charges can be subdivided into:

- permanent charges
- variable charges

Permanent surface charges can be related to the substitution of metals into the crystal lattice (isomorphism). Since the substitution usually occurs by metals with a low charge, an overall deficit in positive charge results for the crystal. To balance this, a negative potential forms at the surface causing positively charged metals to sorb. The surface charges of clay minerals can be predominantly related to isomorphism, therefore they are permanent to a great portion. However, this is not true for all clay minerals; for kaolinite it is less than 50% (Bohn et al., 1979).

Besides the permanent charge, there are variable surface charges, which depend on the pH of the water. They arise from protonation and deprotonation of functional groups at the surface. Under acid conditions, protons are sorbed on the functional groups that cause an overall positive charge on the surface. Thus the mineral or parts of it behave as an anion exchanger. With high pH, the oxygen atoms of the functional groups stays deprotonized and the mineral, or parts of it, shows an overall negative charge; therefore cations can be sorbed.

For every mineral there is a pH value at which the positive charge caused by protonization equals the negative charge caused by deprotonization, so that the overall charge is zero. This pH is called the pH_{PZC} (Point of Zero Charge). If only deprotonization and protonization have an influence on the surface charge this value is called ZPNPC (zero point of net proton charge) or IEP (iso-electric point). This point is around pH 2.0 for quartz, around pH 3.5 for kaolinite, for goethite, magnetite, and hematite approximately between pH 6 and 7, and for corundum around pH 9.1 (Drever 1997). Fig. 11 shows the pH-dependent sorption behavior of iron hydroxide surfaces. The overall potential of the pH-dependent surface charge does not depend on the ionic strength of water.

Natural systems are a mixture of minerals with constant and variable surface charge. Fig. 12 shows the general behavior in relation to anion and cation sorption. At values exceeding pH 3 the anion exchange capacity decreases considerably. Up to pH 5 the cation exchange capacity is constant, rising extremely at higher values.

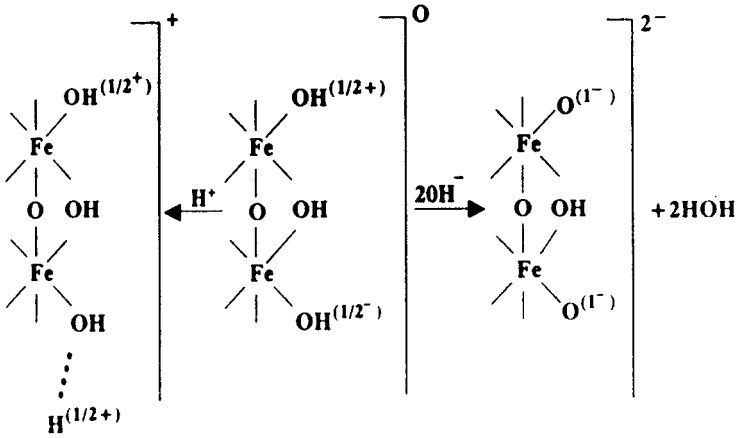

Fig. 11 Schematic depiction of the pH-dependent sorption behaviors of iron hydroxide surfaces at accretion of the H+ and OH- ions (after Sparks 1986).

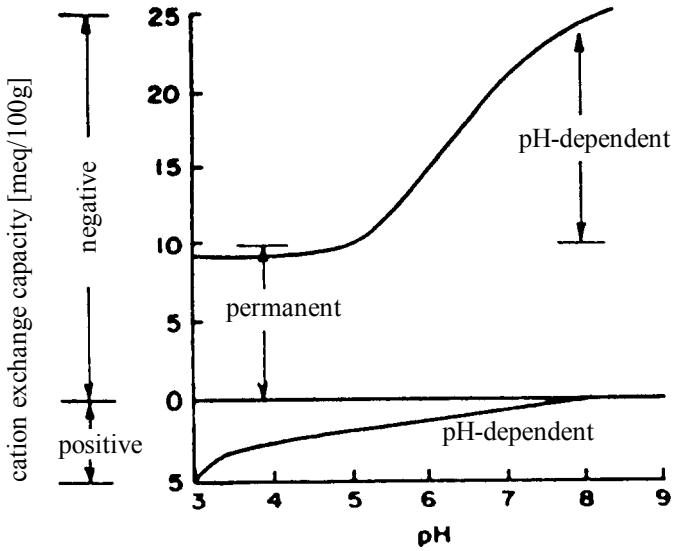

Fig. 12 Cation and Anion exchange behavior of minerals as a function of the pH (after Bohn et al. 1979); "negative" and "positive" relates to the charge of the surfaces, so that "negatives" are cation exchanger and "positives" anion exchanger.

1.1.4.2.3. Mathematical description of the sorption

There is a range of equations used describing the experimental data for the interactions of a substance as liquid and solid phases. They extend from simple empirical equations (sorption isotherms) to complicated mechanistic models based on surface complexation for the determination of electric potentials, e.g. constant-capacitance, diffuse-double layer and triple-layer model.

Empiric models- sorption isotherms

Sorption therms are the depiction of sorptional interactions using simple empirical equations. Initially, the measurements were done at constant temperature, that is why the term isotherm was introduced.

Linear regression isotherm (Henry isotherm)

The most simple form of a sorption isotherm is the linear regression equation.

$$C^* = K_d \cdot C \qquad \text{Eq.(44.)}$$

with C* = mass of substance, sorbed at a mineral (mg/kg)
K_d = distribution coefficient
C = concentration of the substance in water (mg/L)

Linear sorption terms have the advantage of simplicity and they provide the possibility to convert them into a retardation factor Rf, so that the general transport equation can be easily expanded by applying the correction term:

$$Rf = 1 + \frac{Bd}{q} \cdot \frac{C^*}{C} = 1 + \frac{Bd}{q} \cdot K_d \qquad \text{Eq.(45.)}$$

with Bd = bulk density
q = water content

A serious disadvantage is that the relation is linear, so that there is no upper limit to the sorption.

Freundlich isotherms

Using the Freundlich isotherm, an exponential relation between sorbed and dissolved molecules is used.

$$C^* = K_d \cdot C^n \qquad \text{Eq.(46.)}$$

$$Rf = 1 + \frac{Bd}{q} \cdot n \cdot K_d \cdot C^{n-1} \qquad \text{Eq.(47.)}$$

A further empirical constant n is introduced, which is usually less than 1. The Freundlich isotherm is based on a model of a multi-lamellar coating of the solid surface assuming *a priori* that all sites with the largest binding energy (of

electrostatic forces) are occupied (steep section of the curve) and with increasing grade, sites with lower binding energy (flattening of the curve) are occupied.

Using the Freundlich isotherm the shortfall of limitlessness is removed, moreover, as with the linear model, a transformation into a retardation factor Rf is possible.

Langmuir isotherm

The Langmuir isotherm was developed to describe sorbents with a limited number of sorption sites on their surface

$$C^* = \frac{a \cdot b \cdot C}{1 + a \cdot C} \qquad \text{Eq.(48.)}$$

with a = sorption constant
b = maximum sorbable mass of the substance (mg/kg)

$$Rf = 1 + \frac{Bd}{q} \cdot \left[\frac{a \cdot b}{(1 + a \cdot C)^2} \right] \qquad \text{Eq.(49.)}$$

From the scientific point of view, however, all approaches in the sense of the K_d concept (Henry, Freundlich or Langmuir isotherm) are unsatisfactory, since the complex processes on surfaces cannot be described by empirical fitting parameters. Boundary conditions like pH value, redox potential, ionic strength, competition reactions for binding sites are not considered. Thus results from laboratory and field experiments are not transferable to real systems. They are only advisable to provide a suitable prognosis model, if no changes concerning boundary conditions are to be expected and if no parameters for deterministic or mechanistic approach can be determined.

Mechanistic models for surface complexation

Surface complexation is a theory to describe the phenomenon of sorption. At the surface of iron, aluminum, silica, and manganese hydroxides as well as humic substances, there are cations that are not completely surrounded by oxygen ions in contrast to the cations of the inner parts of the crystal lattice. Because of their valence electrons they may bind water molecules. These water molecules distribute after the accretion such that for every sorbed oxygen ion, one hydrogen ion remains. The second hydrogen ion is bound to the oxygen ions in the lattice that is between the lattice cations (Fig. 13). Thus there is a layer of functional groups always containing O, S, or N on the surface of the mineral (double layer).

After Stumm and Morgan (1996) the reaction can be described as follows:

$$\{GH\} + Me^{z+} \leftrightarrow \{GMe^{z-1}\} + H^+ \qquad \text{Eq.(50.)}$$

Here, GH is a functional group as $(R\text{-}COOH)_n$ or $(=AlOH)_n$. The capability of functional groups to form complexes strongly depends on the acid-base behavior and, hence, the change of pH in an aquatic system.

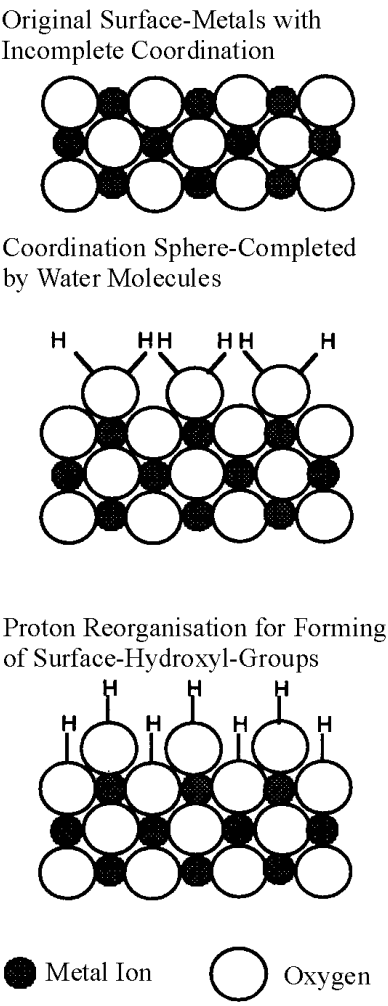

Fig. 13 The process of surface complexation (after Drever 1997)

Similar to solution complexation, surface complexation can be distinguished between inner-spherical complexes (e.g. phosphate, fluoride, copper), where the ion is directly bound to the surface, and outer-spherical (e.g. sodium, chloride) complexes where the ion is covered by a hydration sleeve with the attraction working only electrostatically. The inner-sphere complex is much stronger and not dependent on electrostatic attraction, i.e. a cation can also be sorbed on a positively charged surface (Drever 1997).

On this basis, three models will be discussed, which enable a calculation of the electrical potential, namely the constant-capacitance, the diffuse-double-layer, and the triple-layer model.

Diffuse Double-Layer Model (DDLM)
This model is based on the Gouy-Chapman theory (diffuse double-layer theory). The theory states that in the area of the boundary layer between solid and aqueous phase, independently of the surface charge, increased concentrations of cations and anions within a diffuse layer exists because of electrostatic forces. In contrast to the constant-capacitance model, the electrical potential does not change up to a certain distance from the phase boundaries and is not immediately declining in a linear manner (Fig. 14 a). Diffusion counteracts these forces, leading to dilution with increasing distance from the boundary. This relation can be described physically by the Poisson-Boltzmann equation.

Constant-Capacitance Model (CCM)
The constant-capacitance model assumes that the double layer on the solid-liquid phase boundary can be regarded as a parallel-plate capacitor (Fig. 14 b).

Tripel-Layer Model (TLM)
While CCM and DDLM assume that all ions are at one plane, the triple layer includes different planes, in which the surface complexes are bound. In the original version of Davis et al. (1978) the protons and hydroxide ions are bound at the layer (o-plane) close to the phase boundary, whereas inner-sphere complexes are bound in a β-plane somewhat dislodged. Both planes are assumed as constant-capacity layers. The range outside the β-plane containing the outer-sphere complexes is modeled as a diffuse layer (Fig. 14 c).

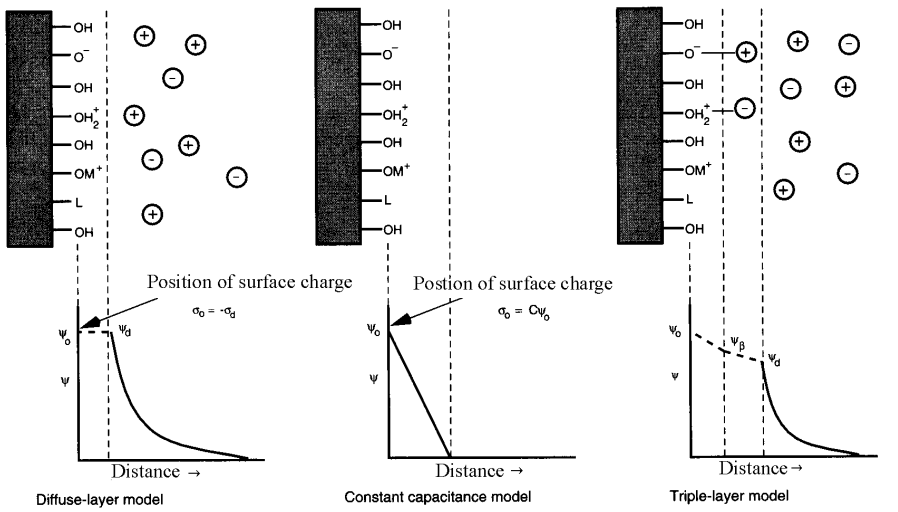

Fig. 14 Idealized distribution of the electrical potential in the vicinity of hydrated oxide surfaces after the (a) diffuse-layer model; (b) the constant-capacitance model; (c) triple-layer model (after Drever 1997).

1.1.5 Interactions in the liquid phase

1.1.5.1 Complexation

Complexation has a significant influence on dissolution and precipitation of minerals as already described in chapter 1.1.4.1.3. In contrast to the dissolution of minerals, complexation is a homogeneous reaction. It can be described by the mass-action law. The complexation constant, K, gives information about the complex stability. Large complex constants indicate a strong tendency for complexation, or high complex stability.

Positively charged, zero charged, and negatively charged complexes can be distinguished. Contaminants for instance have an especially high mobility if they occur as zero charged complexes, since they undergo almost no exchange processes, whereas (positively or negatively) charged complexes show interactions with other ions and solid surfaces.

A complex can be defined as a coordination compound of a positively charged part with a negatively charged part, the ligand. The positively charged part is usually a metal ion or hydrogen, but may also be another positively charged complex. Ligands are molecules, which have at least one free pair of electrons (bases). This ligand can either be free anions like F^-, Cl^-, Br^-, I^- or negatively charged complexes as OH^-, HCO_3^-, CO_3^{2-}, SO_4^{2-}, NO_3^-, and PO_4^{3}.

From the periodic table of elements the following elements can be possible ligands:

Group	4	5	6	7
	C	N	O	F
		P	S	Cl
		As	Se	Br
			Te	I

Beside these inorganic ligands there are also organic ligands like humic or fulvic acids, which occur naturally in almost all waters, but also NTA and EDTA, which enter the hydrosphere as phosphate substitutes in detergents (Bernhardt et al. 1984) and can mobilize metals.

The complex binding can be electrostatic, covalent, or a combination of both. Electrostatically bound complexes, where the metal atom and the ligand are separated by one or more hydrogen molecules, are called outer-sphere complexes. They are less stable and are formed when hard cations come into contact with hard ligands (Table 10).

The Pearson concept of “hard” and “soft” acids and bases considers the number of electrons in the outer shell. Elements with a saturated outer shell and low tendency for polarization (noble gas configuration) are called “hard” acids, while elements with only partially filled outer shell, low electronegativity, and high tendency for polarization are “soft” acids.

Inner-sphere complexes, with covalent bounds between a metal atom and a ligand, form from soft metal atoms and soft ligands or soft metal atoms and hard ligands or hard metal atoms and soft ligands and are much more stable.

Table 10 Classification of metal ions into A and B- type and after the Pearson concept into hard and soft acids with preferred ligands (after Stumm and Morgan 1996)

Metal cations type A („hard spheres“)	Transition metal cations	Metal cations type B („soft spheres“)
H^+, Li^+, Na^+, K^+, Be^{2+}, Mg^{2+}, Ca^{2+}, Sr^{2+}, Al^{3+}, Sc^{3+}, La^{3+}, Si^{4+}, Ti^{4+}, Zr^{4+}, Th^{4+}	V^{2+}, Cr^{2+}, Mn^{2+}, Fe^{2+}, Co^{2+}, Ni^{2+}, Cu^{2+}, Ti^{3+}, V^{3+}, Cr^{3+}, Mn^{3+}, Fe^{3+}, Co^{3+}	Cu^+, Ag^+, Au^+, Tl^+, Ga^+, Zn^{2+}, Cd^{2+}, Hg^{2+}, Pb^{2+}, Sn^{2+}, Tl^{3+}, Au^{3+}, In^{3+}, Bi^{3+}
according to Pearson concept		
hard acids	Transition range	soft acids
all metal cations type A plus Cr^{3+}, Mn^{3+}, Fe^{3+}, Co^{3+}, UO^{2+}, VO^{2+}	all divalent transition metal cations plus Zn^{2+}, Pb^{2+}, Bi^{3+}	all metal cations type B except for Zn^{2+}, Pb^{2+}, Bi^{3+}
preference for ligand atom		
N >> P, O >> S, F >> Cl		P >> N, S >> O, Cl >> F

Chelates are complexes with ligands that form more than one bond with the positively charged metal ion (multidentate ligands). Such complexes show an especially high stability. Complexes with more than one metal atom are called multi- or polynucleus complexes.

By means of complexation, a metal can occur in normally unknown or rare oxidation states. For instance, Co^{3+}, being a strong oxidizing agent, is normally not stable in aqueous solutions, but it is stable as $Co(NH_3)_6^{3+}$. Furthermore, complexation can prevent disproportionation, as in the case of Cu^+ e.g., which converts into Cu^{2+} and Cu(s) in an aqueous solution, although it is stable as $Cu(NH_3)_2^+$.

General statements about the stability of different complexes are problematic. Inferences from the ionic strength or more general subdivisions into good and poor chelating agents based on the periodic table of elements lead to contradictory statements. They do not appear practical, because the tendency of elements to form complexes critically depends on the corresponding ligand, as Table 11 shows for some examples. And last, but not least, the concentration of the ligand in the solution (main or trace element) is of crucial importance.

Table 11 Complexation constants for hydroxide, carbonate, and sulfate complexes (data from WATEQ4F and (*) CHEMVAL data base); Me = metal cations, n = oxidation state of the cations (n = 1, 2, 3)

Element	Hydroxo complex $Me^n + H_2O = MeOH^{n-1} + H^+$	Carbonate complex $Me^n + CO_3^{2-} = MeCO_3^{n-2}$	Sulfate complex $Me^n + SO_4^{2-} = MeSO_4^{n-2}$
Na^+	-13.9 (*)	1.27	0.7
K^+	-14.5 (*)	no data available	0.85
Ca^{2+}	-12.78	3.224	2.3
Mg^{2+}	-11.44	2.98	2.37
Mn^{2+}	-10.59	4.9	2.25
Ni^{2+}	-9.86	6.87	2.29
Fe^{2+}	-9.5	4.38	2.25

Element	Hydroxo complex $Me^n + H_2O = MeOH^{n-1} + H^+$	Carbonate complex $Me^n + CO_3^{2-} = MeCO_3^{n-2}$	Sulfate complex $Me^n + SO_4^{2-} = MeSO_4^{n-2}$
Zn^{2+}	-8.96	5.3	2.37
Cu^{2+}	-8.0	6.73	2.31
Fe^{3+}	-2.19	no data available	4.04

1.1.5.2 Redox processes

Together with acid-base reactions, where a proton transfer occurs (pH-dependent dissolution/ precipitation, sorption, complexation) redox reactions play an important role for all interaction processes in aqueous systems. Redox reactions consist of two partial reactions, oxidation and reduction, and can be characterized by oxygen or electron transfer. Many redox reactions in natural aqueous systems can actually not be described by thermodynamic equilibrium equations, since they have slow kinetics. If a redox reaction is considered as a transfer of electrons, the following general reaction can be derived:

$$\{\text{oxidized species}\} + n \cdot \{e^-\} = \{\text{reduced species}\} \qquad \text{Eq.(51.)}$$

with n = number of electrons, e^-.

1.1.5.2.1. Measurement of the redox potential

Inserting an inert but highly conductive metal electrode into an aqueous solution allows electrons to transfer both from the electrode to the solution and vice versa. A potential difference (voltage) builds up, which can be determined in a current-less measurement. Per definition, this potential is measured relative to the standard hydrogen electrode with $P(H_2)$ = 100 kPa, pH = 0, temperature = 20°C and a potential of

$$E^o\left(\frac{H^+}{H_2}\right) = 0\,\text{mV} \qquad \text{Eq.(52.)}$$

In the aqueous solution, the potential is measured as an integral over all existing redox species (mixed potential).

Since the use of the standard hydrogen electrode in the field would be very tedious, other reference electrodes are used. Those reference electrodes have a defined Eigenpotential, E_B, which is added to the determined value E_M, to obtain the solution potential, or E_H, with reference to the standard hydrogen electrode. Mostly Ag/AgCl or mercury chloride (Hg_2Cl_2)/ platinum electrodes are used as reference electrodes. The advantage of Ag/AgCl electrodes is the fast response rate, whereas the mercurial chloride/platinum-electrode yields a slower responding rate but a higher precision. In practice, the measurement of the redox potential is, independent of the reference electrode, highly problematic, since natural waters are likely not to be in thermodynamical redox equilibrium and redox species are present in concentrations too low to give an electrode response (Nordstrom and

Munoz 1994). Furthermore the electrode is highly susceptible to contamination effects. While contaminations of a platinum electrode can be disposed of managed, thermodynamic disequilibrium and low concentrations can not. Therefore redox measurements should be aborted after 1 hour if no steady value is reached. The statement derived from the measurement in that case is, that the water is redox species are not in thermodynamical redox equilibrium with the platinum electrode.

1.1.5.2.2. Calculation of the redox potential

The equilibrium redox potential can be calculated from the following Nernst equation:

$$E_h = E^o + \frac{R \cdot T}{n \cdot F} \ln \frac{\{ox\}}{\{red\}} \qquad \text{Eq.(53.)}$$

E^o = standard redox potential of a system where the activities of the oxidized species equal the activities of the reduced species
R = ideal gas constant (8.315 J/K mol)
T = absolute temperature (K)
n = number of transferred electrons (e^-)
F = Faraday constant (96484 C/mol = J/V mol)
{ox} = activity of the oxidized species
{red} = activity of the reduced species

Eq. 53 shows the calculation of single redox potentials, unlike the measured redox potential, which may be a mixed potential of several redox reactions not in equilibrium.

It is important for the determination of the redox potential to provide the redox reaction equation. A reversion of the equation causes a change in the sign.

Table 12 shows some redox sensitive elements in the periodic system of the elements, Table 13 depicts standard potentials for some important redox pairs in aqueous systems.

The equation for the calculation of redox potentials (Eq. 53) derives from the equation of the Gibbs free energy (compare also Eq. 6).

$$G = G^0 - R \cdot T \cdot \ln \frac{\{red\}}{\{ox\}} \qquad \text{Eq.(54.)}$$

$$E_H = -\frac{G}{n \cdot F} \qquad \text{Eq.(55.)}$$

$$-\frac{G}{n \cdot F} = -\frac{G^o}{n \cdot F} - \frac{R \cdot T}{n \cdot F} \cdot \ln \frac{\{red\}}{\{ox\}} \qquad \text{Eq.(56.)}$$

Table 12 Redox sensitive elements in the PSE (bold = most common oxidation states in natural aqueous systems) (after Emsley 1992, Merkel and Sperling 1996, 1998)

H **+1** **0** -1																	**He**
Li **+1** 0	**Be** **+2** 0											**B** **+3** 0	**C** **+4** +2 0 -2 **-4**	**N** **+5** +4 **+3** +2 +1 **0** -1 -2 **-3**	**O** **0** -1 **-2**	**F** **-1** 0	**Ne**
Na **+1** 0	**Mg** **+2** +1 0											**Al** **+3** 0	**Si** **+4** +2 0 **-4**	**P** **+5** **+3** 0 -2 **-3**	**S** **+6** +5 **+4** +3 +2 0 **-2**	**Cl** +7 +5 +3 +1 0 **-1**	**Ar**
K **+1** 0	**Ca** **+2** 0 -2	**Sc** **+3** 0	**Ti** **+4** +3 +2 0	**V** +5 +4 **+3** **+2** 0	**Cr** +6 +5 +4 **+3** **+2** +1 0	**Mn** **+7** **+6** **+5** **+4** **+3** **+2** **+1** **0**	**Fe** +6 +4 **+3** **+2** 0	**Co** +6 +5 +4 **+3** **+2** +1 0 -1	**Ni** +6 +4 **+2** 0	**Cu** **+3** **+2** **+1** **0**	**Zn** **+2** 0	**Ga** **+3** **+2** **0**	**Ge** **+4** **+2** 0	**As** **+5** **+3** 0 **-3**	**Se** **+6** +4 0 **-2**	**Br** +7 +5 +1 0 **-1**	**Kr**
Rb **+1** 0	**Sr** **+2** 0 -2	**Y** **+3** 0	**Zr** **+4** 0	**Nb** +5 **+3** 0	**Mo** +6 +5 +4 **+3** +2 0	**Tc** +7 +6 +5 +4 0	**Ru** +8 +7 +6 +4 **+3** **+2** 0	**Rh** **+3** 0	**Pd** +4 **+2** 0	**Ag** +3 **+2** **+1** 0	**Cd** **+2** 0	**In** **+3** **+1** 0	**Sn** **+4** **+2** 0 -4	**Sb** **+5** +4 **+3** 0 **-3**	**Te** **+6** +4 0 -1 **-2**	**I** +7 +5 +1 0 **-1**	**Xe**
Cs **+1** 0	**Ba** +4 **+2** 0 -2	**Lu** **+3** 0	**Hf** **+4** 0	**Ta** **+5** 0	**W** **+6** **+5** **+4** **0**	**Re** +7 +6 +4 +3 0 **-1**	**Os** **+8** **+6** **+3** **+2** **0**	**Ir** +4 **+3** 0	**Pt** **+6** **+4** **+2** **0**	**Au** **+3** **+1** 0	**Hg** **+2** **+1** 0	**Tl** **+3** **+1** 0	**Pb** **+4** **+2** 0 -2	**Bi** **+5** **+3** 0 -3	**Po** +6 +4 **+2** 0 -2	**At** +5 +1 0 **-1**	**Rn**
Fr **+1**	**Ra** **+2**																

Lanthanides and actinides

La	**Ce**	**Pr**	**Nd**	**Pm**	**Sm**	**Eu**	**Gd**	**Tb**	**Dy**	**Ho**	**Er**	**Tm**	**Yb**
+3	**+4**	**+4**	**+4**	**+3**	**+3**	**+3**	**+3**	**+4**	**+4**	**+3**	**+3**	**+3**	**+3**
0	**+3**	**+3**	**+3**	0	**+2**	**+2**	0	**+3**	**+3**	0	0	**+2**	**+2**
	0	0	**+2**		0	0		0	**+2**			0	0
			0						0				
Ac	**Th**	**Pa**	**U**	**Np**	**Pu**	**Am**	**Cm**	**Bk**	**Cf**	**Es**	**Fm**	**Md**	**No**
+3	**+4**	+5	**+6**	+7	+7	+6	**+4**	**+4**	**+3**	**+3**	**+3**	**+3**	**+3**
0	0	**+4**	+5	+6	+6	+5	**+3**	**+3**	**+2**	**+2**	**+2**	**+2**	**+2**
	-3	0	**+4**	+5	+5	**+4**	0	0	0	0	0	0	0
	-4		+3	**+4**	**+4**	**+3**							
			+2	**+3**	**+3**	0							
			0	0	0								

Table 13 Standard potentials and E_H in volts for some important redox couples in aqeous systems at 25°C (modified after Langmuir 1997)

Reaction	**E° Volt**	**E_H Volt / pH 7.0**	**assumptions**
$4H^+ + O_{2(g)} + 4e^- = 2\ H_20$	1.23	0.816	P_{02}=0.2 bar
$NO_3^- + 6\ H^+ + 5e^- = 0.5\ N_{2(g)} + 3\ H_2O$	1.24	0.713	10^{-3} mol N, P_{N2}=0.8 bar
$MnO_2 + 4\ H^+ + 2\ e^- = Mn^{2+} + 2\ H_2O$	1.23	0.544	$10^{-4.72}$ mol Mn
$NO_3^- + 2\ H^+ + 2e^- = NO_2^- + H_2O$	0.845	0.431	NO_3^-=NO_2^-
$NO_2^- + 8\ H^+ + 6\ e^- = NH_4^+ + 2\ H_20$	0.892	0.340	NO_3^-=NH_4^+
$Fe(OH)_3 + 3\ H^+ + e^- = Fe^{2+} + 3\ H_2O$	0.975	0.014	$10^{-4.75}$ mol Fe
$Fe^{2+} + 2\ SO_4^{2-} + 16\ H^+ + 14\ e^- = FeS_2 + 8\ H_2O$	0.362	-0.156	10^{-475} mol Fe, 10^{-3} mol S
$SO_4^{2-} + 10\ H^+ + 8e^- = H_2S_{(aq)} + 4\ H_2O$	0.301	-0.217	SO_4^{2-}=H_2S
$HCO_3^- + 9\ H^+ + 8\ e^- = CH_{4(aq)} + 3\ H_2O$	0.206	-0.260	HCO_3^-=CH_4
$H^+ + e^- = 0.5\ H_{2(g)}$	0.0	-0.414	P_{H2}=1.0 bar
$HCO_3^- + 5\ H^+ + 4\ e^- = CH_2O$ (DOM) + $2\ H_2O$	0.036	-0.482	HCO_3^-=CH_2O

$$E_H = E^o - \frac{R \cdot T}{n \cdot F} \cdot \ln \frac{\{red\}}{\{ox\}} \qquad \text{Eq.(57.)}$$

Eq. 53 is obtained from Eq. 57 by inversion of numerator and denominator within the argument of the logarithm. That leads to the minus sign in front of the logarithm.

For standard conditions of 25°C and putting in the gas constant and the Faraday constant, a simplified form ensues:

$$E_H = E^o - \frac{0.0591}{n} \cdot \log \frac{\{red\}}{\{ox\}} \qquad \text{Eq.(58.)}$$

Dealing with pH-dependent redox reactions, as e.g. the oxidation of Cl^- to Cl_2 by permanganite at pH 3, the number of protons used and formed must be considered.

$$E_H = E^o - 2.303 \cdot \frac{m \cdot R \cdot T}{n \cdot F} \cdot pH - 2.30 \cdot \frac{R \cdot T}{n \cdot F} \cdot \log \frac{\{red\}}{\{ox\}} \qquad \text{Eq.(59.)}$$

The factor 2.303 results from the conversion of the natural logarithm to the common logarithm. Since redox potentials cannot be used directly in thermodynamic programs (unit: volt!), the pE value was introduced for mathematical convenience. Analogous to the pH value the pE value is the negative common logarithm of the electron activity. Thus, it is calculated using a hypothetic activity, respectively concentration of electrons, which is actually not present in water. For the calculation of the pE value Eq. 51 is used and the following equation is obtained for the equilibrium constant K:

$$\log K = \log \frac{\{red\}}{\{ox\}\{e^-\}^n} = \log \frac{\{red\}}{\{ox\}} + \log \frac{1}{\{e^-\}^n} = \log \frac{\{red\}}{\{ox\}} - n \cdot \log \{\bar{e}\} \qquad \text{Eq.(60.)}$$

$$- n \cdot \log \{e^-\} = \log K - \log \frac{\{red\}}{\{ox\}} \qquad \text{Eq.(61.)}$$

$$- \log \{e^-\} = \frac{1}{n} \log K - \frac{1}{n} \log \frac{\{red\}}{\{ox\}} \qquad \text{Eq.(62.)}$$

$$pE = \frac{1}{n} \log K - \frac{1}{n} \log \frac{\{red\}}{\{ox\}} \qquad \text{Eq.(63.)}$$

The conversion from pE to the measured redox potential E_H follows from:

$$pE = -\log \{e^-\} = \frac{F}{2.303 \cdot R \cdot T} \cdot E_H \qquad \text{Eq.(64.)}$$

F, R, and T=25°C put in again, the following simplified form results [E_H in V]:

$$pE \approx 16.9 \cdot E_H \qquad \text{Eq.(65.)}$$

For the system H_2/H^+ the following is applicable:

$$E_H = E^o \left(\frac{H^+}{H_2} \right) + \frac{R \cdot T}{n \cdot F} \cdot \ln \frac{\{H^+\}^2}{\{H_2\}} \qquad \text{Eq.(66.)}$$

$$E_H = 0 + \frac{R \cdot T}{n \cdot F} \cdot \ln \{H^+\}^2 - \frac{R \cdot T}{n \cdot F} \cdot \ln \{H_2\} \qquad \text{Eq.(67.)}$$

$$E_H = 0 + \frac{2.303 \cdot R \cdot T}{2 \cdot F} \cdot 2 \cdot \log\{H^+\} - \frac{2.303 \cdot R \cdot T}{2 \cdot F} \cdot \log\{H_2\} \quad \text{Eq.(68.)}$$

$$E_H = 0 - \frac{2.303 \cdot R \cdot T}{F} \cdot pH - \frac{2.303 \cdot R \cdot T}{2 \cdot F} \cdot \log\{H_2\} \quad \text{Eq.(69.)}$$

Putting in the values for R and F, as well as T =25°C and $P(H_2) = 1 \cdot 10^5$ Pa, it follows:

$$E_H = -0.0591 \cdot pH \quad \text{Eq.(70.)}$$

An increase or decrease of one pH unit causes a decrease or increase, respectively, of the Nernst voltage by 59.1 mV.

1.1.5.2.3. Presentation in predominance diagrams

The presentation of the predominant species for each redox system is called stability (or better) predominance diagram (also called E_H-pH or pE-pH diagrams). Predominance diagrams are extremely dependent on which elements in which concentrations and at which ionic strength are considered. Usually only the species dissolved in water are depicted (Fig. 15 left). However, if the concentration or activity falls below certain limits, which can be defined by the diagram designer, often the (predominant) precipitating mineral phase is outlined (Fig. 15 right). The lines limiting the single predominance ranges show the pE/pH conditions, under which the activities of two neighboring species equal each other.

How such a E_H-pH diagram can be determined analytically is explained below using the example of the Fe-O_2-H_2O diagram shown in Fig. 15 left. In each E_H-pH diagram the occurrence of the aqueous species is limited by the stability field of water. Above this field H_2O converts to elementary oxygen, below this field to elementary hydrogen (also see Fig. 16).

According to Eq. 71 every oxygen concentration is (analytically) assigned to a certain hydrogen content. This means that oxygen saturated (i.e. completely oxidized) water with the partial pressure of $P(O_2) = 1 \cdot 10^5$ Pa is in equilibrium with hydrogen with a partial pressure of $P(H_2) = 10^{-42.6} \cdot 10^5$ Pa. The other way round hydrogen saturated (completely reduced) water is in equilibrium with oxygen of a partial pressure $P(O_2) = 10^{-85.2} \cdot 10^5$ Pa.

$$\begin{aligned} 4\,e^- + 4\,H_2O &= 2\,H_2(g) + 4\,OH^- \\ 4\,OH^- &= O_2(g) + 2\,H_2O + 4\,e^- \\ \hline 2\,H_2O &= 2\,H_2(g) + O_2(g) \end{aligned}$$

$$K = \frac{\{pH_2\}^2 \cdot \{pO_2\}}{\{H_2O\}^2} = 10^{-85.2} \quad \text{Eq.(71.)}$$

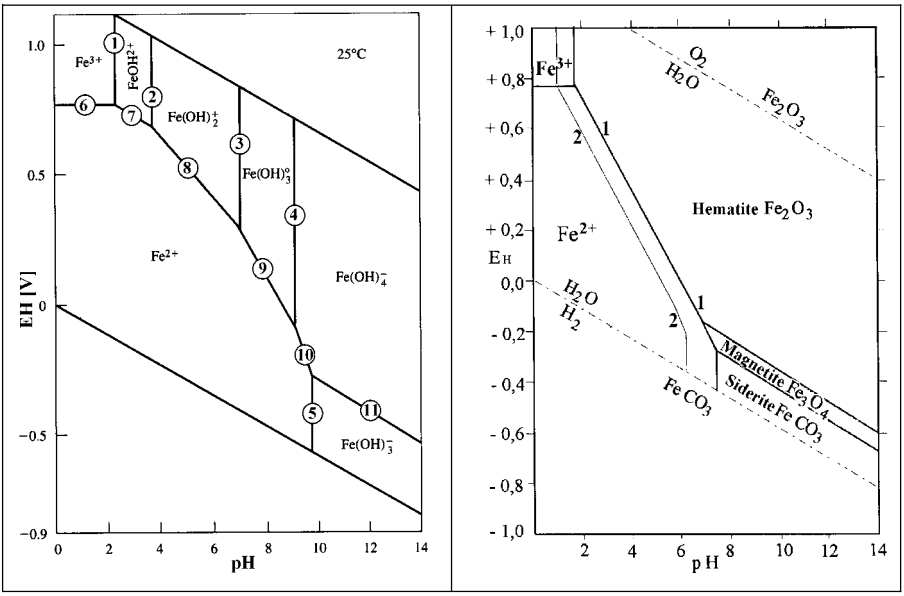

Fig. 15 Left: E_H-pH diagram for the system Fe-O_2-H_2O (at 25°C, the numbers 1-11 correspond to the reaction equations described in the text for the calculation of the stability fields, modified after Langmuir 1997) Right: E_H-pH diagram for the system Fe-O_2-H_2O-CO_2 (at 25°C, $P(CO_2) = 10^{-2}$ atm), for fields where the total activity is < 10^{-6} (1) resp. < 10^{-4} (2) mol/ L the predominant, precipitating mineral phase is outlined (modified after Garrels and Christ 1965).

The diagram´s vertical boundaries (Fig. 15, number 1-5) are reactions that describe a dissolution in water (hydrolysis) independent of the E_H value. The boundaries of the respective predominance fields are calculated via the equilibrium constants for the conversion of the species at each side of the boundary line into each other.

No.	Reaction couples	Reaction equation	-log K = pH
1	Fe^{3+}/ $FeOH^{2+}$	$Fe^{3+} + H_2O = FeOH^{2+} + H^+$	2.19
2	$FeOH^{2+}$/ $Fe(OH)_2^+$	$FeOH^{2+} + H_2O = Fe(OH)_2^+ + H^+$	3.48
3	$Fe(OH)_2^+$/ $Fe(OH)_3^0$	$Fe(OH)_2^+ + H_2O = Fe(OH)_3^0 + H_2O$	6.89
4	$Fe(OH)_3^0$/ $Fe(OH)_4^-$	$Fe(OH)_3^0 + H_2O = Fe(OH)_4^- + H^+$	9.04
5	Fe^{2+}/ $Fe(OH)_3^-$	$Fe^{2+} + 3H_2O = Fe(OH)_3^- + 3H^+$	9.08

In contrast, the conversion of Fe^{3+} into Fe^{2+} (Fig. 15, number 6), is a pure redox reaction, independent of the pH-value (horizontal boundary). It is calculated after Eq. 58:

$$E_H = E^o - \frac{0.0591}{n} \cdot \log \frac{\{red\}}{\{ox\}}$$

For the calculation of the boundary line the activity of both species is equal, i.e. {red} = {ox}. Thus the argument of the logarithm is 1 and the logarithm is 0, i.e. $E_H = E_0$.

No.	Reaction couples	Reaction equation	E_0 (V)	$E_H = E_0$
6	Fe^{3+} / Fe^{2+}	$Fe^{3+} + e^- = Fe^{2+}$	0.770	0.770

The boundaries running diagonally display species transformations, which depend on pH and E_H. After Eq. 59

$$E_H = E^o - 2.303 \cdot \frac{m \cdot R \cdot T}{n \cdot F} \cdot pH - 2.303 \cdot \frac{R \cdot T}{n \cdot F} \cdot \log \frac{\{red\}}{\{ox\}}$$

the calculation of the boundary line ({ox}={red}) follows:

$$E_H = E^o - \frac{0.0591 \cdot m}{n} \cdot pH$$

with m= number of protons used or formed in the reaction

No	Reaction couples	Equation of reaction	E_0 (V)	Equation for boundary line
7	$FeOH^{2+}$/ Fe^{2+}	$FeOH^{2+} + H^+ + e^- = Fe^{2+} + H_2O$	0.899	0.899-0.0591 pH
8	$Fe(OH)_2^+$/ Fe^{2+}	$Fe(OH)_2^+ + 2H^+ + e^- = Fe^{2+} + 2H_2O$	1.105	1.105-0.118 pH
9	$Fe(OH)_3^0$/ Fe^{2+}	$Fe(OH)_3^0 + 3H^+ + e^- = Fe^{2+} + 3H_2O$	1.513	1.513-0.177 pH
10	$Fe(OH)_4^-$/ Fe^{2+}	$Fe(OH)_4^- + 4H^+ + e^- = Fe^{2+} + 4H_2O$	2.048	2.048-0.236 pH
11	$Fe(OH)_4^-$/ $Fe(OH)_3^0$	$Fe(OH)_4^- + H^+ + e^- = Fe(OH)_3^0 + H_2O$	0.308	0.308-0.0591 pH

How E_H-pH-diagrams change if besides O_2, H_2O and CO_2 other species, as e.g. hydrogen carbonate or sulfate, are also considered can be modeled numerically in chapter 3.1.3.1and 3.1.3.2. E_H-pH diagrams can also be used to characterize natural waters at a first approximation (Fig. 16). However, the problems concerning the precision and uncertainties of E_H measurements must be taken into account (chapter 1.1.5.2.1).

Partial pressure or fugacity diagrams provide another possibility of presentation. Analogous to the activity for the concentration the fugacity is an effective pressure, which describes the tendency of a gas for volatilization from a phase (Latin fugere = flee). Under low-pressure conditions, the fugacity equals the partial pressure. In fugacity diagrams the species distribution species is displayed as dependent on the partial pressure of e.g. O_2, CO_2 or S_2 (Fig. 17). Furthermore there is the possibility to show the species distribution in 3-D models (Fig. 18). Such illustrations easily get confusing though.

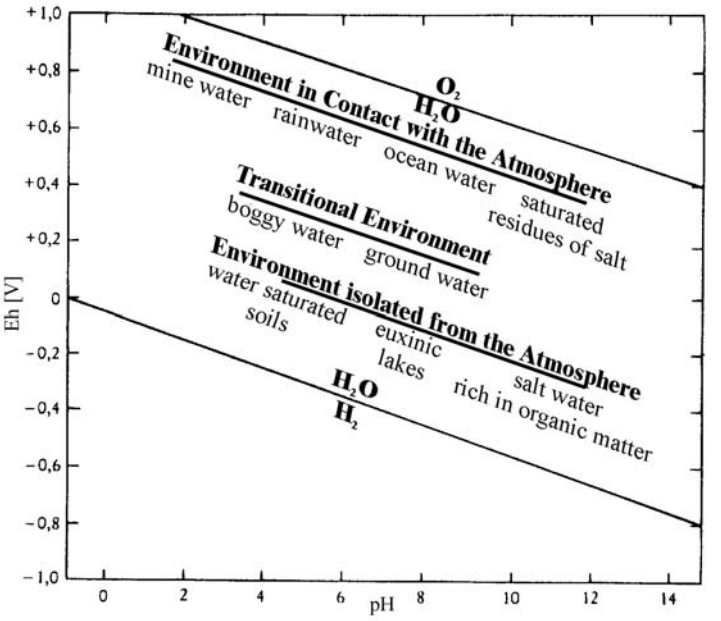

Fig. 16 Classification of natural waters under various E_H/pH conditions (modified after Wedepohl 1978)

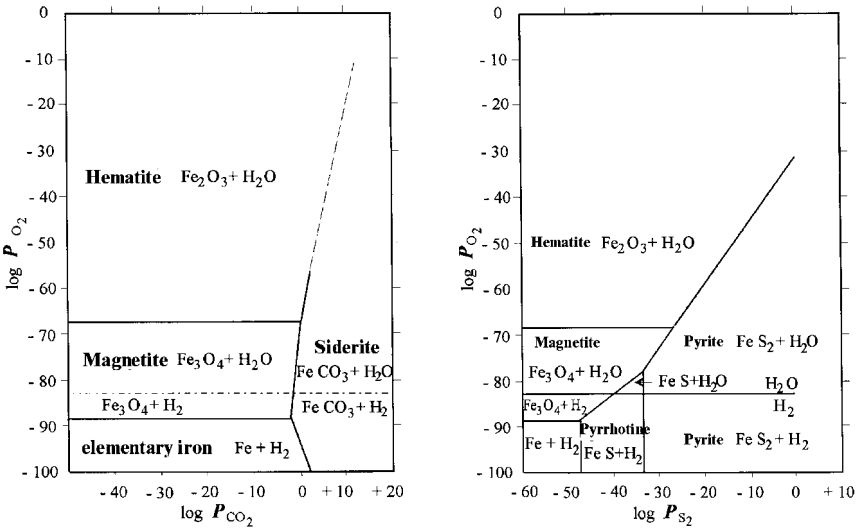

Fig. 17 Left: Fugacity diagram of some iron compounds as a function of $P(O_2)$ and $P(CO_2)$ at 25°C (modified after Garrels u. Christ 1965), Right: Fugacity diagram of some iron and sulfide compounds as a function of $P(O_2)$ and $P(S_2)$ at 25°C (modified after Garrels u. Christ 1965)

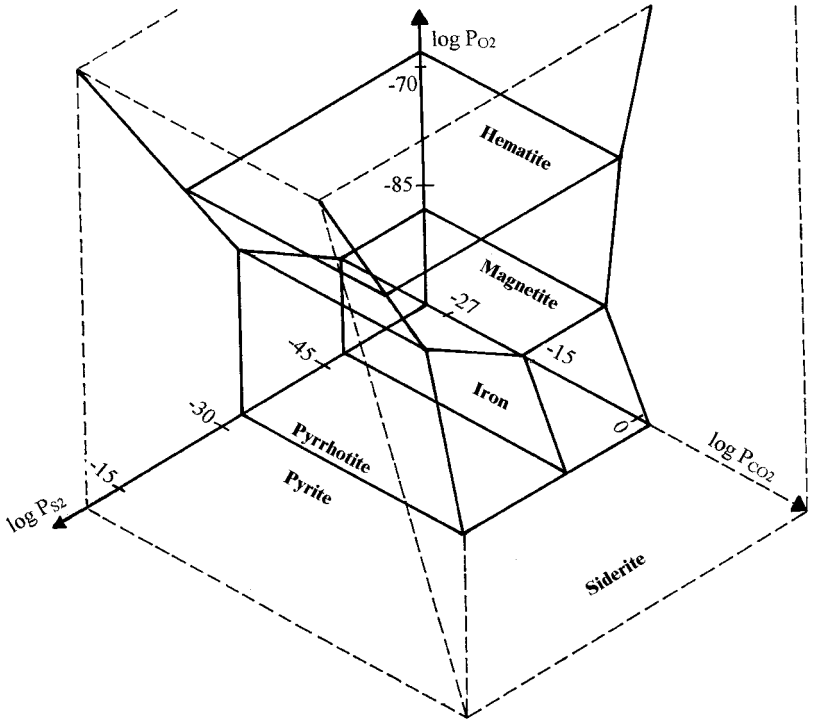

Fig. 18 3-D illustration of a fugacity diagram of some iron compounds as a function of $P(O_2)$, $P(CO_2)$ and $P(S_2)$ at 25°C and a total pressure of 1 atm or higher (modified after Garrels and Christ 1965)

1.1.5.2.4. Redox buffer

Analogous to acid-base-buffers, there are also buffers in the redox system, which can support strong variations of the pE value. Yet the redox equilibrium in ground water can be easily disturbed (Käss 1984). In Fig. 19 some redox buffers are depicted in a pE/pH diagram together with a rough division of ground waters into four ranges. Field 1 characterizes near-surface water with a short residence time, free oxygen, and no degradation processes. Most ground waters lie in the range of field 2 without free oxygen, but also without significant reduction of sulfate. Ground waters with long residence times, a high proportion of organic substances and high concentrations of sulfite plot into the range of field 3. Field 4 contains young mud and peat waters, where a fast degradation of organic material occurs under anaerobic conditions.

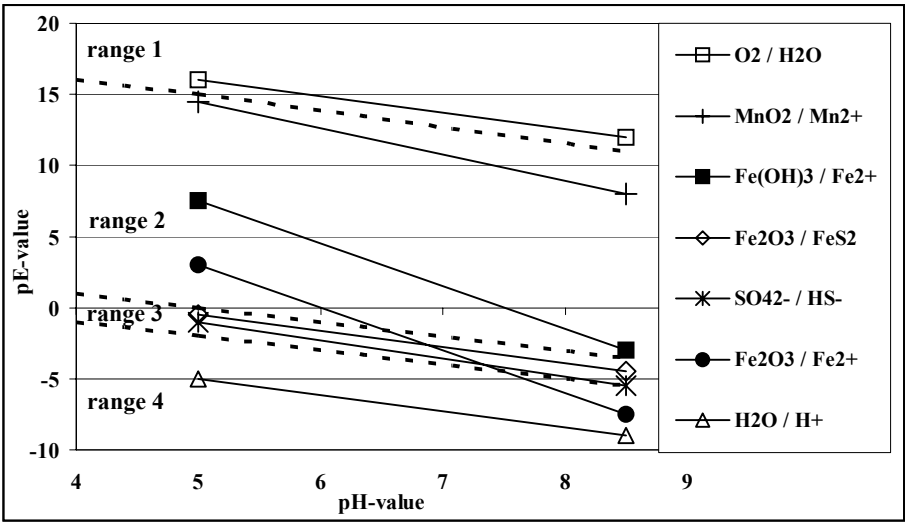

Fig. 19 Redox buffer and subdivision of natural ground waters into 4 redox ranges within the stability field of water; black dashed lines indicate the boundaries of the four redox ranges (after Drever 1997)

1.1.5.2.5. Significance of redox reactions

Oxidation and reduction processes play a major role both in the saturated zone as well as in the unsaturated zone. Within the unsaturated zone there is generally sufficient oxygen from the gas phase to guarantee high redox potentials (500 to 800 mV) in the water. Despite of that, reducing or partly reducing conditions might occur in small pore spaces (micro-milieus). In aquifers close to the surface oxidizing conditions usually prevail too. Thus low redox potentials in such aquifers can indicate anthropogenic contamination.

With increasing depth, even under natural geogenic conditions, oxygen contents and consequently the redox potential in groundwater decreases. Micro-organism, which use the oxygen for their metabolism are the reason for that. If the oxygen, dissolved in water, is used up, they can gain oxygen, respectively energy form the reduction of NO_3^- to N_2 (via NO_2^- and $N_2O(g)$), Fe^{3+} to Fe^{2+} or SO_4^{2-} to $H_2S(aq)$. The occurrence of organically bound carbon in the groundwater or in the aquifer is required for those reductions. Fig. 20 shows some microbially catalysed redox in dependence of pE/E_H conditions.

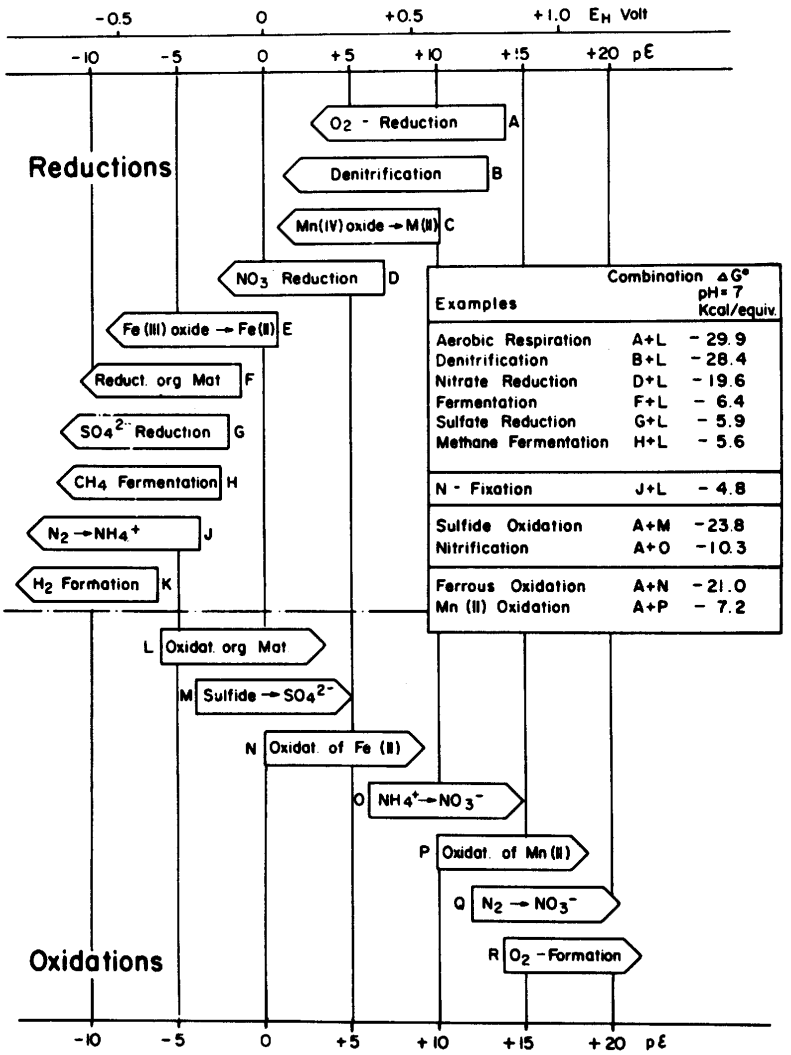

Fig. 20 Microbially catalyzed redox reactions in dependence on pE/E_H value (after Stumm and Morgan 1996)

Fig. 21 schematically shows the most significant hydrogeochemical processes in aqueous systems, and at the water-solid interface.

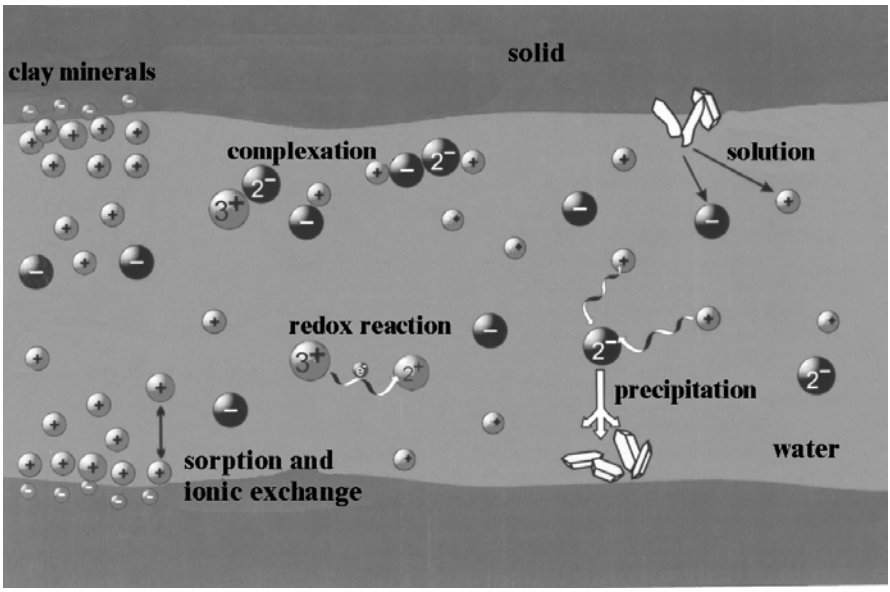

Fig. 21 Synopsis of the interaction processes in aqueous systems

1.2 Kinetics

For the reactions considered in the previous chapter the adjustment of the thermodynamic equilibrium, as the most stable time-independent form of a closed system, was always assumed. To what extent or in which time this equilibrium is reached can not be described by thermodynamic laws. Thus, slow reversible, irreversible or heterogeneous reactions actually require the consideration of kinetics, i.e. of the rate at which a reaction occurs or the equilibrium adjusts.

1.2.1 Kinetics of various chemical processes

1.2.1.1 Half-life

Fig. 22 shows the residence times t_R of waters in the hydrosphere and the half-life $t_{1/2}$ of various reactions. If $t_{1/2} \ll t_R$ then it can be assumed that the system is roughly in equilibrium and thermodynamic models can be used. If, on the other hand, $t_R \ll t_{1/2}$ kinetic models must be applied.

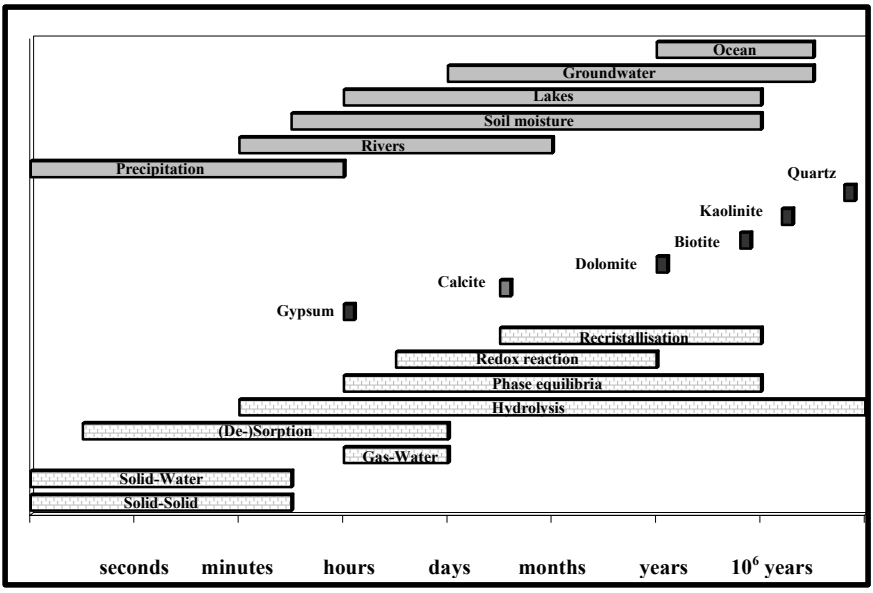

Fig. 22 Schematic comparison between the residence times t_R of waters in the hydrosphere (ocean to rainfall), the dissolution of various minerals in unsaturated solutions at pH 5 (quartz to gypsum) and the half-life $t_{1/2}$ of chemical processes (recristallization to solid-solid reactions) (data after Langmuir 1997, Drever 1997)

Acid-base reactions and complexation processes predominantly with low stability constants (solid-solid, solid-water-interface in Fig. 22) occur within micro- to milliseconds. Unspecific sorption with the formation of a disordered surface film is also a fast reaction, while the kinetics of specific sorption and mineral crystallization generally are considerably slower. For ion exchange the reaction rate depends on the type of binding and exchange. Those processes are the fastest where the exchange only occurs at the edges of mineral grains, as e.g. with kaolinite. Incorporation of ions in mineral sheets is much slower, e.g. into montmorillonite or vermiculite, or the intrusion into basal sheets, as for illite. Dissolution and precipitation processes (the range of phase equilibrium in Fig. 22) sometimes take only hours, but could also need several thousands of years. Redox reactions have long half-lifes in the range of years, especially when catalysts are lacking.

1.2.1.2 Kinetics of mineral dissolution

For interactions between solid and liquid phases, two cases have to be distinguished: weathering of rock-forming minerals and the weathering of trace minerals.

For the weathering of rock-forming minerals, the solution kinetics is determined by the solubility product and transport in the vicinity of the solid-water-interface. If the dissolution rate of a mineral is higher than the diffusive transport from the solid-water interface, saturation of the boundary layer and an exponential decrease with increasing distance from the boundary layer results. In the following text this kind of solution is referred to as solubility-product controlled. If the dissolution rate of the mineral is lower than diffusive transport, no saturation is attained. This process is called diffusion-controlled solution (Fig. 23 right).

In the experiment solubility-product controlled and diffusion-controlled solution can be distinguished by the fact that for diffusion controlled solution an increase in mixing leads to an increase in the reaction rate. Since this assumption is necessarily true the other way round, it is easier to calculate if the reaction proceeds faster or slower than the molecular diffusion. If it is faster, the reaction is controlled by the solubility product; if it is slower, it is diffusion controlled.

For the weathering of trace minerals from the solid matrix, the dissolution occurs selectively on spots where the mineral is exposed to the surface. These mineral surfaces are usually not smooth, but show dislocations (screw, jump, step dislocations) and point defects (vacant sites, interstitial sites) (Fig. 23 left). Dissolved ions are immediately transported from the surface into solution, so that no gradient can develop. Since the total concentrations of trace minerals in the solution are low, no equilibrium can be reached. In the following the dissolution of trace minerals is called surface-controlled.

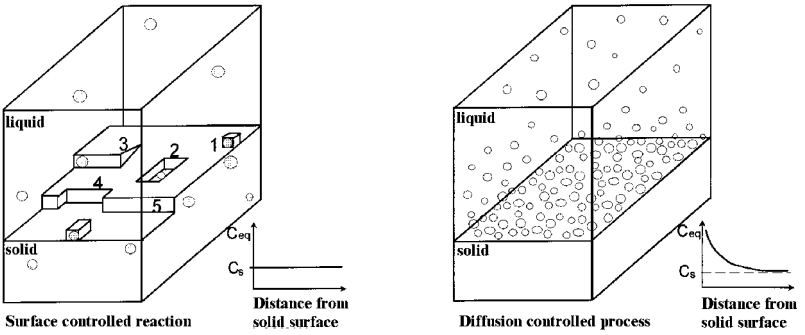

Fig. 23 Comparison between surface-controlled reactions (left; 1= interstitial sites, 2= vacant sites, 3= screw dislocation, 4= jump dislocation, 5=step dislocation) and diffusion-controlled processes (right)

1.2.2 Calculation of the reaction rate

The reaction rate can be determined by inverse geochemical modeling as increase of the products or decrease of the reactants along a flow path over time. In most cases the forward reaction (A + B $\rightarrow$ C) and the simultaneously proceeding reverse reaction (C $\rightarrow$ A + B) have different reaction rates. The total kinetics is the sum of both.

$$v^{+} = k^{+} \prod_{i} (X_i)^{n_i} \qquad \text{Eq. (72.)}$$

$$v^{-} = k^{-} \prod_{i} (X_i)^{n_i} \qquad \text{Eq. (73.)}$$

$$K_{eq} = \frac{k^{+}}{k^{-}} = \prod_{i} (X_i)^{n_i}_{eq} \qquad \text{Eq. (74.)}$$

with:
v^{+} = rate of the forward reaction
k^{+} = rate constant of the forward reaction
v^{-} = rate of the reverse reaction
k^{-} = rate constant of the reverse reaction
X = reactant or product
n = stoichiometric coefficient
K_{eq} = equilibrium constant

Table 14 Calculation of reaction rate, time law and half-life of a reaction in dependence of its order

	chemical reactions	reaction rate time law	half life time
0.order reaction		$v = -K_k$ $(A) = -K_k \cdot t + (A_0)$	$t_{1/2} = \frac{(A_0)}{2 \cdot K_k}$ dependent on concentration
1.order reaction	$A \rightarrow B$ $A \rightarrow B + C$	$\frac{d(A)}{dt} = -K_k \cdot (A)$ $(A) = (A_0) \cdot e^{-K_k \cdot t}$	$t_{1/2} = \frac{1}{K_k} \cdot \ln 2$ independent on concentration
2.order reaction	$A + A \rightarrow C + D$ $A + B \rightarrow C + D$	$\frac{d(A)}{dt} = -K_k \cdot (A) \cdot (B)$ $\frac{d(A)}{dt} = -K_k \cdot (A)^2$ $\frac{1}{(A)} = -K_k \cdot t + \frac{1}{A_0}$	$t_{1/2} = \frac{1}{(A_0) \cdot K_k}$ dependent on concentration
3.order reaction	$A + B + C \rightarrow D$	$\frac{d(A)}{dt} = -K_k \cdot (A) \cdot (B) \cdot (C)$	

Table 14 shows the calculation of the reaction rate, the time law, and the half-life depending on the reaction´s order. The order results from the sum of the exponents of the concentrations. The number does not necessarily have to be an integer. The half-life states in which time half of the reactants is converted into the products. Reaction rate constants k are 10^{12} to 10^{-11} L/s for first order reactions and 10^{10} to 10^{-11} L/(mol∗s) for second order reactions.

1.2.2.1 Subsequent reactions

Frequently chemical processes do not occur in one reaction but as a series of reactions.

$$A + B \xrightarrow{k_1} C \qquad A + B \xleftarrow{-k_1} C$$

$$C \xrightarrow{k_2} D \qquad C \xleftarrow{-k_2} D$$

Eq. (75.)

The equilibrium constant K_{12} is derived from the principle of the microscopic reversibility, i.e. at equilibrium every single and every reversible reaction occurs at the same rate.

$$K_{12} = \frac{\{D\}}{\{A\} \cdot \{B\}} = \frac{k_1 \cdot k_2}{(-k_1) \cdot (-k_2)} \qquad \text{Eq. (76.)}$$

For subsequent reactions the total reaction rate depends on the reaction with the lowest reaction rate.

1.2.2.2 Parallel reactions

For reactions that run independently of each other (parallel reactions) and result in the same product, the reaction with the fastest reaction rate determines the kinetics of the whole process.

$$A + B \xleftrightarrow{k_1} C + D \qquad \text{Eq. (77.)}$$

$$A \xleftrightarrow{k_2} C + E \qquad \text{Eq. (78.)}$$

$$A + F + G \xleftrightarrow{k_3} C + H \qquad \text{Eq. (79.)}$$

With $k_1 > k_2 > k_3$ the reaction of Eq. 77 dominates first. Another reaction can become predominant, when the boundary conditions change in the course of the reaction, as e.g. the pH value during calcite dissolution.

1.2.3 Controlling factors on the reaction rate

The reaction rate mainly depends on the concentration of reactants and products. According to the collision theory, frequent collisions and rapid conversions occur at high concentrations. Yet not all collisions cause conversions, a certain position of the molecules to each other as well as a certain threshold energy are required. Besides the concentration, pH, light, temperature, organics, presence of catalysts, and surface-active trace substances can have a significant influence on reaction rates.

The empirical Arrhenius equation describes the dependency of the reaction rate on the temperature

$$\ln k = \ln A - \frac{E_a}{R} \cdot \frac{1}{T} \qquad \text{Eq. (80.)}$$

with k= velocity constant
A = empiric constant
R = general gas constant (8.315 J/K mol)
T = temperature
E_a = activation energy

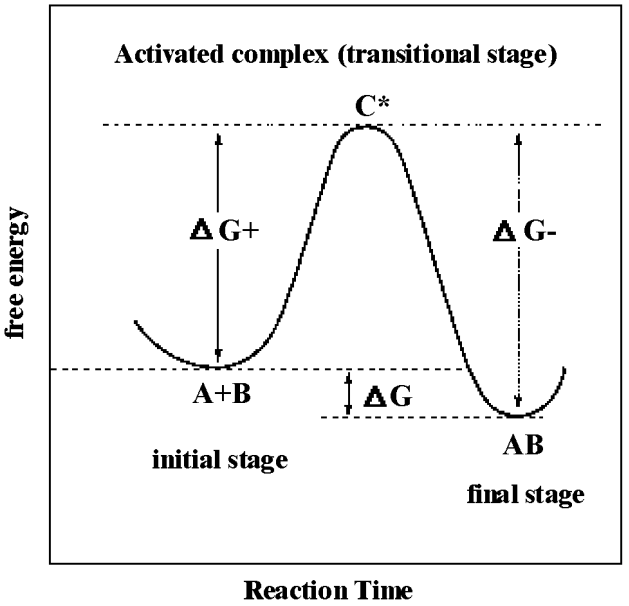

Fig. 24 Scheme of the free energies ΔG and formation of an activated complex C^* as a transitional state of the reaction A+B = AB (after Langmuir 1997)

The activation energy is the energy required for initiating a reaction. According to the theory of the transitional state an instable activated complex forms, which has a fairly high potential energy from the kinetic energy of the reactants and decays within a short period of time. Its energy is converted into the binding energy respectively the kinetic energy of the product (Fig. 24).

Table 15 shows typical values for the activation energy of some chemical processes.

Table 15 Activation energy of some chemical processes (after Langmuir 1997)

Reaction or process	range of typical E_a-values [kcal/mol]
Physical adsorption	2-6
Diffusion in solution	<5
Reactions in cells and organisms	5-20
Mineral solution and precipitation	8-36
Mineral solution via surface controlled reaction	10-20
Ion exchange	>20
Isotope exchange in solution	18 to 48
Solid phase diffusion in minerals at low temperatures	20 to 120

1.2.4 Empiric approaches for kinetically controlled reactions

A kinetically controlled reaction can be described by the equation:

$$\frac{m_i}{d_t} = c_{ik} \cdot k_k \qquad \text{Eq. (81.)}$$

with m_i/dt = converted mass (mol) per time (s)
c_{ik} = concentration of the species i
k_k = reaction rate (mol/kg/s)

The general kinetic reaction rate of minerals is:

$$R_K = r_K \cdot \left(\frac{A_0}{V}\right) \cdot \left(\frac{m_k}{m_{0k}}\right)^n \qquad \text{Eq. (82.)}$$

with r_k = specific reaction rate (mol/m^2/s)
A_0 = initial surface of the mineral (m^2)
V = mass of solution (kg water)
m_{0k} = initial mineral mass (mol)
m_k = mass of the mineral (mol) at a time t
$(m_k/m_{0k})^n$ is a factor, which takes into account the change in A_0 /V during the dissolution. For a steady dissolution from surfaces and cubes n is 2/3. Frequently not all parameters are available, so that simple approaches are useful like:

$$R_K = k_K \cdot (1 - SR)^{\sigma} \qquad \text{Eq. (83.)}$$

In Eq. 83 k_K is an empiric constant and SR is the saturation rate (ion activity product / solubility product). Frequently the exponent σ equals 1. The advantage of this simple equation is that it is valid both for supersaturation and undersaturation. With saturation R_K becomes zero. R_K can also be expressed by the saturation index [log (SR)] (Appelo et al. 1984):

$$R_K = k_K \cdot \sigma \cdot SI \qquad \text{Eq. (84.)}$$

Another example is the Monod equation, which contains a concentration dependent term:

$$R_k = r_{max}\left(\frac{C}{k_m + C}\right) \qquad \text{Eq. (85.)}$$

with r_{max} = maximum reaction rate
k_m = concentration, at which the rate is 50% of the maximum rate
The Monod rate is widely used for the simulation of the degradation of organic matter (van Cappellen & Wang 1996). It can be derived from the general equation for first order kinetics:

$$\frac{ds_C}{dt} = -k_1 s_C \qquad \text{Eq. (86.)}$$

with: s_C = organic carbon content [mol/kg soil]
k_1 = decay constant for first order kinetic reactions [1/s]

If for instance the degradation of organic carbon in an aquifer is considered, a first order degradation parameters ($k_1 = 0.025$ / a for 0.3 mM O_2 and $k_1 = 5 \cdot 10^{-4}$ / a for 3 µM O_2) can be described by the coefficients $r_{max} = 1.57 \cdot 10^{-9}$ / s and $K_m = 294$ µM in the Monod equation, oxygen being the limiting substance. A similar estimation can be done for nitrate as limiting substance: $k_1 = 5 \cdot 10^{-4}$ / a for 3 mM NO_3 and $k_1 = 1 \cdot 10^{-4}$ / a for 3 µM NO_3, which results in $r_{max} = 1.67 \cdot 10^{-11}$ / s and $K_m = 155$ µM. The corresponding Monod equation is as follows:

$$R_C = 6 \cdot s_C \cdot \left(\frac{s_C}{s_{C_0}} \right) \left\{ \frac{1.57 \cdot 10^{-9} m_{O_2}}{2.94 \cdot 10^{-4} + m_{O_2}} + \frac{1.67 \cdot 10^{-11} m_{NO_3^-}}{1.55 \cdot 10^{-4} + m_{NO_3^-}} \right\} \qquad \text{Eq. (87.)}$$

whereas the factor 6 arises, if the concentration s_C is converted from mol/kg soil to mol/ kg pore water. Plummer et al. (1978) found the following rates for the carbonate dissolution and precipitation:

$$r_{Calcite} = K_1 \cdot \{H^+\} + K_2 \{CO_2\} + K_3 \{H_2O\} - K_4 \{Ca^{2+}\} \{HCO_3^-\} \qquad \text{Eq. (88.)}$$

The constants K_1, K_2 and K_3 depend on the temperature and describe the forward reaction:

$$k_1 = 10^{(0.198 - 444.0 / T_K)} \qquad \text{Eq. (89.)}$$

$$k_2 = 10^{(2.84 - 2177.0 / T_K)} \qquad \text{Eq. (90.)}$$

if temperature ≤ 25°C

$$k_3 = 10^{(-5.86 - 317.0 / T_K)} \qquad \text{Eq. (91.)}$$

if temperature > 25°C

$$k_3 = 10^{(-1.1 - 1737.0 / T_K)} \qquad \text{Eq. (92.)}$$

K_4 describes the reverse reaction and can be replaced by the term

$$1 - \left(\frac{IAP}{K_{calcit}} \right)^{\frac{2}{3}} \qquad \text{Eq. (93.)}$$

where IAP is the ion activity product and $K_{calcite}$ is the calcite solubility product.

1.3 Reactive mass transport

1.3.1 Introduction

In the previous part of the book chemical interactions were described without any consideration of transport processes in aqueous systems. Models for reactive mass transport combine these chemical interactions with convective and dispersive transport, so that they can model the spatial distribution coupled to the chemical behavior. Requirement for every transport model is a flow model as accurate as possible.

1.3.2 Flow models

Flow models show potential or velocity fields resulting from the groundwater flow, unsaturated flow, or in the soil. These potential fields adequately describe the flow process together with further boundary conditions, such as pore volume, dispersivity, etc., in order to calculate the transport behavior (Table 16).

Table 16 Description of homogenous, laminar transport processes of a mass C in the saturated and unsaturated zone (without dispersion and diffusion)

	saturated zone	unsaturated zone / soil
effective head	hydraulic head (gravitational and pressure head)	matrix head (gravitational and capillary head)
Model equation	DARCY $\frac{\partial c}{\partial t} = K \frac{\partial h}{\partial l} \cdot \frac{c}{\partial z}$	RICHARDS $\frac{\partial c}{\partial t} = \left(K(P_k) \frac{\partial P_m}{\partial z} \right) \cdot \frac{c}{\partial z}$
Permeability K	Constant	function of matrix head P_m

1.3.3 Transport models

1.3.3.1 Definition

The description of transport is closely connected to the terms convection, diffusion dispersion, and retardation as well as decomposition. First, it is assumed that there are no interactions between the species dissolved in water and the solid phase, through which the water is flowing. Moreover, it is assumed that water is the only fluid phase. The multiphase flow water-air, water-organic phase (e.g. oil or DNAPL) or water-gas is not considered here.

Convection (also known as advection) is the vector, which results from the DARCY or the RICHARDS equations. It describes the flow velocity or the flow distance for a certain time t. In general convection has the major influence on

mass transport. Magnitude and direction of the convective transport are controlled by:

the disposition of the flow field
the distribution of the hydraulic permeabilities within the flow field
the disposition of the water table or the potentiometric surface
the occurrence of sources or sinks

Concentration gradients are leveled out by diffusion by means of molecular motion. The vector of diffusion is generally much smaller than the vector of convection in groundwater. With increasing flow velocity diffusion can be neglected. In sediments, in which the k_f value is very low, and consequently the convective proportion is very small or even converging towards zero (e.g. for clay), the diffusion could become the controlling factor of mass transport.

The third term in mass transport is dispersion. The dispersion describes the mass flow, which results from velocity variations due to the geometry and the structure of the rock system. From this definition it follows that the smaller the vector of convection the smaller the effect of dispersion. The other way round, an increasing effect of dispersion occurs with higher flow velocity. Consequently the mathematical description of the species distribution is an overlap of convection, diffusion, and dispersion.

All phenomena that cause species not to spread with the velocity of the water in soil or in groundwater are called retardation. Retardation is possible without any mass decrease. Frequently, though, retardation is combined with degradation. This "degradation" of the concentration of a species can occur by means of radioactive decay of a radionuclide or biological degradation of an organic substance. Also sorption and cation exchange can be included in this definition of "degradation", because the considered element is entirely or partially removed from the aqueous phase.

Fig. 25 shows a simplified illustration of the described phenomena for the one-dimensional case.

1.3.3.2 Idealized transport conditions

Within the groundwater transport including simple chemical reactions can be described by the following equation in a one-dimensional form:

$$\frac{\partial C_i}{\partial t} = \underbrace{D_l \frac{\partial^2 C_i}{\partial z^2} + D_t \frac{\partial^2 C_i}{\partial z^2}}_{\text{dispersion}} + \underbrace{D \frac{\partial^2 C_i}{\partial z^2}}_{\text{diffusion}} - \underbrace{v \frac{C_i}{\partial z}}_{\text{advection}} + \underbrace{C_{SS}}_{\text{sources/sinks}} \qquad \text{Eq. (94.)}$$

with C_i = concentration for the species i dissolved in water [mol/L]
t = time [s]
D_l = longitudinal dispersion coefficient [m^2/s]
D_t = transversal dispersion coefficient [m^2/s]
D = diffusion coefficient [m^2/s]
z = spatial coordinate [m]

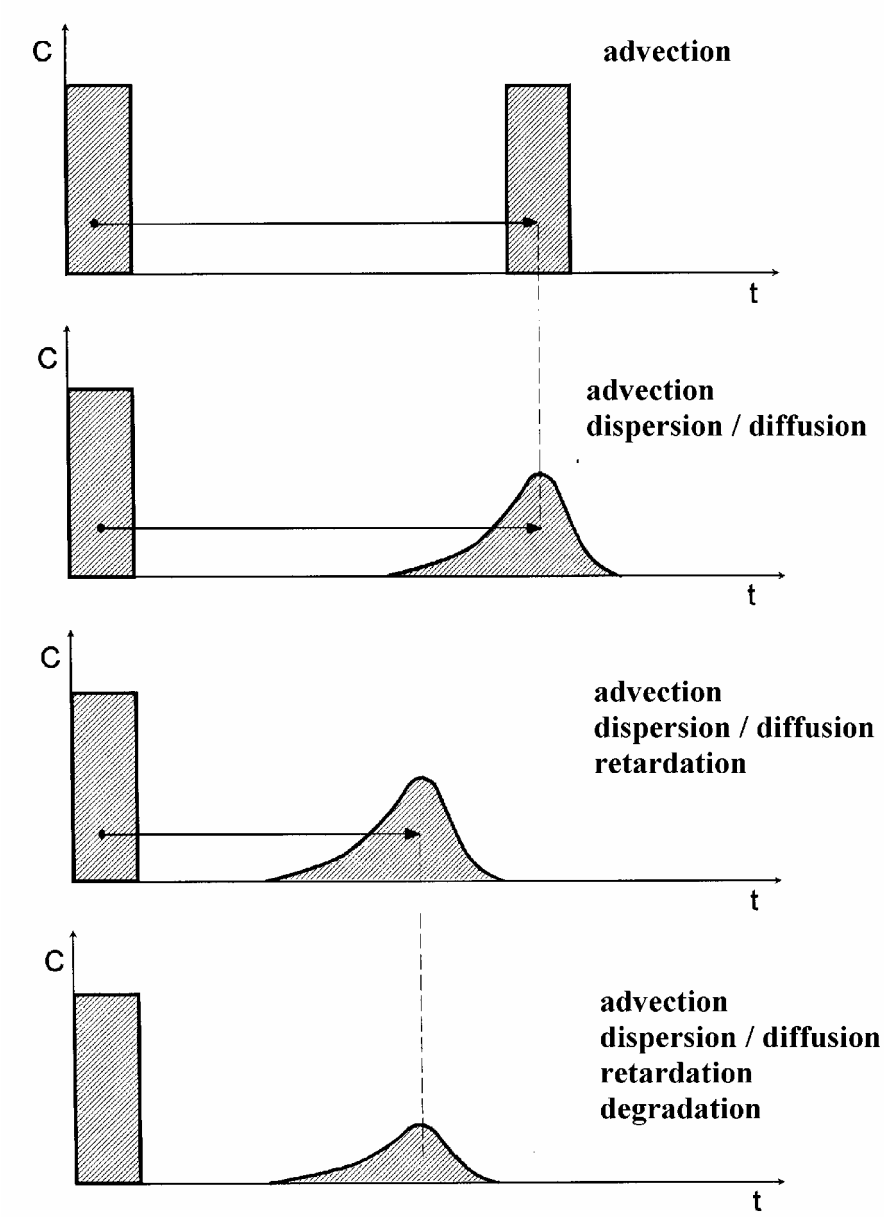

Fig. 25 Convection, dispersion / diffusion, retardation and degradation of a species (single peak input) versus time along a flow path

v = flow velocity [m/s]
C_{SS} = concentration of the species (source or sink)

Assuming some simplifications, analytical solutions for the transport equation may be inferred from arguments by analogy with the basic equations of heat conduction and diffusion (e.g. Lau et al. (1959), Sauty (1980), Kinzelbach (1983), and Kinzelbach (1987)).

1.3.3.3 Real transport conditions

Convection, diffusion, and dispersion can only describe part of the processes occurring during transport. Only the transport of species that do not react at all with the solid, liquid or gaseous phase (ideal tracers) can be described adequately by the simplified transport equation (Eq. 94). Tritium as well as chloride and bromide can be called ideal tracers in that sense. Their transport can be modeled by the general transport equation as long as no double-porosity aquifers are modeled. Almost all other species in water somehow react with other species or a solid phase. These reactions can be subdivided into the following groups, some of which have already been considered in the previous part of the book.

- Reactions between the aqueous and the gaseous phase (chapter 1.1.3)
- Dissolution and precipitation processes (chapter 1.1.4.1)
- Sorption and desorption of species in water on the solid phase (chapter 1.1.4.2)
- Anion and cation exchange (chapter 1.1.4.2.2)
- Formation of colloids
- Sorption on colloids
- Homogeneous reactions within the aqueous phase (chapter 1.1.5)

All chemical reactions comprise at least two species. For models of transport processes in groundwater or in the unsaturated zone reactions are frequently simplified by a basic sorption or desorption concept. Hereby, only one species is considered and its increase or decrease is calculated using a K_s or K_d value. The K_d value allows a transformation into a retardation factor that is introduced as a correction term into the general mass transport equation (chapter 1.1.4.2.3).

As already explained in chapter 1.1.4.2.3, the K_d concept must be rejected in most cases, because of its oversimplification and its low suitability for application to natural systems. For example, in degradation only the degrading substance is considered. This concept might be applicable for radioactive decay, yet if the decomposition of organic matter is considered, it is crucial to consider decomposition products (metabolites) that form and play an important role in transport themselves.

For the saturated and the unsaturated zone, the general mass transport equation can be extended as follows, describing exchange processes with the sediment as well as interactions with the gas phase, and within the aqueous phase.

$$\frac{1}{\partial t}\partial\left(C_i+\left(S_i\frac{d}{n}\right)+\frac{G_i}{n}\right)=D_l\frac{\partial^2 C_i}{\partial z^2}+D\frac{\partial^2 C_i}{\partial z^2}-v\frac{C_i}{\partial z} \qquad \text{Eq. (95.)}$$

with v = pore velocity [m/s]
C_i = concentration of the species i [mol/L]
S_i =concentration of the species i on/ in the solid phase [mol/g]
n = porosity
d = density [g/L]
G_i = concentration of the species i in the gas phase [mol/L]
D_l = longitudinal dispersion coefficient [m^2/s]
D = diffusion coefficient [m^2/s]
z = spatial coordinate [m]
t = time [s]

1.3.3.3.1. Exchange within double-porosity aquifers

Diffusive exchange between mobile and immobile water can be expressed mathematically as a mixing process between two zones: One zone containing stagnant water is coupled to a "mobile" zone, where water flows. The diffusive exchange can be described by first order kinetics.

$$\frac{\partial M_{im}}{\partial t}=\theta_{im}\cdot R_{im}\frac{\partial c_{im}}{\partial t}=\alpha(c_m - c_{im}) \qquad \text{Eq. (96.)}$$

The index "m" stands for mobile and "im" for immobile. M_{im} is the number of moles of a species in the immobile zone and R_{im} the retardation factor of the immobile zone, c_m and c_{im} are the concentrations in mol/kg in the mobile and immobile zone respectively. The symbol α stands for an exchange factor (1/s). The retardation factor R = 1+ (dq/dc) is determined by chemical reactions. The integrated form of Eq. 96 is:

$$c_{im}=\beta\cdot f\cdot c_{m0}+(1-\beta\cdot f)c_{im0}$$
$$\text{with}\quad \beta=\frac{R_m\theta_m}{R_m\theta_m+R_{im}\theta_{im}} \qquad \text{Eq. (97.)}$$
$$f=1-\exp\left(\frac{\alpha t}{\beta\theta_{im}R_{im}}\right)$$

with c_{m0} and c_{im0} being the initial concentrations, and θ_m and θ_{im} the saturated porosities of the mobile and immobile zones respectively. R_m is the retardation factor of the mobile zone. From these the mixing factor $mixf_{im}$ can be defined, which is a constant for a time t.

$$mixf_{in}=\beta\cdot f \qquad \text{Eq. (98.)}$$

If this factor is implemented into the Eq.97, the result is:

$$c_{im} = mixf_{im} \cdot c_{m0} + (1 - mixf_{im}) c_{im0} \qquad \text{Eq. (99.)}$$

Analogously, it follows for the mobile concentration:

$$c_m = (1 - mixf_m) c_{m0} + mixf_m \cdot C_{im0} \qquad \text{Eq. (100.)}$$

The exchange factor α is, according to van Genuchten (1985), dependent on the geometry of the stagnant zone. For a sphere, the relation is:

$$\alpha = \frac{D_e \theta_{im}}{(af_{s\to 1})^2} \qquad \text{Eq. (101.)}$$

with D_e = diffusion coefficient in the sphere (m^2/s)
a = radius of the sphere (m)
f_{s1} = shape factor (Table 17)

Alternatively, the problem can be solved numerically by applying a finite differences grid on the stagnant zone and determining the diffusive exchange iteratively (Parkhurst and Appelo, 1999; Appelo and Postma, 1994).

Table 17 Shape factors for the first order diffusive exchange between mobile and immobile water (Parkhurst & Appelo, 1999)

Shape of stagnant region	Dimensions (x,y,z) or 2 r,z	First-order equivalent $f_{s\to 1}$	Comments
Sphere	2a	0.21	2a = diameter
Plane sheet	2a, ∞, ∞	0.533	2a = thickness
Rectangular prism	2a, 2a, ∞	0.312	Rectangle
	2a,2a,16a	0.298	
	2a,2a,8a	0.285	
	2a,2a,6a	0.277	
	2a,2a,4a	0.261	
	2a,2a,3a	0.246	
	2a,2a,2a	0.22	Cube
	2a,2a,4a/3	0.187	
	2a,2a,a	0.162	
	2a,2a,2a/3	0.126	
	2a,2a,2a/4	0.103	
	2a,2a,2a/6	0.0748	
	2a,2a,2a/8	0.0586	
Solid cylinder	2a, ∞	0.302	2a = diameter
	2a,16a	0.298	
	2a,8a	0.277	
	2a,6a	0.27	
	2a,4a	0.255	
	2a,3a	0.241	
	2a,2a	0.216	

Shape of stagnant region	Dimensions (x,y,z) or 2 r,z	First-order equivalent $f_{s\rightarrow 1}$	Comments
	2a,4a/3	0.185	
	2a,a	0.161	
	2a,2a/3	0.126	
	2a,2a/4	0.103	
	2a,2a/6	0.0747	
	2a,2a/8	0.0585	
Pipe wall (surrounds the mobile pore)	$2r_i$,$2r_0$,		2 r_i = pore diameter
	2a,4a	0.657	2 r_0 = outer diameter of pipe
	2a,10a	0.838	wall thickness (r_0 - r_i) = a (Gl. 99)
	2a,20a	0.976	
	2a,40a	1.11	
	2a,100a	1.28	
	2a,200a	1.4	
	2a,400a	1.51	

1.3.3.4 Numerical methods of transport modeling

The numerical methods for solving the transport equation can be subdivided into two groups:

- Solution of the transport equation including the chemical reactions (one equation system for each species to be solved)
- Coupled methods (transport model coupled with hydrogeochemical code)

For coupled models solving the transport equation can be done by means of the finite-difference method (and finite volumes) and of the finite-elements method. Algorithms based on the principle of particle tracking (or random walk), as for instance the method of characteristics (MOC), have the advantage of not being prone to numerical dispersion (see 1.3.3.4.1).

1.3.3.4.1. Finite-difference / finite-element method

For the finite difference method the area is discretized by rectangular cells. The distance of neighboring nodes can differ. The nodes are usually set in the center of gravity of each cell and present the average concentration of the cells. The mass transport is simulated by modeling the chemical reactions for every node in discrete time intervals. Convective, diffusive, and dispersive mass transport is calculated along the four sides of each cell, e.g. by considering the weighted means of the concentrations of neighboring cells. The ratio between convective and dispersive mass flow is called Grid-Peclet number P_e (Eq. 102).

$$P_e = \frac{|v| \cdot L}{D} \qquad \text{Eq. (102.)}$$

with D= dispersivity
L= cell length

and $|v| = \sqrt{v_x^2 + v_y^2 + v_z^2}$ Eq. (103.)

Both the spatial discretisation and the choice of the type of differences (e.g. uplift differences, central differences) have a strong influence on the result. This fuzziness caused by the application of different methods is subsumed as "numeric dispersion".

Numeric dispersion can be eliminated largely by a high-resolution discretisation. The Grid-Peclet number helps for the definition of the cell size. Pinder and Gray (1977) recommend the P_e to be ≤ 2. The high resolution discretisation, however, leads to extremely long computing times. Additionally the stability of the numeric finite-differences method is influenced by the discretisation of time. The Courant number (Eq. 104) is a criterion, so that the transport of a particle is calculated within at least one time interval per cell.

$$Co = \left| v \frac{dt}{L} \right| < 1 \qquad \text{Eq. (104.)}$$

Methods applying reverse differences in time are called implicit. Generally these implicit methods, as e.g. the Crank-Nicholson method, show high numerical stability. On the other side, there are explicit methods, and the methods of iterative solution algorithms. Besides the strong attenuation (numeric dispersion) there is another problem with the finite differences method, and that is the oscillation.

With the finite-elements method the discretisation is more flexible, although, as with the finite-differences method, numeric dispersion and oscillation effects can occur (Fig. 26).

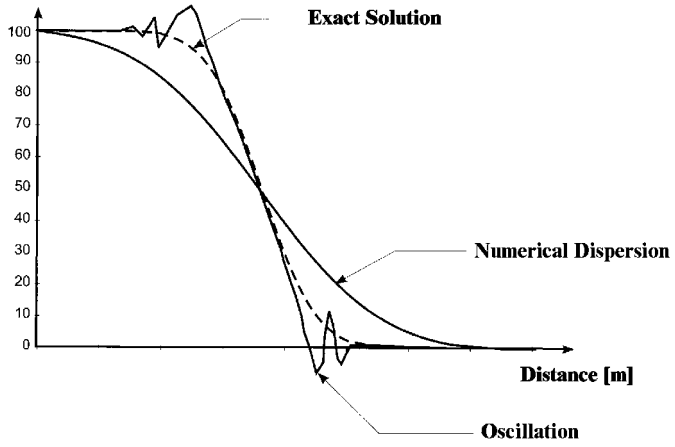

Fig. 26 Numeric dispersion and oscillation effects for the numeric solution of the transport equation (after Kovarik, 2000)

1.3.3.4.2. Coupled methods

In physics, the random walk method has already been in use for decades to understand and model diffusion processes. Prickett et al. (1981) developed a simple model for groundwater transport to calculate the migration of contamination. An essential advantage of the methods of random walk and particle tracking is that they are free of numeric dispersion and oszillations (Abbot 1966).

For the method of characteristics (MOC), the convective term is dealt with separately from the dipersive transport term by establishing a separate coordinate system along the convection vector for solving the dispersion problem. In most modeling programs, the convection is approximated with discrete particles. A certain number of particles with defined concentrations is used and moved along the velocity field (Konikoff and Bredehoeft, 1978).

Particularly sophisticated models deal with reactive mass transport, including both the accurate description of the convective and dispersive transport of species, as well as the modeling of interactions of species in water, with solid and gaseous phases (precipitation, dissolution, ion exchange, sorption).

Coupled reactive transport modeling does the flow modeling separately as first step. After that a modified method of characteristics (MMOC) is carried out based on the calculated flow field. The particles present a complete water analysis or a discrete water volume with certain chemical properties. These particles or water volumes are then moved for every single time step and using a hydrochemical modeling code (e.g. PHREEQC, MINTEQA2), the interactions of the particles with their environment (i.e. rock, gaseous phases), and with each other are calculated. The results of this thermodynamic modeling are subsequently transferred back to the particles before these are “moved” one time step further. Some examples for such models are TREAC, MINTRAN, and PHAST.

An extremely simplified application of the described approach is already implemented in the PHREEQC program. Reactive mass transport can be modeled for the one-dimensional case at constant flow rates considering diffusion and dispersion.

Taking into consideration a high possible number of chemical reactions for the reactive mass transport, like what is done for coupled models, the computing times mainly result from the calculations within the thermodynamic code. The 2d or 3d models easily lead to unreasonably long computing times. Since information on the chemical heterogeneity of an aquifer is frequently lacking, the calculation of a 1d model is generally preferable.

However, there is a severe disadvantage with one-dimensional models: they do not take into account the dilution due to the transversal dispersion. Consequently a mass M, that is not susceptible to any chemical reaction, occurs “blurred” at a point x downstream from x_0 (the location of M input) due to longitudinal dispersion. The dispersion leads to a smaller maximum concentration, however, and the mass integral equals the mass added at x_0. Thus, the impulse of mass remains constant along any simulated one-dimensional distance.

In reality, however, transversal dispersion D_t causes mass exchange in y and z direction leading to dilution. This dilution is a function of D_t and the flow velocity

v. If D_t and v are constant within the flow field, than the resulting dilution can by described by a linear function or a constant factor, respectively. The value for this factor can be determined using a conservative 3d model taking into account the aquifer thickness in particular. If, for instance in a conservative tracer model the contaminant concentration decreases by 50 percent along a certain distance through dispersion, it follows that, using a 1d model of reactive mass transport, half of the water within the column has to be substituted by uncontaminated groundwater.

2 Hydrogeochemical Modeling Programs

2.1 General

A selection of computer programs available is listed in Fig. 27 in chronological order. The first generation of geochemical computer programs was developed and published in the beginnings of the 1970's. New programs appeared at the end of the 1970's with improved features. From the early 1980's it became possible to install these programs on personal computers while mainframes had been the computer platforms until then.

The most frequently used models are MINTEQA2 (Allison et al. 1991),WATEQ4F (Ball & Nordstrom 1991), PHREEQC (PHREEQE) (Parkhurst & Appelo 1999, Parkhurst 1995 & Parkhurst et al. 1980) and EQ 3/6 (Wolery 1992a and 1992b).

2.1.1 Geochemical algorithms

The most common approach used by geochemical modeling codes to describe the water-gas-rock-interaction in aquatic systems is the ion dissociation theory outlined briefly in chapter 1.1.2.6.1. However, reliable results can only be expected up to ionic strengths between 0.5 and 1 mol/L. If the ionic strength is exceeding this level, the ion interaction theory (e.g. PITZER equations, chapter 1.1.2.6.2) may solve the problem and computer codes have to be based on this theory. The species distribution can be calculated from thermodynamic data sets using two different approaches (chapter 2.1.4):

- Determination of the thermodynamically most stable state by minimization of the free energies of reaction (lowest energy state) (e.g. CHEMSAGE) (chapter 2.1.2)
- Solving the non-linear set of equations resulting from equilibrium constants and mass balances in the system (e.g. PHREEQC, EQ 3/6, WATEQ4F, MINTEQA2 etc.) (chapter 2.1.3)

Both processes presuppose the establishment of chemical equilibrium and mass balance. Being in equilibrium, the interrelation between the equilibrium constant K and the free energy is defined as (see also chapter 1.1.2.2):

$$G_0 = -R \cdot T \cdot \ln K \qquad \text{Eq.(105.)}$$

or for T = 25 °C: $G_0 = -5.707 \cdot \ln K$ Eq.(106.)

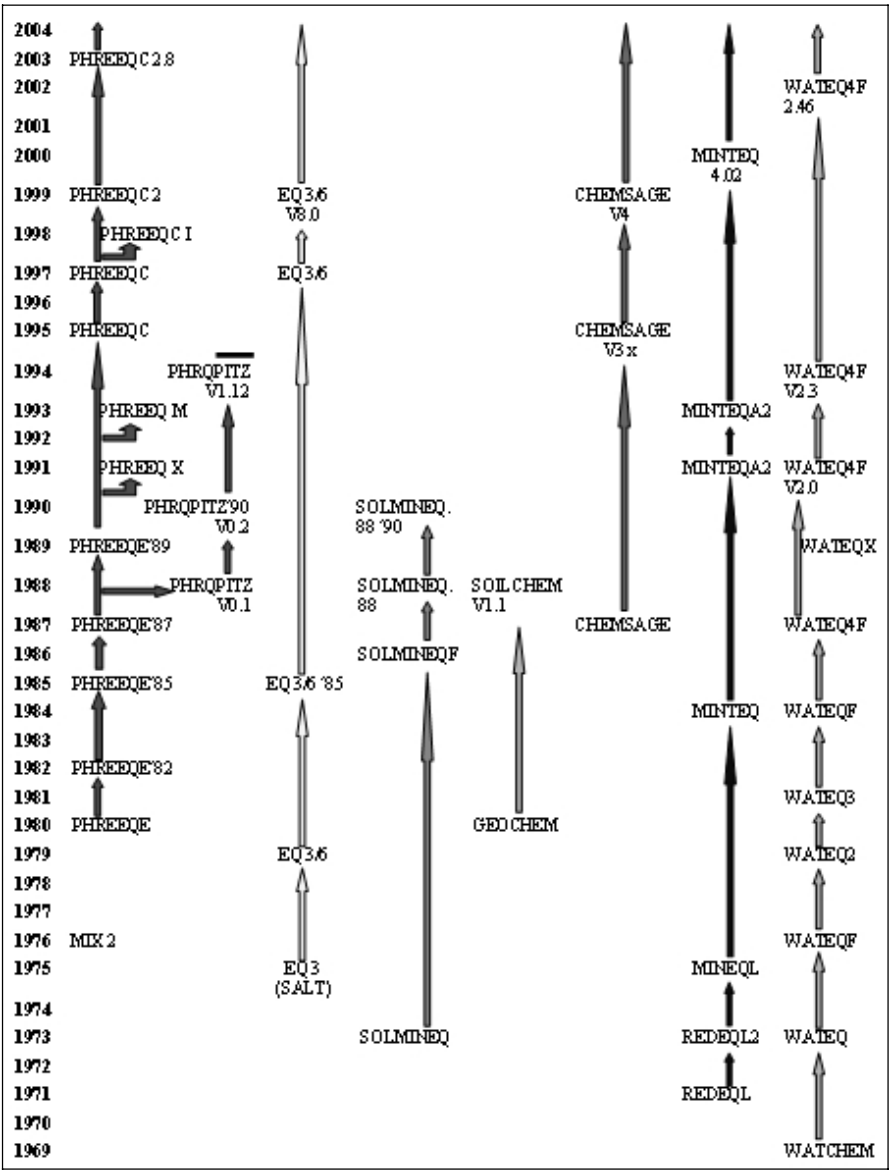

Fig. 27 Overview on hydro-geochemical modeling programs in chronological order

Table 18 gives an example for the calculation of an equilibrium constant from the free energy. Due to the relatively big error for the determination of the free energy, it is not advisable to perform such conversions unless unavoidable. Direct experimental determination of equilibrium constants is often more reliable.

Table 18 Example for the calculation of an equilibrium constant using the standard-free energy.

Species	G [K·J/mol]
Calcite	-1130.61
Ca^{2+}	-553.54
CO_3^{2-}	-527.90
$-G = G_{Calcite}-G_{Ca}-G_{CO3}$ $-G = -1130.61-(553.54)-(-527.90)$ $-G = -49.17$ $\log K_{Calcite} = -49.17 / 5.707 = -8.6157$ for comparison log K from the experiments (Plummer & Busenberg 1982) $\log K_{Calcite} = -8.48 \pm 0.02$	

If the solubility constant for a certain reaction is not explicitly given in a data set, but the solubility constants of partial reactions are known, the solubility constant of the total reaction can be calculated from the solubility constants of the partial reactions (see Table 19).

Table 19 Example for the calculation of the equilibrium constant of a reaction using the equilibrium constants of partial reactions

no equilibrium constant available for the following reaction: $CaCO_3 + CO_2 + H_2O = Ca^{2+} + 2HCO_3^-$	
$CaCO_3 = Ca^{2+} + CO_3^{2-}$	logK = -8.48
$CO_2 + H_2O = H_2CO_3$	logK = -1.47
$H_2CO_3 = H^+ + HCO_3^-$	log K = -6.35
$H^+ + CO_3^{2-} = HCO_3^-$	logK = +10.33
sum of single reactions: $CaCO_3 + CO_2 + H_2O + H_2CO_3 + H^+ + CO_3^{2-} = Ca^{2+} + CO_3^{2-} + H_2CO_3 + H^+ + HCO_3^- + HCO_3^-$ equals: $CaCO_3 + CO_2 + H_2O = Ca^{2+} + 2HCO_3^-$ Sum of logKs = -8.48 + (-1.47) + (-6.35) + 10.33 = **-5.97** (calculated log K for total reaction)	

2.1.2 Programs based on minimizing free energy

CHEMSAGE (ESM (Engineering and Materials Science) Software, http://www.esm-software.com/chemsage/) is a program family based on the minimization of the Gibbs' energy and distributed commercially.

As successor of SOLGASMIX (Besmann 1977), CHEMSAGE is mainly used for technical concerns, e.g. development of alloys, ceramics, semiconductors and superconductors, material processing, and investigation of material behavior.

Dynamic reactions like processes in blast furnaces, roasting processes or the solidification of liquid alloys can be simulated using the REACTOR MODEL

MODULE. Raw material and energy are input parameters. From this reactions in gaseous and condensed phases are simulated under different boundary conditions as well flux of material in different parts of the reactor.

According to the distributor, it is also possible to address geochemical problems, environmental pollution in soil, air and water, and impact of toxic, non-toxic and radioactive waste disposals with the implementation of several modules from the program SUPCRT 92 (Johnson et al. 1992).

However, only few applications in aquatic systems were found in literature. A reason for the rare use in the domains of hydro- and environmental science may also be the commercial marketing of both the program and the accompanying data sets.

2.1.3 Programs based on equilibrium constants

Computer codes used commonly by geo-scientists and environmental engineers are based on equilibrium constants. Frequently used programs are WATEQ4F, MINTEQA2, EQ 3/6 and PHREEQC. Data processing is very convenient in WATEQ4F using standard Excel files, however, limited to calculations of analytical error, speciation and saturation index (http://water.usgs.gov/software/wateq4f.html). Using MINTEQA2, it is possible to calculate the distribution of dissolved and adsorbed species (on solid phases) (http://www.scisoftware.com/products/minteqa2_overview/minteqa2_overview.html). The application spectrum of PHREEQC and EQ 3/6 is far greater. Therefore, these two programs are described in more detail. While PHREEQC is a public domain software (http://wwwbrr.cr.usgs.gov/projects/GWC_coupled/phreeqc/index.html), EQ 3/6 has to be purchased at the Lawrence Livermore National Laboratories (http://www.llnl.gov/IPandC/technology/software/softwaretitles/eq36.php).

2.1.3.1 PHREEQC

The program PHREEQC dates back to 1980 (Parkhurst et al. 1980), at that time written in FORTRAN and named PHREEQE. The option of the program comprised:

- the mixing of waters
- achieve equilibrium with an aquatic phase by dissolution-precipitation reactions
- modeling effects of changes in temperature
- calculation of element concentrations, molalities, activities of aquatic species, pH, pE, saturation index, mole transfer as function of reversible/irreversible reactions

In 1988, a version of PHREEQE was written including PITZER equations for ionic strengths greater 1 mol/L thus applicable for brines or highly concentrated electrolytic solutions (PHRQPITZ, Plummer et al. 1988). PHREEQM (Appelo & Postma 1994) included all options of PHREEQE and additionally a one-

dimensional transport module taking into account dispersion and diffusion. PHRKIN was an add-on module to PHREEQE to model kinetically controlled reactions.

In 1995 PHREEQC (Parkhurst 1995) was completely rewritten using the C programming language. This version removed nearly all limits regarding number of elements, aquatic species, solutions, phases, exchangers and surface complexes and caused the abolition of Fortran formats in the input files. Additionally, the equation solver was revised (more robust now) and several other options were added. With the 1995 version to the present, the following options have been possible:

- to enter the measured concentration of an element in different master species in the input data (e.g. N as NO_3, NO_2 and NH_4)
- to define the redox potential either with the measured E_H value (as pE value) or with a redox couple [e.g. As(III)/As(V) or U(IV)/U(VI)]
- to model surface-controlled reactions such as surface complexation and ion exchange by integrated double-layer models (Dzombak & Morel 1990) and a non-electrostatic model (Davis & Kent 1990)
- to model reactions with multicomponent gas phases as closed or open systems
- to administer the amounts of minerals in the solid phase and to determine automatically thermodynamically stable mineral associations
- to calculate the amount of water and the pE value in the aquatic phase during reaction and transport calculations using hydrogen-oxygen-mole equilibria and thus to model the water consumption or water production correctly
- to model convective mass transport with the help of a one-dimensional transport module
- to model the composition of a given water by inverse modeling based on one, or several, initial waters and chemical changes that occur as a water evolves along a flow

The most recent version, PHREEQC in the version 2 (Parkhurst & Appelo 1999), additionally allows for the following simulations:

- the formation of ideal and non-ideal solid solution minerals
- kinetic reactions with user-defined conversion rate
- dispersion and/or diffusion in 1-D transport and adding immobile cells as option to the mobile cells in a 1-D column
- change the number of exchanger places with dissolution or precipitation of reactants
- Inclusion of isotope balances in inverse modeling

Furthermore, it is possible to shorten the data output user-defined and to export it in a spreadsheet compatible data format. A BASIC interpreter program is implemented for programming user specific questions concerning kinetics and output formats. The BASIC interpreter also supports direct graphic output in

connection with the user interface "PHREEQC for Windows". Several revised versions were made available since 1999 and updates are still ongoing.

The following problems are still unsolved in PHREEQC Version 2 (with the Windows Interface 2.8.03, release April 13, 2004):

- uncertainties of thermodynamically constants are not taken into account
- the ion exchange model is based on the definition activity = equivalent fraction; more complex exchange models are not considered so far.
- the modeling of surface complexation corresponds to a first sensitivity analysis; three- or four-layer models are not taken into account
- simplified assumptions of a steady-state flow in a homogeneous medium with steady-state boundary conditions are made in the 1-D transport model.

2.1.3.2 EQ 3/6

EQ 3/6 is composed of two programs: EQ 3 is a pure speciation code whose results are processed for further questions within EQ 6.

In the version 7.2 of the program EQ 3/6, the modeling of solid-solution minerals using "end-member" and "site-mixing" models (chapter 1.1.4.1.3) had been already realized compared to the PHREEQC version from 1995. Table 20 represents the solid-solution minerals that are considered in Gemboch's data set of EQ 3/6. Using the concept of solid-solution minerals, surface complexation can be modeled as well.

Table 20 "Solid-solution" minerals of the Gembochs data set of the program EQ 3/6

Mineral name	Formularies
Biotite	$K(Mg,Fe)_3AlSi_3O_{10}(OH)_2$
Carbonate-Calcite	$(Ca,Mn,Zn,Mg,Fe,Sr)CO_3$
Chlorite-ss	$(Fe,Mg)_5Al_2Si_3O_{10}(OH)_8$
Clinoptilolite-hy-ss	$(Na,K,Cs,NH_4,Ca_{.5},Sr_{.5})_{3.467}Al_{3.45}(Fe^{3+})_{0.017}Si$
Clinoptilolite-ss	$(Na,K,Cs,NH_4,Ca_{.5},Sr_{.5})_{3.467}Al_{3.45}(Fe^{3+})_{0.01}7Si$
Epidote-ss	$Ca_2(Fe,Al)Al_2Si_3O_{12}(OH)$
Garnet-ss	$Ca_3(Al,Fe)_2Si_3O_{12}$
Olivine	$(Fe,Mg)_2SiO_4$
Orthopyroxene	$(Fe,Mg)SiO_3$
Plagioclase	$CaAl_2Si_2O_8$-$NaAlSi_3O_8$
Sanidine-ss	$(K,Na)AlSi_3O_8$
Saponite-tri	$(Ca_{.5},H,K,Mg_{.5},Na)_{.33}Mg_3Al_{.33}Si_{3.67}O_{10}(OH)_2$
Smectite-di	$(Na,K,Ca_{.5},Mg_{.5})_{.33}(Al,Mg,Fe)_2(Si,Al)_4O_{10}(OH)_2$

Furthermore, compared to the PHREEQC version from 1995, it was already possible to model kinetically controlled reactions with EQ 3/6. An advantage of EQ 3/6 over the recent PHREEQC version is that it can use both the ion dissociation theory and the PITZER equations for solutions with higher ionic strengths.

2.1.3.3 Comparison PHREEQC – EQ 3/6

In comparison with the PHREEQC version from 1995, EQ 3/6 offered the above-mentioned possibilities for considerations of solid-solution minerals and kinetically controlled reactions. Both are found now in the PHREEQC version from 1999 and the use of EQ 3/6 holds hardly any more advantages with the exception of the modeling of solutions with high ionic strengths, where the application of the PITZER equations is required. As a matter of fact, the complex data format of both the thermodynamic constants and the input files in EQ 3/6 have to be regarded as disadvantage. Moreover, the advantage of the PHREEQC data format is that the reaction equations are written in the syntax of chemical formulas. This aspect is demonstrated with the example of the mineral rutherfordine (UO_2CO_3) (Fig. 28 and Fig. 29).

```
Rutherfordine                606
UO2CO3 = UO2+2 + CO3-2
log_k     -14.450
delta_h    -1.440 kcal
```

Fig. 28 Excerpt from the WATEQ4F database for PHREEQC; definition of the mineral rutherfordine

```
   UO2CO3
     date last revised =  02-jul-1993
   keys   = solid
      V0PrTr =   0.000 cm**3/mol (source =
  *     mwt    =   330.03690 g/mol
      3 chemical elements =
       1.0000 C          5.0000 O      1.0000 U
      4 species in data0 reaction
     -1.0000  UO2CO3             -1.0000  H+
      1.0000  HCO3-               1.0000  UO2++

  *    log k grid (0-25-60-100/150-200-250-300 C) =
         -3.8431   -4.1434   -4.4954   -4.7855
         -5.0616   -5.2771  500.0000  500.0000
  * Extrapolation algorithm: constant enthalpy approxi-
mation
```

Fig. 29 Excerpt from the NEA data set for EQ 3/6; definition of the mineral rutherfordine (elements which exist in a similar form in the PHREEQC data set are boldly marked; the different log_k values are due to different reaction equations (also compare to chapter 2.1.5))

A comparison of Fig. 28 and Fig. 29 shows how complicated the declaration of a mineral phase in EQ 3/6 is. Moreover, there is the problem that FORTRAN data

formats are used in EQ 3/6. Errors in the format (placement within a row) can easily lead to fatal errors.

Next, it will be shown how a simple input file looks like with PHREEQC and EQ 3/6 (Fig. 30 and Fig. 31) simulating the dissolution of the mineral rutherfordine in a water with 1 mmol/L sodium-chloride and low sulfate concentrations (0.0001 mmol/L) under oxidizing conditions (pE = 14) at 25 °C and at a CO_2 partial pressure of 0.033 kPa (atmospheric concentration).

```
TITLE   solution Rutherfordine as function of CO2 partial pressure

SOLUTION 1      water with 1 mmol/L Na and Cl
units           mmol/kgw
temp            25
pH      7
pe      14
Na      1
S(6)    1E-7
Cl      1

EQUILIBRIUM_PHASES 1
CO2(g)  -3.481
Rutherfordine           0

END
```

Fig. 30 Example for a PHREEQC input file (dissolution of the mineral rutherfordine as a function of the CO_2 partial pressure)

Here too, it is clearly visible that the definition of a problem is much more easily and quickly done with PHREEQC. A Windows user interface for PHREEQC, freely available by internet (http://www.geo.vu.nl/users/posv/phreeqc.html), simplifies the input even more.

Overall, it seems that PHREEQC, except for the problems with high ionic strengths that require the application of PITZER equations, is the optimal program for the solution of both simple and more complex exercises and for one-dimensional transport modeling with regard to user-friendliness, numerical stability, compactness and clarity of the data format as well as flexibility. It will be used for the solution of the exercises in chapter 3. The utilization of PHREEQC is presented in detail in chapter 2.2.

```
   EQ3NR input file name= co3aqui.3i
    Description= "Uranium Carbonate solution"
    Version level= 7.2

    endit.
       Tempc=  2.50000E+01
           rho=   1.00000E+00     tdspkg=   0.00000E+00
tdspl=  0.00000E+00
         fep=  0.00000E+00    uredox=
      tolbt=  0.00000E+00    toldl=  0.00000E+00   tol-
sat=  0.00000E+00
      itermx=  0
  *            1   2   3   4   5   6   7   8   9  10
    iopt1-10=    0   0   0   0   0   0   0   0   0   0
    iopg1-10=    0   0   0   0   0   0   0   0   0   0
    iopr1-10=    0   0   0   0   0   0   0   0   0   0
    iopr11-20=    0   0   0   0   0   0   0   0   0   0
    iodb1-10=    0   0   0   0   0   0   0   0   0   0
       uebal= H+
       nxmod=  0
    data file master species= Na+
     switch with species=
     jflag=  0   csp=  1.00000E-03
    data file master species= UO2++
     switch with species=
     jflag= 19   csp=       0.
     Mineral= UO2CO3
    data file master species= HCO3-
     switch with species=
     jflag= 21   csp=  -3.481
       gas= CO2(g)
    data file master species= SO4--
     switch with species=
     jflag=  0   csp=  1.00000E-10
    data file master species= Cl-
     switch with species=
```

Fig. 31 Example for an EQ 3/6 input file (dissolution of the mineral rutherfordine as a function of the CO_2 partial pressure)

2.1.4 Thermodynamic data sets

2.1.4.1 General

Thermodynamic databases are the primarily source of information of all geochemical modeling programs. Basically, it is possible to create one's own thermodynamic dataset with almost any program. However, it is a considerable effort and requires great care. Normally one accesses already existing data sets.

Table 21 shows a variety of thermodynamic data collections and the elements considered. The thermodynamic data are usually not available in a current database format (exception: CHEMVAL 6 as dBASE file) but in a form which is needed for the specific program. To use thermodynamic data in PHREEQC which are applicable e.g. for EQ 3/6 or PHREEQC, they have to be converted into the respective format (e.g. PHREEQC) using a transfer program.

With the help of appropriate filters it is also possible to create a partial data set out of the standard data set. Especially when a huge number of analyses have to be calculated - as with a coupled model (transport plus reaction) - CPU-time can be saved with a reduced data set. However, it must be verified that the partial data set yields comparable results to the original data set.

Table 21 Thermodynamic data sets with elements considered

Database	NEA	PHREEQC	WATEQ4F [1]	CHEM-VAL6	HATCHES	NAGRA / PSI TDB	MINEQL [2]	MINTEQA2 [3]	LLNL.dat [4]
Last update	1999	2003	2003	1999	1999	2002	2003	2003	2003
Ag	+		+				+	+	+
Al	+	+	+	+	+	+	+	+	+
Am	+			+	+	+			+
Ar									+
As	+		+	+	+	+	+	+	+
Au							+		+
B	+	+	+	+	+	+	+	+	+
Ba	+	+	+	+	+	+	+	+	+
Be							+	+	+
Br	+	+	+	+	+	+	+	+	+
C	+	+	+	+	+	+	+	+	+
Ca	+	+	+	+	+	+	+	+	+
Cd	+	+	+	+			+	+	+
Ce							+		+

Database	NEA	PHREEQC	WATEQ4F [1]	CHEM-VAL6	HATCHES	NAGRA / PSI TDB	MINEQL [2]	MINTEQA2 [3]	LLNL.dat [4]
Last update	1999	2003	2003	1999	1999	2002	2003	2003	2003
N	+	+	+	+	+	+	+	+	+
Na	+	+	+	+	+	+	+	+	+
Nb						+			
Nd				+					+
Ne									+
Ni			+	+	+	+	+	+	+
Np				+	+	+			+
O	+	+	+	+	+	+	+	+	+
P	+	+	+	+	+	+	+	+	+
Pa				+					
Pb	+	+	+	+				+	+
Pd					+	+			+
Pm				+					+
Pr				+					+

Database	NEA	PHREEQC	WATEQ4F [1]	CHEM-VAL6	HATCHES	NAGRA / PSI TDB	MINEQL [2]	MINTEQA2 [3]	LLNL.dat [4]
Cl	+	+	+	+	+	+	+	+	+
Cm				+					
Co							+		+
Cr							+	+	+
Cs	+		+	+		+	+		+
Cu	+	+	+	+			+	+	+
Dy									+
Er									+
Eu						+			+
F	+	+	+	+	+	+	+	+	+
Fe	+	+	+	+	+	+	+	+	+
Ga									+
Gd									+
H	+	+	+	+	+	+	+	+	+
Hf									+
He									+
Hg	+						+	+	+
Ho									+
I	+		+	+	+	+	+	+	+
In									+
K	+	+	+	+	+	+	+	+	+
Kr									+
La							+		+
Li	+	+	+	+	+	+	+	+	+
Lu									+
Mg	+	+	+	+	+	+	+	+	+
Mn		+	+	+	+	+	+	+	+
Mo					+	+	+		+

Database	NEA	PHREEQC	WATEQ4F [1]	CHEM-VAL6	HATCHES	NAGRA / PSI TDB	MINEQL [2]	MINTEQA2 [3]	LLNL.dat [4]
Pu				+	+	+			+
Ra				+		+			+
Rb	+		+				+	+	+
Re									+
Rn									+
Ru									+
S	+	+	+	+	+	+	+	+	+
Sb							+	+	+
Sc							+		+
Se	+		+		+	+	+	+	+
Si	+	+	+	+	+	+	+	+	+
Sm				+					+
Sn	+				+	+	+		+
Sr	+	+	+	+	+	+	+	+	+
Tb				+					+
Tc				+	+	+			+
Th				+	+	+	+		+
Ti							+		+
Tl							+	+	+
Tm				+					+
U	+		+	+	+	+	+	+	+
V							+	+	+
W							+		+
Xe									+
Y									+
Yb				+					+
Zn	+	+	+				+	+	+
Zr					+	+			+

[1] additionally considered in WATEQ4F.dat: fulvate and humate

[2] addtionally considered in MINEQL.dat: acetate, butanole, citrate, DCTA, DIP, diethane, dimethane, EDTA, formate, fulvate, hexane, humate, isopropane, isobutyl, methane, n-propane, NTA, phthalate, propanole, salicyle, tartrate, trimethane, TRIS, valerate, glutamate, glycine

[3] additionally considered in MINTEQ.dat: cyanide, cyanate, benzoate, para-acetate, isophthalate, diethylamine, n-butylamine, methylamine, dimethylamine, tributylphosphate, hexylamine, ethylenediamine, n-propylamine, isopropylamine, trimethylamine, citrate, NTA, EDTA, propanoate, butanoate, isobutyrate, 2-methylpyridine, trimethylpyridine, 4-methylpyridine, formate, isovalerate, valerate, acetate, tartrate, glycine, salicylate, glutamate, phthalate

[4] additionally considered in LLNL.dat: acetate, ethylene, orthophthalate

2.1.4.2 Structure of thermodynamic data sets

A thermodynamic geochemical data set is divided into several blocks with different variables. If it is defined as relational database, several tables (relations) with different variables are necessary. However, many programs (among them PHREEQC and EQ 3/6) read the data from a plain ASCII file that is separated in logical blocks by keywords. Each logical block has a different syntax for reading and interpreting data. In PHREEQC, there are the following blocks:

- master species in solution (Table 22) (SOLUTION_MASTER_SPECIES)
- species in solution (Table 23) (SOLUTION_SPECIES)
- phases: solid phases and gas phases (PHASES)
- exchange of master species (EXCHANGE_MASTER_SPECIES)
- exchange of species (EXCHANGE_SPECIES)
- surface master species (SURFACE_MASTER_SPECIES)
- surface species (strong and week binding species, sorted by cations and anions) (SURFACE_SPECIES)
- reaction rates (RATES)

Table 22 Example for the declaration of master species in solution (SOLUTION_MASTER_SPECIES) from the PHREEQC data set WATEQ4F.dat

Element	Master species	Alkalinity	mole mass in mg/L	atomic mass of elements
C	CO3-2	2.0	61.0173	12.0111
H	H+	-1.0	1.008	1.008
Fe	Fe+2	0.0	55.847	55.847
Fe(+3)	Fe+3	-2.0	55.847	
N	NO3-	0.0	14.0067	14.0067
N(-3)	NH4+	0.0	14.0067	
N(0)	N2	0.0	14.0067	
N(+3)	NO2-	0.0	14.0067	
N(+5)	NO3-	0.0	14.0067	
P	PO4-3	2.0	30.9738	30.9738
S	SO4-2	0.0	96.0616	32.064
Si	H4SiO4	0.0	60.0843	28.0843

The contribution of each master species to the alkalinity in Table 22 is calculated according to the predominant species at a pH of 4.5. For example, Fe^{3+} forms at pH 4.5 the predominant species $Fe(OH)_2^+$ with two OH^--ions that are able to bind two H^+-ions. Therefore a factor of -2 results for the alkalinity. For inorganic C with the dominant species H_2CO_3 and two H^+-ions the factor will be +2.

Column 4 in Table 22 specifies in which way the input in mg/L has to be done. In this example, C has to be defined as carbonate, however, nitrate, nitrite, ammonia each defined as elementary nitrogen, P as elementary phosphorous, S as sulfate and Si as SiO_2. If, for example, P is input as phosphate in mg/L, all

subsequent calculations would be wrong. A thorough study of the respective data sets is thus absolutely necessary with each input. These problems can be avoided by declaring all concentrations in mol/L.

For all reactions being put in data sets manually, the used master species, if not yet existent, have to be defined using the keyword SOLUTION_MASTER_SPECIES.

Table 23 Example of declaration of species in solution (SOLUTION_SPECIES) from WATEQ4F.dat

```
CO3-2 primary master species
      CO3-2 = CO3-2
      log_k      0.0
     -gamma    5.4     0.0
CaCO3                          78
     Ca+2  +  CO3-2  =  CaCO3
     log_k       3.224
     delta_h     3.545 kcal
     -analytical -1228.732     -0.299444     35512.75     485.818       0.0
S2-2                           502
     HS-  =  S2-2  +  H+
     log_k       -14.528
     delta_h      11.4kcal
     -no_check
     -mole_balance   S(-2)2
     -gamma      6.5     0.0
```

For the species in solution (SOLUTION_SPECIES, Table 23), listed in the top row with current number, solubility constant log k and enthalpy delta h are given in kcal/mol or kJ/mol at a temperature of 25 °C. Using the sub-key-word “gamma” parameters for the calculation of the activity coefficient γ according the WATEQ-DEBYE-HÜCKEL ion dissociation theory (compare to chapter 1.1.2.6.1) are given. With the sub-key-word “analytical”, coefficients A_1 to A_5 are defined to calculate the temperature dependence of the solubility-product constant.

Reaction equilibrium, which should not be used to compensate charge balances, has to be marked with “no check”. If the stoichiometry of a species has to be defined explicitly, like the polysulphide species (see Table 23, S_2^{2-} contains 2 S atoms, but only one will be used for the combination of HS^-), the declarations have to be made under “mole balance”.

The specification of reactions with solid or gaseous phases (PHASES) is done similarly to one of the species in solution. While looking for equilibrium constants it is important to look under the correct keywords. The equilibrium constant of the reaction $CaCO_3 = Ca^{2+} + CO_3^{2-}$ describing the dissolution of the mineral calcite (log K = -8.48, under the keyword PHASES) differs totally from the equilibrium constant of the reaction $Ca^{2+} + CO_3^{2-} = CaCO_3^0$ describing the formation of the aquatic complex $CaCO_3^0$ (log K = 3.224 under the keyword SOLUTION_SPECIES) even though the reactions may look alike at a first glance.

EXCHANGE_MASTER_SPECIES defines the interrelation between the name of an exchanger and its master species. Based on this, EXCHANGE SPECIES describes a half-reaction and requires a selectivity coefficient for each exchanger species. In contrast to stability constants or dissociation constants, these selectivity coefficients are dependent on the respective solid phase with the specific features of their inner and outer surfaces (see also chapter 1.1.4.2). Therefore, within thermodynamically data collections they are only to be seen as placeholders that have to be changed according to site specific exchange constants.

SURFACE_MASTER_SPECIES defines analogously the interrelation between the name of surface binding sites and the surface master species, whereas SURFACE_SPECIES describes reactions for any surface species sorted by cations and anions as well as by strongly and weakly bound partners.

Following the keyword RATES, reactions rates and mathematical equations are listed from different references to describe the kinetics of K-feldspar, albite, calcite, pyrite, organic carbon, and pyrolusite reactions. Again, these entries have to be seen as examples that often have to be replaced or adjusted by site-specific data.

2.1.5 Problems and sources of error in geochemical modeling

Hydrochemical analyses should be as complete and correct as possible because they are the basic prerequisite of a reliable hydrogeochemical model. They represent the essential information and errors propagate from them to the final result. Fig. 32 to Fig. 34 show an example of the saturation index calculation for calcite and dolomite, of the CO_2 equilibrium partial pressure, and of the consequences an incomplete analysis may have. The following analysis is given (pH = 7.4, temp. = 8.1°C, conductivity = 418 µS/cm, concentrations in mg/L):

Ca^{2+}	74.85	Cl^-	2.18	Fe^{2+}	0.042	Mn^{2+}	0.014
Mg^{2+}	13.1	HCO_3^-	295.0	Pb^{2+}	0.0028	Zn^{2+}	0.379
Na^+	1.88	SO_4^{2-}	2.89	Cd^{2+}	0.0026	SiO_2	0.026
K^+	2.92	NO_3^-	3.87	Cu^{2+}	0.030	DOC	8.8255

Assumptions made in hydrogeochemical modeling programs complicate the transferability to natural systems, e.g. assuming thermodynamic equilibrium. This assumption is often not true especially for redox reactions being dominated by kinetics and catalyzed by microorganisms, and precipitation of certain minerals. Both processes can maintain disequilibria over a long time period.

Numerical dispersion or oscillation effects can occur as accidental source of error when using finite differences and finite element methods while modeling mass transport. Utilizing the criteria of numerical stability (Grid-Peclet number or Courant number) or the random walk procedure, these errors can be either reduced or even eliminated.

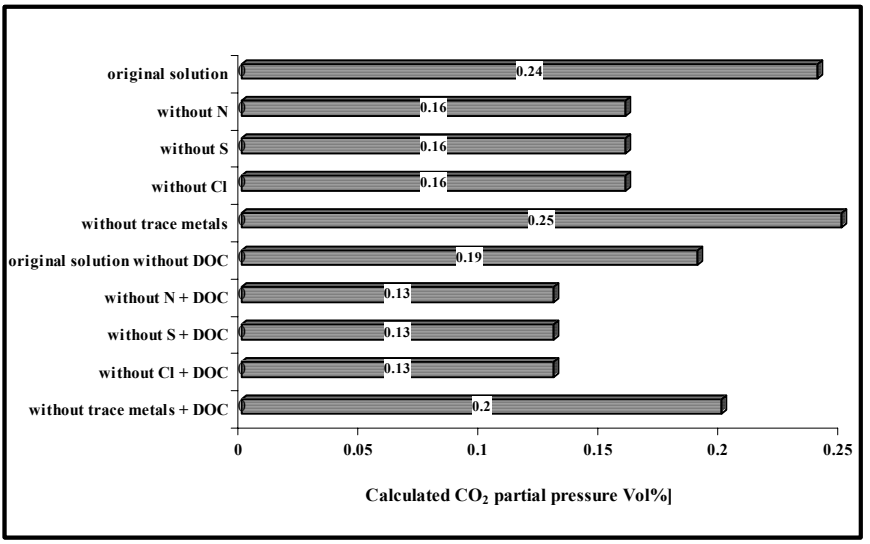

Fig. 32 CO_2 equilibrium partial pressure of complete and incomplete water analyses (calculated with PHREEQC after data by Merkel 1992)

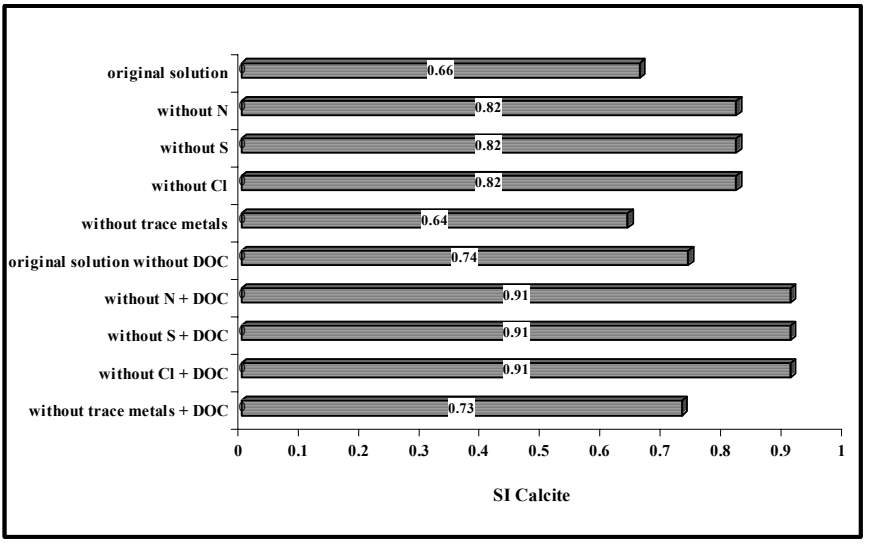

Fig. 33 Calcite saturation index of complete and incomplete water analyses (calculated with PHREEQC after data by Merkel 1992)

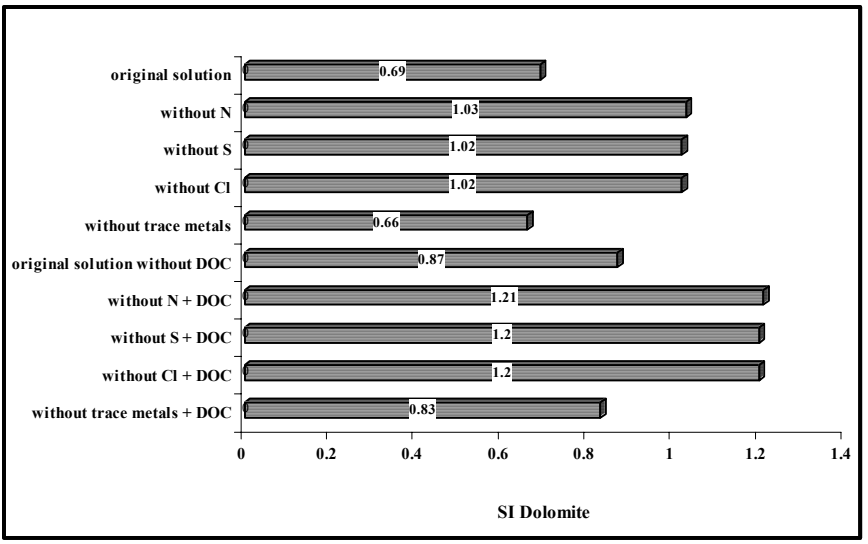

Fig. 34 Dolomite saturation index of complete and incomplete water analyses (calculated with PHREEQC after data by Merkel 1992)

However, the most common sources of different results are both based on the approach used for the calculation of the activity coefficient (chapter 1.1.2.6) and the thermodynamic data sets themselves (chapter 2.1.4), which provide the respective program with the fundamental geochemical information of each single species. The thermodynamic databases available partly use severely differing data with different solubility products, different species, minerals and reaction equations. Nordstrom et al (1979, 1990), Nordstrom & Munoz (1994), Nordstrom (1996, 2004) discuss this inconsistency of thermodynamic datasets in detail. For some species, for which stability constants have been published, not even the existence of the respective species has been proved doubtless, as can been shown in the following example.

Two surveys consider uranium species in the year 1992 (Grenthe et al. 1992 [NEA 92] and Fuger et al. 1992 [IAEA 92]) lead to quite different interpretations regarding some hexavalent uranium-hydroxo-species. These differences do influence considerably the species distribution of a measured total uranium concentration at neutral and basic pH values (Table 24).

Even greater differences exist for the mineral barium arsenate $Ba_3(AsO_4)_2$. While this mineral is not contained in PHREEQC.dat, CHEMVAL.dat, and EQ 3/6.dat, it is listed in MINTEQ.dat as well as in WATEQ4F.dat with such a low solubility product, that this mineral may readily regarded as Arsenic limiting phase during thermodynamic modeling. However, it is not $Ba_3(AsO_4)_2$ but $BaHAsSO_4 \cdot H_2O$ that might be a limiting mineral phase under certain conditions (Planer-Friedrich et al. 2001). The quoted low solubility product for $Ba_3(AsO_4)_2$ is based on a misinterpretation of the precipitating mineral (Chukhlantsev 1956).

That had been already known since 1985 (Robins 1985), but has never been changed in the above cited thermodynamic data sets (Zhu & Merkel 2001).

Table 24 Dissociation constants for U (6) hyrdoxo species (* = no data available)**

Species	NEA (92) log(K)	IAEA (92) log(K)
UO_2OH^+	-5.2	-5.76
$UO_2(OH)_2^0$	< -10.3	-13
$(UO_2)_2(OH)_2^{2+}$	-5.62	-5.54
$(UO_2)_3(OH)_5^+$	-15.55	-15.44
$(UO_2)_3(OH)_2^+$	-11.9	***
$(UO_2)_2(OH)_3^+$	-2.7	-4.06
$(UO_2)_4(OH)_7^+$	-21.9	***
$UO_2(OH)_3^-$	-19.2	***
$(UO_2)_3(OH)_7^-$	-31	***
$UO_2(OH)_4^{2-}$	-33	***

Furthermore it is of great importance that solubility products and complexation constants taken from the literature are clearly attached to the appropriate reaction equation. The example of the definition of the mineral rutherfordine (UO_2CO_3) in PHREEQC (Fig. 28) and EQ 3/6 (Fig. 29) shows that different reaction equations can be used for the same mineral. Whereas PHREEQC uses the chemical equation $UO_2CO_3 = UO_2^{2+} + CO_3^{2-}$, EQ 3/6 applies the equation $UO_2CO_3 + H^+ = HCO_3^- + UO_2^{2+}$. Because of the different reaction equations, the solubility product will not be identical.

Additionally, thermodynamic data are yielded by laboratory tests under defined boundary conditions (temperature, ionic strength) that apply to natural, geogenic circumstances only to a limited extent, e.g. for uranium thermodynamic data sets were derived from nuclear research that deals with uranium concentrations in the range of 0.1 mol/L. But in natural aquatic systems, concentrations are in the range of nmol/L.

In the laboratory, often relatively high ionic strengths (0.1 or 1 molar solution) are used. For the retrograde calculation of the complexation constants or the solubility products to an ionic strength of zero, the same procedures as for the calculation of the activities from measured concentrations can be applied (e.g. extended DEBYE-HÜCKEL equation). However, because the validity of the ion dissociation theory ends with 1 molar solutions, such experiments are in a range that is no longer valid with the ion dissociation theory. If solubility products and complexation constants are extracted from literature, data will be gathered that have been yielded under different experimental boundary conditions, and different calculation procedures considering the extrapolation of constants to an ionic strength of zero. Sometimes these data are not even recalculated to an ionic strength of zero at all.

Progress toward an internally consistent and reliable thermodynamic data set for geochemical calculations is a tedious, slow, and poorly supported enterprise. For some applications, a smaller but consistent subset of data is sufficient. Some

aqueous species forms can be determined analytically and this approach should be used to confirm the reliability of computed species to build general confidence in these calculations.

It is also important to indicate the range of the error of each species for calculated species distributions. The pH value is a significant parameter to be measured. In practice, it can be measured with an accuracy of ± 0.1 pH units. Particularly with respect to reactions, in which several protons occur, this uncertainty may have a significant impact on the result (Fig. 35). Sensitivity analyses can be performed by simply entering the anticipated error in the analytical data (such as a ± 0.1 pH change) and propagating this change through a speciation and saturation index calculation. This type of error propagation can demonstrate the effect of errors from analytical data on geochemical calculations.

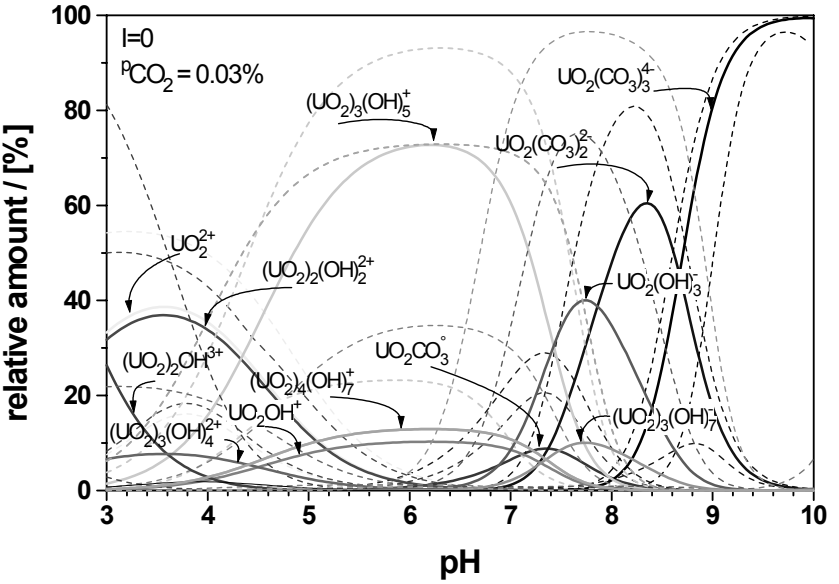

Fig. 35 Uranyl species in dependence on the measured pH value taking into account a error estimate (after Meinrath 1997)

2.2 Use of PHREEQC

2.2.1 Structure of PHREEQC under the Windows surface

The program, the Windows user interface and the respective manual are freely available by internet:
Program: http://wwwbrr.cr.usgs.gov/projects/GWC_coupled/phreeqc/index.html
Windows surface: http://www.geo.vu.nl/users/posv/phreeqc.html
PHREEQC Manual: ftp://brrcrftp.cr.usgs.gov/geochem/unix/phreeqc/manual.pdf
(pdf format (Adobe Acrobat Reader), size 1.1MB)

The file unpacks and installs itself independently and is started via PHREEQC.exe. After the start of the program, a window with four tab pages opens: INPUT (chapter 2.2.1.1), DATABASE (chapter 2.2.1.2), GRID (chapter 2.2.1.4), and CHART (chapter 2.2.1.5).

2.2.1.1 Input

The input window consists of two windows. The left, initially blank window is the space to enter the chemical analysis to be modeled together with the commands to perform the particular modeling task. PHREEQC keywords and PHREEQC BASIC statements may be listed in the right window. A mouse click on the "+" symbol displays the list of keywords. The utilization of the BASIC commands is explained in chapter 2.2.2.2.2.

A simple input comprises the three keywords TITLE, SOLUTION and END. However, just using the keyword SOLUTION is sufficient. END is not necessarily to be used for simple tasks, but for separation of multistage tasks. TITLE is exclusively used for documentation of the particular task. These keywords can be inserted to the left windows from the list on the right hand side by double-clicking on the respective commands. The structure of an input file will be explained by means of the example of the following seawater analysis. The order of the details in example SOLUTION 1 seawater analysis corresponds to a certain logic. However, it does not matter in which order the details are entered in the input file. They only have to appear under the keyword SOLUTION.

```
TITLE           Example analysis of seawater
SOLUTION 1          seawater
        units       mg/L
        pH          8.22
        temp        25.0
        density     1.023
        pe          8.451
        redox       O(0)/O(-2)

        Ca          412.3
        Mg          1291.8
        Na          10768.0
        K           399,1
        Fe(3)       0.002
        Fe(2)       0.0005
        Si          4.28
        Mn          0.0002

        Alkalinity  141.682     as HCO3
        N8-39       0.03        as NH4
        N(5)        0.29        gfw 62.0
```

```
    S(6)        28.25       mmol/L

    Cl          19353.0     charge
    O(0)        1.0         O2(g) –7
    U           3.3         ug/L    N(5)/N(-3)
END
```

The unit used for the input of concentrations can be defined with the keyword units. Possible units are mass or moles per liter solution, moles per kg solution or moles per kg water. Concentrations thereby can be given in g, mg, ug (not µg) or mol, mmol, and umol. Temperature (temp) is denoted in °C. The density (density) can be entered in g/cm3, with a default of 0.9998. That information is especially important for highly mineralized waters, like e.g. seawater. To input the measured E_H value a conversion to the pE value is necessary (see chapter 1.1.5.2.2, Eq. 65). If no pE value is given, pE is assumed to be 4 by default. A redox couple (redox) can be defined to calculate the pE value that will be used to model the species distribution of redox sensitive elements if no pE is given.

A list of element concentrations follows. Whereas ions like Ca, Mg, etc. that occur only in one redox stage are indicated as elements, ions whose concentration is determined in different redox states are denoted individually with their valence in parentheses, as in the example of Fe^{3+} and Fe^{2+}. However, the syntax is defined in the database (*.dat) not in the PHREEQC code. For complexes like HCO_3^-, NO_3^-, SO_4^{2-}, three input options exist:

[ion] ([valence]) [concentration in mg/L] **as** [complex form] *in the example for HCO_3, NH_4*
[ion] ([valence]) [concentration in mmol/L] **gfw**[molar mass of the complex]
gfw = gram formular weight, in the example for NO_3^-
[ion] ([valence]) [concentration in mmol/L] **mmol/L** *in the example for SO_4^{2-}*

In the latter case, mmol/L defines a unit different from the default unit (units). It is important that the reference value (in the example for liter) is the same as that used with units and with individual elements. Alternatively, ppm could be defined under units and ppb or mg/kgw (kg water) and mol/kgw could be added behind individual elements.

Furthermore, the command **"charge"** can be used with any element, the pH or the pE value, but it may **only** appear **once** in the whole input file (as in the example with chloride). The use of "**charge**" enforces a total charge compensation by means of the chosen element or the pH or the pE value, respectively and thus maintains electrical balance. The element with the highest concentrations might be chosen to keep the relative error as small as possible by means of an arbitrary increase or decrease of the concentration for charge compensation. The keyword "charge" may not be used with "Alkalinity".

The pH, pE or individual elements may be combined with a mineral or gas phase and a saturation index (in the example: **O(0) 1.0 O2(g) –0.7**). It causes a change in concentration of the respective element to obtain an equilibrium or a

defined disequilibrium in terms of that mineral or gas phase. If no saturation index is given along with the phase name, the default SI = 0 (equilibrium) will be used. For gases, the logarithm of the partial pressure is specified in bar instead of the saturation index: -0.7 in the example thus means a O_2 partial pressure of $10^{-0.7}$ = 0.2 bar or 20 Vol-%.

A redox couple can be separately defined according to a redox sensitive element (in the example:U according to **N(5)/N(-3)** redox couple) that can be given either as total concentration (like U) or as partial concentrations of the respective species (like Fe). The input enforces a calculation of a redox equilibrium of the redox sensitive elements by means of the given redox couple. In this example the standard pE value for the standard redox couple will not be used for this element (in the example of uranium) to calculate the uranium species.

The shortcut **STRG+T** opens a list of the species defined in the dataset, **STRG+H** a list of the minerals and gases. Marking a species or phase and pressing ENTER transfers the desired species or phase into the input file.

Alternatively to the keyword SOLUTION, SOLUTION_SPREAD can be used for the input of solution. The input is transposed compared to the input for SOLUTION, i.e. the rows of input for SOLUTION become the columns of input for SOLUTION_SPREAD. It is especially convenient to define more than one aqueous solution composition using this tab-limited format. Data obtained e.g. from a laboratory spreadsheet format can be copied directly into the PHREEQC input file. SOLUTION_SPREAD is compatible with the format of many spreadsheet programs, as e.g. Excel. The column headings are element names, element valence state names or isotope names. One subheading can be used to define speciation (e.g. „as SO4“, or „as NO3“), specify element specific units, redox couples, phase names and saturation indices. All succeeding lines are the data values for each solution, with one solution defined on each line.

As PHREEQC for Windows does not use an extension for saving (like e.g. “.doc” for word documents), it is advisable to either create an extension of one’s own (e.g. “phr”) or to save all input files in a separate directory. The input files are plain ASCII files that can be read and edited with any editor.

To model balanced reactions, kinetics or reactive transports, more keywords besides TITLE, SOLUTION and END are needed, which will be listed in the following. Furthermore, the individual input parameters are described in detail in the PHREEQC manual.

ADVECTION
-cells *cells*
-shifts *shifts*
-time_step *time step*
-initial_time *initial_time*
-print_cells *list of cell numbers*
-print_frequency *print_modulus*
-punch_cells *list of cell numbers*
-punch_frequency *punch_modulus*
-warnings [*True* or *False*]

END
EQUILIBRIUM_PHASES [*number*] [*description*]
phase name [*saturation index* [(*alternative formula* or *alternative phase*) [*amount*]]
EXCHANGE [*number*] [*description*]
exchange formula, name, [(equilibrium_phase or kinetic_reactant)],
exchange_per_mole
-equilibrate number
EXCHANGE_MASTER_SPECIES
exchange name, exchange master species
EXCHANGE_SPECIES
Association reaction
log_k *log K*
delta_h *enthalpy,* [*units*]
-analytical_expression *A 1 , A 2 , A 3 , A 4 , A 5*
-gamma *DEBYE-HÜCKEL a, DEBYE-HÜCKEL b*
-Davies
-mole_balance *formula*
GAS_PHASE
Three options are available to model gas phases:
Fixed-pressure gas phase
GAS_PHASE [*number*] [*description*]
-fixed_pressure
-pressure *pressure*
-volume volume
-temperature *temperature*
phase name partial pressure
Fixed-volume gas phase: Define initial moles of components with partial pressures
GAS_PHASE [*number*] [*description*]
-fixed_volume
-volume *volume*
-temperature *temperature*
phase name, partial pressure
Fixed-volume gas phase: Define initial moles of components by equilibrium with a solution
GAS_PHASE [*number*] [*description*]
-fixed_volume
-equilibrium *number*
-volume *volume*
phase name
INCREMENTAL_REACTIONS [*True* or *False*]
INVERSE_MODELING [*number*] [*description*]
-solutions *list of solution numbers*
-uncertainty *list of uncertainty limits*

-phases *phase name* [force] [dissolve or precipitate] [*list of isotope name, isotope ratio, isotope uncertainty limit*]
-balances *element or valence state name,* [*list of uncertainty limits*]
-isotopes *isotope_name,*[*list of uncertainty limits*]
-range [*maximum*]
-minimal
-tolerance *tolerance*
-*force_solutions list of* [*True* or *False*]
-uncertainty_water *moles*
-mineral_water *[True* or *False*]
KINETICS [*number*] [*description*]
rate name
-formula *list of formula,* [*stoichiometric coefficient*]
-m *moles*
-m0 *initial moles*
-parms *list of parameters*
-tol *tolerance*
-steps *list of time steps*
-step_divide *step_divide*
-runge_kutta (1, 2, 3, or 6) Equal-increment definition of steps
-steps *total time* [in *steps*]
KNOBS (changing numerical convergence criteria)
-iterations *iterations*
-convergence_tolerance *convergence_tolerance*
-tolerance *tolerance*
-step_size *step_size*
-pe_step_size *pe_step_size*
-diagonal_scale [*True* or *False*]
-debug_diffuse_layer [*True* or *False*]
-debug_inverse [*True* or *False*]
-debug_model [*True* or *False*]
-debug_prep [*True* or *False*]
-debug_set [*True* or *False*]
-logfile [*True* or *False*]
MIX [*solution number*] [*ratio*]
PHASES
Phase name
Dissolution reaction
log_k *log K*
delta_h enthalpy [*units*]
-analytical_expression *A 1 , A 2 , A 3 , A 4 , A 5*
-no_check
PRINT
-reset [*True* or *False*]
-eh [*True* or *False*]
-equilibrium_phases [*True* or *False*]

-exchange [*True* or *False*]
-gas_phase [*True* or *False*]
-headings [*True* or *False*]
-inverse_modeling [*True* or *False*]
-kinetics [*True* or *False*]
-other [*True* or *False*]
-saturation_indices [*True* or *False*]
-solid_solutions [*True* or *False*]
-species [*True* or *False*]
-surface [*True* or *False*]
-totals [*True* or *False*]
-user_print [*True* or *False*]
-selected_output [*True* or *False*]
-status [*True* or *False*]
RATES
name of rate expression
-start
numbered BASIC statements
-end
REACTION [*number*] [*description*]
(*phase name* or *formula*), [*relative stoichiometry*]
list of reaction amounts, [*units*]
Equal increment definition of steps
reaction amount [*units*] [in *steps*]
REACTION_TEMPERATURE [*number*] [*description*]
list of temperatures
Equal increment definition of steps
temp 1 , temp 2 , in *steps*
SAVE *keyword*, *number*
SELECTED_OUTPUT
-file *file name*
-selected_out *[True or False*]
-user_punch [*True* or *False*]
-high_precision [*True* or *False*]
-reset [*True* or *False*]
-simulation [*True* or *False*]
-state [*True* or *False*]
-solution [*True* or *False*]
-distance [*True* or *False*]
-time [*True* or *False*]
-step [*True* or *False*]
-pH [*True* or *False*]
-pe [*True* or *False*]
-reaction [*True* or *False*]
-temperature [*True* or *False*]
-alkalinity [*True* or *False*]

-ionic_strength [*True* or *False*]
-water [*True* or *False*]
-charge_balance [*True* or *False*]
-percent_error [*True* or *False*]
-totals *element list*
-molalities *species list*
-activities *species list*
-equilibrium_phases *phase list*
-saturation_indices *phase list*
-gases *gas-component list*
-kinetic_reactants *reactant list*
-solid_solutions *component list*
-inverse_modeling [*True* or *False*]
SOLID_SOLUTIONS [*number*] [*description*]
solid-solution name
-comp *phase name, moles*
-comp1 *phase name, moles*
-comp2 *phase name, moles*
-temp *temperature in Celsius*
-tempk *temperature in Kelvin*
-Gugg_nondim *a0, a1*
-Gugg_kJ *a0, a1*
-activity_coefficients *x 1 , x 2*
-distribution_coefficients *x 1 , x 2*
-miscibility_gap *x 1* , *x 2*
-spinodal_gap *x 1 , x 2*
-critical_point *x cp , t cp*
-alyotropic_point *x aly* ,
-Thompson *wg 2 , wg 1*
-Margules alpha *2 , alpha 3*
SOLUTION_MASTER_SPECIES
element name, master species, alkalinity, (*gram formula weight* or *formula*)*, gram formula weight of element*
SOLUTION_SPECIES
Association reaction
log_k *log K*
delta_h *enthalpy* [*units*]
-analytical_expression *A 1 , A 2 , A 3 , A 4 , A 5*
-gamma *DEBYE-HÜCKEL a, DEBYE-HÜCKEL b*
-no_check
-mole_balance *formula*
SOLUTION_SPREAD
-temp *temperature*
-pH *pH*
-pe *pe*
-redox *redox couple*

-units *concentration units*
-density *density*
-water *mass*
-isotope *name, value,* [*uncertainty_limit*]
-isotope_uncertainty *name, uncertainty_limit*
column headings
[subheadings]
chemical data
SURFACE [*number*] [*description*] Implicit definition of surface composition
-equilibrate *number*
surface binding-site name, sites, specific_area_per_gram, mass
surface binding-site formula, name, [(equilibrium_phase or kinetic_reactant)],
sites_per_mole,
specific_area_per_mole
-no_edl
-diffuse_layer *[thickness*]
-only_counter_ions
SURFACE [*number*] [*description*] Explicit definition of surface composition
surface binding-site formula, sites, specific_area_per_gram, mass
surface binding-site formula, name, [(equilibrium_phase or kinetic_reactant)],
sites_per_mole,
specific_area_per_mole
SURFACE_MASTER_SPECIES
surface binding-site name, surface master species
SURFACE_SPECIES
Association reaction
log_k *log K*
delta_h enthalpy, [*units*]
-analytical_expression *A 1 , A 2 , A 3 , A 4 , A 5*
-no_check
-mole_balance *formula*
TITLE *comment*
comment
TRANSPORT
-cells *cells*
-shifts *shifts*
-time_step *time step*
-flow_direction *(forward, back, or diffusion_only)*
-boundary_conditions *first, last*
-lengths *list of lengths*
-dispersivities *list of dispersivities*
-correct_disp [*True* or *False*]
-diffusion_coefficient *diffusion coefficient*
-stagnant *stagnant_cells* [*exchange_factor*]
-thermal_diffusion *temperature retardation factor, thermal diffusion coefficient*
-initial_time *initial_time*

-print_cells *list of cell numbers*
-print_frequency *print_modulus*
-punch_cells *list of cell numbers*
-punch_frequency *punch_modulus*
-dump *dump file*
-dump_frequency *dump_modulus*
-dump_restart *shift number*
-warnings [*True* or *False*]
USE *keyword*, (*number* or none)
USER_PRINT
-start
numbered BASIC statements
-end
USER_PUNCH
-headings *list of column headings*
-start
numbered BASIC statements
-end

2.2.1.2 Thermodynamic data

The data sets WATEQ4F.dat, MINTEQ.dat, PHREEQC.dat and LLNL.dat are automatically installed with the program PHREEQC and can be chosen from the menu item Calculations/File under Database File. The internal structure of these thermodynamic data sets has already been explained in great detail in chapter 2.1.4.2 by means of the example WATEQ4F.dat.

Lines beginning with "#" are only commends, e.g. each first line of the species defined in the block SOLUTION_SPECIES.

When modeling rare elements, one will often recognize that not all necessary data are available in an existing data set. Thus, there is principally the option to create/add own data sets (e.g. as combination of different data sets) or to change already existing ones. In chapter 2.1.4.1 and chapter 2.1.5, associated problems concerning data set maintenance, verification of the data set consistency or existence of species, and differences in the conditions under which the solubility constants have been determined, have already been discussed. Using the data browser of PHREEQC in the folder DATABASE nothing can be changed in a data set. To make modifications, the desired data set has to be opened and changed in any editor, e.g. WORDPAD and saved as ASCII file.

If elements, species, stability constants, and/or solubility constants that are unavailable in an existing data set, should be used for one task only, it is advisable to define them directly in the input file rather than to change the data set itself. As a declaration in an input file always has a higher rank, it overwrites information of a data set. Like in a data set, the keyword SOLUTION_MASTER_SPECIES has to be used to define the element (e.g. C), the ionic form (e.g. CO3-2), the contribution of the element to alkalinity (e.g. 2.0), the mole mass of the species for

the input in mg/L (e.g. 61.0171), and the atomic mass of the element (e.g. 12.0111) (see also Table 22). When entering the keyword SOLUTION_SPECIES a reaction, the respective solubility constant log k and the enthalpy delta h in kcal/mol or kJ/mol at 25 °C additionally have to defined (for further operations see also Table 23), e.g.

Reaction	CO3-2 = CO3-2
Solubility constant	log k 0.0
Enthalpy	-gamma 5.4 0.0

2.2.1.3 Output

The modeling can be started either via Calculations/Start or by the icon "pocket calculator". A "PHREEQC for Windows-progress" window opens showing input, output and data set file as well as the calculation progress in line 4. DONE appears when the calculation is performed or terminated. By clicking on DONE, the progress window closes and the output folder opens.

An output file is automatically created with the name of the input file and the additional extension "out". If one explicitly wants to enter a different name, it can be done under Calculations/Files Output-File.

The output consists of a standard output plus additional results per input. The standard output has the following structure:

- Reading data base (the data set is read in and the keywords will be assumed)
- Reading input data (repetition of data and keywords from the input file)
- Beginning of initial solution calculation (standard calculations)
  solution composition: element concentration in mol/kg (molality) and mol/L (moles)
  description of solution: pH, pE, activity, charge balance, ionic strength, error of analysis, etc.
  distribution of species: in each first line total concentration of an element in mol/L, followed by the species of that element with concentration c in mol/L, activity a in mol/L, log c, log a, and log Gamma (= log activity coefficient = log (activity/concentration) = log a – log c; see also chapter 1.1.2.4)
  saturation indices: saturation indices with mineral name, SI, log IAP, log KT (SI = log IAP – log KT; see also chapter 1.1.4.1.2), and mineral formula; positive values mean super-saturation, negative values under-saturation with regard to the respective mineral phase.

If redox sensitive elements (e.g. NO_3^-, NH_4^+ in the case of the seawater analysis) are declared in the input file, a paragraph "redox couples" will be displayed in the output after "description of solution" that contains all individual redox couples (in the example N(-3)/N(5)) with their respective redox potentials as pE, and E_H value in volts.

Following the standard output (beginning of initial solution calculation) the task-specific results are printed, i.e. of a modified solution. The structure of the output file is displayed by a tree index on the right in the window. By double-clicking the tree-structure one gets to the beginning of the desired chapter in the

output. Especially when having long output files, the search via tree index can be of significant help so as not to get lost in a complex output file.

2.2.1.4 Grid

The GRID folder offers to plot data in spreadsheet format. However, a file name ("example.csv") and the desired information has to be defined by using the command SELECTED_OUTPUT in the input file, e.g. the saturation indices of anhydrite and gypsum,

```
SELECTED_OUTPUT
      -file   example.csv
      -si     anhydrite gypsum
```

In that particular example the spreadsheet file has to be opened in the folder GRID (does not happen automatically). Files with the extension ".csv" (Microsoft Excel – files delimited by comma) can be directly opened in the GRID folder. If no file name is entered in the command line, "selected.out" will be used as default. This file can be opened in GRID also, but is not displayed automatically (to open "selected.out" the file tye "all files" (*.*) must be chosen). For other graphical representations it is recommended to open the SELECTED_OUTPUT file in a spreadsheet program (e.g. EXCEL) to make further changes and take advantage of graphical options in those programs.

2.2.1.5 Chart

By marking a respective data area in the folder GRID and by clicking on the right mouse button ("Plot in chart") it is possible to plot the data in CHART. By doing so, the values of the first marked column will be considered as x-values and all values of the following columns as y-values. A second possibility is using the keyword USER_GRAPH where one may directly declare in the input file the parameters to be plotted in the CHART diagram (see exercise chapter 3.3.3).

Using the right mouse button, the diagram area can be formatted by "format chart area" (font, background). With "chart options", it is possible to add a second y-axis, a legend, titles, and labels for the x- and y-axis. The axes, the legend, and the graph itself can be formatted by selecting and clicking the right mouse button.

2.2.2 Introductory Examples for PHREEQC Modeling

2.2.2.1 Equilibrium reactions

Equilibrium reactions (theory see chapter 1.1) are the simplest form of hydrogeochemical modeling. In the following, the modeling of such a reaction by means of PHREEQC is explained using two simple examples. For both calculations the data set WATEQ4F.dat is used.

2.2.2.1.1. Example 1: Standard output – seawater analysis

By means of the example of the seawater analysis already discussed in chapter 2.2.1.1 it is shown what results can be taken from the standard output.

General information can be taken from the paragraphs "**solution composition**" and "**description of solution**". Looking at the molarities of the solution composition it is obvious that the water is of Na-Cl-type (Cl = 0.55 mol/L, Na = 0.47 mol/L; seawater).

The ionic strength of 0.6594 mol/L found in "description of solution" represents the high total mineralization of the seawater. To verify the accuracy of the analysis, the electrical charge balance and the analytical error are considered (electrical balance (eq) = $7.370 \cdot 10^{-04}$; percent error, 100*(Cat-|An|)/(Cat+|An|) = 0.06). Note: In Germany, the equation 100*(Cat-|An|)/[0.5*(Cat+|An|) is often used (Hölting 1996, DVWK 1990). This alternate form of the charge balance equation is also used in WATEQ4F (Ball and Nordstrom, 1991). Thus the error would be 0.12 %. Anyway, the accuracy of the analysis is very good and the analysis can be used for further modeling. If the command "charge" is put behind chloride, as shown in the example in chapter 2.2.1.1, a total charge compensation will be enforced [electrical balance ($1.615 \cdot 10^{-16}$) and analytical error (0.00)]. Under "redox couples" the redox potential for each single redox couple is listed as pE- or E_H value.

Not only the total concentration of each element can be taken from "distribution of species" but also the distribution of species, i.e. the portion of free cations, negatively charged, positively charged and zero charged complexes. Thus one is able to draw conclusions about oxidative/reductive ratios, mobility, solubility, or even toxicity of elements and species. The cations Na, K, Ca, and Mg mainly exist (87-99 %) in form of their respective free cations, only 1-13 % account for metal-sulfate-complexes. Chloride is available as free ion to nearly 100 %. It hardly reacts with other bonding partners. C(4) occurs predominantly as HCO_3^- ion (70 %), yet reacts to a lower percentage with Mg and Na forming HCO_3^- and CO_3^{2-} complexes. S(6) behaves similarly as C(4) forming predominantly SO_4^{2-}. N(5) and N(-3) occur predominantly as NO_3^- and to a less amount as NH_4^+. The simplest form to represent species distribution is a pie chart. Fig. 36 shows exemplarily the species distribution for C(4) and S(6).

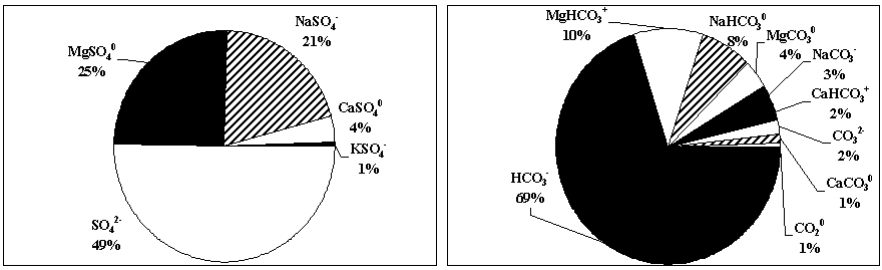

Fig. 36 EXCEL pie charts to represent the species distribution of S(6) and C(4)

The ratio N(5)/N(-3) is approximately 3:1. The Fe(3)/Fe(2) ratio is 4:1. Thereby it is important to see that Fe(2) exists in form of the free cations Fe^{2+} or as positively charges complex $FeCl^{+}$ and thus is subject to cation exchange, while Fe(3) occurring mainly in form of the zero charged complex $Fe(OH)_3^0$ is not. U(6) clearly dominates compared to U(5) and U(4). In contrast to U(4), U(6) is considerably soluble and thus more mobile. But the predominant U(6) species are the negatively charged complexes ($UO_2(CO_3)_3^{4-}$, $UO_2(CO_3)_2^{2-}$), which are subject to interactions with e.g. iron hydroxides and thus mobility may be limited. The different proportions of the reduced form of the total concentration for N, Fe, and U are in accordance with the theoretical oxidation/reduction succession (see also Fig. 20). The oxidation of Fe(2) to Fe(3) already starts at pE values of 0, the oxidation of N(-3) to N(5) only at pE= 6, while the oxidation of uranium is already finished at a pE value of 8.451, which was determined in the seawater sample.

Hints for super- or undersaturation of minerals can be found in the last paragraph of the initial solution calculations entitled “saturation indices”. Graphical representation of saturation proportions is often done by means of bar charts, whereas SI = 0 marks the point of intersection between the x-axis and the y-axis, and the bars of super-saturated phases point upwards and those for under-saturated phases downwards (example Fe-bearing mineral phases Fig. 37).

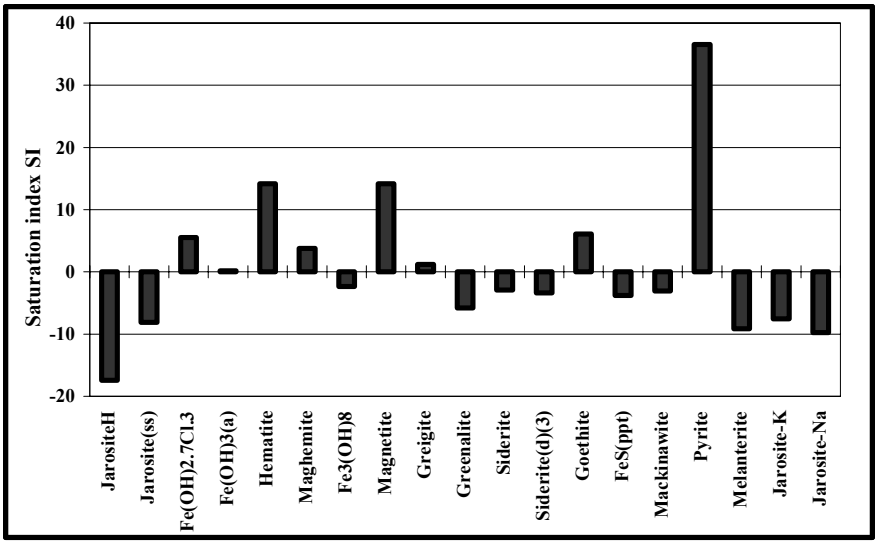

Fig. 37 EXCEL bar chart to represent all super- and undersaturated iron-bearing mineral phases

It is important to note that not all mineral phases with an SI > 0 necessarily will be precipitated because low reaction rates and prevailing boundary conditions may lead to the preservation of disequilibria over long periods. Therefore, dolomite will not precipitate from seawater despite its distinctly positive SI of 2.37 (or 1.82

for dolomite(d); d = dispersedly distributed) due to its inertness, while a rapid precipitation can be expected for calcite having an SI of 0.74. Referring to the iron represented in Fig. 37, a fast precipitation reaction of amorphous iron hydroxide can be anticipated. Thereby, only a moderate super-saturation occurs (SI = +0.18). Pyrite is significantly supersaturated and will likely precipitate with time, after amorphous iron hydroxide, forming finely distributed crystals. Hematite, magnetite, and goethite are generally formed from $Fe(OH)_3(a)$ during conversion reactions and will not precipitate directly. Altogether, it can be observed that the total concentration of iron with Fe = 0.0025 mg/L is very low and thus surely not all precipitation reactions with iron will run completely.

2.2.2.1.2. Example 2 equilibrium – solution of gypsum

The question "How much gypsum can be dissolved in distilled water?" shall be answered by manual calculation and then by means of PHREEQC for comparison [pK gypsum = 4.602 (at T = 20 °C)].

Calculation

The chemical equation for the dissolution of gypsum is:

$CaSO_4 \leftrightarrow Ca^{2+} + SO_4^{2-}$

$$K_{gypsum} = \frac{\{Ca^{2+}\} \cdot \{SO_4^{2-}\}}{\{CaSO_4\}}$$

$K = [Ca^{2+}] * [SO_4^{2-}] = 10^{-4.602}$ (as $[CaSO_4] = 1$)

as $[Ca^{2+}] = [SO_4^{2-}]$ $K = [SO_4^{2-}]^2$ $[SO_4^{2-}] =$ **0.005 mol/L = 5 mmol/L**

This answer does not give us a concentration but an activity since the law of mass action concerns activities (chapter 1.1.2). The conversion from activity to concentration is carried out using the activity coefficient (Eq. 10). The ionic strength is calculated after Eq.12:

$$I = 0.5 \cdot \sum m_i \cdot z_i^2$$

where m is the concentration in mol/L and z the oxidation state of the species i. Since the concentration is unknown, iterative calculation has to be performed with a first approximation that the activity of 5 mmol/L replaces the concentration. The results for Ca^{2+} and SO_4^{2-} are:

$$I = 0.5 \cdot \sum 5 \cdot 2^2 + 5 \cdot 2^2 = 20\,\text{mmol/L}$$

From the graphical correlation between ionic strength and activity coefficient (Fig. 2) an activity coefficient f_1 of about 0.55 and a concentration c_1 of $a_i/f_i = 0.005 / 0.55 = 0.009$ mol/L = 9 mmol/L, respectively is found. If this first approximation for the concentration is now used in the equation for the ionic strength, the following results will be obtained: $I_2 = 36$ mmol/L, $f_2 = 0.5$, $c_2 = 0.010$ mol/L = 10

mmol/L; I_3 = 40 mmol/ L, f_3 = 0. 48, c_3 = 0.0104 mol/L = 10.4 mmol/L, etc. With three iterative steps a concentration of about **10 mmol/L of gypsum is calculated.**

Modeling

In comparison to this calculation, the dissolution of gypsum in distilled water shall now be modeled by means of PHREEQC The input is very simple as it concerns distilled water and thus, the SOLUTION block contains only pH = 7 and temperature = 20 °C. To force equilibrium with gypsum, the keyword EQUILIBRIUM_PHASES and the saturation index of 0 are used.

The input file looks as follows:

```
TITLE example 2 dissolution of gypsum
SOLUTION 1
        temp                    20
        pH                      7.0
EQUILIBRIUM_PHASES
gypsum  0
END
```

The output file contains an additional block “beginning of batch-reaction calculations”, and a “phase assemblage“ block besides the already known paragraphs solution composition, description of solution, distribution of species, saturation indices. Phase assemblage contains: mineral phase – SI – log IAP – log KT – initial (initial amount of gypsum, 10 mol/kg by default) – final (amount of gypsum, which still exists as solid after dissolution) – delta (amount of dissolved gypsum = final – initial; negative value stands for dissolution, positive values indicate precipitation).

As distilled water (with no constituents) is used, the amount of dissolved gypsum (phase assemblage delta) is equal to the amount of Ca^{2+} and SO_4^{2-} (solution composition molality, respectively distribution of species).

The result of the dissolution of gypsum is $1.532*10^{-2}$ = **15.32 mmol/L**, in comparison to about 10 mmol/L of the preceding calculation. Looking at the species distribution it can be seen that besides of the free ions Ca^{2+} and SO_4^{2-} the following complexes have been formed as well: $CaSO_4^0$, $CaOH^+$, HSO_4^- and $CaHSO_4^+$. Due to the formation of the $CaSO_4^0$ complex (**4.949 mmol/L**), the dissolution of gypsum will be clearly increased (see also chapter 1.1.4.1.1). It is a process that had not been considered in the simple calculation above.

Already, by means of this first simple example, the complexity of describing the hydrogeochemistry of aquatic systems and the limitations of interpretations without computer-aided modeling can be understood.

2.2.2.2 Introductory examples for kinetics

Even more complicated than equilibrium modeling is the modeling of kinetically controlled processes (for theory see chapter 1.2). Normally the reaction rate varies

with the reaction process and this leads to a set of simple differential equations. The integration of the reaction rates over time can be carried out e.g. with the help of the Runge-Kutta algorithm. The implementation of Fehlberg (1969) within PHREEQC offers the possibility to evaluate the derivatives in partial steps by performing an error estimation and comparing it with a user predetermined tolerance limit (Cash & Karp 1990).

For kinetic modeling in PHREEQC two keywords are necessary: KINETICS n (n = number of SOLUTION, for which the kinetics shall be calculated) and RATES. For both keywords, a "rate name" has to be entered, e.g. calcite when the dissolution of calcite shall be kinetically modeled. The general syntax within the keyword KINETICS is as shown in Table 25.

Table 25 Syntax within the keyword kinetics in PHREEQC

KINETICS m-n	[m<n]
rate name	*rate name* and its associated rate expression must be defined within a RATES data block, e.g. pyrite, or any aquatic species
-formula	chemical formula or the name of a phase
-m	current moles of reactant [default = m0]
-m0	initial moles of reactant
-parms	a list of numbers may be entered that can be used in a BASIC program within the rate expressions, for example constants, exponents, or half saturation constants
-tol	Tolerance for integration procedure [default = $1 \cdot 10^{-8}$ mol/L], the value of *tolerance* is related to the concentration differences that are considered significant for the elements in the reaction. Smaller concentration differences that are considered as significant require smaller tolerances.
-steps	Time steps over which the rate expressions is integrated, n in m steps [default: n = 1] in seconds, e.g. 500 in 3 steps or 100 300 500
-step_divide	If *step_divide* is greater than 1.0, the first time interval of each integration is set to *time* = step / step_divide; if step_divide is less than 1.0, then *step_divide* is the maximum moles of reaction that can be added during a kinetic integration subinterval.
runge_kutta	(1,2,3 or 6) designates the preferred number of time subintervals to use when integrating (default 3)

The general syntax for RATES is "rate name" and -start -end. A BASIC program is obligatory between -start and -end (see chapter 2.2.2.2.1).

2.2.2.2.1. Defining reaction rates

As reaction rates can be fitted mathematically in very different manners, there is an option (and need) in PHREEQC to declare any mathematical term in the form of a little BASIC program within the keyword RATES as will be shown in the following example of a **time-dependent calcite dissolution**:

```
SOLUTION 1 distilled water
pH 7
temp 10
EQUILIBRIUM_PHASES
CO2(g) -3.5
KINETICS 1
 Calcite
          -tol       1e-8
          -m0        3e-3
          -m         3e-3
          -parms              50         0.6
          -steps 36000 in 20 steps              // 36.000 seconds*
          -step_divide 10000                    // first interval calculated with 3.6 sec.*
RATES
Calcite
 -start
  1 rem Calcite solution kinetics according to Plummer et. al 1978
  2 rem               parm(1) = A/V, 1/dm        parm(2) = exponent for m/m0
  10  si_cc = si("Calcite")
  20    if (m <= 0  and si_cc < 0) then go to 200
  30  k1 = 10^(0.198 - 444.0 / (273.16 + tc) )
  40  k2 = 10^(2.84 - 2177.0 / (273.16 + tc) )
  50    if tc <= 25 then k3 = 10^(-5.86 - 317.0 / (273.16 + tc) )
  60    if tc > 25 then k3 = 10^(-1.1 - 1737.0 / (273.16 + tc) )
  70  t = 1
  80    if m0 > 0 then t = m/m0
  90    if t = 0 then t = 1
  100 moles = parm(1) * 0.1 * (t)^parm(2)
  110 moles = moles * (k1 * act("H+") + k2 * act("CO2") + k3 * act("H2O"))
  120 moles = moles * (1 - 10^(2/3*si_cc))
  130 moles = moles * time          //this line is a ”must“ for each BASIC-program*
  140   if (moles > m) then moles = m
  150   if (moles >= 0) then goto 200
  160 temp = tot("Ca")
  170 mc  = tot("C(4)")
  180   if mc < temp then temp = mc
  190   if -moles > temp then moles = -temp
  200 save moles                    //this line is a “must” for each BASIC-program*
 -end
SELECTED_OUTPUT
-file 4_Calcite.csv
-saturation_indices calcite
end
```

* the ´///´ included comments cannot appear like this in a PHREEQC-BASIC script as the BASIC interpreter is trying to interpret them. It is only possible by means of REM (remark) to include commentary lines at the beginning of a line.

Fig. 38 shows that settling of the calcite equilibrium is very rapid at low CO_2 partial pressures (in the example 0.03 Vol-%), but distinctly slower at increased CO_2 partial pressures (in the example 1 Vol-%).

Further examples can be found as already quoted in chapter 2.1.4.2 for K-feldspar, albite, calcite, pyrite, organic carbon and pyrolusite in the data set PHREEQC.dat or WATEQ4F.dat with the keyword RATES. There, all parameters are marked as comments by means of the # sign in the block KINETICS.

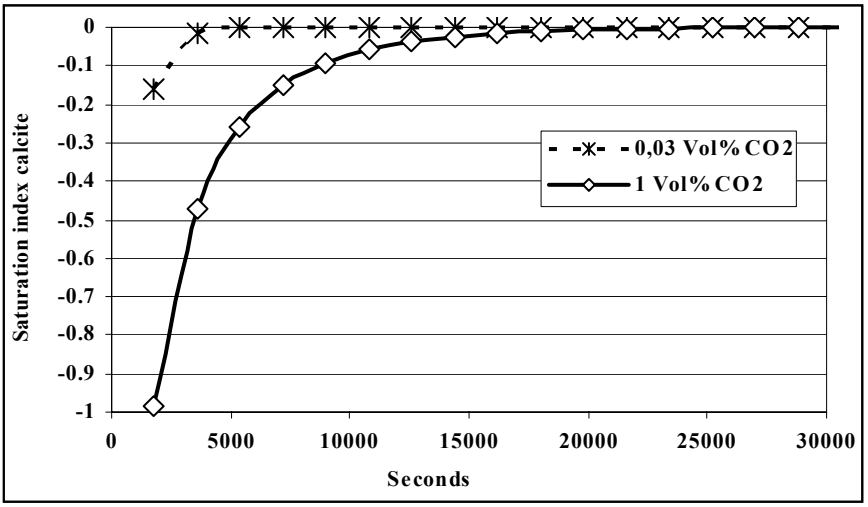

Fig. 38 Time-dependent calcite dissolution at 0.03 Vol% CO_2 (atmospheric pressure) and increased CO_2 partial pressure (1 Vol%)

In the following, an example for the definition of **pyrite weathering rates** is given:

```
KINETICS
# example for KINETICS data block for pyrite
        -tol      1e-8                      # tolerance for Runge_Kutta
        -m0       5e-4                      # initial amount of pyrite in mol
        -m        5e-4
        -parms -5.0    0.1    .5    -0.11   # parameter in kinetics equation
#       parm(1) = log10(A/V) in 1/dm
#       parm(2) = exponent for (m/m0)
#       parm(3) = exponent  for O2
#       parm(4) = exponent for H+
```

```
RATES
Pyrite
  -start
     5 rem Pyrite weathering rates
   10 if (m <= 0) then goto 200                  // m = mole of reactant *
   20 if (si("Pyrite") >= 0) then goto 200       // si = saturation index *
   20  rate = -10.19 + parm(1) \
   21     + parm(3)*lm("O2")  \
   22     + parm(4)*lm("H+")  \
   23     + parm(2)*log10(m/m0)                  // parm(i) = parameter*
                                                 // lm= log10 molality *
   30  moles = 10^rate * TIME                    // time interval defined in steps*
   40 if (moles > m) then moles = m
   50 if (moles >= (mol("O2")/3.5)) then moles = mol("O2")/3.5
   200 save moles
  -end
```

* the ´//´ included comments cannot appear like this in a PHREEQC-BASIC script since the BASIC interpreter is trying to interpret them. It is only possible to include commentary lines at the beginning of a line by means of REM (remark).

To be able writing own kinetics programs it is necessary to get familiarized with the programming language BASIC and particularly with the special BASIC-codes within PHREEQC.

2.2.2.2.2. BASIC within PHREEQC

The BASIC interpreter, which comes along with the Linux operating system (Free Software Foundation, Inc.), is implemented in PHREEQC. Amongst others things as already demonstrated, it is used for the integration of kinetic rates to determine converted quantities of substance in mol with respect to a given time. Therefore, a BASIC program for each kinetic reaction has to be ready either in the data set (PHREEQC.dat, WATEQ4F.dat, etc.) or in the respective input file. Each programs stands for itself (no global variables) and lines have to be numbered consecutively (e.g. 10, 20, 30,…). The transfer of data between the BASIC programs and PHREEQC is done by using the command GET and PUT as well as the command TIME. The final result of a kinetic calculation is acquainted to PHREEQC by means of SAVE. Thereby, no rates but quantities of moles are transferred that have reacted with a positive sign when the concentration of the reactant in solution has increased and vice verse a negative sign when the concentration has decreased.

The BASIC code can be used within the keyword RATES, but also for USER_GRAPH, USER_PRINT and USER-PUNCH and always occurs between the commands

-start
-end.

Table 26 presents a list of the standard commands within the BASIC interpreter of PHREEQC, Table 27 the special codes in BASIC of PHREEQC.

Table 26 List of standard commands within the BASIC interpreter of PHREEQC (Parkhurst & Appelo 1999)

+, -, *, /	Add, subtract, multiply, and divide
String1 + String2	String concatenation
a ^ b	Exponentiation
<, >, <=, >=, <>, =,AND, OR, XOR, NOT	Relational and Boolean operators
ABS(a)	Absolute value
ARCTAN(a)	Arctangent function
ASC(character)	ASCII value for character
CHR$(number)	Convert ASCII value to character
COS(a)	Cosine function
DIM a(n)	Dimension an array
DATA list	List of data
EXP(a)	e^a
FOR i = n TO m STEP k …….. NEXT I	"For" loop
GOTO line	Go to line number
GOSUB line	Go to subroutine
IF (expr) THEN statement ELSE state ment	If, then, else statement (on one line; a '\' may be used to concatenate lines)
LEN(string)	Number of characters in *string*
LOG(a)	Natural logarithm
LOG10(a)	Base 10 logarithm
MID$(string, n)	Extract characters from position *n* to end of *string*.
MID$(string, n, m)	Extract *m* characters from *string* starting at position *n*.
a MOD b	returns remainder a / b
ON expr GOTO line1, line2, ... ON expr GOSUB line1, line2, ...	If the expression's value, rounded to an integer, is *N*, go to the *N*th line number in the list. If *N* is less than one or greater than the number of line numbers listed, execution continues at the next statement after the ON statement
READ	Read from DATA statement
REM	At beginning of line, line is a remark with no effect on the calculations
RESTORE line	Set pointer to DATA statement of *line* for subsequent READ
RETURN	Return from subroutine
SGN(a)	Sign of *a*, +1 or -1
SIN(a)	Sine function
SQR(a)	a^2
SQRT(a)	$\sqrt{a}$
STR$(a)	Convert number to a string

TAN(a)	Tangent function
VAL(string)	Convert string to number.
WHILE (expression) … WEND	"While" loop

Table 27 Special codes in BASIC of PHREEQC

ACT("HCO3-")	Activity of an aqueous, exchange, or surface species
ALK	Alkalinity of solution
CELL_NO	Cell number in **TRANSPORT** or **ADVECTION** calculations
CHARGE_BALANCE	Aqueous charge balance in equivalents
DIST	Distance to midpoint of cell in **TRANSPORT** calculations, cell number in **ADVECTION** calculations, "-99" in all other calculations
EQUI("Calcite")	Moles of a phase in the pure-phase (equilibrium-phase) assemblage
EXISTS(i1[, i2, ...])	Determines if a value has been stored with a PUT statement for the list of one or more subscripts. The function equals 1 if a value has been stored and 0 if no value has been stored. Values are stored in global storage with PUT and are accessible by any BASIC program. See description of PUT for more details.
GAS("CO2(g)")	Moles of a gas component in the gas phase
GET(i1[, i2, ...])	Retrieves the value that is identified by the list of one or more subscripts. Value is zero if PUT has not been used to store a value for the set of subscripts. Values stored in global storage with PUT are accessible by any BASIC program. See description of PUT for more details
KIN("CH2O")	Moles of a kinetic reactant
LA("HCO3-")	Log10 of activity of an aqueous, exchange, or surface species
LM("HCO3-")	Log10 of molality of an aqueous, exchange, or surface species
M	Current moles of reactant for which the rate is being calculated (see **KINETICS**)
M0	Initial moles of reactant for which the rate is being calculated (see **KINETICS**)
MISC1("Ca(x)Sr(1-x) SO4")	Mole fraction of component 2 at the beginning of the miscibility gap, returns 1.0 if there is no miscibility gap (see **SOLID_SOLUTIONS**)
MISC2("Ca(x)Sr(1-x) SO4")	Mole fraction of component 2 at the end of the miscibility gap, returns 1.0 if there is no miscibility gap (see **SOLID_SOLUTIONS**)
MOL("HCO3-")	Molality of an aqueous, exchange, or surface species
MU	Ionic strength of the solution (mol)
PARM(i)	Parameter array defined in **KINETICS** data block
PERCENT_ERROR	Percent charge-balance error [100(cations-|anions|)/(cations + |anions|)]
PRINT	Write to output file
PUNCH	Write to selected-output file
PUT(x, i1[, i2, ...])	Saves value of *x* in global storage that is identified by a sequence of one or more subscripts. Value of *x* can be retrieved with GET(*i1*,[, *i2, ...*]) and a set of subscripts can be tested to determine if a value has been stored with EXISTS(*i1*[*, i2, ...*]). PUT may be used in

	RATES, **USER_PRINT**, or **USER_PUNCH** BASIC programs to store a value. The value may be retrieved by any of these BASIC programs. The value persists until overwritten using a PUT statement with the same set of subscripts, or until the end of the run. For a **KINETICS** data block, the BASIC programs for the rate expressions are evaluated in the order in which they are defined in the input file.
RXN	Amount of reaction (moles) as defined in **-steps** in **REACTION** data block for a batch-reaction calculation, otherwise zero
SAVE	Last statement of BASIC program that returns the moles of kinetic reactant, counted positive when the solution concentration of the reactant increases
SI("Calcite")	Saturation index of a phase, *Log*10 (*IAP/K)*
SIM_NO	Simulation number, equals one more than the number of **END** statements before current simulation
SIM_TIME	Time (s) from the beginning of a kinetic batch-reaction or transport calculation
SR("Calcite")	Saturation ratio of a phase, (IAP/K)
STEP_NO	Step number in batch-reaction calculations, or shift number in **ADVECTION** and **TRANSPORT** calculations
S_S("MgCO3")	Current moles of a solid-solution component
TC	Temperature in Celsius
TK	Temperature in Kelvin
TIME	Time interval for which moles of reaction are calculated in rate programs, automatically set in the time-step algorithm of the numerical integration method
TOT("Fe(2)")	Total molality of element or element redox state. TOT("water") is total mass of water (kg)
TOTAL_TIME	Cumulative time (s) including all advective (for which **-time_step** is defined) and advective-dispersive transport simulations from the beginning of the run or from last **-initial_time** identifier

2.2.2.3 Introductory example for reactive mass transport

After equilibrium reactions and kinetically controlled reactions, the reactive mass transport will be described as a final introductory example (for theory see chapter 1.3). Within PHREEQC there are two options to simulate one-dimensional transport with constant velocity. Using the keyword ADVECTION, simple simulations can be carried out by a mixing cell approach. Applying the keyword TRANSPORT, dispersion, diffusion and double porosity (mobile and immobile pores) can be taken into account. The units used are basically meter and seconds. One-dimensional modeling are well suited for simulating laboratory column experiments or to model processes in an aquifer along a theoretical flow path. Concerning the consideration of dilution processes during 1d-modeling in groundwater, see chapter 1.3.3.4.2.

The following example shows the result of a column experiment with an 8 m long column filled with a cation exchanger. First of all, the column was

equilibrated with a conditioning solution containing 1 meq/L $NaNO_3$ and 0.2 meq/L KNO_3. This solution had been added as long as the input solution leaked at the outlet. Thus, the cation exchanger was in equilibrium with the solution. Then the input solution was changed into a 0.5 meq/L $CaCl_2$ solution. The concentrations monitored at the outlet can be seen in Fig. 39. The time scale on the x-axis starts at 0 at the time of changing the input solution. The x-axis is scaled in water volumes and represents a threefold exchange of the water within the column (shift = 120).

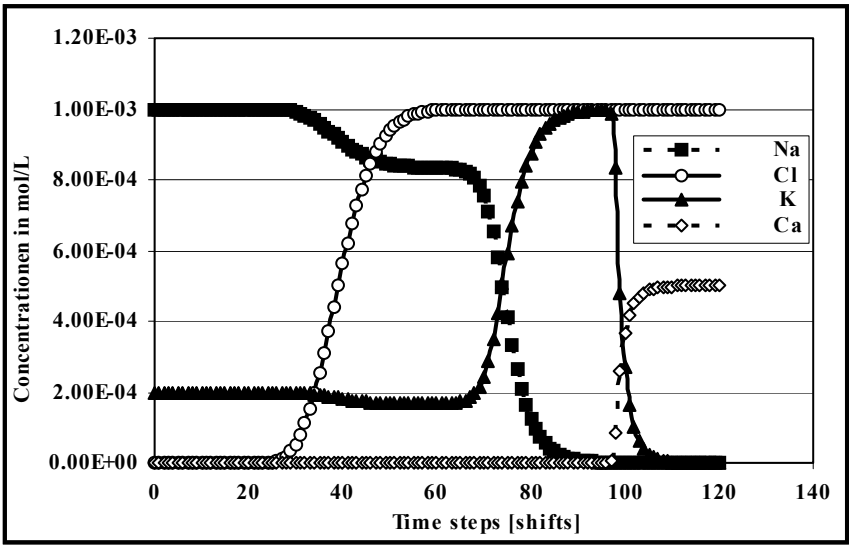

Fig. 39 Laboratory column experiment: course of the concentration at the column runoff; 40 "shifts" correspond to a complete exchange of water within the column

Chloride behaves like an ideal tracer and is only affected by dispersion. Calcium is still not in solution even after a single exchange of all water within the column (shift = 40) as it is exchanged for Na and K. When all sodium has been removed from the exchanger, Ca can only be exchanged for K that leads to a peak in the K-concentration. Only after the water of the column has been exchanged about 2.5 times, the concentration of calcium increases at the outlet.

In the next example the PHREEQC job is presented that simulates the experiment. To adjust the model to the data observed, the exchange capacity (X under EXCHANGE, here 0.0015 mol per kg water), the selectivity coefficients in the data set WATEQ4F.dat and the chosen dispersivity (TRANSPORT, dispersivity, here 0.1 m) are decisive besides the spatial discretisation (number of cells, here 40). If one sets the dispersivity to a very small value (e.g. $1 \cdot 10^{-6}$) in the input file "Exchange" and rerun the job, one will see that no numerical dispersion occurs showing that numerical stability criteria are maintained properly.

```
TITLE  column experiment with exchangers
PRINT
    -reset false                          # create no standard output
SOLUTION 0  CaCl2                         # new solution: CaCl2
      units        mmol/kgw
      temp         25.0
      pH           7.0    charge
      pe           12.5   O2(g)   -0.68
      Ca           0.5
      Cl           1.0
SOLUTION 1-40  Initial solution for column        # NaNO3 + KNO3
      units        mmol/kgw
      temp         25.0
      pH           7.0    charge
      pe           12.5   O2(g)   -0.68
      Na           1.0
      K            0.2
      N(5)         1.2
EXCHANGE 1-40                             # all cells of column (exchanger)
      equilibrate 1                       # equilibrate with solution 1
      X            0.0015                 # exchanger capacity in mole
TRANSPORT
      -cells       40                     # 40 cells
      -length      0.2                    # each 0.2 m; 40*0.2= 8 m length
      -shifts      120                    # refill each cell 120 times
      -time_step   720.0                  # 720 s per cell; --> v = 24 m/day
      -flow_direction  forward            # forward simulation
      -boundary_cond   flux   flux        # flow boundary condition at inlet and
                                          outlet
      -diffc       0.0e-9                 # diffusion coefficient m2/s
      -dispersivity  0.1                  # dispersivity in m
      -correct_disp  true                 # correction for dispersivity: yes
      -punch_cells   40                   # only cell 40 in Selected_Output
      -punch_frequency 1                  # print each time interval
      -print       40                     # print only cell 40 (outlet)
SELECTED_OUTPUT
      -file        exchange.csv           # output in this file
      -reset       false                  # print no standard output
      -step                               # default
      -totals      Na Cl K Ca             # output total concentrations
END
```

It is important to notice that a SOLUTION has to be given by default for all 40 cells of the column, at the beginning of the job (SOLUTION 1-40). When additionally kinetics and equilibrium reactions have to be taken into account, the same is true for the keywords KINETICS and EQUILIBRIUM_PHASES. Writing

KINETICS 1 instead of KINETICS 1-40, the kinetic reaction would only be taken into account for cell 1. The syntax of the keyword TRANSPORT is explained in detail in Table 28.

Table 28 Syntax of the keyword TRANSPORT in PHREEQC (Parkhurst & Appelo 1999)

Keyword	example	default	comments
TRANSPORT			
-cells	5	0	Number of cells in a 1D column to be used in the advective-dispersive transport simulation
-shifts	25	1	number of advective shifts or time steps, which is the number of times the solution in each cell will be shifted to the next higher or lower numbered cell; the total time simulated is *shifts * time_step*
-time_step	3.15e7	0	Time, in seconds, associated with each shift or diffusion period
-flow_direction	forward	forward	forward, back, or diffusion_only
-boundary_ conditions	flux constant	flux flux	constant, closed, flux for first cell and last cell
-lengths	4*1.0 2.0	1	Length of each cell (m). Any number of *lengths* up to the total number of cells (*cells*) may be entered
-dispersivities	4*0.1 0.2	0	Dispersivity assigned to each cell (m). Any number of *dispersivities* up to the total number of cells (*cells*) may be entered.
-correct_disp	true	true	true or false: When *true*, dispersivity is multiplied with (1 + 1/*cells*) for column ends with flux boundary conditions. This correction is recommended when modeling effluent composition from column experiments.
-diffusion_ coefficient	1.0e-9	0.3e-9	Diffusion coefficient in m^2/s
-stagnant	1 6.8e-6 0.3 0.1 5	0 0 0 0	Defines the maximum number of stagnant (immobile) cells associated with each cell in which advection occurs (mobile cell). The immobile cells are usually defined to be a 1D column that is connected to the mobile cell; however, the connections among the immobile cells may be defined arbitrarily with **MIX** data blocks. Each immobile cell that is used must have a defined solution and either a **MIX** data block must be defined or, for the first-order exchange model, the *exchange_factor* must be defined, for details refer to manual
-thermal_diffusion	3.0 0.5e-6	2 1e-6	temperature-retardation-factor and thermal diffusion coefficient; for details refer to manual
-initial_time	1000	cum mulativ	Time (seconds) at the beginning of the transport simulation. The identifier sets the

		e time	initial value of the variable controlled by **-time** in the **SELECTED_OUTPUT** data block.
-print_cells	1-3 5	1-n	Identifier to select cells for which results will be written to the output file.
-print_frequency	5	1	Identifier to select shifts for which results will be written to the output file.
-punch_cells	2-5	1-n	Identifier to select cells for which results will be written to the selected-output file.
-punch_frequency	5	1	Identifier to select shifts for which results will be written to the selected-output file.
-dump	dump.file	phree qc.dmp	Identifier to write complete state of a advective-dispersive transport simulation after every *dump_modulus* advection shifts or diffusion periods. The file is formatted as an input file that can be used to restart calculations.
-dump_frequency	10	shifts/2 or 1	Complete state of a advective-dispersive transport simulation will be written to dump file after *dump_modulus* advection shifts or diffusion periods.
-dump_restart	20	1	Starting shift number for the calculations, if restarting from a dump file. The shift number is written in the dump file by PHREEQC. It equals the shift number at which the dump file was created
-warnings	false	true	If true, warning messages are printed to the screen and the output file

3 Exercises

With the installation of the PHREEQC program, 18 examples are automatically installed in the folder "Examples". They include:
Example 1.--Speciation calculation
Example 2.--Equilibration with pure phases
Example 3.--Mixing
Example 4.--Evaporation and homogeneous redox reactions
Example 5.--Irreversible reactions
Example 6.--Reaction-path calculations
Example 7.--Gas-phase calculations
Example 8.--Surface complexation
Example 9.--Kinetic oxidation of dissolved ferrous iron with oxygen
Example 10.--Aragonite-strontianite solid solution
Example 11.--Transport and cation exchange
Example 12.--Advective and diffusive flux of heat and solutes
Example 13.--1D transport in a dual porosity column with cation exchange
Example 14.--Advective transport, cation exchange, surface complexation, and mineral equilibria
Example 15.--1D Transport: Kinetic biodegradation, cell growth, and sorption
Example 16.--Inverse modeling of Sierra spring waters
Example 17.--Inverse modeling with evaporation
Example 18.--Inverse modeling of the Madison aquifer

A detailed description of the solutions for these examples can be found in the PHREEQC manual (Parkhurst & Appelo 1999). In addition, the following exercises for equilibrium reactions (chapter 3.1), kinetics (chapter 3.2) and transport (chapter 3.3) will help the user to become familiar with the possibilities and limitations of the program. The solutions of all exercises are explained in detail in chapter 4.

All exercises have been modeled with PHREEQC version 2.8.03. This latest version, available at the time of book printing, can be found on the enclosed CD (there are different versions of installation for Windows, Mac or Unix workstations).

3.1 Equilibrium reactions

3.1.1 Groundwater - Lithosphere

3.1.1.1 Standard-output well analysis

The following hydrogeochemical analysis (Table 29) is given for the drinking water well ("B3") in the model area shown in Fig. 40 (concentrations in mg/L):

Table 29 Hydrogeochemical analysis of the drinking water well B3 from Fig. 40

Temperature = 22.3°C	pH = 6.7	pE = 6.9	
Ca = 75.0	Mg = 40.0	K = 3.0	Na = 19.0
HCO_3^- = 240.0	SO_4^{2-} = 200.0	Cl^- = 6.0	NO_3^- = 1.5
NO_2^- = 0.05	PO_4^{3-} = 0.60	SiO_2 = 21.59	F^- = 1.30
Li = 0.030L	B = 0.030	Al = 0.056	Mn = 0.014
Fe = 0.067	Ni = 0.026	Cu = 0.078	Zn = 0.168
Cd = 0.0004	As = 0.005	Se = 0.006	Sr = 2.979
Ba = 0.065	Pb = 0.009	U = 0.003	

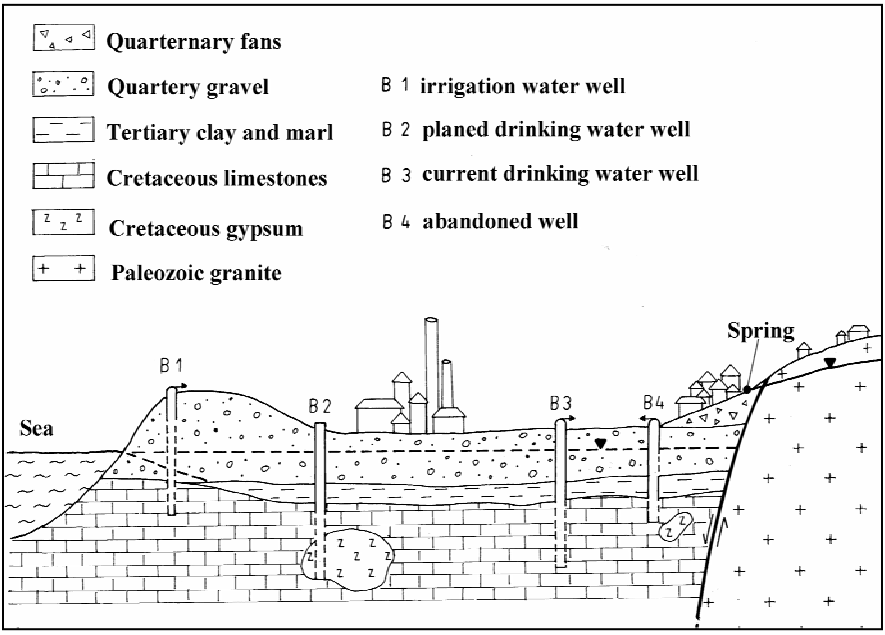

Fig. 40 Model area for exercises in the chapters 3.1.1.1 - 3.1.1.8, chapter 3.1.4.1, chapter 3.1.4.3, chapters 3.1.5.2 - 3.1.5.5

How would you interpret the analysis? Have a close look at the redox sensitive elements (which elements do not fit in the general scheme and why?). Present the species distribution of the Ca-, Mg-, Pb- and Zn-species in the form of a pie chart

(what is remarkable?). Illustrate the supersaturated Fe- and Al-mineral phases by means of two bar charts.

3.1.1.2 Equilibrium reaction - solubility of gypsum

The town council plans to drill a new well for drinking water supply. From a logistic point of view (lengths of water pipes), it should be closer to the town than the present drinking water well B3. The new, planned location can be found as "B2" in Fig. 40. Is the planned location advisable from a hydrogeochemical point of view? Assume that the general direction of groundwater flow is from the East to the West. Furthermore, regard the analysis of the drinking water well B3 as characteristic for the aquifer east of the B2. Point out changes in the water chemistry and take into account drinking water standards when drawing a final conclusion.

3.1.1.3 Disequilibrium reaction - solubility of gypsum

How does the water quality change when assuming that the retention times in the underground are so short that only a 50 %-saturation with regard to the predominant mineral phase will occur? (*Note: Using the key word* EQUILIBRIUM_PHASES, *it is not only possible to specify equilibria, but to determine defined disequilibria with the help of the saturation index as well. A saturation of 80% (undersaturation) would mean e.g.: IAP/KT = 80 % = 0.8; log IAP/KT = SI = log 0.8 ≈ -0.1; see also Eq.35*).

3.1.1.4 Temperature dependency of gypsum solubility in well water

Data of more recent drilling holes show a certain geothermal influence in the area of B2. How would different temperatures in the underground affect the water quality in the planed well B2 (simulation range 10, 20, 30, 40, 50, 60, 70°C with a saturation of 50 %)? [*key word* REACTION_TEMPERATURE]

3.1.1.5 Temperature dependency of gypsum solubility in distilled water

Only for comparison: How much gypsum will be solved in distilled water at the same temperatures? How can the difference be explained in comparison to the well water?

3.1.1.6 Temperature and $P(CO_2)$ dependent calcite solubility

In the well B3, seasonally changing amounts of calcium have been measured. This phenomenon is ascribed to karst weathering, which is not only dependent on

temperature but also on the CO_2 partial pressure in the soil (often increased CO_2 concentrations in the soil are a product of microbial decomposition reactions). Simulate the theoretical solubility of calcite for a whole year with temperatures on winter days of 0 °C and a low CO_2 partial pressure (corresponding to the value of the atmosphere) up to temperatures of 40 °C and a high bioproductivity ($P(CO_2)$ = 10 Vol%) during summer times.

The following pairs of temperature and CO_2 partial pressure are given:

Temp.(°C)	0	5	8	15	25	30	40
CO_2 (Vol%)	0.03	0.5	0.9	2	4.5	7	10

Where is the maximum of karst weathering (tabular and graphic illustration) and why?

[Note: Gas phases can be put into equilibrium like mineral phases. Instead of SI use the gas partial pressure p: Convert CO_2 Vol% into [bar] and form the logarithm; e.g. 3 Vol% = 0.03 bar = -1.523 $P(CO_2)$.]

3.1.1.7 Calcite precipitation and dolomite dissolution

What happens when not only pure calcium carbonate (calcite) but also magnesium calcium carbonate (dolomite) exists? Present your results graphically. How is this kind of reaction called? [*For simulation use mineral phase dolomite(d) = dispersive distributed dolomite*]

3.1.1.8 Calcite solubility in an open and a closed system

While simulating the two previous exercises 3.1.1.6 and 3.1.1.7 you always assumed that the amount of CO_2 was unlimited. Such systems are called “open systems”. In reality, this is very rare. Usually, there is only a restrained amount of gas available (closed system).

Simulate for the drinking water well B3 the solution of calcite for an open and a closed system using a temperature of 15 °C and partial pressures of 2 and 20 Vol% respectively. Where is the difference between the two systems? What changes with increasing partial pressure and why? Consider, besides the solution of calcite, changes in pH values, too.

[*Note: closed system: key word GAS_PHASE; here, the following parameters have to be defined: the total pressure = 1 bar, the volume = 1 L gas per L water, and the temperature of the gas = 35 °C; additionally: which gas is being used (CO_2) and which partial pressure exists (here not the log $P(CO_2)$ is used like in EQUILIBRIUM_PHASES, but the CO_2 partial pressure in bars!*]

3.1.1.9 Pyrite weathering

Many reactions are so slow that it is impossible to describe them using equilibrium reactions (e.g. the weathering of quartz, or pyrite in the absence of microorganisms). However, it is often interesting to figure out to what extent these

slow transformations affect the pH value or other (equilibrium) reactions in solution. Therefore, transformations are experimentally modeled to find out possible relations between the amount of reaction products and the time from sections of linear correlations.

When flooding an abandoned mine processes of oxidation and reduction are of great importance. Due to the supply of oxygen, protons and sulfate are formed changing the chemistry of ground water fundamentally, e.g. mobilisation of metals as a result of the decrease of the pH value ("acidification").

Model the oxidation of pyrite with different oxygen supplies (0.0, 0.001, 0.005, 0.01, 0.05, 0.1, 0.3, 0.6, 1.0 mol), and show the changes graphically for the two major elements building up from pyrite dissolution as well as for the pH value of the ground water given in Table 30.

Table 30 Water analysis of a ground water (concentrations in mg/L).

pH	6.5		
Redox potential	-120 mV	Al	0.26
Temperature	10.7 °C	SiO_2	24.68
O_2	0.49	Cl	12.76
Ca	64.13	HCO_3	259.93
Mg	12.16	SO_4	16.67
Na	20.55	H_2S	2.33
K	2.69	NO_3	14.67
Fe	0.248	NH_4	0.35
Mn	0.06	NO_2	0.001

[Note: The key word for the addition of definite amounts of a reactant to a solution is REACTION. The command SELECTED_OUTPUT, which has already been mentioned in chapter 2.2.1.4, is very useful here. It directly displays all required data in an extra file in a spreadsheet format, so the user does not have to look through the whole output manually. Under "molalities" and under "totals" the species of interest and the total concentration of an element can be issued, respectively.

In the data set used so far (WATEQ4F), NH_4 is not included. Therefore, it has to be defined as an additional species. It can be done either directly in the data set or – like in this example – in the input file (see chapter 2.2.1.1). For that, NH_4 has to be defined as a species and a respective reaction equation has to be included. The key words are the same as for their definition in the data set:

```
SOLUTION MASTER SPECIES
N(-3)     NH4                 0.0                 14.0067
SOLUTION_SPECIES
#NH4 secondary master species 127
          NO3- + 10H + 8e- =NH4+ + 3 H2O
          log_k               119.077
          delta h –187.055 kcal
```

Anything in the input file always overwrites information in the database. Thus, NH_4 can be defined as a species only for this exercise without changing the whole WATEQ4F data set and without having problems with regard to the maintenance of the data set, the verification of the consistency of the data sets, the existence of the products, and the differences in the conditions under which the solubility constants as well as the absolute values have been determined (see also chapter 2.1.4.1 and chapter2.1.4.2).]

Additionally, show if it is possible to attenuate the reactions when adding calcium carbonate. Add U_3O_8(c) as a mineral phase and test if a diminution in the concentration of uranium can be observed when adding calcium carbonate.

[It is worthwhile remarking that a lot of these slow reactions do not proceed linearly and therefore they can only be modeled to a first approximation. The weathering of pyrite, e.g., will be catalyzed by microbes which are subject to exponential growth and death. These kinetics are taken into consideration in chapter 3.2.1.]

3.1.2 Atmosphere – Groundwater – Lithosphere

3.1.2.1 Precipitation under the influence of soil CO_2

Considerable amounts of carbon dioxide are produced in the soil as a result of microbial degradation reactions. Particularly during the summer, concentrations of CO_2 soil gas of approximately 1-5 Vol% can be reached under humic climate. This amount is a significant increase compared to CO_2 partial pressures in the atmosphere of 0.03 Vol% (see also the exercise in chapter 3.1.1.6). Simulate the effect that a soil CO_2 partial pressure of 1 Vol% has on the following rainwater: Na = 8, K = 7, Ca = 90, Mg = 29, SO_4^{2-} = 82, NO_3^- = 80, C(+4) = 13 and Cl = 23 [all units in µmol/L]. Value of pH: 5.1, temperature: 21°C.

Attention: In PHREEQC, C(+4) has indeed to be expressed as C(+4) and not as alkalinity as we did it so far. Because of the low concentrations in rainwater, a "conventional" determination of the alkalinity is not possible, only the determination of the TIC (total inorganic carbon, C(+4)) can be done.

3.1.2.2 Buffering systems in the soil

How do the different buffer systems in the soil (Al-hydroxide-, exchanger- (50 % NaX, 30 % CaX_2, 20 % MgX_2), carbonate-, Fe-hydroxide-, Mn-hydroxide buffer) affect the chemical composition of the rainwater of the previous exercise (chapter 3.1.2.1) when it infiltrates in the soil (CO_2 partial pressure 1 Vol%)?

[For modeling the exchanger buffer use the key word EXCHANGE and then define the exchanger species and their respective amounts (e.g. NaX 0.5).]

3.1.2.3 Mineral precipitates at hot sulfur springs

The following analysis of a sulfur-rich thermal water is given (Table 31):

Table 31 Water analysis of a sulfur-rich thermal water (concentration in mol/L)

pH	4.317	pe	-1.407	Temperature	75°C
B	2.506e-03	Ba	8.768e-08	C	1.328e-02
Ca	7.987e-04	Cl	5.024e-02	Cs	9.438e-06
K	3.696e-03	Li	1.193e-03	Mg	2.064e-06
Na	4.509e-02	Rb	1.620e-05	S	8.660e-03
Si	7.299e-03	Sr	3.550e-06		

Model what happens when this water discharges at a spring outlet and comes into contact with atmospheric oxygen and CO_2. Take into account that the diffusion of gas in water proceeds relatively quickly but that the contact with oxygen results in redox reactions which much slower kinetics. Therefore, restrict the addition of oxygen with the help of the command REACTION from 1 mg O_2/L to the maximum amount of O_2 that can be dissolved assuming that the water close to the spring cools down to 45 °C (gas solubility decreases with increasing temperature, see chapter 1.1.3.1).

[Hint: Table 32 presents the O_2 gas solubility in cm^3 per cm^3 water at a partial pressure of 100 Vol%):

Table 32 Dependence of O_2 solubility on temperature at P(O_2) = 100 %

Temperature	Gas solubility	Temperature	Gas solubility	Temperature	Gas solubility
0	0.0473	20	0.0300	50	0.0204
5	0.0415	25	0.0275	60	0.0190
10	0.0368	30	0.0250	70	0.0181
15	0.0330	40	0.0225	90	0.0172

Estimate from Table 32 how much O_2 per liter water is dissolved at the given temperature and at an atmospheric O_2 partial pressure. For this approximation it can further be assumed that there is 1 mole O_2 in 22.4 liter gas.]

3.1.2.4 Formation of stalactites in karst caves

The rainwater of exercise chapter 3.1.2.1 infiltrates in a karst area. There is enough time that an equilibrium regarding the predominant mineral phase and an elevated CO_2 partial pressure of 3 Vol% can be reached.

In the underground, there is a karst cavern with an extension of 10 m length, 10 m width and 3 m height connected via a natural tunnel to the atmosphere. Approximately 100 liter of the infiltrated, calcareous water is dripping daily from the ceiling into the cavern, in which the CO_2 partial pressure is the same as in the atmosphere. Stalactites are forming (Fig. 41) – why and in which amount per year?

How many mm per year do the stalactites grow assuming that the density of calcite is 2.7 g/cm^3 and that approximately 15 % of the cavern ceiling is covered with stalactites?

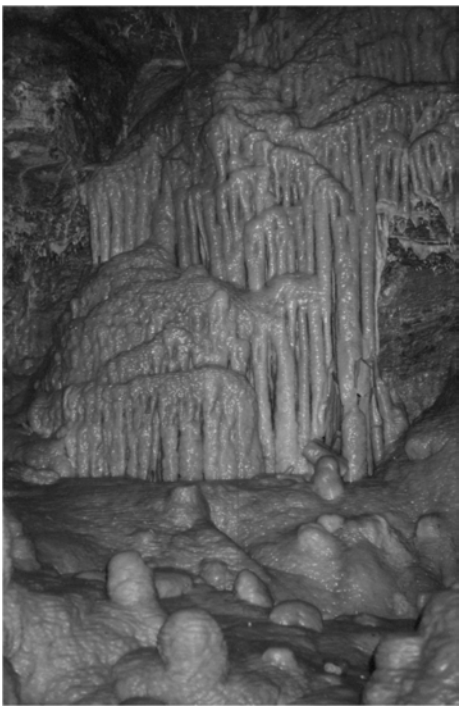

Fig. 41 Formation of stalactites in karst caverns

3.1.2.5 Evaporation

Evaporation changes the rainwater chemistry in the sense of a relative depletion of volatile components and a relative enrichment of non-volatile components.

As the calculation of the evaporation is quite tricky in PHREEQC, the following example is given for orientation. It is important to know that 1 kg of water consists of approximately 55.5 mol of H_2O. First, a titration with a negative amount of water (in mol) will be done, in order to remove pure water. Afterwards, the resulting, enriched solution has to be reconverted to 55.5mol by mixing the solution with itself.

```
Title 90 % evaporation as example
Solution 1 rainwater
…….
REACTION 1              # evaporation
H2O     -1.0            # remove water by -H2O!
```

```
        49.95 moles     #90 % evaporation; 100% = 1 kg H2O = 55.5 mol =>
                        #90% = 49.95 mol
                        #the resulting 10 % of the original amount of water
                        #have the same chemical composition as the 100 %
                        #before => the same amount of substance in less
                        #solvent, i.e. an enrichment has taken place
save solution 2
END
MIX
2       10              # mix SOLUTION 2 10 times with itself
                        # to get back to 100 % of enriched solution
save solution 3
END
….further reactions, e.g. equilibrium reactions etc.
```

Calculate the composition of seepage water with and without considering evaporation assuming that the annual average precipitation in an area is 250 mm, the current evaporation is 225 mm and the surface runoff is 20 mm. Use the rainwater analysis of exercise chapter 3.1.2.1. Furthermore, there is an increased CO_2 partial pressure of 0.01 bar in the unsaturated zone. This unsaturated zone consists mainly of limestone and sandstone.

Calculate the amount of calcite being dissolved every year in an area of 50 km · 30 km. How large is the volume of cavities created by this kind of karst weathering assuming a density of calcite of 2.6 g/cm^3? How much is the theoretical subsidence resulting from the calcite dissolution per year over the whole area of 50 km · 30 km? (Formation of caverns first prevents an immediate subsidence. Only after those caverns collapse, site specific subsidence structures appear at the surface. This aspect of time and spatial distribution shall be neglected for the calculations above.)

3.1.3 Groundwater

3.1.3.1 The pE-pH diagram for the system iron

In chapter 1.1.5.2.3, using the example of the system Fe-O_2-H_2O, it was demonstrated that the distributions of species can be determined analytically under different pH- and redox conditions and illustrated in a pE-pH-diagram. In the following examples, the numerical solution will be modeled with the help of PHREEQC.

The modeling is relatively simple. In the input file, certain pE- and pH values have to be defined besides the species in solution. After the modeling, the dominant species (i.e. the species with the highest concentration) has to be determined from the species distribution in the output. Varying the pH value between e.g. 0 (acid) and 14 (alkaline) as well as the pE value between e.g. -10 (reducing) and +20 (oxidizing) and listing the dominant species for each pE-pH

combination creates a pE-pH-diagram as a raster image. The smaller the increment (=step width) for the variation of pE and pH is chosen, the finer the raster of the pE-pH-diagram will be.

To avoid entering every pE and pH combination individually (e.g.: using an increment of 1 for pH and pE there would be 15 pH values x 31 pE values = 465 combinations!), a BASIC program was written. It copies a PHREEQC master input file, in which the job is defined for any pE and pH value once, and changes pE and pH step by step. The program can be found on the CD enclosed in this book ("ph_pe_diagramm.exe"). The program is asking for pH- and pE minimum values, maximum values and the increment ("delta"). Furthermore, the existing PHREEQC master input file and a new output file have to be chosen.

The program takes into account that aquatic species are limited in every pE-pH-diagram by the stability field of water. Therefore, the program deletes automatically all pE-pH combinations lying above the line of transformation O_2-H_2O or below the line of transformation H_2O-H_2. Assistance to the program can be found within the menu HELP.

When considering the increment of 1 for pE and pH, i.e. 15 pH values · 31 pE values, the output file would comprise 465 jobs, numbered from SOLUTION 1 to SOLUTION 465, each containing different pE- and pH values. In fact, there will be only 377 jobs since the SOLUTIONs with pE-pH values above or below the stability field of water are missing. The water constituents defined under SOLUTION (e.g. Fe, Ca, Cl, C, S, etc.) are alike in all 377 jobs. Opening this input file takes about 30 seconds. Because files larger than 32 k cannot be opened in the Windows environment of PHREEQC either they have to be divided into smaller files or they have to be started directly with phreeqc.exe in the DOS prompt (phreeqc Input-File-Name Output-File-Name Database name).

To avoid looking for the predominant species in 377 output jobs manually after modeling, two means are offered: At first, a SELECTED_OUTPUT (see also chapter 2.2.1.4) has to be defined in the PHREEQC master input file. Besides pE and pH, it will output all species of interest, for example all Fe species, in a .csv file. These species have to be specified explicitly under the sub key word "-molalities", e.g. Fe2+, Fe3+, FeOH+, etc. The BASIC-reproduction program inserts the 377 SOLUTION jobs before the key word SELECTED_OUTPUT. Since the SOLUTIONs are not separated by an END, a SELECTED_OUTPUT will be created out of all SOLUTIONs displaying for each of the 377 jobs a row with the columns pH, pE, m_Fe2+ (concentration of Fe2+ in mol/L), m_Fe3+, m_FeOH+, etc.

To open and to view this csv file use GRID in PHREEQC. The species with the highest concentration (predominant species) have to be determined for each row (i.e. for each pE-pH combination). To avoid doing this manually, the data have to be copied into EXCEL and to be treated with a macro, which can also be found on the CD enclosed in this book. The macro can be activated by opening the Excel file "macro.xls" from the book´s CD and by clicking on "activate macros". Now, one can either copy data instead of the given test data into table 1 or open the .csv file directly in Excel. The activated macro is available for all open Excel files. The macro itself can be opened under menu Extras / Macro / Macros under the name

"maxwert". Using the menu "edit", the macro can be viewed and edited. Also the data range as well as the number of rows and columns for the data range has to be defined under "edit". The definition for the test data follows:

```
Sub maxvalue
‘ adjust N% and M% as well as the data range
N% = 6: M% = 4    ‘ N% = number of rows, M% = number of columns
Dim name As Range
Dim wert As Range
Set name = Worksheets("Table1").Range("A1:D1")
Set wert = Worksheets("Table1").Range("A1:D6")
```

The values marked in bold have to be changed according to the current data range. If data has been pasted into table 1 replacing the test data, the name of the worksheet needs no further modification. If the .csv file has been opened directly, the name of the current worksheet has to be entered in the macro.

The macro is started using the play button (▸) or the menu Execute/Execute SubUserForm. Then the macro automatically scans each row for the cell with the highest value (= the highest concentration). The columns pH and pE are skipped automatically. For each cell found with a maximum value the respective header cell is written into the first empty row right next to the defined data range. The completed EXCEL table finally has one column more than the original .csv file, in which the names of the predominant species for each pE-pH combination are given (Attention: If the data range has been defined too small by mistake, the program will overwrite a column of the original data!). Note: The macro neither closes automatically nor displays the end of the calculation. The calculation will be finished after approximately 5 seconds at the most. After that, the Microsoft Visual BASIC window has to be closed manually to go back to the modified EXCEL table.

With the 3 columns pE, pH and predominant species, a pE-pH-diagram can be generated as a raster image in Excel. The first step is to sort all three columns according to the column "predominant species" (menu Data / Sorting). The most suitable diagram type is scatter plot (XY) with X = pH and Y = pE. When highlighting the columns pE and pH and creating a scatter diagram all points will appear automatically in the same color (Note: To obtain a raster object choose a filled rectangle as point symbol by double-clicking on the XY points. Vary the size of the rectangles so that a completely filled surface results, approximately 20 pt).

If the individual predominant species appear each in a different color, click with the right mouse button in the diagram and choose the window "data source". Under "row" you can define a data series for each species (per default, there is only one data set with the name "pe" comprising all species). Further data series can be defined by using "Add", e.g. the series Fe2+, with name (Fe2+), X value (as found in the table, e.g. in column A from row 146 to 268) and the respective Y values (B 146 – B 268). The X and Y values can be defined most simply by clicking with the mouse on the red arrow beside the cells for X values and Y

values and mark the respective cells in the table (A146-A268 for X, B146-B268 for Y). As soon as a data set has been defined for each species, different colors will be assigned to them automatically. A raster-pe-pH-diagram is obtained reflecting the predominance of individual species by differently colored zones.

Create a pE-pH-diagram of the predominant iron species in a solution, which contains 10 mmol/L Fe and 10 mmol/L Cl. Vary pH and pE values from 0 to 14 and from -10 to +20, respectively, in steps of 1 as well as of 0.5.

Note: When varying pH and pE in steps of 0.5 the generated PHREEQC input file will be too large to open it within the PHREEQC Windows environment. Therefore, either start PHREEQC from the DOS-prompt or divide the input file in 4 files (a = pH 0-7, pE -10 to +5; b = pH 0-7, pE 5.5-20; c = pH 7.5-14, pE -10 to +5; d = pH 7.5-14, pE 5.5-20).

3.1.3.2 The Fe pE-pH diagram considering carbon and sulfur

How does the pE-pH diagram created in chapter 3.1.3.1 change when 10 mmol/L S(6) or 10 mmol/L C (4) in solution are taken into account?

3.1.3.3 The pH dependency of uranium species

An acid mine water mixes downstream of a mine with groundwater of the following chemical composition (Table 33).

Table 33 Water analysis of an acid mine drainage AMD (pH = 2,3) and of a groundwater GW (pH = 6,6) (concentrations in mg/L)

	GW	AMD		GW	AMD		GW	AMD
pE	6.08	10.56	Cu	0.005	3	Ni	0.005	5
Temperature	10	10	F	0.5	1	NO_3^-	0.5	100
Al	3.0	200	Fe	0.6	600	Pb	0.05	0.2
As	0.004	2	K	1.5	4	pH	6.6	2.3
C(4)	130		Li	0.02	0.1	Si	3.64	50
Ca	36.6	400	Mg	3.5	50	SO_4^{2-}	14.3	5000
Cd	0.0003	1	Mn	0.07	20	U	0.005	40
Cl	2.1	450	Na	5.8	500			

How do the uranium species change? Which species predominate at which pH value? What are the effects of the change in uranium species concerning processes of transport and sorption?

Note: The PHREEQC key word for the mixing of two waters is MIX. Here you have to enter the number of the solution and the percentage, to which the solution contributes to the mixture. Assuming a mixture of 25 % from solution 1 and 75 % from solution 2 may be expressed in the one or the other form:

MIX MIX
1 0.25 1 1
2 0.75 2 3

When mixing the acid mine drainage, assume that it will be diluted 1:1 with groundwater. Dilute this water again 1:1 with groundwater and so on until you obtain more or less pure groundwater. Save the first 1:1 diluted solution using the key word SAVE_SOLUTION 3, terminate the job with END, and start the next job with USE_SOLUTION 3, etc.

3.1.4 Origin of groundwater

Inverse modeling

The determination of the origin of groundwater is an important aspect of hydrogeological investigations. For establishing drinking water protection zones e.g. it is necessary to know the groundwater´s origin to determine possible geogenic or anthropogenic contamination potential and its impact on the extracted groundwater.

The basic idea is to reconstruct geochemical evolution of the groundwater from its chemical composition. For example, knowing the chemical composition of a well on the one hand and an analysis of the rainwater on the other, it will be possible to reconstruct which geological formation the rainwater must have passed after its infiltration to change its chemical composition as the result of reactions with mineral and gas phases (dissolution, precipitation, degassing) in a way that accounts for the composition of the water from the well.

The key word in PHREEQC is "Inverse Modeling". The primary solution(s) (rainwater) and the final product (well water) have to be defined as SOLUTION as well as the involved mineral- and gas phases as PHASES. The structure of such a job follows:

```
TITLE Inverse Modeling
SOLUTION 1                # original water (rainwater)
SOLUTION 2                # water after the reaction with minerals and gases
                          # (well water)
INVERSE MODELING
        - solutions 1 2   # solution 1 transforms into solution 2
        - uncertainty 0.1 # 10 % uncertainty equally defined for all elements in
                          #the analysis and both waters 1 and 2
        - balance Ca  0.2  0.3    # for special elements higher uncertainties can
                                  # be defined, e.g. for elements whose
                                  # determination underlies a greater error,
                                  # e.g. 20 % error for the amount of Ca in
                                  # solution 1 and 30 % error for the amount of
                                  # Ca in solution 2
        - phases                  # definition of involved phases
```

```
    K-mica     dissolve      # mica can only be dissolved
    CO2(g)                   # both dissolution and degassing possible
    SiO2(a)                  # both dissolution and precipitation possible
Kaolinite      precip        # allow only for precipitation

END                          # end of the job
```

Note: For each element in solution 1 or solution 2, a mineral or gas phase has to be defined under PHASES that contains this element. Otherwise PHREEQC reports the following problem: "element is included in solution 1, but is not included as a mass-balance constraint". The modeling can still be continued, however the respective element is not considered for the mass balance.

The number of the mineral phases as well as the size of the uncertainty should be varied to simulate different possible situations. Maybe the program does not find a valid model after the first calculation. Then the mineral phases have to be changed or completed or the uncertainty has to be increased, whereas of course uncertainties of > 10 % do not permit any reliable predictions anymore. Also including as many mineral and gas phases as possible, does not help. The main goal is to exclude as many reaction pathways as possible and find others with a minimum of necessary gas and mineral phases.

Depending on the number of mineral phases and the uncertainty chosen the program displays one or more models in the output. Each model describes how much of each mineral was dissolved or precipitated to transform solution 1 (rainwater) into solution 2 (well water) (key word: phase mole transfers). If you enter several initial solutions (e.g. 5 analyses of rainwater from 5 individual altitudes), the program will also calculate the share of the respective rainwater solutions contributing to the final solution (well water).

3.1.4.1 Origin of spring water

Inverse modeling is to be carried out for the spring water in the eastern part of the model area (Fig. 40) to determine the geological formation from which the spring water originates. The hydrogeochemical data can be found in Table 34.

Table 34 Water analysis of a spring water (concentrations in mg/L)

pH	6.5		
Redox potential	-120 mV	Al	0.26
Temperature	10.7 °C	SiO_2	24.68
O_2	0.49	Cl	12.76
Ca	64.13	HCO_3	259.93
Mg	12.16	SO_4	16.67
Na	20.55	H_2S	2.33
K	2.69	NO_3	14.67
Fe	0.248	NH_4	0.35
Mn	0.06	NO_2	0.001

Analysis of the rainwater:
Na=323, K=65, Ca=165, Mg=120, SO_4^{2-}=712, NO_3^-=205, HCO_3^- =527, Cl=234 [concentrations in µg/L]; pH: 5.1, temperature: 21°C.

Mineralogical investigations showed that the following trace minerals exist additionally to the main minerals in the following geological formations:

- $Fe(OH)_{2.7}Cl_{0.3}$, FeS_2, MnO_2, arsenolite in the crystalline basement
- NaCl and $CaMg(CO_3)_2$ in the Cretaceous limestones
- FeOOH, Ca-montmorillonite and K-mica in the Quaternary sediments

Proceed with the assumption that neither feldspars nor mica nor halite nor gypsum will form under the given conditions. However, clay minerals such as Ca montmorillonite can precipitate.

Give reasons for your chosen model regarding the special geological location of the spring and try to use a minimum of mineral phases.

[see exercise chapter 3.1.1.9 for definition of a data set of non-existent species]

3.1.4.2 Pumping of fossil groundwater in arid regions

50 L/s groundwater of the following composition (Table 35) are extracted from a well in an arid zone.

Table 35 Water analysis of a groundwater (pH = 6.70, temperature = 34.5 °C, concentrations in mg/L)

K	2.42	Na	12.96	Ca	247.77	Mg	46.46
Alkalinity	253.77	Cl	6.56	NO_3^-	2.44	SO_4^{2-}	637.75
SiO_2	4.58	^{13}C	-6 ± 0.8	^{2}H	-68 ± 0.6	^{18}O	-9.6 ± 0.3

It is known that only a small amount of the extracted groundwater originates from recent groundwater resources (Table 36). The rest is extracted from a reservoir of fossil water that has been formed 20.000 years ago when temperatures were considerably lower in that area than they are today.

The fossil water is characterised by high total mineralization as a result of long residence times in the subsurface as well as by lower ^{2}H and ^{18}O isotope values as a result of the lower temperatures during formation (Table 37). The different amounts of ^{13}C can be explained by the establishment of equilibrium of the fossil groundwater with marine limestones with higher amounts of ^{13}C than recent groundwater, which reflects the lower concentrations of ^{13}C in the atmosphere.

Table 36 Water analysis of a recent groundwater (pH = 6.70, temperature = 28.0 °C, concentrations in mg/L)

K	2.87	Na	14.60	Ca	72.60	Mg	20.50
Alkalinity	247.97	Cl	4.00	NO_3^-	4.52	SO_4^{2-}	69.96
SiO_2	32.16	^{13}C	-22 ± 1.4	^{2}H	-52 ± 0.5	^{18}O	-7.5 ± 0.3

Table 37 Water analysis of a fossil groundwater (pH = 6.90, temperature = 40 °C, concentrations in mg/L)

K	3.33	Na	18.41	Ca	351.80	Mg	65.96
Alkalinity	298.29	Cl	9.00	NO_3^-	1.35	SO_4^{2-}	906.15
SiO_2	20.74	^{13}C	0 ± 0.4	^{2}H	-76 ± 0.7	^{18}O	-10.5 ± 0.4

Apply inverse modeling to determine how much of the extracted groundwater originates from the reservoir of fossil water. Also take into account that the extracted groundwater has been in contact with sandstones, dolomitic limestones, gypsum and halite and that under the given conditions neither dolomite nor gypsum nor halite are formed. Assume precipitation for calcite and degassing of CO_2.

If the amount of fossil water in the extracted groundwater is known an estimation can be given on how long it will take to completely exploit the approximately 5 m high, 1 km wide and 10 km long reservoir assuming a constant rate of production of 5 L/s.

Note: Remember the explanation in the introduction of chapter 3.1.4 that the portions of several initial solutions on the final solution can be modeled with the help of the inverse modeling!

To include the isotopes in the modeling, they have to be defined under each respective SOLUTION using the sub keyword "isotope".

```
SOLUTION
    -isotope [name of the isotope in the following form: mass number element]
[value in %, pmc or as ratio] [uncertainty in % (possible, but not necessary)], e.g.
    -isotope   13C   -6   0.8
    Instead of the sub key words –isotope the abbreviation –i can be used.
    Isotope data can only be used for inverse modeling. There, the respective
isotopes have to be listed again under the key word Inverse_Modeling and under
the sub key word –isotopes, e.g.
    INVERSE_MODELING
        -isotopes
        13C
        2H
        18O
    Additionally for each mineral or gas phase containing these isotopes their
share has to be defined (mean value, in the example 2 ‰ and deviation, in the
example ± 2 ‰) and whether the respective phase shall be dissolved or
precipitated, e.g.
        -phases
        calcite          pre      13C      2.0      2
```

Consider an average concentration of 13C between 1-5 ‰ for dolomite, 0-4 ‰ for calcite and -20 to -30 ‰ for CO_2. The isotopes ^{2}H and ^{18}O can only be found in the water molecule. Therefore they do not have to be defined for a mineral phase.

If you want to keep the option of dissolution or precipitation open, define the mineral phases twice, once using dis (dissolve), and a second time using pre (precipitate).

3.1.4.3 Salt water / fresh water interface

As a result of the groundwater extraction in coastal areas, seawater intrusions occur, leading to a mixture of salt water and fresh water. Such a mixed ground water of the following chemical composition is extracted from the irrigation water well B1 in the model area west of the town (Fig. 40): pH = 6.58, temperature = 13.4 °C, Ca = 3.724e-03 mol/L, Mg = 1.362e-02mol/L, Na = 1.080e-01 mol/L, K = 2.500e-03 mol/L, C = 7.067e-03 mol/L, S = 6.780e-03 mol/L, Cl = 1.261e-01 mol/L, P = 7.542e-06 mol/L, Mn = 8.384e-10 mol/L, Si = 1.641e-05 mol/L, Fe = 8.248e-09 mol/L.

The results of the analysis of the seawater are as follows: pH = 8.22, temperature = 5.0 °C, Ca = 412.3 mg/L, Mg = 1291.8 mg/L, Na = 10768.0 mg/L, K = 399.1 mg/L, HCO_3^- = 141.682 mg/L, SO_4^{2-} = 2712.0 mg/L, Cl = 19353.0 mg/L, Si = 4.28 mg/L, Mn = 0.0002 mg/L, Fe = 0.002 mg/L. Furthermore, consider a higher density for seawater (1.023 g/cm^3)!

The following analysis is given for the Quaternary aquifer: pH = 6.9, temperature = 18 °C, Ca = 65.9 mg/L, Mg = 40.1 mg/L, Na = 3.5 mg/L, K = 7.5 mg/L, HCO_3^- = 405.09 mg/L, SO_4^{2-} = 23.4 mg/L, Cl = 15.8 mg/L, PO_4^{3-} = 0.921 mg/L.

Determine the origin of the mixed ground water (i.e. the share of seawater and fresh ground water) taking into account the geological features around the irrigation water well. Keep in mind that there is no distinct aquiclude between the Quaternary and the Cretaceous aquifer.

Note: In general, check each analysis regarding the analytical error and enforce, if necessary, a charge balance when the deviations are too high before starting the modeling.

3.1.5 Anthropogenic use of groundwater

3.1.5.1 Sampling: Ca titration with EDTA

To determine the amount of calcium in a water sample, e.g. the titration with EDTA (ethylenediaminetetraacetate, $C_2H_4N_2(CH_2COOH)_4$) can be used. First of all, NaOH is added to the sample to obtain a pH value of at least 12. Then, a color indicator is admixed and titration with EDTA performed until the color changes. In doing so, all Ca is converted to a Ca-EDTA complex and detected in this form.

Model the determination of the concentration of Ca of the following analysis with PHREEQC: pH = 6.7, temperature = 10.5 °C, Ca^{2+} = 185 mg/L, Mg^{2+} = 21 mg/L, Na^+ = 8 mg/L, K^+ = 5 mg/L, C(4) = 4.5 mmol/L, SO_4^{2-} = 200 mg/L, Cl = 90 mg/L, NO_3^- = 100 mg/L.

The amount of EDTA that has to be added until the color changes is unknown. Therefore, EDTA is added step by step and the titration is continued beyond the point of color change. The point of color change will be determined afterwards using the obtained graph.

[EDTA cannot be found in the previously used data set WATEQ4F.dat. It is only defined in the data set MINTEQ.dat. Therefore, use this one. The key word for the addition of EDTA is the same as for the exercise in chapter 3.1.1.9.]

3.1.5.2 Carbonic acid aggressiveness

In drinking water standards it is often required that "water should not be aggressive". In most cases this "aggressiveness" refers to the carbonic acid. The reason for the requirement of a low aggressiveness is not of toxicological but of technical nature since carbonic acid waters easily corrode materials of pipelines (concrete, metals, plastics). Regulations therefore recommend, that the measured pH value shall only differ ± 0.2 pH units from the pHc (the pH value at calcite saturation) ($\Delta pH = pH - pHc$). The aim is to have a pH value that is slightly above the pHc value (0.05 pH units) because then a protective layer can develop on the pipe walls. On the contrary, significant supersaturation ($\Delta pH > 0.2$) lead to noticeable calcite deposits within the pipes and calcite scales are as undesirable as undersaturation ($\Delta pH < -0.2$), which leads to corrosion.

Additionally, potable water should not exceed pH values of 9.5 or fall below pH values of 6.5.

Consider these technical requirements when checking if the potable water extracted from the drinking water well B3 in the model area (chapter 3.1.1.1, Fig. 40) can be used without further treatment.

3.1.5.3 Water treatment by aeration - well water

Check whether an open aeration from equilibrium with atmospheric CO_2 (open system) would help to meet the requirements concerning the pH as well as the ΔpH for the drinking water which is extracted from well B3 in the model area (Fig. 40).

[Note: For simulating the open aeration and the calculation of the new pHc in one job, use the commands SAVE_SOLUTION, END and USE_SOLUTION 1 like in the exercise in chapter 3.1.3.3.]

3.1.5.4 Water treatment by aeration - sulfur spring

For the little village as well as for some individual farms in the eastern part of the model area (Fig. 40), a possibility for drinking water supply is sought. The spring discharging east of the village shall be investigated for suitability. Its chemical composition is given in chapter 3.1.4.1, where its geological origin has already been modeled.

Illustrate the species distribution for the elements aluminium, iron(II) and iron(III). Then, model a water treatment in terms of an open aeration with atmospheric oxygen (oxidation!). What happens to the Al- and Fe species? Which mineral phases will presumably precipitate during the aeration?

Vary the partial pressure of oxygen. What is remarkable?

Is the pH value after the aeration still within the limits required for potable water?

To set up the dimensions of a water treatment plant correctly, it is important to know the amount of sludge that will form every day as the result of the precipitation of mineral phases. Enforce the precipitation of the mineral phases that are most likely to precipitate during aeration in your model and calculate the accumulating amount of sludge per day assuming a production rate of 30 L/s in the future water treatment plant. Do not forget that sludge does not only consist of the precipitated mineral phases but mainly of water (60-90 %).

Evaluate your model with regard to the elements N and S. What will the results rather look like in reality and why?

3.1.5.5 Mixing of waters

Not far from the drinking water well B3 in the model area (Fig. 40) there is an older, abandoned well B4 that has been shut down for several years as it did not meet the quality requirements for potable water anymore. Recent investigations showed the following result: pH = 6.99, temperature = 26.9°C, Ca^{2+} = 260 mg/L, Mg^{2+} = 18 mg/L, Na^{+} = 5 mg/L, K^{+} = 2 mg/L, HCO_3^{-} 4 = mmol/L, SO_4^{2-} = 260 mg/L, Cl^{-} = 130 mg/L, NO_3^{-} = 70 mg/L.

It is planned to reactivate the well B4 to support peak times of water consumption and to mix the extracted water with that of the current drinking water well B3. Check with the help of PHREEQC modeling if and in which shares this can be done with regard to general requirements of drinking water standards and to the technical requirements in terms of the calcite-carbondioxide equilibrium (chapter 3.1.5.2). *[key word for mixing of two waters see the exercise in chapter 3.1.3.3.]*

3.1.6 Rehabilitation of groundwater

3.1.6.1 Reduction of nitrate with methanol

Groundwater from the exercise in chapter 3.1.5.1 in an area with intensive agriculture shows extremely high concentrations of nitrate due to years of excessive fertilization. Methanol as a reducing agent shall be pumped into the aquifer via infiltration wells to reduce the pentavalent nitrogen (nitrate) to the zero valent gas nitrogen. The latter can degas leading to a decrease of nitrate concentrations in the aquifer. How many liters of a 100 % methanol solution (density of methanol = 0.7 g/cm^3) per m^3 aquifer have to be pumped into the

aquifer to guarantee an effective reduction of nitrate concentrations? What effect could an "overdose" of methanol have?

3.1.6.2 Fe(0) barriers

Reactive barriers of elemental iron are used to reduce groundwater constituents in-situ and thus, to convert e.g. mobile uranium(VI) into uranium(IV) that precipitates as uraninite (UO_2). At the same time, the elemental iron in the reactive barriers oxidizes and iron hydroxide and, secondary, crusts of iron oxide form. Precipitated iron hydroxides and uraninite reduce the reactivity of the barrier after a certain time.

The uranium containing mine water of the exercise in chapter 3.1.3.3 shall be cleaned by means of such a reactive barrier. How much iron per m^2 has to be used considering a percolation of the reactive barrier of 500 $L/d \cdot m^2$ to reduce the amount of uranium from 40 mg/L to at least one third taking into account that the barrier shall be in operation for approximately 15 years? How much uraninite will precipitate?

3.1.6.3 Increase in pH through a calcite barrier

To increase the pH of the acid mine drainage from the exercise in chapter 3.1.6.2 a reactive wall of 1 m thick calcite (density of calcite = 2500 kg/m^3) shall be installed within the aquifer. Thickness and permeability of the wall are chosen in a way that a 50 % saturation of lime in the aquifer can be reached with a daily percolation of 500 L/m^2.

Does the calcite wall lead to the desired increase of the pH value? And why are there still objections against the reactive calcite wall taking into account the long-term efficiency and premature alteration? Which carbonates could be chosen alternatively to calcium carbonate to avoid a premature alteration?

3.2 Reaction kinetics

3.2.1 Pyrite weathering

Diffusion calculations for a covered heap containing pyrite rocks show that 0.1 m^3 of oxygen enter the heap every day by diffusion. It is assumed that this oxygen is completely consumed by pyrite oxidation within one day. Therefore, reaction kinetics is exclusively determined by the diffusion rate of the oxygen into the heap. An average of 0.1 mm of rainwater infiltrates through the heap cover daily. The rainwater has a pH of 5.3, a temperature of 12 °C and is in equilibrium with the CO_2 and O_2 partial pressure of the atmosphere. The heap covers an area of 100 m x 100 m, has a height of 10 m, and a pyrite concentration of 2 Vol%. The following questions are to be solved:

1. What is the chemical composition of the seepage water discharging at the foot of the heap along the base sealing?
2. What happens when water at the foot of the heap gets in contact with atmospheric oxygen?
3. How many years will it take until all pyrite in the heap is exhausted?
4. How much carbonate has to be added during the heap construction to neutralise the pH value? Is it possible to reduce the amount of sulfate at the same time?
5. How does the necessary amount of carbonate change when assuming that a CO_2 partial pressure of 10 Vol% will develop within the heap as a result of the decomposition of organic matter?

Instead of assuming an oxygen diffusion rate as in this example, it is also possible to define a pyrite oxidation rate R that is a function of e.g. O_2, pH, temperature, the amount of microorganisms and the nutrient supply. Examples using direct reaction rates in PHREEQC follow in the next exercises.

3.2.2 Quartz-feldspar-dissolution

Model the dissolution of quartz and K-feldspar (adularia) over time. Are the parameters temperature and CO_2 partial pressure of any importance? Within the key word RATES use the BASIC program from the data set PHREEQC.dat. The calculation is done with distilled water (pH = 7, pE = 12) as a batch reaction over a time span of 10 years in 100 time steps at a temperatures of 5 °C and of 25 °C and at CO_2 partial pressures of 0.035 Vol% (atmosphere) and of 0.7 Vol% (soil). Calculate also the kinetics of the dissolution with 0.035 Vol% CO_2 and 25 °C for a period of 10 minutes.

[Note: The data set WATEQ4F.dat uses the name adularia for K-feldspar. Use EQUILIBRIUM_PHASES to fix the oxygen concentration to 21 Vol%. Enter quartz with "0 0" under the same key word. While the first zero limits the solubility to 100% saturation, the second zero indicates the possible amount of quartz added in moles. Zero means no further quartz addition (dissolution), i.e. that the 100% saturation can only be achieved through precipitation at supersaturation, but not through dissolution at undersaturation. This step is necessary, since the dissolution will be defined using KINETICS and RATES. It is quite useful, too, to limit the solubility of aluminium by the precipitation of e.g. kaolinite. In the simplest case this can be done by EQUILIBIUM_PHASES as well since this precipitation occurs spontaneous and fast. Thus, a kinetic modeling is not necessary.

Using the minerals quartz and kaolinite in EQUILIBRIUM_PHASES causes a problem in PHREEQC regarding the elements Si and Al because they do not occur within the key word SOLUTION. Therefore you have to specify them in very small quantities in the solution (e.g. 1 µg/L). Furthermore, the sub key word -step_divide 100 within the key word KINETICS is necessary. The output can be obtained most effectively using SELECTED_OUTPUT.]

3.2.3 Degradation of organic matter within the aquifer on reduction of redox sensitive elements (Fe, As, U, Cu, Mn, S)

The degradation of organic matter results in the consumption of oxygen. Under certain circumstances, this may lead to the reduction of oxygen-containing anions like nitrate (see also the exercise in chapter 3.1.6.1) and sulfate, as well as to the reduction of redox sensitive elements like iron, manganese, or uranium. The decomposition of organic matter depends on the presence of microorganisms and is thus always connected to kinetics.

The reactions in an aquifer shall be modeled in the presence of calcite and large concentrations of pyrite and organic matter for the acid mine drainage from the exercise in chapter 3.1.3.3. As no inorganic carbon is given in the analysis and calcite is to be used as kinetically reacting mineral in the model, the analysis has to be completed by e.g. 1 mg/L carbon, formally.

PHREEQC always refers to one liter or one kg of water. The model describes a batch reaction with 1 liter water. 10 mmol calcite as well as 1 mol pyrite and 1 mol organic matter shall be present in the respective sediment/rock. To describe the kinetics of calcite and pyrite, the BASIC program given at the end of the data set PHREEQC.dat is used. For the degradation of organic matter the PHREEQC.dat notation is used, too. However, the lines 50 and 60 have to be changed as follows to accelerate the decomposition of the organic matter. Nitrate is not taken into account in this example.

```
50   rate = 1.57e-7*mO2/(2.94e-4 + mO2)
60   rate = rate + 1.e-10*mSO4/(1.e-4 + mSO4)
```

Since there is no general definition for organic matter in any of the three data sets which are installed with the PHREEQC program, a name has to be assigned in the kinetics data block (e.g Organic_C) and the organic matter has to be specified using the key word "-formula". Use the general formula CH_2O.

```
-formula CH2O
```

KINETICS needs three subdivisions for organic matter, pyrite and calcite, respectively. It is not relevant, in which block the time steps are defined. Using "-step_divide 1000000", the step width is cut down at the beginning of the kinetic calculations according to the quotient total time/step_divide.

Since all calcite is dissolved after 100 days at the latest, the following line for the calcite kinetics is inserted at the beginning of the BASIC program to save calculation time:

```
5 if time > 8640000 then goto 200
```

The simulation time is 10.000 days in 100 intervals (steps). For a higher temporal resolution at the beginning of the simulation, another model with only 600 days in 100 intervals will be calculated afterwards.

3.2.4 Degradation of tritium in the unsaturated zone

If the unsaturated zone is composed of relatively fine sediment (silt and fine sands) a quasi-uniform seepage flow can be assumed for the unsaturated zone in humid climate zones over long time spans. Therefore, the transport of infiltration water can be simulated in PHREEQC as a monotonous movement in accordance with the ”piston flow” model. A constant flow of infiltration water of 0.5 m per year is assumed for the following simulation. Furthermore, it is considered simplistically that the infiltrating precipitation has a tritium activity of 2000 TU (tritium units) over a period of 10 years. Then, it is assumed that the tritium activity decreases to zero again.

The following example shows how this can be modeled in PHREEQC. First of all, a master- and a solution species tritium T or T^+ have to be defined. Since the input of data for log_k und –gamma within the key word SOLUTION_SPECIES is required, but unknown, any value can be entered here as a free parameter (“dummy”, e.g. 0.0). This value is not used for kinetic calculations and thus, does not cause any problems. However, all results based on equilibrium calculations (e.g. the calculation of the saturation index) are nonsense for this “species”. The tritium values have to be entered in tritium units. However, in order not to have to define or convert them in an extra step, they are entered fictitiously with the unit umol/kgw instead of TU in PHREEQC. As no interactions of tritium with any other species are defined, the unit is eventually irrelevant. After modeling, remember that the result is displayed in mol/kgw as always in PHREEQC and has to be recalculated to the fictitious tritium unit umol/kgw. Entering mol/kgw in the input file, the solution algorithm quits due to problems with too high total ionic strengths.

The unsaturated zone is 20 m and is subdivided into 40 cells, 0.5 m each so that a “time step” is exactly 1 year = 86400 * 365 seconds = 3.1536e+7 seconds. The half-life of tritium (12.3 years) has to be entered in seconds in PHREEQC. First, the created 1d soil column is saturated with water containing no tritium (solution 1-40). Then, water with 2000 TU is added over a period of 10 “shifts” (= 10 years) *(Note: solution 0 is always the solution which is added on top of the column)*. After this high tritium impulse, the solution is changed again to water containing no tritium, which percolates through the column for another 30 years. The two changes from water with 0 TU to 2000 TU and back again from 2000 TU to 0 TU are two different jobs that have to be separated by END.

The degradation of tritium is described as a 1st order kinetic reaction as follows (see also Table 14):

$$\frac{\mathrm{d(A)}}{\mathrm{dt}} = -K_{\mathrm{k}} \cdot \mathrm{(A)}$$

$$t_{1/2} = \frac{1}{\mathrm{K_k}} \cdot \ln 2$$

```
PHREEQC Job: Tritium in the unsaturated zone – impulse like input function
TITLE                                   tritium in the unsaturated zone
PRINT
        -reset false                            # no standard output
SOLUTION_MASTER_SPECIES  # define master species tritium
T       T+      -1.0    T       1.008
SOLUTION_SPECIES                        # define solution species tritium
T+ = T+
        log_k   0.0                     # dummy
        -gamma  0.0     0.0             # dummy
   SOLUTION 0  tritium 1.phase          # tritium concentration 2000 TU after
                                        # the initial column water with 0 TU
        units   umol/kgw
        temp    25.0
        pH      7.0
        T       2000                    # unit umol/kgw, only fictitious
SOLUTION 1-40                           # initial column water without tritium
        units   umol/kgw
        temp    25.0
        pH      7.0
END                                     # end of the 1st job
RATES                                   # define degradation
T                                       # for tritium
-start
        10 rate = MOL("T+") * -(0.63/parm(1))     # 1st order kinetics (Table 14)
        20 moles = rate * time
        30 save moles
-end                                    # end of the 2nd job
KINETICS 1-40
T
        -parms  3.8745e+8               # 12.3 years in seconds (half-life of
                                        tritium)
TRANSPORT
        -cells      40                  # 40 cells
        -length     0.5                 # 0.5 m each, 40 * 0.5 = 20 m length)
        -shifts     10                  # 10 years
        -time_step          3.1536e+7   # 1 year in seconds
        -flow_direction forward         # forward simulation
        -boundary_cond   flux    flux   # flow boundary condition at inlet
                                        # and outlet
        -diffc      0.0e-9              # diffusion coefficient
        -dispersivity   0.05            # dispersivity
        -correct_disp    true           # correction of dispersivity yes
        -punch_cells    1-40            # cell 1 to 40 in Selected_output
        -punch_frequency 10             # print every 10th time interval
```

```
SELECTED_OUTPUT
        -file       tritium.csv          # output to this file
        -reset      false                # no standard output
        -totals     T                    # print total tritium concentration
        -distance true
END                                      # end of 3rd job
SOLUTION 0                               # no more tritium after 10 years of
        units       umol/kgw             # infiltrating water with 2000 TU
        temp        25.0
        pH          7.0
TRANSPORT
        Shifts      30                   # for another 30 years
END
```

Fig. 42 shows a vertical cross section of tritium concentrations resulting from an impulse-like input of tritium into the unsaturated zone after 10, 20, 30 and 40 years. The tritium peak moves downward and widens continuously.

The actual task now is to change the PHREEQC job in such a way that the tritium input function is not impulse-like but more realistic. Fig. 43 illustrates the increase of tritium concentrations in precipitation water from 1962 to 1963 and the subsequent decrease from 1963 to 1997, as determined at the climate station Hof-Hohensaas, Germany.

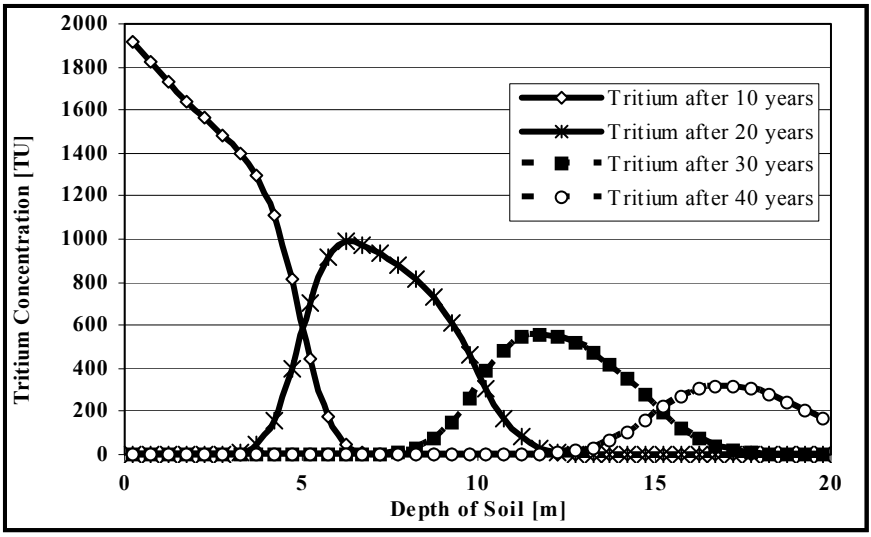

Fig. 42 Vertical cross section of tritium in the unsaturated zone (0-20 m depth) for the time intervals 10, 20, 30, 40 years assuming an impulse-like input during the first ten years

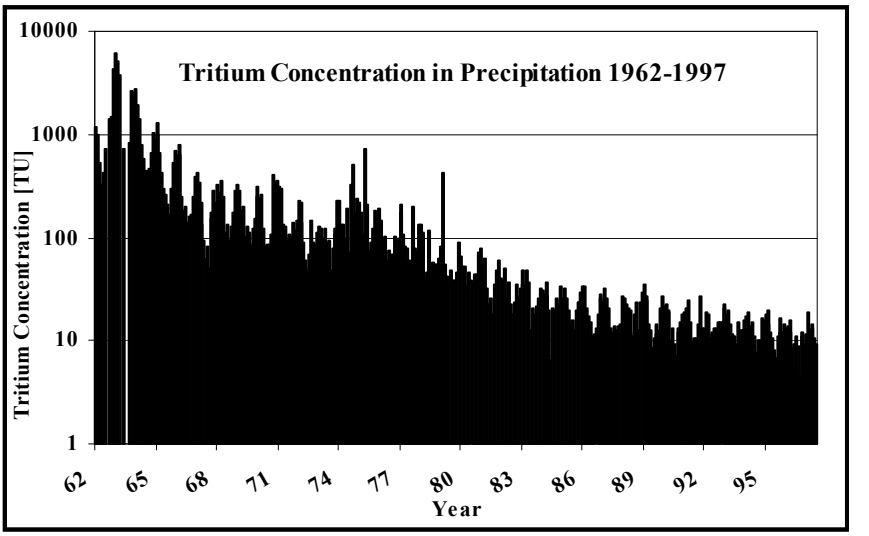

Fig. 43 Tritium concentration in rainwater, measured at the station Hof-Hohensaas, Germany (latitude 50.32 °N, longitude 11.88 °E, height 567 m NN) from 1962 to 1997

The definition of a more realistic tritium input function based on the available data of the tritium concentrations in the rainwater is done in time intervals of 5 years each (Table 38).

Table 38 Tritium concentrations in the atmosphere from 1962 to 1997

Intervall of 5 years	Tritium in the atmosphere (TU)
1 (06/1962 - 06/1967)	1022
2 (07/1967 - 07/1972)	181
3 (08/1972 - 08/1977)	137
4 (09/1977 - 09/1982)	64
5 (10/1982 - 10/1987)	24
6 (11/1987 - 11/1992)	17
7 (12/1992 - 12/1997)	13

Remodel the degradation of tritium in the unsaturated zone with this new input function. Compare your results with the results obtained from the assumption of an impulse-like tritium input in Fig. 42.

3.3 Reactive transport

3.3.1 Lysimeter

A lysimeter filled with sediments was equilibrated with the following water (concentrations in mmol/L):
pH = 8.0, pE = 12, temperature = 10.0 °C, Ca = 1, C = 2.2, Mg = 0.5, K = 0.2, SO_4^{2-} = 0.5

At a time T1, an acid mine drainage of the following composition is added (concentration in mmol/L):
pH = 3.2, pE = 16, temperature = 10.0° C, Ca = 1, C = 2.0, Mg = 0.5, K = 0.2, SO_4^{2-} = 4.0, Fe = 1, Cd = 0.7, Cl = 0.2

Calculate the distribution of the concentrations within the lysimeter column taking into account the cation exchange (discretisation and time steps as in the example in chapter 2.2.2.3). Selectivity coefficients are taken from the exemplary data of WATEQ4F.dat data set and an exchange capacity of 0.0011mol per kg water is assumed. Neither diffusion nor dispersion is considered. Present your results graphically.

3.3.2 Karst spring discharge

A karst water has the following chemical composition:
pH = 7.6, pE = 14.4, temperature = 8.5 °C, Ca = 147, HCO_3^- = 405, Mg = 22, Na = 5, K = 3, SO_4^{2-} = 25, Cl = 12, NO_3^- = 34

It is in equilibrium with a CO_2 partial pressure of 0.74 Vol% and is slightly supersaturated with regard to calcite (SI = 0.45). This karst water discharges at a spring with a mean discharge of 0.5 L/s and flows in a small channel downhill with a mean velocity of 0.25 m/s. Due to the turbulent flow, CO_2 will degas spontaneously until equilibrium is reached with the CO_2 partial pressure of the atmosphere. Because of the resulting carbonate precipitation, the creek forms a small carbonate ridge over the years, on top of which it flows in a small channel (Fig. 44).

Model the carbonate precipitation in this carbonate channel by means of a 1d transport with 40 cells of 10 m length each. Dispersivity is assumed with 1m. Use the key words KINETICS and RATES and the BASIC program for calcite from the data set PHREEQC.dat describing the kinetics for both the calcite dissolution and the calcite precipitation. How much calcite precipitates each year within the channel´s first 400 meter after the discharge? How much CO_2 degasses at the same time?

[Note: For all n cells a SOLUTION has to be defined at the beginning of the modeling (SOLUTION 1-n). The same applies for the key words KINETICS and EQUILIBRIUM_PHASES. If you use 1 instead of 1-n, the kinetic or the equilibrium reactions would only be modeled for the first cell.]

Fig. 44 Calcite ridge at a karst spring discharge near Weißenburg, Germany.

3.3.3 Karstification (corrosion along a karst fracture)

Talking about karstification often the question arises why karst phenomena do not only occur at the surface but in greater depths as well. The reason is that the carbonate dissolution is a comparatively fast process, but still takes some time, while water may cover quite a long distance along a fracture.

This shall be modeled with the following example. A fracture with an extension of 300 meters is given. Assume that, at the beginning of the simulation, this fracture is filled with groundwater that is in carbonate equilibrium. To simplify matters the following data shall be used:

pH	7.32
Temp	8.5
C	4.905 mmol/L
Ca	2.174 mmol/L

Infiltrating rainwater now dissolves CO_2 according to the increased partial pressure of 1 Vol% in the unsaturated zone. Thus, the seepage water has the following characteristics:

pH	4.76
Temp	8.5
C	0.5774 mmol/L

This water enters the model fracture with a velocity of 10 m per 6 minutes. Calculate the carbonate dissolution in the 300 meter long fracture, that will be

modeled as a one dimensional pipe with 30 elements of 10 m length each. Furthermore, consider a dispersivity of 0.5 m and assume that the whole water column will be exchanged once. Moreover, the fracture is not completely filled with water, but contains air, too. This air has a CO_2 partial pressure of 1 Vol%. The kinetics of the carbonate dissolution shall be assumed according to chapter 2.2.2.2.1. Further, use the key word USER_GRAPH to visualize the result graphically within PHREEQC. The concentrations of Ca and C as well as the calcite saturation index shall be displayed along the 300 m long fracture after a single exchange with the infiltrating rainwater.

3.3.4 The pH increase of an acid mine water

Acid mine drainages (AMD) cause great problems in the mining industry as they typically contain high concentrations of iron, sulfate and protons due to the pyrite oxidation. Consequently, other elements (e.g. metals and arsenic) may be increased as well. A simple method of water treatment is to conduct these acid waters through a carbonate channel. This process causes an increase of the pH value due to carbonate dissolution. Furthermore it can result in supersaturation of other minerals that can precipitate spontaneously. The high sulfate concentrations combined with increasing calcium values from the calcite dissolution often exceed the gypsum solubility product. Iron minerals are also supersaturated as a result of these reactions, and consequently e.g. amorphous iron hydroxide precipitates spontaneously. Even though the dissolution of calcite is relatively fast this exercise shows that the reaction kinetics still has to be taken into account to plan the dimensions of such a carbonate channel correctly. An acid mine drainage ("AMD") and a natural surface water are given (Table 39).

Table 39 Water analysis of an acid mine drainage ("AMD") and of a natural surface water ("SW")

Parameter	AMD	SW
pe	6.08	6.0
Temp.[°C]	10	10
pH	1.61	8.0
Al	1.13e-04 mol/L	
As	5.47e-07 mol/L	
TIC*)	3.18e-03 mol/L	
HCO_3^-		130 mgl/L **)
Ca	9.19e-04 mol/L	36.6 mgl/L***)
Cd	2.27e-07 mol/L	
Cl	6.07e-05 mol/L	2.1 mgl/L
Cu	8.06e-07 mol/L	
F	2.69e-05 mol/L	
Fe	2.73e-02 mol/L	0.06 mgl/L

Parameter	AMD	SW
K	3.93e-05 mol/L	1.5 mgl/L
Li	2.95e-06 mol/L	
Mg	1.47e-04 mol/L	3.5 mgl/L
Mn	1.30e-06 mol/L	
NO_3^-	2.47e-04 mol/L	0.5 mgl/L
Na	2.58e-04 mol/L	5.8 mgl/L
Ni	8.72e-07 mol/L	
Pb	2.47e-07 mol/L	
SO_4^{2-}	5.41e-02 mol/L	14.3 mgl/L
Si	6.20e-05 mol/L	3.64 mgl/L
U	2.15e-07 mol/L	
Zn	1.09e-05 mol/L	

*) total inorganic carbon
**) adjust inorganic C to the partial pressure of the atmosphere (CO2(g) -3.5)
***) set Ca to "charge" in the PHREEQC input file

At the beginning of the modeling the 500 m long carbonate channel is filled with the surface water ("SW"). Then, the acid mine water is added. Calculate how the composition of the mine water changes, how much calcite is dissolved and how much gypsum and iron hydroxide precipitate. Additional problems like coating of the carbonate by gypsum and iron hydroxide crusts as well as the kinetics of the formation of gypsum and iron hydroxide are ignored in this model.

Apply 1 m/s as flow velocity so that the total contact time in the channel is 500 seconds. The modeling should be done as 1d transport model with 10 cells (dispersivity: 0.1 m) and last over 750 seconds. Also take into account the contact with the atmosphere. Therefore, run the model once with a CO_2 partial pressure of 0.03 Vol% and a second time with 1 Vol%, both times assuming an oxygen partial pressure of 21 Vol% O_2. The latter case corresponds rather to a closed carbonate channel.

Illustrate the results of the model by presenting the water characteristics over the whole length of the channel at the end of the modeling (pH value, SI calcite, Ca, Fe, C, SO_4^{2-}, $CaSO_4^0$). Additionally indicate the amounts of calcite dissolved and of gypsum and iron hydroxide precipitated.

3.3.5 In-situ leaching

Aquifers with double porosity (e.g. sandstones with fractures and pore volume) require special considerations with regard to transport modeling even if no reactive mass transport in its proper sense is taken into account. This problem is demonstrated with the following example of an aquifer regeneration in an uranium mine. The ore was leached in this mine by in-situ leaching (ISL) using sulfuric acid. The hydrochemical composition of the water that is in the aquifer after this in-situ leaching process is shown as "ISL" in Table 40:

Table 40 Water analysis of a natural groundwater (GW) and groundwater influenced by in-situ leaching (ISL) (concentrations in mg/L)

Parameter	GW	ISL	Parameter	GW	ISL	Parameter	GW	ISL
pe	6.08	10.56	Cu	0.005	3	Ni	0.005	5
Temp.	10 °C	10	F	0.5	1	NO_3^-	0.5	100
Al	3.0	200	Fe	0.6	600	Pb	0.05	0.2
As	0.004	2	K	1.5	4	pH	6.6	2.3
C(4)	130		Li	0.02	0.1	Si	3.64	50
Ca	36.6	400	Mg	3.5	50	SO_4^{2-}	14.3	5000
Cd	0.0003	1	Mn	0.07	20	U	0.005	40
Cl	2.1	450	Na	5.8	500			

The simulation will be done in a zone of 200 m between an infiltration well and a pumping well. This zone shows a k_f value of $5 \cdot 10^{-5}$ m/s along the fracture and 10^{-8} m/s within the pores (those k_f values are only for orientation and are not needed directly for the modeling). The flow velocity is 10 m/day due to the potential head.

The dispersivity is 2 m. Natural groundwater ("GW" in Table 40) will be infiltrated in the infiltration well and extracted at the pumping well.

Assume that the exchange between pores and fractures only takes place by diffusion ($2 \cdot 10^{-10}$ m^2/s). The fracture volume is 0.05, and the pore volume is 0.15. Presuppose that the fractures are planar and that the distance between them is 20 cm. Thus, on average each fracture has a pore matrix of 10 cm thickness to each side. Homogeneous and heterogeneous reactions shall be ignored.

The simulation time is supposed to be 200 days. Thus, the water of the fractures will be exchanged 10 times in the 200 m long aquifer section.

The discretisation shall be carried out in elements of 10 m length. The connection of the immobile cells to the mobile cells is done by a box for each cell (Fig. 45) and the exchange between mobile and immobile cells by the means of a 1st order reaction (for theory see chapter 1.3.3.3.1). Present the concentrations of the elements U, Fe, Al, and S at the pumping well over a period of 200 days.

Change the parameter "immobile pore volume" from 0.15 to 0.05 and the matrix thickness on each side of each fracture from 0.1 to 0.01. Compare the results.

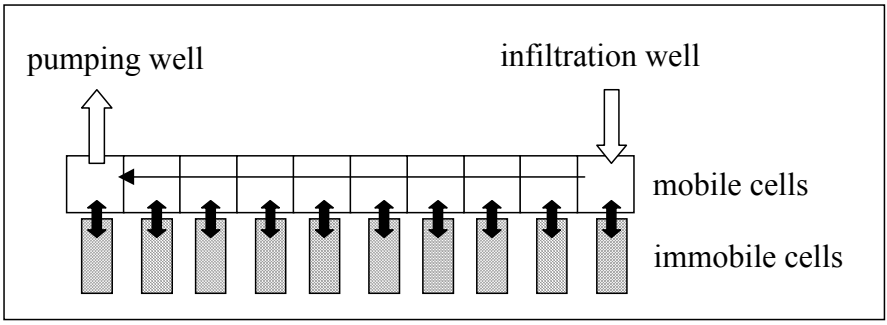

Fig. 45 Scheme for the model approach of a double porosity aquifer

4 Solutions

4.1 Equilibrium reactions

4.1.1 Groundwater- Lithosphere

4.1.1.1 Standard-output well analysis

The water sample shows a low to average mineralization (ionic strength I = 1.189e-02 mol/L „description of solution“). It can be classified as Ca-Mg-HCO_3-type (Ca 1.872 mmol/L, Mg 1.646 mmol/L, HCO_3^- 3.936 mmol/L; „solution composition“). The analytical accuracy is sufficient with an electrical balance (eq) of -3.407e-04 and a percent error (100*(Cat-|An|)/(Cat+|An|)) of -2.36%.

In terms of redox sensitive elements it is remarkable that for As, Cu, Fe, N, and U the respective oxidized forms predominated, while Mn predominantly occurs as Mn (+2) and Se as Se (+4). Fig. 20 shows that the Mn oxidation does not start up to a pE > +10, while the analysis on hand has a pE of 6.9. The oxidation of Se starts at lower values so that Se (-2) is already completely oxidized, and there are small quantities of Se(+6). However, the partly reduced form Se(+4) still predominates.

The species distribution of Ca, Mg, Zn, and Pb can be seen in Fig. 46. It is noteworthy that Ca, Mg, and Zn predominantly occur as free ions in contrast to lead, which typically forms complexes. The most important complexing anion for calcium and magnesium is sulfate, for lead and zinc it is hydrogen carbonate.

Fig. 47 and Fig. 48 show the supersaturated Al and Fe mineral phases. As already mentioned in chapter 2.2.2.1.1, the amorphous mineral phases precipitate initially. In this example, it is only $Fe(OH)_3(a)$ because $Al(OH)_3(a)$ is undersaturated. Because of the low total concentrations of 0.056 mg/L for Al and 0.067 mg/L for Fe, further mineral precipitations are unlikely to occur.

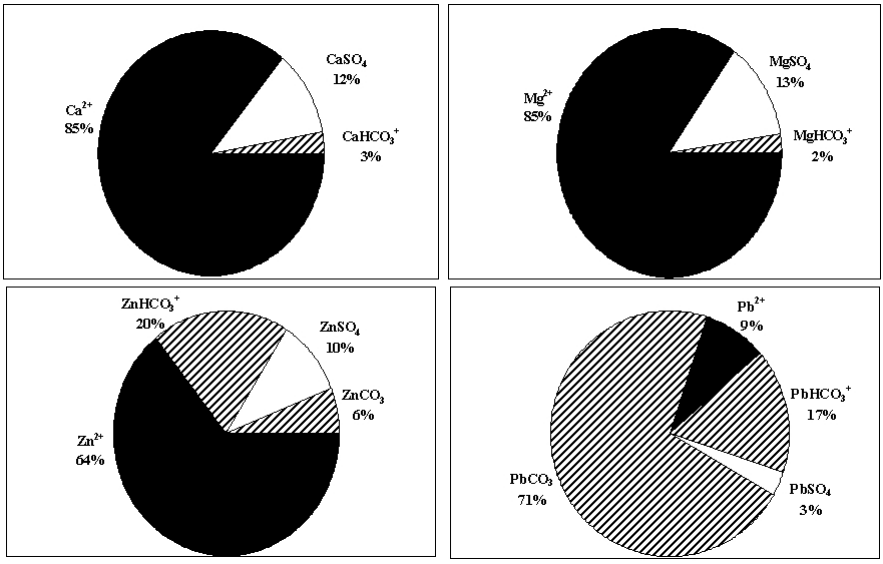

Fig. 46 EXCEL pie chart presenting the species distribution for Ca, Mg, Zn, and Pb

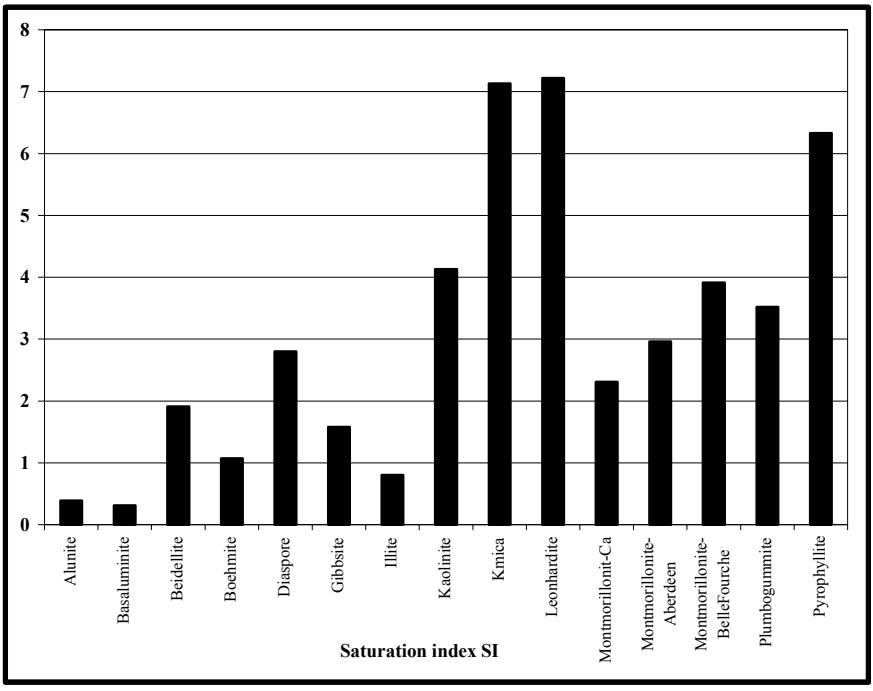

Fig. 47 EXCEL bar chart presenting the supersaturated aluminum mineral phases

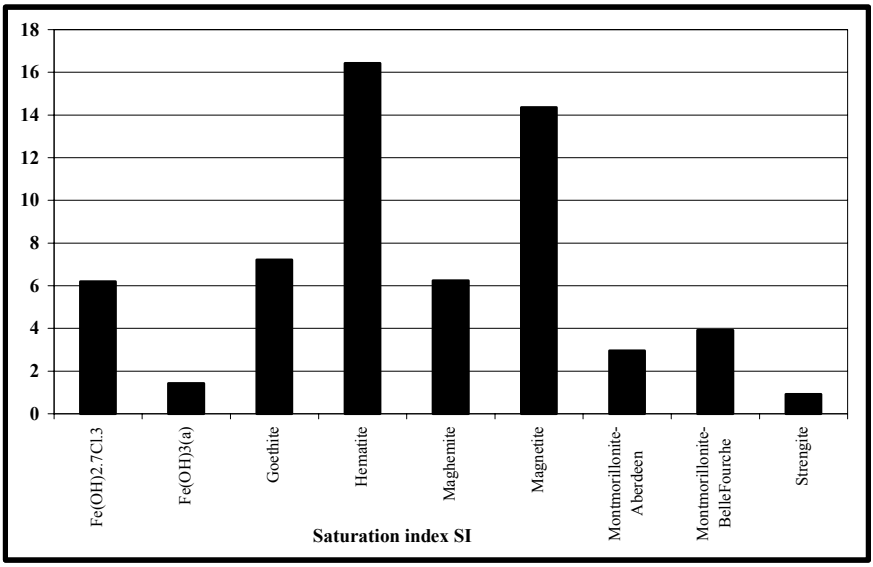

Fig. 48 EXCEL bar chart presenting the supersaturated iron mineral phases

4.1.1.2 Equilibrium reaction- solubility of gypsum

Because of its general flow direction from the east to the west the groundwater flows through the gypsum deposit before in enters the planned new well. In contact with the mineral deposit 1.432e-02 mol/L gypsum can dissolve (Delta gypsum from the section "phase assemblage", the minus sign indicates that gypsum dissolves). Thus, the total mineralization increases from 1.190e-02 mol/L in the old well (assumed to be characteristic for this aquifer) to 4.795e-02 mol/L, which is 4 times higher than the initial value. The Ca concentration increases from 1.872e-03 mol /L (75 mg/L) for the old well to 1.618e-02 mol/L (645 mg/L) and the sulfate concentration from 2.083e-03 mol/L (200 mg/L) to 1.639e-02 mol/L (1570 mg/L).

Thus, the drinking water standards of 400 mg/L for Ca and 240 mg/L for SO_4^{2-} are exceeded by far. While the level for Ca is of rather technical significance, since high Ca values may lead to calcite precipitation in the pipe system (also see chapter 3.1.5.2), the sulfate standard has a medical background, because sulfate can cause diarrhea in high concentrations.

To calculate the sulfate content, not only the SO_4^{2-} ion as listed in the species distribution but all S(6) species were considered. Most analytical methods determine all S(6) compounds as "sulfate" and, moreover, also the drinking water standard refers to this rather "theoretical" total sulfate content.

4.1.1.3 Disequilibrium reaction – solubility of gypsum

Assuming an incomplete dissolution of gypsum (50% → log 0.5 = 0.3 → EQUILIBRIUM_PHASES gypsum 0.3) only 7.832e-03 mol/L of gypsum dissolve. After the reaction, the total mineralization is 3.259e-02 mol/L, the Ca content 388 mg/L, sulfate 950.4 mg/L. Hence, the Ca content is slightly below the standard, while the limit for sulfate is still clearly exceeded. All in all, the planned well location can not be recommended. At least the high sulfate concentrations would make an expensive water treatment indispensable.

4.1.1.4 Temperature dependency of gypsumsolubility in well water

The following amounts of gypsum dissolve at the corresponding temperatures:
Δ gypsum -7.217e-03 mol/L at 10°C
Δ gypsum -7.736e-03 mol/L at 20°C
Δ gypsum -8.074e-03 mol/L at 30°C
Δ gypsum -8.229e-03 mol/L at 40°C
Δ gypsum -8.213e-03 mol/L at 50°C
Δ gypsum -8.047e-03 mol/L at 60°C
Δ gypsum -7.753e-03 mol/L at 70°C

The maximum solubility of gypsum occurs at 40°C (Fig. 49). The first increase of solubility with temperature is related to the endothermic formation of the $CaSO_4^0$ complex, the significance of which was already shown in the example 2 in chapter 2.2.2.1.2 ($\Delta H(CaSO_4^0) = +1.6 \rightarrow \Delta G > 0$, since $\Delta G = -R \cdot T \cdot \ln K$ it follows, if T ↑ -lnK ↓, thus K ↑). The solubility of the mineral phase $CaSO_4$(s) on the other hand decreases with increasing temperature (exothermic process) ($\Delta H(CaSO_4(s)) = -0.1 \rightarrow \Delta G < 0$, since $\Delta G = -R \cdot T \cdot \ln K$ it follows, if T ↑ lnK ↓, thus K↓). Both effects overlap and lead to the fact that the maximum gypsum solubility occurs at some medium temperature, at which the formation of the $CaSO_4^0$ complex is already increased and the decreasing solubility of $CaSO_4$(s) does not predominate yet. As a consequence of the decreasing mineral solution over 40°C, also the amount of $CaSO_4^0$ declines.

4.1.1.5 Temperature dependency of gypsum solubility in distilled water

Compared to well water, distilled water can dissolve more gypsum (Fig. 49), since the initial concentrations of calcium and sulfate are lower.

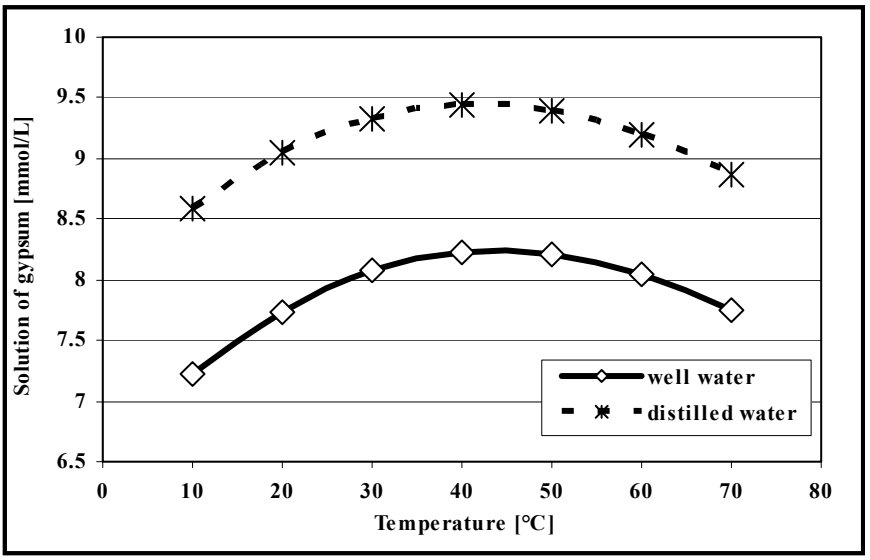

Fig. 49 Temperature dependency of gypsum solubility in well water and in destilled water.

4.1.1.6 Temperature and P(CO_2) dependent calcite solubility

The optimum calcite solubility occurs at 30°C (Fig. 50), not at the maximum temperature of 40°C (Table 41).

Table 41 Dependence of calcite solubility on temperature and P(CO_2)

Temperature [°C]	CO_2 [Vol%]	P(CO_2)	Calcite [mmol/L]
0	0.03	-3.5	1.07
5	0.5	-2.3	-0.08
8	0.9	-2.05	-0.40
15	2	-1.70	-0.83
25	4.5	-1.3	-1.32
30	7	-1.15	-1.46
40	10	-1	-1.34

Different factors have an influence on the calcite solubility. First of all, like for gypsum (chapter 4.1.1.4) the formation of the $CaCO_3^0$ complex is endothermic ($\Delta H(CaCO_3^0) = +3.5$), while the mineral dissolution is exothermic ($\Delta H(CaCO_3(s)) = -2.3$). Thus, the maximum solubility occurs at some medium temperature, at which the formation of the $CaCO_3^0$ complex is already increased and the decreasing solubility of $CaCO_3(s)$ does not predominate yet.

Furthermore, calcite solubility does not only depend on temperature but also on P(CO_2).

Calcite solution:	$CaCO_3$	$\leftrightarrow$	Ca^{2+}	+ $\mathbf{CO_3^{2-}}$
Autoprotolysis of water:	H_2O	$\leftrightarrow$	$\mathbf{H^+}$	+ OH^-
Subsequent reaction:		$\mathbf{CO_3^{2-}} + \mathbf{H^+}$	$\leftrightarrow$	HCO_3^-

As can be seen from the equations above, an increase of H^+-ions causes a consumption of CO_3^{2-} forming the HCO_3^- complex. Thereby $CaCO_3$ dissolution is increased. An increase in H^+-ions can be caused e.g. by acids (HCl, H_2SO_4, HNO_3) but also by an increase of CO_2 concentration, since H^+ ions form with the dissolution of CO_2 in water.

$$CO_2 + H_2O \leftrightarrow H_2CO_3 \leftrightarrow H^+ + HCO_3^-$$

Although the immediate dissociation of H_2CO_3 to $H^+ + HCO_3^-$ only makes up 1%, subsequent reactions cause a much higher CO_2 dissolution.

That means, the higher the $P(CO_2)$, the more $CaCO_3$ can be dissolved. Yet, the solubility of CO_2 as gas in water depends on the temperature: The higher the temperature the lower the gas solubility. Consequently, initially, the calcite solubility increases with temperature due to the endothermic reaction of $CaCO_3^0$ complexation, but with increased temperature the exothermic reaction of $CaCO_3$(s) dissolution and the significantly reduced CO_2 dissolution decrease the total calcite solubility.

4.1.1.7 Calcite precipitation and dolomite dissolution

In the presence of both calcite and dolomite, dolomite dissolves while calcite precipitates (Table 42, Fig. 50), because the solubility product of $CaCO_3$ is exceeded. This process is called incongruent dissolution (see chapter 1.1.4.1.3). The maximum of dissolution/ precipitation shifts to lower temperatures (6°-7°C).

Table 42 Dependence of calcite dissolution and dolomite precipitation on temperature

Temperature [°C]	CO_2 [Vol%]	Calcite [mmol/L]	Dolomite [mmol/ L]
0	0.03	2.68	-1.11
5	0.5	4.10	-2.90
8	0.9	4.19	-3.17
15	2	3.79	-3.12
25	4.5	3.02	-2.86
30	7	2.60	-2.65
40	10	1.79	-2.00

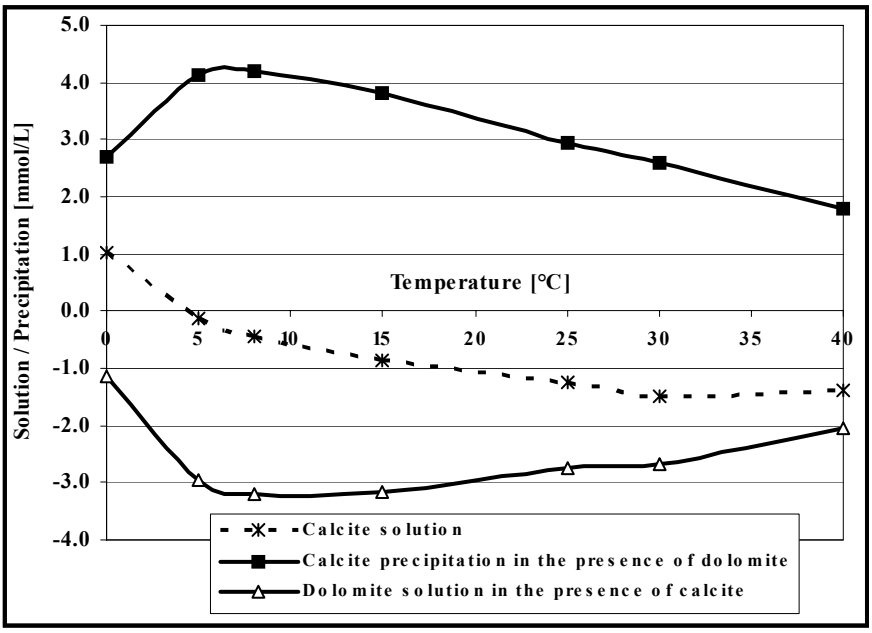

Fig. 50 Calcite solubility and incongruent solution calcite-dolomite (calcite – precipitation and dolomite dissolution)

4.1.1.8 Comparison of the calcite solubility in an open and a closed system

At a $P(CO_2)$ of 2 vol% the calcite dissolution is lower in the open system (hence the pH value higher) than in the closed system. At 20 vol% $P(CO_2)$ it is the other way around, in the open system the calcite dissolution is higher, the pH value is lower (Table 43).

Table 43 Calcite dissolution in an open and a closed system at $P(CO_2)$ = 2 vol%, respectively $P(CO_2)$ = 20 vol%

	2 Vol% open system	2 Vol% closed system	20 Vol% open system	20 Vol% closed system
pH	7.144	7.028	6.485	6.594
Calcite [mmol/L]	-0.8290	-1.250	-4.385	-3.552

The explanation can be found by modeling the well analysis without any equilibrium reactions. The well sample itself already has a CO_2 partial pressure of 3.98 vol% (under „initial solution“ - „saturation indices“ SI $CO_2(g)$ = -1.40 → $P(CO_2)$ = 3.98 vol%), i.e. the following processes occur in the open and the closed system:

in the open system: a complete gas exchange is possible:

2 vol% complete degassing from 3.98 vol% to 2 vol%

20 vol% complete dissolution from 3.98 vol% to 20 vol%

in the closed system: the gas exchange is suppressed (ideally no exchange at all)

2 vol% minor degassing from 3.98 vol% to 3.02 vol% (SI = -1.52 for CO_2(g) under „batch reaction calculations“ - „saturation indices“ → $P(CO_2)$ = 3.02 vol%), since only a limited amount of gas (1liter) is assumed for the reaction. Because in the open system the partial pressure $P(CO_2)$ = 2 vol% is lower than in the closed system (3.02 vol%), the calcite dissolution is less.

20 vol% minor dissolution from 3.89 vol% to 13.49 vol% (SI = -0.87 for CO_2(g) under „batch reaction calculations“ - „saturation indices“ → $P(CO_2)$ = 13.49 vol%)%), since only a limited amount of gas (1liter) is assumed for the reaction. Therefore, in the open system the CO_2 partial pressure is higher (20 vol%) than in the closed system (13.49 vol%), and, consequently, the calcite dissolution is higher too.

4.1.1.9 Pyrite weathering

As can be seen from Fig. 51, with increasing oxygen the pyrite weathering has a crucial influence on the concentrations of Fe^{2+} and SO_4^{2-}, which increase from 0.001 mol/L to 1 mol/L O_2 by about 3 orders of magnitude. The pH value drops significantly from 6.3 to 0.7. The resulting water is extremely acid.

In the presence of calcite, the total concentration of SO_4^{2-} at oxygen concentrations exceeding 0.05 mol/L strongly increases compared to the pyrite weathering in the absence of calcite. The reason for this increase is that H^+ ions are consumed for the formation of the HCO_3^- complex, which results from calcite dissolution. This consumption of H^+ reduces the formation of the HSO_4^- complex, and the formation of SO_4^{2-} is increased. The Fe^{2+} concentration on the other hand decreases. Significant amounts of Fe^{2+} are bound in the $FeHCO_3^+$-complex due to higher concentrations of HCO_3^- in the presence of calcite. Most important, however, is the influence of calcite on the pH value, which is decreasing from 6.9 to 5.1 only. The presence of calcite causes a significant buffering of the waters formed during pyrite weathering.

In the presence of the mineral phase U_3O_8, $5.32 \cdot 10^{-8}$ (at 0.001 mol/L O_2), $1.98 \cdot 10^{-1}$ mol/L uranium (at 1 mol/L O_2) can dissolve (Fig. 52). In the absence of calcite, the pH value drops from 6.3 to 2.0. In the presence of calcite the pH value is buffered as in the example described above (6.9 to 5.1). Up to an oxygen concentration of 0.005 mol/L the uranium solubility in the presence of calcite is higher than in its absence because more uranium carbonate complexes can form. However, at higher oxygen contents, the uranium solubility in the presence of calcite is significantly restricted. It reaches $3.56 \cdot 10^{-6}$ mol/L at 1 mol/L O_2, hence only one hundred thousandth of the amount that is soluble in the absence of calcite. Thus, calcite effectively contributes to the reduction of uranium concentrations in the groundwater during pyrite weathering.

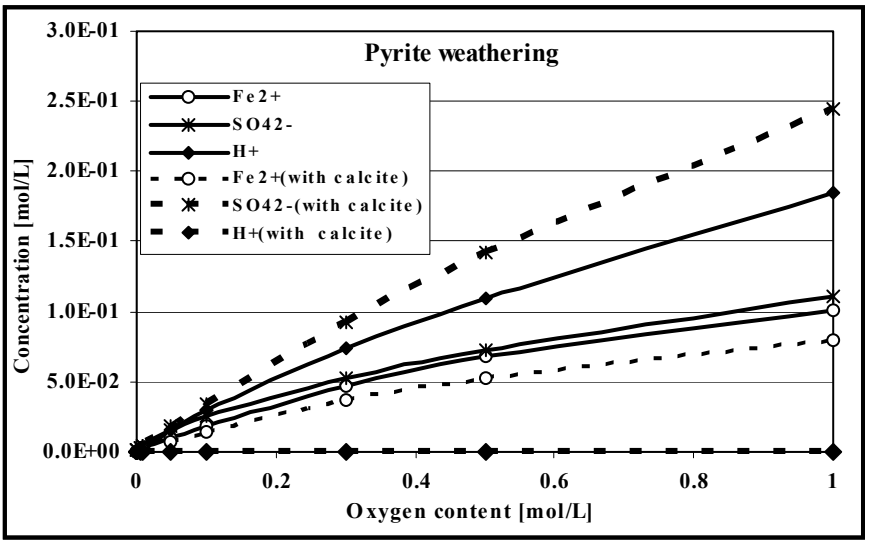

Fig. 51 Effects of pyrite weathering on the concentrations of Fe^{2+}, SO_4^{2-} and H^+ in the absence and in the presence of calcite

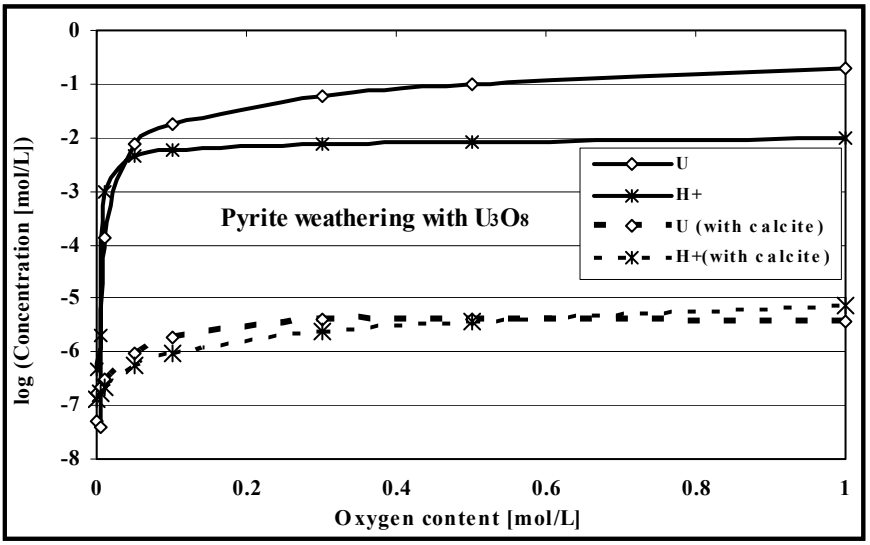

Fig. 52 Effects of pyrite weathering in the presence of the mineral phase U_3O_8 on the concentrations of uranium and H^+ in the absence and in the presence of calcite (y-axis logarithmic).

4.1.2 Atmosphere – Groundwater – Lithosphere

4.1.2.1 Precipitation under the influence of soil CO_2

The increased soil CO_2 partial pressure of 1 vol% - compared to atmospheric $P(CO_2)$ = 0.03 vol% - causes an increase in the concentration of the H^+ ions (see chapter 3.1.1.6). Thus, the pH value of the rainwater decreases from 5.1 to 4.775, while at the same time the concentration of dissolved carbon increases from 13 µmol/L to 390 µmol/L.

4.1.2.2 Buffering systems in the soil

The pH value of the infiltrating rainwater under increased CO_2 partial pressures in the soil is 4.775. In this pH range the iron hydroxide buffer shows no effect at all. The pH value remains at 4.775 even after the reaction with goethite. Iron buffers only play a role for reactions in very acid mine waters (pH 2 to 4), by the transformation of goethite into Fe (III) under proton consumption: $FeOOH + 3H^+ = Fe^{3+} + 2H_2O$. The reaction with aluminum hydroxide (boehmite $AlOOH + H_2O + 3H^+ = Al^{3+} + 3H_2O$) shows little buffering capacity. The pH is 4.91 after the reaction. Similarly manganese hydroxides ($MnOOH + 3H^+ + e^- = Mn^{2+} + 2H_2O$) buffers only slightly from pH 4.775 to 5.032. In the exchanger buffering system the protons are sorbed on the exchanger while (earth) alkaline ions are released. The buffered pH value is 6.718 and thus almost in the neutral pH range. The most effective buffer is the carbonate buffer, which is responsible for buffering most of the systems in the pH range of 5.5 to 8.0. After the reaction with calcite, the pH of rainwater increases from 4.775 to 7.294.

Because of the slow kinetics of feldspar weathering, the modeling of a silicate buffer is impossible by equilibrium reactions only. Kinetics must be considered, which will not be done here.

4.1.2.3 Mineral precipitations at hot sulfur springs

At 45°C a maximum of about 6.5 mg O_2 can dissolve in one liter of water. The gas solubilities given in Table 44 first must be recalculated to the respective temperatures (T)., for 0 °C e.g.:

0.0473 cm^3 water / cm^3 water = 0.0473 L gas / L water;

since 22.4 L = 1 mol gas: 0.0473 : 22.4 mol gas / L water = $2.11 \cdot 10^{-3}$ mol/L

since the mole mass of O_2 = 32 g/mol: $2.11 \cdot 10^{-3}$ mol/L · 32 g/mol = 0.0676 g/L = 67.6 mg/L

The calculated value would be correct for 100 vol% O_2. However, there are only 21 vol% in the atmosphere, 67.6 mg/L so that value must be multiplied by 0.21 and one gets 14.19 mg/L O_2-solubility at 0°C.

Table 44 Dependence of O_2 solubilities on temperature at $P(O_2)$ =21 vol%

T	Gas solubility [cm^3/cm^3]	Gas solubility [mg/L]	T	Gas solubility [cm^3/cm^3]	Gas solubility [mg/L]	T	Gas solubility [cm^3/cm^3]	Gas solubility [mg/L]
0	0.0473	14.19	20	0.0300	9.00	50	0.0204	6.12
5	0.0415	12.45	25	0.0275	8.25	60	0.0190	5.70
10	0.0368	11.04	30	0.0250	7.50	70	0.0181	5.43
15	0.0330	9.90	40	0.0225	6.75	90	0.0172	5.16

Thus, using REACTION 1, 2, 3, 4, 5, 6, and 6.5 mg/L O_2 (converted into mol/L) are added. For CO_2, equilibrium with the atmospheric partial pressure can be defined simply by using the key word EQUILIBRIUM_PHASES, since all the subsequent reactions depend only on the diffusion of the CO_2 and its dissociation in water. Contrary to redox reactions with oxygen both processes are fast reactions, hence can be described by equilibrium reactions, neglecting kinetics.

As long as sulfur-rich thermal waters circulate in the underground, all mineral phases except for the Si compounds are undersaturated. Upon discharge as spring water, the exposure to a small quantity of oxygen is sufficient to reach a supersaturation with regard to elemental sulfur (SI = 0.04 at 1 mg O_2/L to SI = 0.47 at 6.5 mg O_2/L). Even at higher O_2 contents, gypsum stays undersaturated (SI = -6.6 at 1 mg O_2/L to -3.25 at 6.5 mg O_2/L). Close to the spring´s discharge the supersaturated sulfur precipitates spontaneously together with SiO_2(a) forming the characteristic yellow – red sulfur sinter incrustations. Depending on the O_2 content the amount of precipitating sulfur varies from 0.419 mg S/L to 11.26 mg S/ L at maximum O_2 - solubility.

4.1.2.4 Formation of stalactites in karst caves

The rainwater infiltrates in the soil of the karst area. Under the increased CO_2 partial pressure of 3 vol% in the soil the dissolution of 2.613 mmol/L calcite (simulation1 / batch reactions / phase assemblage) occurs and karst cavities form. From the cave ceilings, water saturated with regard to calcite drips. As soon as the infiltrating water creates a karst drainage system, which finally discharges to a river, the CO_2 content drops to the level of atmospheric partial pressure (0.03 vol%). With decreasing $P(CO_2)$, calcite precipitation inevitably results (see also chapter 3.1.1.6), leading to the precipitation of 2.116 mmol/L (simulation2 / batch reactions / phase assemblage) or 211.6 mg/L $CaCO_3$ (2.116mmol/L · mole mass 100 mg/mmol = 211.6 mg/L). Assuming a daily amount of 100 liter of water dripping from the cave´s ceiling, that amounts to 211.6 mg/L · 100 L/d = 21.16 g/d, or for one year (365 day) about 7.7 kg/a.

Taking 2.7 g/cm^3 as density, a precipitated volume of calcite of 7.7 kg/a : 2.7 kg/dm^3 = 2.86 dm^3/a results. Because only about 15% of the ceiling of the karst cave is covered by stalactites, this volume is spread on 0.15 ·10 m (length) · 10 m (width) = 15 m^2. Thus the stalactites grow by 2.63 dm^3/a : 15 : 10^2 dm^2 = 0.0019 dm/a = 0.19 mm/a.

4.1.2.5 Evaporation

The negative amount of water, which must be used for titration, equals 54.38 moles. The rainfall of 250 mm must be reduced by 20 mm for the runoff, which leaves 230 mm for infiltration. That comes up with 225 mm evaporation / 230 mm infiltration = 98 % of evaporation; this means that 98% of the amount of water (pure H_2O without any ions) must be removed (98% of 55.5 moles = 54.38 moles). That leaves 2% of highly concentrated solution, which must be multiplied 50 times with itself to get back to 100% of highly concentrated solution (50 · 2% = 100%). Additionally, equilibrium with calcite, quartz, and 0.01 bar of CO_2 (CO_2(g) -2.0) must be adjusted.

This calculation results in the solution composition shown in Table 45 with and without consideration of evaporation (in mol/L).

Table 45 Groundwater recharge with and without consideration of evaporation

Groundwater recharge without consideration of evaporation		Groundwater recharge with consideration of evaporation	
C	3.85e-03 mol/L	C	3.11e-03 mol/L
Ca	1.84e-03 mol/L	Ca	4.61e-03 mol/L
Cl	2.30e-05 mol/L	Cl	7.95e-04 mol/L
K	7.00e-06 mol/L	K	2.42e-04 mol/L
Mg	2.90e-05 mol/L	Mg	1.00e-03 mol/L
N(5)	8.00e-05 mol/L	N(5)	2.77e-03 mol/L
Na	8.00e-06 mol/L	Na	2.77e-04 mol/L
S(6)	8.20e-05 mol/L	S(6)	2.83e-03 mol/L
Si	9.13e-05 mol/L	Si	9.10e-05 mol/L
pH = 7.294		pH = 7.161	
SI (gypsum) = -2.60		SI (gypsum) = -0.93	

Considering evaporation, the elements Cl, K, Mg, N(5), Na, and S(6) yield a concentration about 35 times higher than without considering evaporation. For Ca, Si, and HCO_3 the difference is smaller, since for those elements an additional input - independent of the evaporation - is assumed by the equilibrium reactions in the underground. The increase in the gypsum saturation index is remarkable, showing that at high evaporation rates even gypsum precipitation might occur.

Under PHASE ASSEMBLAGE one can find the amount of calcite dissolved (-2.169 mmol/L, respectively 2.169/L · 100 mg/mmol = 216.9 mg/L). The groundwater recharge can be calculated from 5 mm/a (250 mm rainfall - 20 mm runoff - 225 mm evaporation) related to the recharge area of 50 km · 30 km to 5 mm/a · 1500 km^2 = 0.005 m/a · 1.5 · 10^9 m^2 = 7.5 · 10^6 m^3/a or 7.5 · 10^9 L/a. For this groundwater recharge, a dissolved amount of calcite of 216.9 mg/L · 7.5 · 10^9 L/a = 1.627 · 10^{12} mg/a = 1627 t/a results.

For a calcite density of 2.6 g/dm^3 that amounts to a cavity volume of 1627 t/a : 2.6 · 10^{-6} t/dm^3 = 6.25 · 10^8 dm^3/a or 6.25 · 10^5 m^3/a. Recalculated to an area of 50 km · 30 km, a subsidence of 6.25 · 10^5 m^3/a : (50 km · 30 km) = 6.25 · 10^5 m^3/a : 1.5 · 10^9 m^2 = 4.17 · 10^{-4} m/a = 0.4 mm/a can be calculated.

4.1.3 Groundwater

4.1.3.1 The pE-pH diagram for the system iron

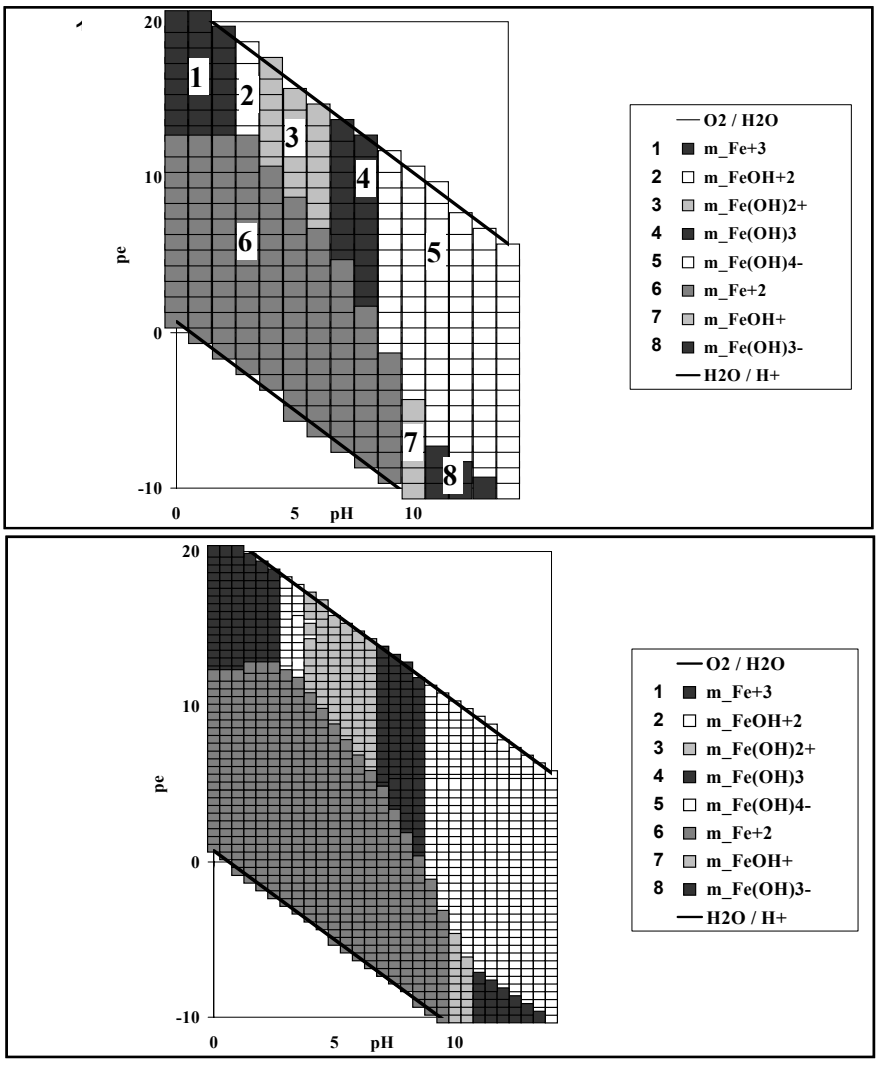

Fig. 53 pe-pH diagram for the system iron (initial solution 10 mmol Fe + 10mmol Cl); Variation of pE, pH in steps of 1 (above) and 0.5 (below, higher raster resolution, numbers as indicated in the figure above)

The following species must be defined within the key word SELECTED_OUTPUT to assess whether they predominate and if so, under which pH-pe-conditions: Fe^{2+}, Fe^{3+}, $FeCl^{+}$, $FeOH^{+}$, $Fe(OH)_2$, $Fe(OH)_3^{-}$, $Fe(OH)_2^{+}$, $Fe(OH)_3$, $FeOH^{2+}$, Fe^{3+}, $Fe_2(OH)_2^{4+}$, $Fe(OH)_4^{-}$, $Fe_3(OH)_4^{5+}$, $FeCl_2^{+}$, $FeCl^{2+}$, $FeCl_3$.

Fig. 53 shows the predominance diagram as a result of the modeling. The second raster, created by the 4-fold number of data by cutting down the step width by half, reveals a higher resolution. However, no additional species appear, that might have been missed by the lower resolution in the first raster. The gaps within the 0.5-step raster at the pH-pE combinations of pH 3.5 / pE 12.5, pH 3.5 / pE 13, pH 4 / pE 14.5, pH 4 / pE 15.5 and pH 3.5 / pE 16 arise from numerical problems that occurred during the modeling and allowed no convergence of the model. The corresponding SOLUTIONS were removed from the PHREEQC input file.

Comparing the created pE-pH diagram to the one for the system Fe-O_2- H_2O according to Langmuir (1997; Fig. 15), clear similarities can be shown. Just the $Fe(OH)_3^-$-field is somewhat smaller in the example and an additional field for the $FeOH^+$ species is indicated, which is lacking in the diagram of Langmuir (1997).

4.1.3.2 The Fe pE-pH diagram considering carbon and sulfur

In SELECTED_OUTPUT $FeHCO_3^+$, and $FeCO_3$ for the iron - carbon system as well as $FeSO_4^+$, $FeHSO_4^{2+}$, $Fe(SO_4)_2^-$, $FeHSO_4^+$, and $FeSO_4$ for the iron - sulfur system must be defined for the output besides the iron species from chapter 4.1.3.1. For both systems numerical problems occur at pH 4 and pH 14.

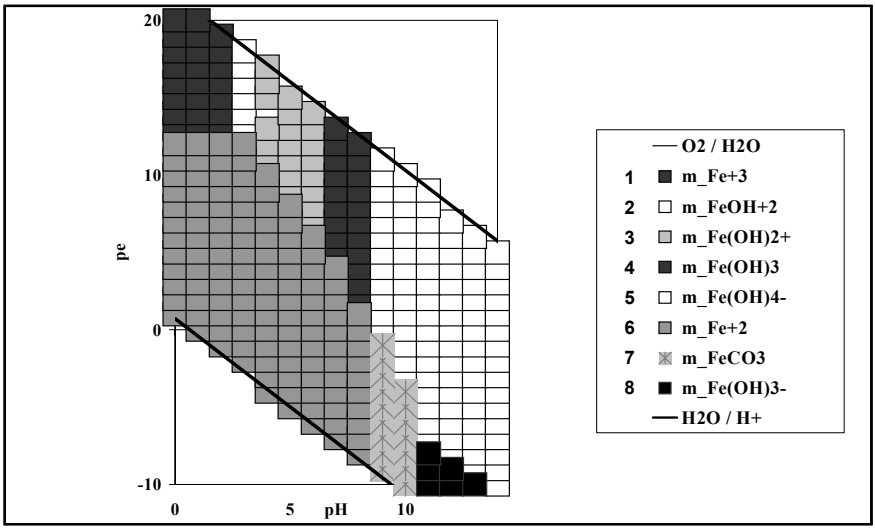

Fig. 54 pe-pH-diagram for the system iron-carbon (initial solution 10 mmol Fe + 10 mmol Cl + 10 mmol C), numbers as indicated in Fig. 53

In the iron - carbon system (Fig. 54) the $FeOH^+$ - field vanishes, the zero charged $FeCO_3^0$ - field predominating instead under the same pE - pH conditions. In the iron - sulfur system (Fig. 55) the predominance field of the iron - sulfate species $FeSO_4^+$ enlarges at the expense of Fe^{3+}, while $FeOH^{2+}$ disappears completely.

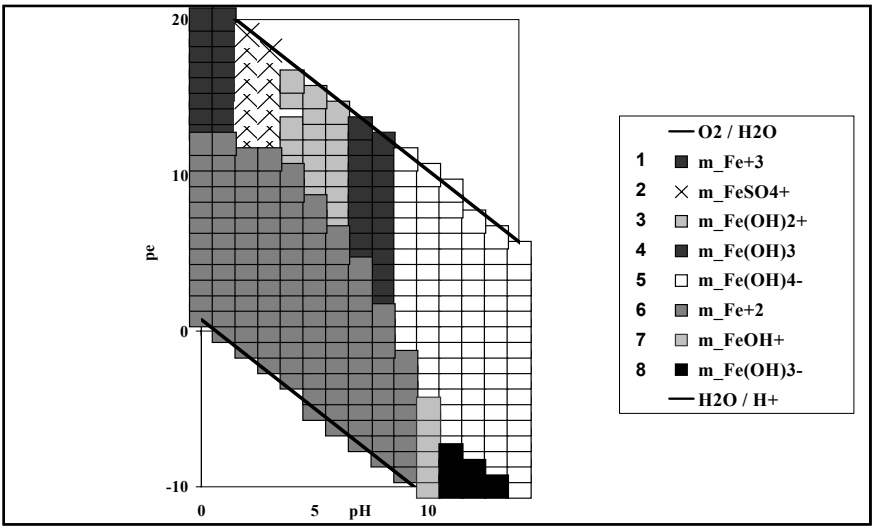

Fig. 55 pe-pH diagram for the system iron – sulfur [initial solution 10 mmol Fe + 10 mmol Cl + 10 mmol C], numbers as indicated in Fig. 53

The pE-pH diagrams, as the ones modeled and presented in Fig. 53 to Fig. 55, provide a good overview of possible predominating species. However, they have the significant disadvantage that for setting up a complete diagram covering all ranges (i.e. from extremely oxidizing to extremely reducing, and from extremely acid to extremely alkaline) only idealized solutions can be modeled. Those idealized solutions contain only few defined species, as e.g. in the example, only C or S apart from Fe and Cl as the corresponding anion. The ion balance frequently shows larger deviations than 2%. The requirement of a constant ionic strength through all pE - pH fields can only be partially maintained. Moreover, species that occur in almost the same concentration as the predominating species, and are possibly significant for reactive transport, are totally neglected in predominance diagrams. These weaknesses of pE - pH diagrams must be kept in mind for modeling and interpretation.

4.1.3.3 The pH dependency of uranium species

First of all both solutions, the acid mine water and the groundwater, are defined in the PHREEQC input file and mixed applying the keyword MIX. Then this solution is saved as solution 3 (SAVE_SOLUTION) and the job is finished by END. A second job follows, which uses again SOLUTION 2 (groundwater) and SOLUTION 3 (1:1 diluted water) via the key word USE, once again mixes both solutions 1:1, and saves the result as SOLUTION 4, etc. SELECTED_OUTPUT facilitates the further data processing in EXCEL by providing the pH values and the “molalities” of all uranium species. The key word itself has to be repeated for every job, as well as the definition of the desired parameters pH and molalities.

Yet the file name (e.g. 3_uranium_species_pHdependent.csv) should only appear within the first SELECTED_OUTPUT block and not be repeated. This way PHREEQC writes the parameters of all modeling in one single SELECTED_OUTPUT file. The headline, however, is repeated for every modeling run. The sub key word "- reset false", also applied just once within the first SELECTED_OUTPUT block, suppresses the standard output for all other modeling, which are written into the same file.

With seven mixings plus the initial solution of acid mine water and the resulting solution of groundwater the variations in uranium species are as shown in (Fig. 56).

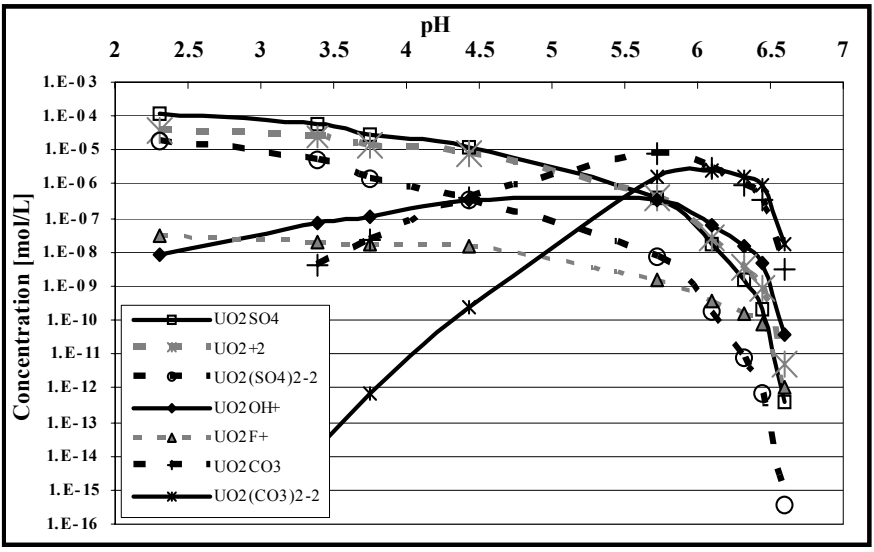

Fig. 56 Development of uranium species during the mixing of an acid mine water (pH= 2.3) with a groundwater (pH=6.6)

For low pH values the zero charged $UO_2SO_4^0$ complex predominates. The positively charged UO_2^{2+} complex reaches similar concentrations though. From pH=5 on, the carbonate complexes predominate, first the zero charged $UO_2CO_3^0$ complex, at pH values exceeding 6 the negatively charged $UO_2(CO_3)_2^{2-}$ complex. Both carbonate complexes are of no importance in an acid environment (pH values < 3.5). For transport and sorption processes, especially the zero charged complexes have to be taken into account, since they show only little interactions, hence can hardly be retarded.

4.1.4 Origin of groundwater

4.1.4.1 Origin of spring water

For inverse modeling there is never just one "correct" solution but a number of possible ways, one of which is shown here. No model could be found explaining the chemical composition of the spring only from the influence of the crystalline basement or just from the Quaternary, as might have been assumed from the location of the spring.

With an uncertainty of 0.06, the use of the gaseous phase CO_2 and the mineral phases calcite, dolomite, and halite (from the Cretaceous limestone), quartz, K-mica, albite, anorthite, and Ca-montmorillonite (from the Quaternary aquifer) as well as $Fe(OH)_{2.7}Cl_{0.3}$ pyrite, pyrolusite (from the crystalline basement) and assuming additionally that halite, K-mica, albite, and anorthite can only be dissolved while Ca-montmorillonite can only precipitate, the following model was found (Table 46).

Table 46 Model for the origin of a spring water (precipitating mineral phases +, dissolving mineral phases -, concentration in mol/L)

$CO_2(g)$	1.06E+03	Albite	4.00E-04
Calcite	-1.06E+03	Anorthite	1.23E+03
Dolomite (d)	4.07E-04	K-Mica	3.59E-05
Halite	2.29E-04	$Fe(OH)_{2.7}Cl_{0.3}$	-3.25E-05
Montmorillonite	-1.06E+03	Pyrite	3.69E-05
Quartz	1.42E+03	Pyrolusite	1.09E-06

Besides the clay mineral Ca-montmorillonite, calcite and $Fe(OH)_{2.7}Cl_{0.3}$ also form. All other mineral phases remain dissolved. The hypothesis that there is a hydrochemical influence from the Cretaceous limestone and from the Quaternary sediments because the spring is located above an apparently hydraulically active fault, seems to be correct. The influence of the crystalline basement results from the general groundwater flow from east to west. The model uncertainty is acceptable with 6%.

4.1.4.2 Pumping of fossil groundwater in arid regions

The mineral phases calcite, dolomite, halite, and gypsum for the Cretaceous limestone, as well as albite, quartz, anorthite, K-mica for the sandstone, and the gaseous phase CO_2 have to be defined. Furthermore it is assumed that dolomite, gypsum, and halite only dissolve, while calcite precipitates and CO_2 degasses. Under those conditions and with an uncertainty of 4%, two models are obtained (Table 47).

Both models differ only slightly; model 2 does not use quartz as a mineral phase. The ratio fossil to recent groundwater is equal for both models: 62%:38%, which means that almost two thirds of the extracted groundwater is not recharged.

With a pumping rate of 50 L/s or 50 · 60 · 60 · 24 L/ d = 4,320,000 L/d, 0.6211 · 4,320,000 L/d = 2,683,152 L/d fossil water are extracted. For a reservoir of 5 m · 1000 m · 10,000 m = 50,000,000 m^3 or 50,000,000,000 L it takes 50,000,000,000 L : 2,683,152 L/d = 18635 d or 18635 d : 365 = approximately 51 years until the reservoir is completely exploited, and only recent groundwater is available anymore. Thus, assuming a constant supply, this amount will be only 38% of the present production, i.e. 19 L/s instead of 50 L/s, which are also subject to larger variations independent of the rainfall.

Table 47 Two models, showing the share of fossil groundwater compared to recent groundwater in an arid region (precipitating mineral phases +, dissolving mineral phases -, concentration in mol/L)

Isotopic composition of phases	**Model 1**		**Model 2**	
13C Calcite	2 + -2 = 0		2 + -2 = 0	
13C CO2(g)	-25 + -5 = -30		-25 + -5 = -30	
Solution fractions	share	percentage	share	percentage
Solution 1 (fossil water)	6.21E-01	62.11	6.21E-01	62.11
Solution 2 (recent groundwater)	3.79E-01	37.89	3.79E-01	37.89
Solution 3	1.00E+00	100.00	1.00E+00	
Phase mole transfers				
Calcite CaCO3	-2.59E-04	pre	-2.59E-04	pre
CO2(g)	-2.48E-04	pre	-2.48E-04	pre
Quartz SiO2	7.69E-06	dis		
Kmica KAl3Si3O10(OH)2	-1.88E-05	pre	-1.88E-05	pre
Albite NaAlSi3O8	-1.75E-04	pre	-1.71E-04	pre
Anorthite CaAl2Si2O8	1.16E-04	dis	1.14E-04	dis
Gypsum CaSO4	2.80E-04	dis	2.82E-04	dis

4.1.4.3 Salt water / fresh water interface

Just as with every task of inverse modeling there is not one correct solution, but a number of possible solutions. First, by means of the sub key word “charge” the electrical balance must be corrected because the analytic error is too high with -4.65%. The best way is to use calcium to attain a balanced charge.

With a very small uncertainty of 0.006 for the gaseous phase CO_2, the mineral phases gypsum and halite (for the marine environment), quartz, K-mica, albite, and anorthite (from the Quaternary aquifer) as well as calcite and dolomite (from the Cretaceous limestone) and assuming that halite, gypsum, K-mica, albite, and anorthite can only be dissolved, the following three models were found (Table 48).

Since quartz, feldspar and mica are considered as significant mineral phases in the Quaternary aquifer and these are only represented in the first model, this one is chosen. Independent of that, the proportion of seawater to groundwater is 22.55% to 77.45% in all three models.

Table 48 3 models for the determination of the proportion of sea water relative to fresh water in the irrigation water (precipitating mineral phases +, dissolving mineral phases -, concentration in mol/L)

Model 1		**Model 2**		**Model 3**	
CO2(g)	4.91E-04	CO2(g)	4.93E-04	CO2(g)	4.93E-04
Gypsum	1.25E-04	Gypsum	1.28E-04	Gypsum	1.28E-04
Quartz	9.79E-06	Calcite	-2.00E-04	Quartz	-9.71E-08
K-Mica	1.65E-06	Dolomite	-1.16E-04	Calcite	-2.00E-04
Albite	-4.94E-06			Dolomite	-1.16E-04
Calcite	-1.97E-04				
Dolomite	-1.17E-04				

4.1.5 Anthropogenic use of groundwater

4.1.5.1 Sampling: Ca titration with EDTA

In order to get the sample alkaline first, 0.1 mol NaOH is added using the key word REACTION. This addition causes an increase in pH value from 6.7 to 13.343. This alkaline solution is saved, and called up again in a second job. Using REACTION, EDTA is added (for this example 1e-5, 5e-5, 1e-4, 5e-4, 1e-3, 5e-3, 1e-2, 5e-2, 1e-1, 5e-1, 1, 5 and 10 mol/L).

Fig. 57 shows the predominant Ca-complexes under the described conditions.

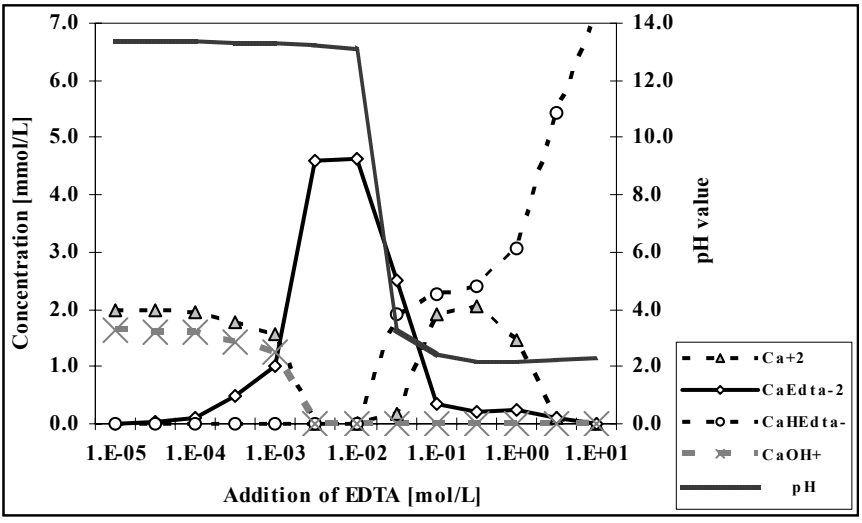

Fig. 57 Stability of the Ca-EDTA complex upon addition of 5e-3 to 1e-2 mol/L EDTA to a solution, which is made basic with 0.1 mol NaOH to a pH of 13.34; larger amounts of EDTA in solution lead to deprotonization and thus to a decrease in pH value, EDTA is preferably bound to H^+ ions, the $CaEdta^{2-}$ complex loses significance.

Upon addition of small quantities of EDTA to the alkaline solution, free Ca^{2+} cations and the Ca-hydroxo complex $CaOH^+$ predominate. From about 0.5 to 1 mmol/L EDTA the Ca-$EDTA^{2-}$ complex gains significance. Between 5 to 10 mmol/L EDTA at last all Ca is bound as Ca-$Edta^{2-}$ complex and is determined by means of a color indicator. If more than 10 mmol/L of EDTA are added, the pH drops immediately from 13 to about 3, since the deprotonization of the acid EDTA exceeds the alkaline buffering with NaOH. Preferably H^+-EDTA-complexes form ($EdtaH_2^{2-}$, $EdtaH_3^-$, etc.). For Ca only a limited amount of EDTA is available. The $CaHEdta^-$ complex and again free Ca^{2+}-cations predominate.

Using 1 mol NaOH instead of 0.1 mol in the beginning of the titration the stability range of the Ca-$Edta^{2-}$ complex enlarges. Using 0.01 mol NaOH, Ca-$Edta^{2-}$ does not predominate in any range anymore.

4.1.5.2 Carbonic acid aggressiveness

Considering calcite equilibrium a pHc of 7.076 results, that is 0.376 pH units above the measured pH value of 6.7. The permitted deviation of 0.2 is exceeded. Since pH-pHc is negative, the water is calcite aggressive, i.e., it can still dissolve calcite and present a danger for pipe corrosion. Undersaturation can also be determined without calculation of the pHc, because within "initial solution calculations" in the PHREEQC output, calcite already shows a saturation index of -0.63 (= 23% saturation).

4.1.5.3 Water treatment by aeration - well water

After aeration by adjustment of an equilibrium with the atmospheric CO_2 partial pressure (0.03 Vol%, CO_2(g) -3.52) the pH value increases to 8.783, the pHc to 7.57. Thus ΔpH is +1.213, i.e., the water is supersaturated with regard to calcite and calcite precipitation might occur in the pipe systems. The SI calcite (under "batch reaction calculations") is +1.35. Thus, aeration deteriorates the initial conditions regarding calcite equilibrium. The drinking water standards are exceeded by far.

4.1.5.4 Water treatment by aeration - sulfur spring

The species distribution of Al, Fe(II), and Fe(III) is depicted in Fig. 58. Al(III) and Fe(II) predominate as OH-complexes. There are almost no free Al^{3+} or Fe^{3+} cations, while the majority of Fe(II) occurs as free cations (71%), followed by the $FeHCO_3^+$ complex (21%). Considering the total iron content, the concentration of Fe(II) ($4.44 \cdot 10^{-6}$ mol/L) is significantly higher than Fe(III) ($5.69 \cdot 10^{-15}$ mol/L).

After aeration there are no significant species changes (Fig. 59), beside the fact that the $Fe^{II}(HS)_2$ complex is not formed under oxidizing conditions anymore. Iron is almost completely oxidized to Fe(III) ($4.44 \cdot 10^{-6}$ mol/L compared to $1.41 \cdot 10^{-14}$

mol/L for Fe(II)). $Al(OH)_3(a)$ and $Fe(OH)_3(a)$ are precipitating mineral phases, possibly also some more.

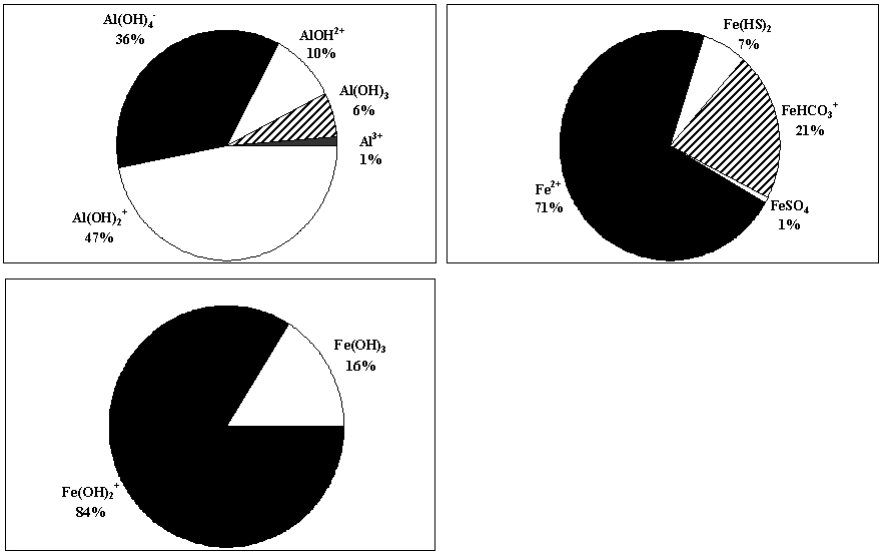

Fig. 58 Al-, Fe(II)- and Fe(III) species distribution prior to aeration

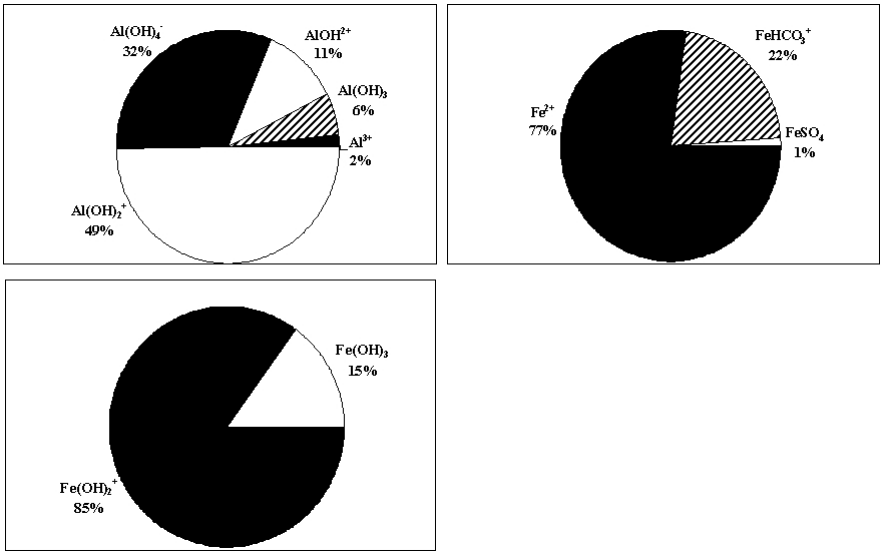

Fig. 59 Al-, Fe(II)- and Fe(III) species distribution after aeration

Variation of the oxygen partial pressure scarcely leads to any changes because in an open system under steady state conditions any amount of oxygen can be dissolved. Hence, all species can be oxidized almost independent of the partial pressure. The concentration of Fe(III) does not change at all, while slight changes

occur for Fe(II). For $P(O_2)$ = 1 Vol% Fe (II) is at $3.019_{.} \cdot 10^{-14}$mol/L and for $P(O_2)$ = 100 Vol% at $9.547 \cdot 10^{-15}$ mol/L.

The pH value of 6.462 after aeration is too low according to the drinking water standards. Further water treatment is required.

The amounts of the precipitating mineral phases $Al(OH)_3$(a) and $Fe(OH)_3$(a) can be found under "phase assemblage". Multiplying these concentrations (in mol/L) with the molecular weight in g/mol and the production rate of the waterworks (in L/s) one gets a concentration (in g/s), which in turn can be transformed into kg/d (Table 49).

Table 49 Accumulating amounts of sludge resulting from the precipitation of $Al(OH)_3$ and $Fe(OH)_3$

	mol/L	mole mass	yield	kg/day
$Al(OH)_3$(a)	$6.139_{.}$·10-6	78	30 L/s	1.24
$Fe(OH)_3$(a)	$4.425_{.}$·10-6	106.8		1.22

The amount of sludge, resulting from precipitation of Al- and Fe-hydroxides, sums up to 2.46 kg/d of dry mineral phases. Considering the high content of water in the sludge yields a factor of 2.5 (for 60% water content) to 10 (for 90% water content) and an amount of sludge of 6.15 kg/d or 24.6 kg/d, or about 185 - 740 kg/month.

In the simulation, N and S get completely oxidized, which is not necessarily true for a water treatment plant, since redox reactions show appreciable kinetics (slow reactions). Partly reduced forms may keep metastable over long periods of time.

4.1.5.5 Mixing of waters

In the abandoned well SO_4^{2-} with 260 mg/L and NO_3^- with 70 mg/L exceed the drinking water standards of 240 mg/L, and 50 mg/ L respectively. In the well currently used there are problems concerning the calcite aggressiveness, as modeled in chapter 3.1.5.2. Therefore these parameters must be taken into account while modeling the mixing of the two waters. The following values were obtained (Table 50).

Table 50 pH, pHc, SO_4^{2-} and NO_3^- concentrations for different mixing ratios between the water from the abandoned (old) and the current (new) well

new : old	pH	pHc	ΔpH	SO_4^{2-} [mmol/L]	SO_4^{2-} [mg/L]	NO_3^- [mmol/L]	NO_3^- [mg/L]
0:100	6.99	6.84	0.15	2.707	**260.00**	1.129	**70.01**
10:90	6.95	6.86	0.09	2.644	**253.95**	1.019	**63.18**
20:80	6.91	6.87	0.04	2.582	**248.00**	0.908	**56.33**
30:70	6.87	6.89	-0.02	2.520	**242.04**	0.798	49.50
40:60	6.84	6.91	-0.07	2.457	235.99	0.688	42.67

new : old	pH	pHc	ΔpH	SO_4^{2-} [mmol/L]	SO_4^{2-} [mg/L]	NO_3^- [mmol/L]	NO_3^- [mg/L]
50:50	6.81	6.93	-0.12	2.395	230.03	0.577	35.78
60:40	6.79	6.95	-0.16	2.333	224.08	0.467	28.95
70:30	6.76	6.98	**-0.22**	2.270	218.03	0.356	22.05
80:20	6.74	7.01	**-0.27**	2.208	212.07	0.246	15.28
90:10	6.72	7.04	**-0.32**	2.146	206.12	0.136	8.45
100:0	6.70	7.08	**-0.38**	2.083	200.07	0.024	1.50

If a proportion of the water from the old well is too high, the mixed water shows sulfate and nitrate concentrations exceeding drinking water standards (bold), if it is too low, the mixture is calcite aggressive (bold), which may lead to pipe corrosion. The optimum ratio is between 40 : 60 to 60:40, where the water can be discharged to the drinking water distribution net without any further treatment.

4.1.6 Rehabilitation of groundwater

4.1.6.1 Reduction of nitrate with methanol

To determine the amount of methanol required to reduce the nitrate, one has to proceed iteratively, i.e. a certain amount of methanol is added step by step using the keyword REACTION (e.g. 0.1 1 5 10 50 100 mmol/L) and according to the results the step width is refined. In this example a higher resolution was chosen between 1.3 and 1.35 mmol/L. The following result is obtained (Fig. 60).

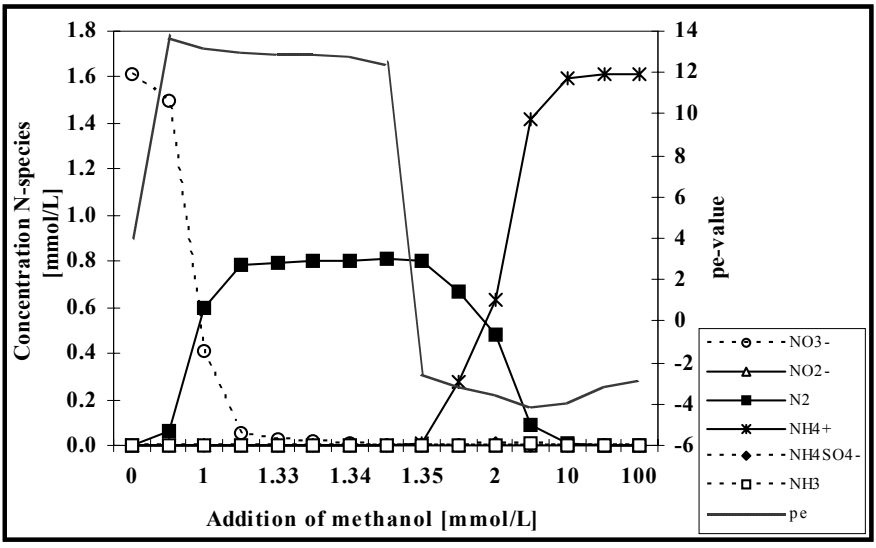

Fig. 60 Successive reduction of penta-valent NO_3 in an aquifer into zero valent N_2 and -3-valent NH_4^+ by addition of methanol (the species NO_2^-, $NH_4SO_4^-$, NH_3 occur in trace amounts only)

Already upon addition of small amounts of methanol (<1 mmol/L) a significant decomposition of NO_3 to N_2 occurs, the pE being in the oxidizing range (12 to 14). With 1.345 mmol/L methanol, the nitrate concentration decreases from 1.614 mmol/L to 0.155 µmol/L N(5) by more than 4 orders of magnitude. If the addition is further increased, the pE value drops notably (pE approx. –2) and N_2 is further reduced to NH_4^+, which is an undesirable side effect for the groundwater rehabilitation.

Thus, 1.345 mmol/L CH_3OH is the necessary amount for a total reduction of nitrate. Methanol has a density of 0.7 g/cm^3 = 700 g/dm^3 = 700 g/L and a molecular weight of 32 g/mol, therefore a 100% methanol-solution has 700g/L : 32 g/mol = 21.875 mol CH_3OH per liter of methanol solution. Thus 1.345 mmol CH_3OH per liter of groundwater : 21875 mmol CH_3OH per liter of methanol solution = $6.15 \cdot 10^{-5}$ L methanol solution per liter groundwater are required, or related to 1 m^3 groundwater 0.06 L of a 100% methanol solution.

4.1.6.2 Fe(0) barriers

Like the previous exercise (3.1.6.1) the question about the dimension of the reactive iron barrier and the corresponding uraninite precipitation must be solved iteratively. Elemental iron is added step by step via the key word REACTION and the saturation index of uraninite is registered. If for instance 1, 2, 3, 4, and 5 mmol/L of Fe are added, the following saturation indices are obtained: -14.3401, -13.6202, -12.8359, -11.3031, +9.5288, i.e. uraninite gets supersaturated when adding between 4 and 5 mmol/L of Fe. Further refining the range, one can assess the supersaturation at 4.40 mmol/L. The results in Table 51 are obtained, promoting uraninite precipitation and registering the amount of uranium that stays in the solution after the reduction of U(VI) to U(IV) by Fe and the subsequent precipitation as (probably amorphous) UO_2.

Table 51 Decrease of the uranium concentration using Fe^0 barriers of different iron concentrations

Fe [mmol/L] in reactive barrier	4.40	4.42	4.43	4.44	4.46	4.48
U [mol/L] in solution after reaction	8.7366 e-05	6.7663 e-05	5.7854 e-05	4.8089 e-05	2.8811 e-05	1.0582 e-05
U [mg/L] in solution after reaction	20.79	16.10	13.77	11.45	6.86	2.52

Since the requirement was to reduce uranium at least to one third of the initial quantity of 40 mg/L, the target concentration is 13 mg/L. Thus, at least 4.43 mmol/L = 247.4 mg/L of Fe have to be available. Assuming a flow through of 500 L/dm^2 these are 247.4 mg/L · 500 L/d·m^2 = 123.7 g/d·m^2. Furthermore, if the barrier is to be in effective operation for about 15 years (5475 days) then 123.7 g/d·m^2 · 5475 d = 677.3 kg of Fe per m^2 must be used. During operation 0.1115

mmol/L UO_2(a) will precipitate, that is 30.1 mg/L, or 82.4 kg/m^2 for a flow through of 500 L/d·m^2 in 15 years.

4.1.6.3 Increase in pH through a calcite barrier

By setting up a reactive calcite barrier in the aquifer, the pH value of the initial acid mine water is increased from 2.3 to 6.25 at a calcite saturation of 50%. Hereby, 17.3 mmol/L or 1.73 g/L calcite dissolves, i.e. for a flow of 500 L/d·m^2 this amount is 1.73 g/L · 500 L/d·m^2 = 865 g/d·m^2. The available 2500 kg/m^2 of calcite would thus be sufficient for 2500 kg/m^2 : 865 g/d·m^2 = 2890 days or 7.9 years, before the calcite barrier would be completely dissolved.

Yet after the reaction with calcite the water is strongly supersaturated with regard to gypsum, which consequently must be precipitated. After the precipitation of gypsum the pH is even slightly higher (6.356) than for pure reaction with calcite, 20.8 mmol/L, or 2.08 g/L of calcite dissolve. At a rate of 500 L/d·m^2 there would be 1040 g/d, i.e. it would take only 2402 days or 6.6 years until the barrier is completely used up. Far more complicated is the precipitation of 17.5 mmol/L or 2.38 g/L of gypsum. For the assumed flow of 500 L/d·m^2 this quantity is 1190 g of gypsum precipitating each day, forming a coating on the calcite barrier, decreasing the permeability and thereby obstructing or even completely preventing any further calcite dissolution.

Alternatively dolomite (as a mixed mineral of Mg and Ca carbonate) or pure Mg carbonate (magnesite) could be used. Dolomite causes a pH increase to 6.439 dissolving 11.45 mmol/L or 2.11 g/L of dolomite. For a flow of 500 L/d·m^2 there are 1050 g/d, using up the supply of 2500 kg dolomite within 2500 kg : 1050 g/d = 2373 days or 6.5 years. As for the reaction with calcite, gypsum becomes supersaturated (SI gypsum = 0.26) and will precipitate. The resultant pH is 6.470 and dolomite dissolution is 12.15 mmol/L = 2.24 g/L (complete dissolution of the dolomite barrier after 2237 days or 6.1 year). Gypsum precipitation produces 9.475 mmol/L or 1.29 g/L gypsum, which is a reduction of 644.3 g/d (at a flow of 500 L/d·m^2) compared to the pure calcite barrier, even though it is still too much for an effective long-term run of the reactive barrier.

For a pure magnesite barrier the pH increases to 6.533. Gypsum stays slightly undersaturated (SI = -0.08), thus is not precipitating and not forming disturbing incrustations. An amount of 26.4 mmol/L or 2.22 g/L of magnesite is dissolved, resulting in an average life of 2252 days or 6.2 years. The higher cost for pure magnesite can be justified by the long-term effectiveness compared to a calcite or dolomite barrier.

4.2 Reaction kinetics

4.2.1 Pyrite weathering

Question 1: What is the chemical composition of the seepage water discharging at the foot of the heap along the base sealing?

The heap is covering an area of 100 · 100= 10.000 m^2. Hence with a daily infiltration rate of 0.1 mm, 1000 liter of rainwater infiltrate every day. The volume of 0.1 m^3 O_2 equals 100 liter O_2 that are entering the heap each day by diffusion. Because one mol of gas equals 22.4 L gas at atmospheric pressure, 100 liter equal (100/22.4) 4.463 mol of O_2. The PHREEQC job for the solution of this task is done as follows: Distilled water (rainwater) is equilibrated with the CO_2- and O_2-partial pressures of the atmosphere, then the extra oxygen from the diffusion into the heap is added by using REACTION and at last the resulting water is put into equilibrium with pyrite.

In the process 1.347 mmol of pyrite dissolve per day and per liter, that equals 1.347 mol for 1000 liters. The pH value is 2.65 and the pE 2.79. Because the modeling started with distilled water, it contains only carbon (0.01704 mmol/L as CO_2), iron (1.347 mmol/L as Fe^{II}) and sulfur (2.695 mmol/L as S(6)) after the reaction. The element S(6) occurs in the following species (Fig. 61):

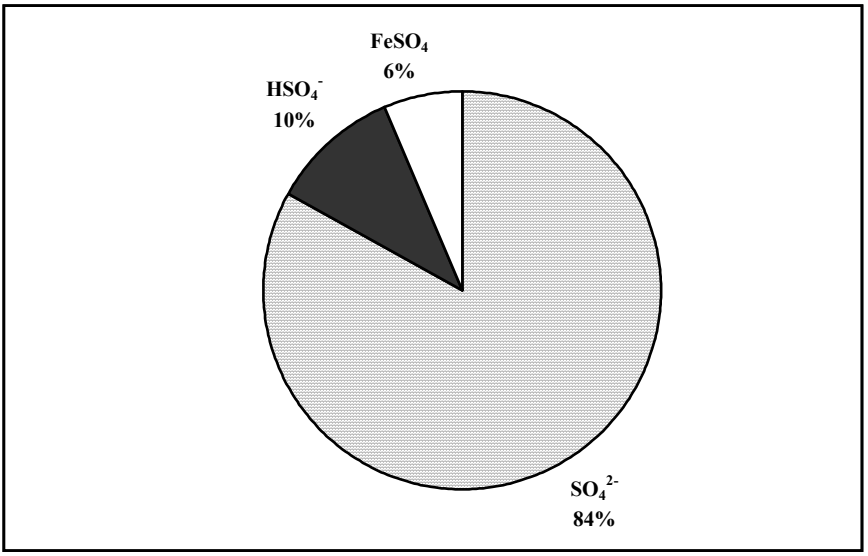

Fig. 61 Species distribution for the element sulfur in the seepage water discharging at the foot of the heap along the base sealing

2. What happens when water at the foot of the heap is in contact with atmospheric oxygen?

To answer this question, the result of question 1 has to be saved in the PHREEQC input file with SAVE_SOLUTION 3, called up in a new job by USE_SOLUTION 3, and subsequently equilibrium with the atmospheric partial pressure has to be adjusted.

The divalent iron is oxidized by atmospheric oxygen into trivalent iron, but only 13% of this iron occurs as free Fe^{3+} cation. The rest is bound in hydroxo and sulfur complexes (Fig. 62).

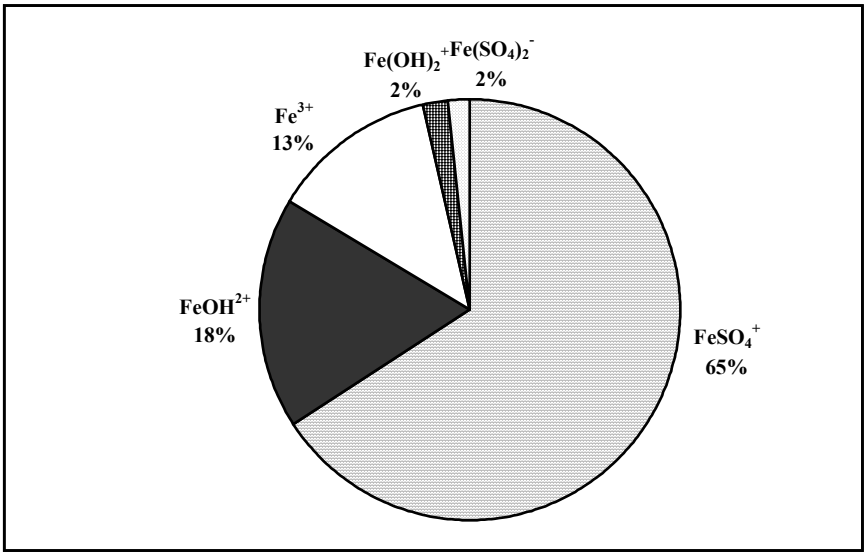

Fig. 62 Species distribution for trivalent iron in the seepage water discharging at the foot of the heap along the base sealing

After the reaction the following minerals are close to saturation or supersaturated (Table 52).

Table 52 Saturation index for some mineral phases after the discharge of the seepage water at the foot of the heap along the base sealing and contact with atmospheric oxygen

Mineral	SI	Mineral	SI	Mineral	SI
$Fe(OH)_3(a)$	-0.41	JarositeH	-0.27	Goethite	5.48
Magnetite	-0.4	Maghemite	2.57	Hematite	11.93

Amorphous iron hydroxide, which precipitates rather spontaneously, is still undersaturated. Maghemite, goethite, and hematite do not usually precipitate spontaneously, but form as secondary mineral phases from hydroxides. That means the trivalent iron mainly remains in solution through complexation reactions.

3. How many years will it take until all pyrite in the heap is exhausted?

To answer this question one does not even have to use PHREEQC. The heap has a volume of 100,000 m^3 (100·100·10 m). 2% of it are 2,000 m^3 of pyrite, which with a density of 5.1 t/m^3 mounts up to 10.200 t or 10,200,000,000 g / 119.8 g/mol = 85,141,903 mol. With a pyrite dissolution of 1.347 mol/d it takes 85,141,903 mol / 1.347 mol/d = 63,208,539 days or 173,174 years until all pyrite is gone. During that time the water has a pH 2.65, and contains 215 mg/l of sulfate and 75 mg/l of iron (as Fe(II)). This result is only valid if there is no passivation of the pyrite surfaces and the mineral is not imbedded in a rock matrix that is weathering more slowly.

4. How much carbonate has to be added during the heap construction to neutralise the pH value? Is it possible to reduce the amount of sulfate at the same time?

The existing input file is extended by setting up equilibrium not only with pyrite but also with calcite. 2.621 mmol of calcite dissolve. The amount of pyrite dissolved is the same as in the absence of calcite (1.347 mmol). The pH value of 7.58 is in the neutral range. Thus, to neutralize the pH approximately 2 moles of calcite must be added for every mol of pyrite. The saturation index of gypsum is still clearly undersaturated (SI = -1.09), i.e. that gypsum is not a limiting mineral phase and hence the sulfate contents stay more or less invariable.

5. How does the necessary amount of carbonate change when assuming that a CO_2 partial pressure of 10 Vol% will develop within the heap as a result of the decomposition of organic matter?

The increased CO_2 partial pressure is implemented using the logarithm of its partial pressure in bar under the key word EQUILIBRIUM_PHASES. For a partial pressure of 10 vol% CO_2 considerable more calcite must be available in the heap, since a significant amount of the CO_2 is used for the dissolution of calcite. To reach equilibrium now 6.288 mmol of calcite are needed. For one mol of pyrite 4.7 mol of calcite must be added. The pH value is with 6.65 compared to 7.58 lower by almost one order of magnitude. Again no saturation is reached for gypsum.

4.2.2 Quartz-feldspar-dissolution

The input file for the solution of this task consists of the keywords SOLUTION, EQUILIBRIUM_PHASES, KINETICS, RATES, and SELECTED_OUTPUT. In the KINETICS block the total time in seconds and the number of steps must be defined by the sub key word -step. This step is only done once and it does not matter for which mineral. Numerical problems must be solved by choosing suitable parameters for -tol and -step divide.

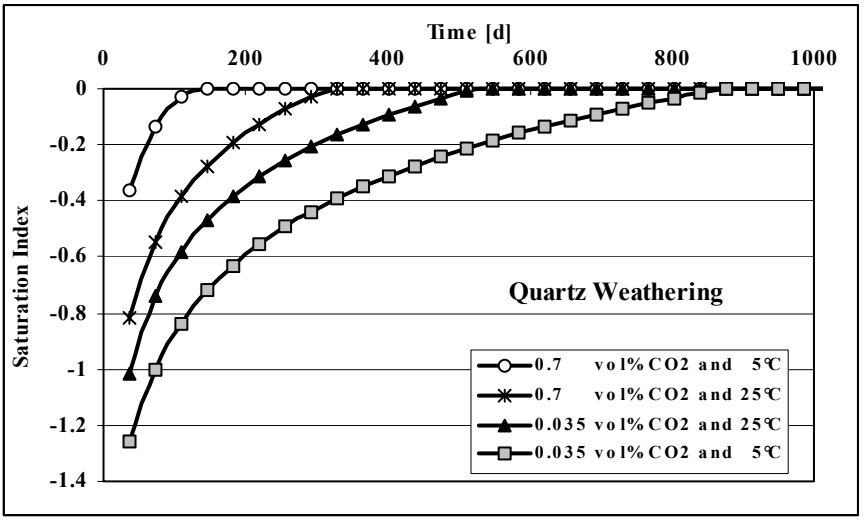

Fig. 63 Kinetics of the dissolution of quartz for four models with different temperatures and partial pressures

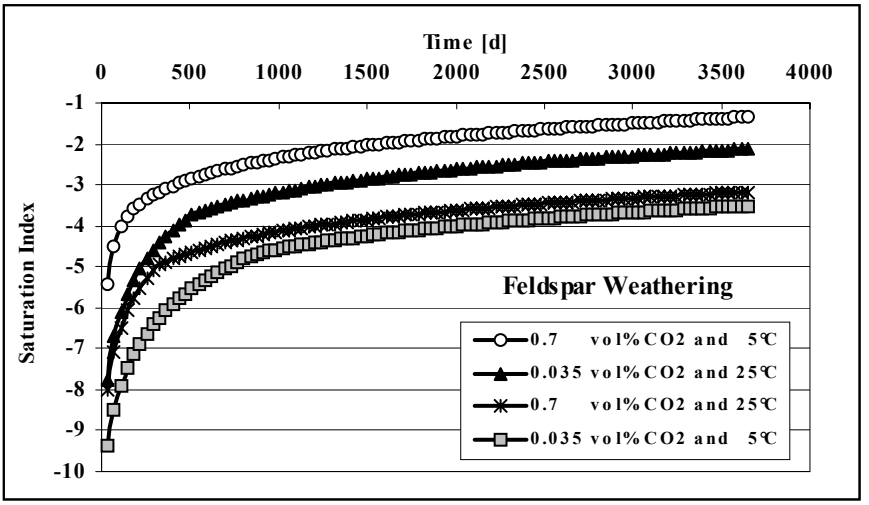

Fig. 64 Kinetics of the dissolution of K-feldspar for four models with different temperatures and partial pressures

Fig. 63 and Fig. 64 show, that both quartz and K-feldspar show different dissolution kinetics depending on temperature and CO_2 partial pressure. The difference between quartz and K-feldspar is significant: while quartz reaches dissolution equilibrium after 150 to 550 days, K-feldspar does not show any equilibration even after 10 years for all of the four possible scenarios. To reach saturation for K-feldspar in all four models, the simulation time would have to be about 1000 years.

4.2.3 Degradation of organic matter within the aquifer on reduction of redox sensitive elements (Fe, As, U, Cu, Mn, S)

At the beginning of the degradation of organic matter the pE-value decreases significantly (Fig. 65). During this decrease the sulfate contents increase by the dissolution of pyrite. From a pE value of +2.7 onwards pyrite is supersaturated and precipitates, which causes a continuous decrease of the sulfate content. The zero charged $CaSO_4^0$ complex copies this behavior to some extent. The pH decreases slightly at the beginning and finally steadies at a value just over 6.

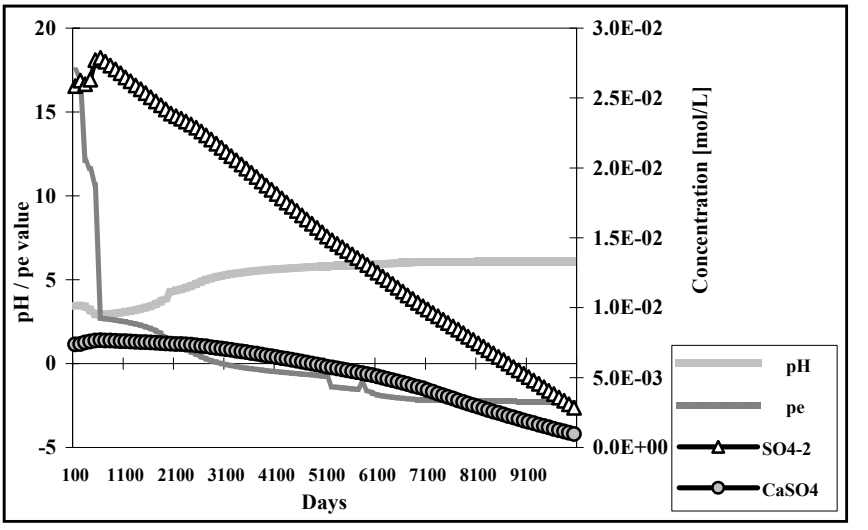

Fig. 65 pH, pE and sulfate concentration over a period of 10,000 days (approximately 27 years) by degradation of organic matter

Fig. 66 shows the undersaturation of some mineral phases of interest. If the saturation index is attained, the respective mineral is precipitated by the model and acts as a limiting phase (kinetics are not considered). The possible limitation by coffinite, uraninite, and pyrite from 500 days onwards (not distinguishable in the figure; coffinite is not a limiting mineral phase any more from 2000 days on; furthermore it is questionable that coeffinite forms under this conditions) is remarkable. Kaolinite is supersaturated after 2000, calcite after 7000, and $Al(OH)_3$

after 10.000 days. Jurbanite is supersaturated from the beginning. An important statement is that, at least under the defined boundary conditions, pyrite can form simultaneously with uranium minerals from a pE value of approximately 2.7 and lower. Before that, the occurrence of pyrite has no significant influence on the concentration of uranium. Moreover, it is important to note that organic matter is available over the whole period of time, in contrast to calcite, which is already used up during the first reaction step. The continuous increase of inorganic carbon results from the formation of CO_2 by the degradation of organic matter. Regarding CO_2 the model assumes a closed system: CO_2 degassing is excluded. The overall influence of calcite is rather small. It causes the pH increase at the beginning of the modeling from 2.3 to 3.39 and has influence on the time of calcite precipitation. Since at the beginning only a small amount of calcite is dissolved, the saturation index of gypsum stays in equilibrium and no precipitation of gypsum was considered.

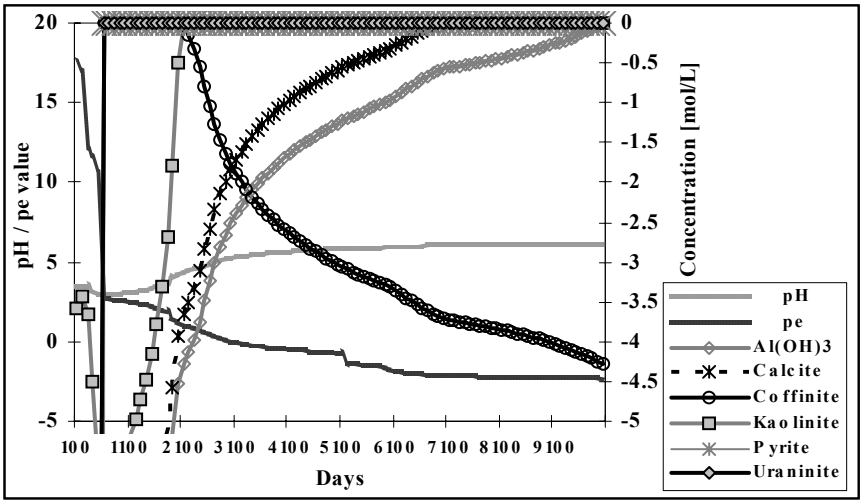

Fig. 66 Selected saturation indices compared to pE and pH values during the degradation of organic matter over a period of 10,000 days

Manganese does not change during the whole time of modeling and occurs as Mn^{2+}. Copper behaves in a different way; it is in the end responsible for the sudden changes in the pE value. The occurrence of Cu^{+} together with As^{3+} (Fig. 67) and the re-transformation into Cu^{2+} at pE-values below -1.87 is also interesting.

For a closer look on the reactions at the beginning of the degradation, the modeling was redone with unchanged boundary conditions in 100 time steps for a period of 600 days. Fig. 68 shows better than Fig. 65 and Fig. 66 the step wise decrease of the pE value. The first drop is connected to the occurrence of Fe^{2+}, the second to the elimination of Fe^{3+} and the reduction of As^{5+} to As^{3+}. Shortly after that the reduction of U^{6+} to U^{4+} occurs. In the model uraninite and coffinite

precipitate spontaneously and hence the uranium concentrations are significantly reduced.

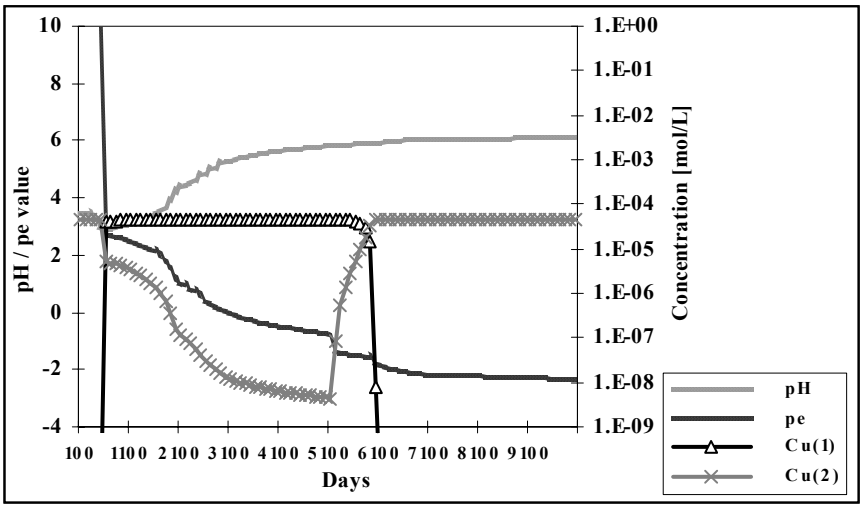

Fig. 67 Changes in the speciation of Cu^{+} and Cu^{2+} in relation to pE and pH values during the degradation of organic matter over a period of 10,000 days

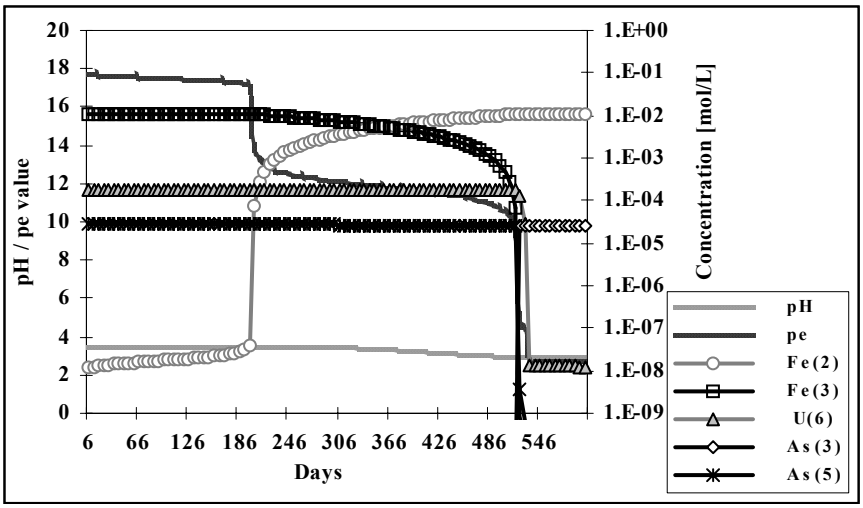

Fig. 68 Changes in the speciation of iron, arsenic, and uranium compared to pE and pH values during the degradation of organic matter over a period of 600 days

4.2.4 Degradation of tritium in the unsaturated zone

Instead of the fictitious initial solution given in the example of an impulse-like input function of a tritium concentration of 2000 TU, a solution of the averaged concentration over a period of 5 years is used (climate station: 06/1962 - 06/1967 1022 TU). The "punch frequency" under the keyword TRANSPORT must be changed from 10 to 5, since every fifth time step (5 years) shall be printed in the output. The six further solutions from 1967-1997 with decreasing tritium concentrations are used as SOLUTION 0 instead of the modeling "30 years no tritium". The jobs are input one after another separated by END. The definition of the transport parameters (number and length of the cells, time steps etc.) must only be done once, when the keyword TRANSPORT is used for the first time (for the modeling of the first 5 years). For the modeling of the further 6 times 5 years only the keyword TRANSPORT is sufficient, all parameters defined in there are taken over from the first definition.

Fig. 69 shows the modeled tritium concentrations in the unsaturated zone after 5, 10, 15, 20, 25, 30, and 35 years. Contrary to the modeling with an impulse-like tritium input (Fig. 42) the concentrations in the uppermost meters of the soil do not immediately drop back to zero because some tritium-containing water keeps infiltrating, even though with lower tritium concentrations. Thus, the tritium peaks do not show a symmetrical curve as with the impulse-like input, but a slightly left-inclined distribution.

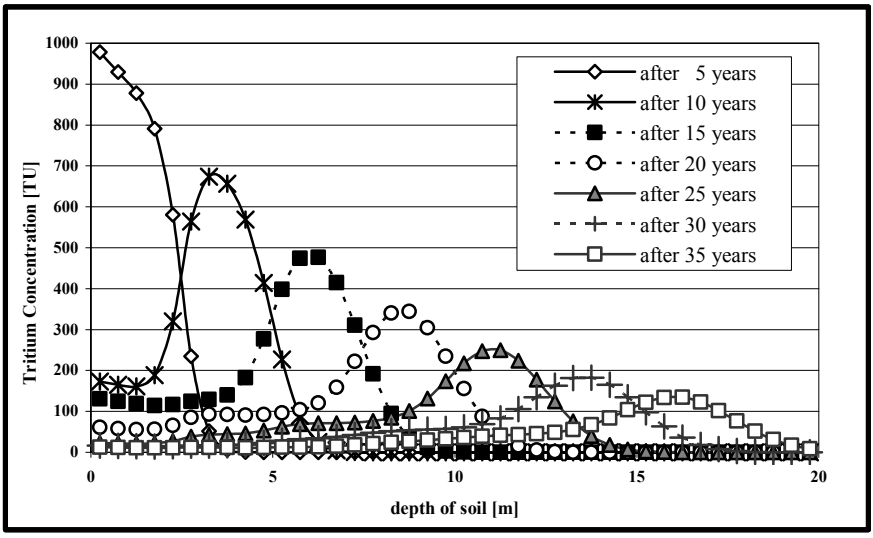

Fig. 69 Vertical cross section of tritium in the unsaturated zone (0-20 m depth) for the climate station Hof-Hohensaas, Germany after 5, 10, 15, 20, 25, 30, and 35 years

4.3 Reactive transport

4.3.1 Lysimeter

Fig. 70 shows the concentration distribution of Ca, Mg, K, Cl, Fe, and Cd in the lysimeter column. Chloride behaves like an ideal tracer and flows through the lysimeter column only influenced by dispersion. Iron apparently does the same, but this is an artifact because no selectivity constant is defined for the predominating species Fe^{3+}. There is one selectivity constant defined for Fe^{2+}, but this species only occurs in negligible amounts (1.459e-07 mol/L). Calcium and magnesium are preferably exchanged for cadmium. This leads to the peaks, occurring after one complete column exchange, that are the sum of the concentrations in the initial water and the acid mine water. As soon as calcium and magnesium are completely exchanged for cadmium, the concentrations decrease to the level of the acid mine water, which is further added to the column. Cadmium only appears at the column´s outlet, when all exchanger sites are occupied, i.e. when the entire volume of the column is exchanged 1.5 times. Thereby, Cd^{2+} ions occupy both the exchanger sites of Mg^{2+} and of Ca^{2+}. That is why cadmium already appears after 1.5 and not only after 2 exchanged column volumes. Potassium is only exchanged to a small extent, sorption and desorption balance one another.

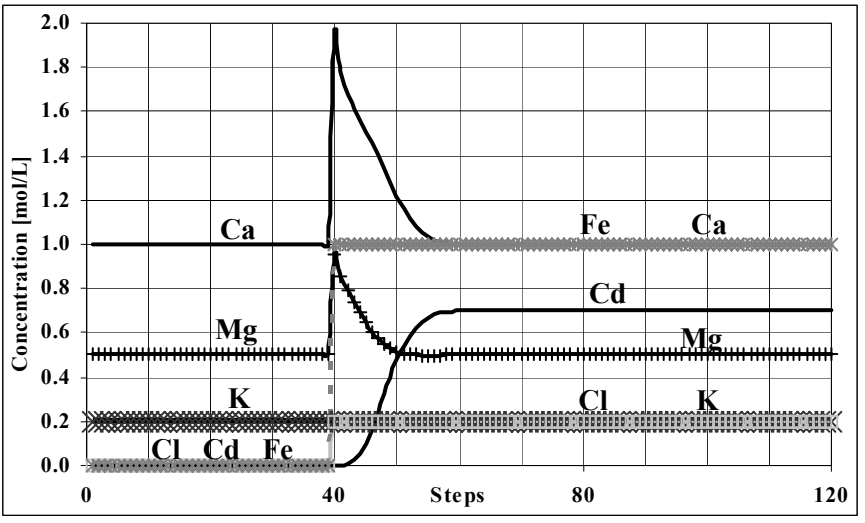

Fig. 70 Concentration distribution of Ca, Mg, K, Cl, Fe, and Cd in the lysimeter column

4.3.2 Karst spring discharge

Using the keyword TRANSPORT PHREEQC always expects an initial solution in the cells, defined as SOLUTION 1-n (here: 1-40). For this exercise it is possible to

simply use the analysis of the water flowing in the karst channel. The same analysis is used as SOLUTION 0 (input solution). The only difference is that for the kinetic transport modeling the partial pressures for CO_2 and O_2 are adjusted to atmospheric conditions by means of EQUILIBRIUM_PHASES 1-40. It is important that also within the keywords KINETICS, RATES and TRANSPORT all 40 cells are considered. A number of 50 shifts is sufficient for the complete exchange of the water, after which a virtually steady state is attained. The results of PHREEQC always refer to one liter of water. Thus the respective conversions must be done; from the stated value in mol calcite/L · 0.5 L/s (discharge) · 86400 · 365 s/a to mol calcite / a, and then from mol calcite / a · 100 g/mol to g calcite / a.

The result of the modeling is depicted in Fig. 71 as the precipitated amount of calcite per year in kg/a for the modeled 400 m in the karst channel after the discharge. The calcite supersaturation decreases within 400 m respectively 27 minutes from 1.58 to 0.16. Despite of the small discharge of 0.5 L/s, the amount of precipitation is 3354.85 kg of calcite per year within the first 400m with an associated release of 1727.5 kg of CO_2 into the atmosphere.

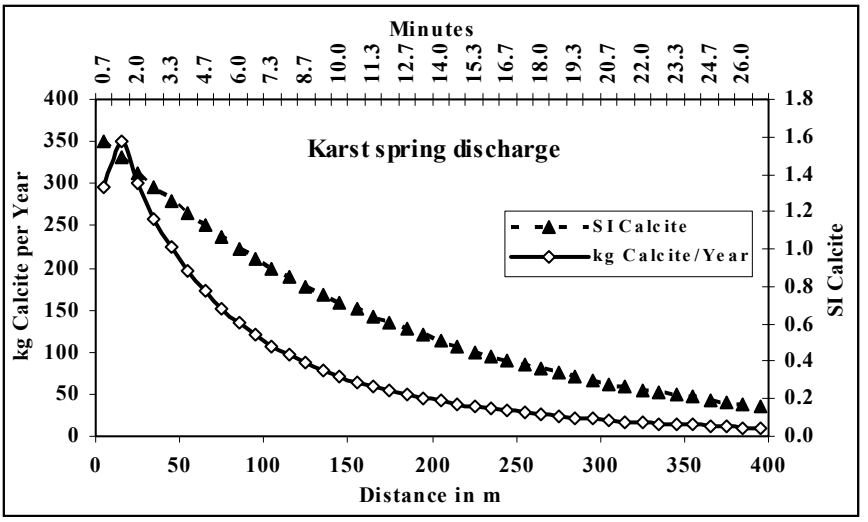

Fig. 71 Calcite saturation index and amount of calcite precipitated per year for a discharge of 0.5 L/s in a 400m long karst channel with a flow velocity of 0.25 m/s assuming turbulent mixing ($P(CO_2)$ = 0.03 Vol%).

The amount of CO_2 can be calculated from the difference of the concentrations of inorganic carbon dioxide at the beginning (6.64 mmol/L) and at the end of the channel (2.02 mmol/L). This amount is 4.62 mmol/L or 873.72 kg C/a. Furthermore, it is known that 3354.85 kg of calcite precipitate per year, which amounts to 402.58 kg of carbon per year (3354.85 kg/a / 100 mol/L (molecular weight of $CaCO_3$)·12 mol/ L (molecular weight of carbon)). The difference between the initial carbon concentration and the concentration, that is lacking at

the end of the channel but was not precipitated, must be the quantity released: 873.72 kg C/a - 402.58 kg C/a = 471.14 kg C/a or 1727.5 kg of CO_2/a. Alternatively, it is possible to calculate the difference between the amount of CO_2 at the begin and at the end of the karst channel (2.55 mmol/ L - 0.45 mmol/L = 2.10 mmol/L), then reduce the difference of the contents of inorganic carbon at the beginning and at the end by that value (4.62 mmol/L - 2.10 mmol/L = 2.52 mmol/L) and finally convert the result, as explained above, into kg of CO_2/a (1748.4 kg CO_2 /a). The deviations resulting from the two different ways of calculation (1727.5 kg CO_2/a versus 1748.4 kg CO_2/a) are within the limits of rounding errors.

4.3.3 Karstification (corrosion along a karst fracture)

To model the karst fracture the keyword TRANSPORT is used and 30 elements are defined by the sub key word -cells. For the fracture being 300 m long the length of the cells is 10 m each. The number of 30 shifts is required to exchange the water volume one time completely. According to the assumed flow velocity the variable -time step is set to 360 seconds (= 0.1 hours). With -punch 1-30 all 30 cells are printed in the output, with -punch frequency 30 only the result after 30 shifts is considered for all of those 30 cells. The adjustment of the equilibrium during transport can be done using EQUILIBRIUM_PHASES. It is important to add 1-30 behind the key words SOLUTION, EQUILIBRIUM_PHASES and KINETICS in order to consider all 30 cells.

By using the key word USER_GRAPH, data are directly written to the spreadsheet GRID within PHREEQC and the graph is created automatically in the folder CHART. The script is as follows:

```
USER_GRAPH
-headings x Ca C SI(calcite)
-chart_title Karstification
-axis_titles "distance [m]"  "concentration [mol] and SI-calcite"
-axis_scale y_axis 0 0.005
-axis_scale secondary_y_axis -3   0.0  1.0
-initial_solutions false
-plot_concentration_vs x
10 GRAPH_X DIST
20 GRAPH_Y tot("Ca"), tot("C")
30 GRAPH_SY SI("Calcite")
```

To display the secondary Y-axis for the calcite saturation index besides the primary Y-axis with the concentrations for Ca and C, “Chart options” / “Show secondary y-axis” must be chosen by click on the right mouse button in the graph. The result of the modeling can be seen in Fig. 72. The figure depicts a convergence to the calcite equilibrium. However, the saturation index shows that

even in the last cell the equilibrium is not reached yet, and thus, carbonate is still dissolved in small quantities (corrosion).

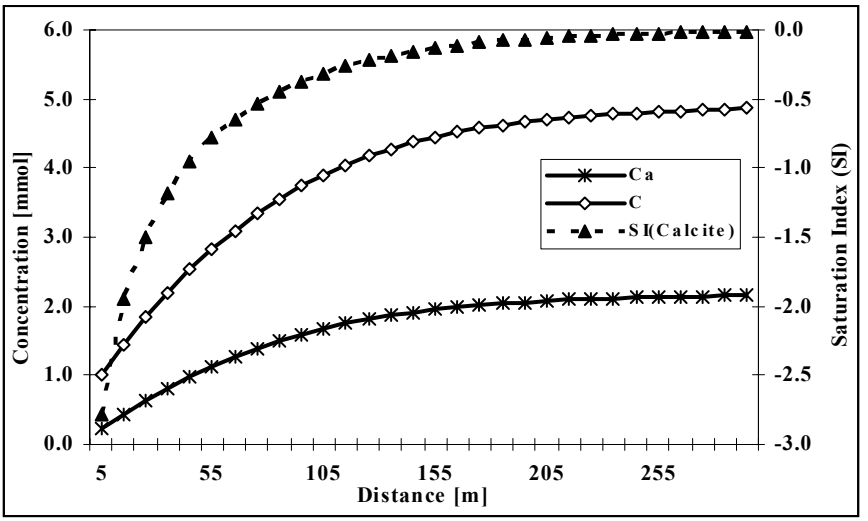

Fig. 72 Corrosion in a fracture showing convergence to the calcite equilibrium with increasing distance

4.3.4 The pH increase of an acid mine water

The acid mine water is defined as SOLUTION 0 and the water in the carbonate channel as SOLUTION 1. Within the key word KINETICS 1-10 the calculation tolerance as well as the initial and the total mole mass of calcite can be defined. Obligatory are only the parameter 50 and 0.6. These are needed by the BASIC program, which must be implemented within the key word RATES. Here, we use the BASIC program listed at the end of the database PHREEQC.dat. If the database PHREEQC.dat is used (which is not free of troubles, since there are, e.g., no data for uranium) or if the paragraph is copied into another database, it is not necessary to define a RATES block in the input file. PHREEQC uses automatically the RATES block from the database. Yet, if any other kinetic rates are to be used, the BASIC program must be copied into the input file under RATES. In any case, the KINETICS block is required.

Using the key word TRANSPORT the model is built from 10 cells and 15 shifts. Flow velocity is defined to 1 m/s by setting -length and -time_step to 50. By that, the total length of the channel is 500 m and the total exposure time 500 s. To get the required information in a selected output file, the input definition must look as follows:

```
SELECTED_OUTPUT
-file    amd_kin.csv
-totals  Ca C Fe
```

```
-molalities SO4-2 CaSO4
-saturation_indices  gypsum calcite
-kinetic_reactants calcite          # how much calcite is dissolved by KINETICS?
-equilibrium_phases gypsum          Fe(OH)3(a)        # how much gypsum and
                                                      # Fe(OH)3 is dissolved by
                                                      # EQUILIBRIUM?
```

Fig. 73 shows that the largest changes in pH value take place in the middle of the carbonate channel. There also the decrease of iron concentrations due to iron hydroxide precipitation takes place. Slightly more moderate are the increase of Ca by calcite dissolution and the decrease of sulfate by gypsum precipitation. The significant decrease of inorganic carbon in the acid mine drainage at the beginning of the channel is caused by degassing of CO_2 to the atmosphere.

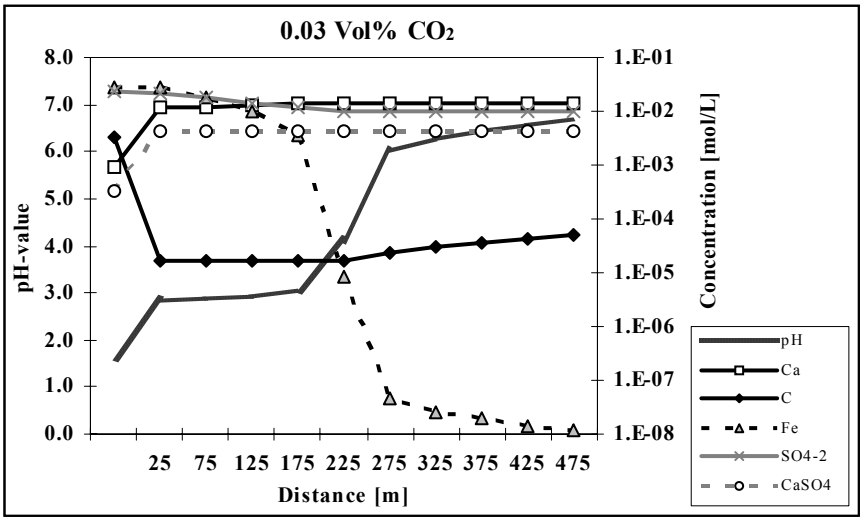

Fig. 73 Concentration changes in an acid mine water while flowing thorough a 500m long carbonate channel

Fig. 74 shows the saturation index for calcite, which increases from almost -12 to about -2.27 in acid mine water, but does not reach saturation. Furthermore, the figure depicts the amounts of dissolved calcite in mol as well as the amounts of precipitated gypsum and iron hydroxide over the simulation time. It can be seen that a channel of 300 m would have a very similar treatment effect as the one modeled 500 m long. Yet modeling of gypsum and iron hydroxide precipitation was done without considering kinetics; it assumed a spontaneous precipitation. The modeling with a partial pressure of 1 vol% CO_2 shows the same behavior at lower pH values (approx. 0.5 pH units) and higher carbon contents.

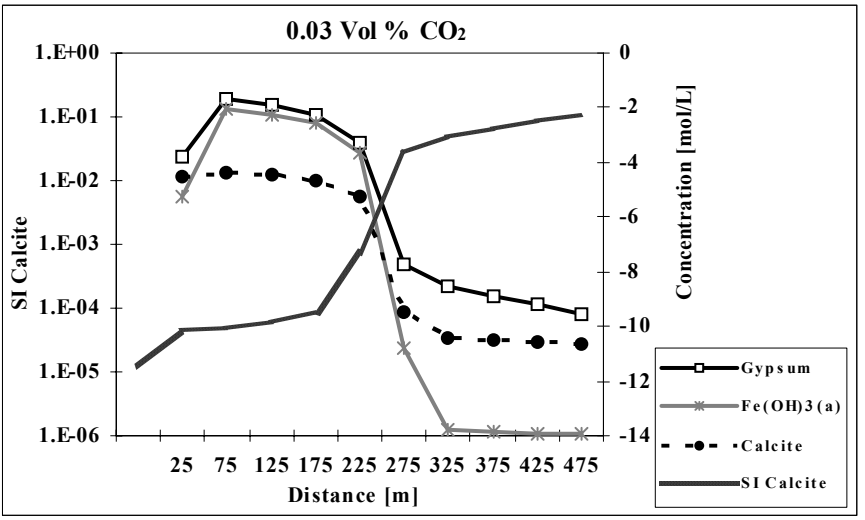

Fig. 74 Dissolution of calcite, precipitation of gypsum and iron hydroxides and the development of the calcite saturation index for the AMD water shown in Fig. 73

4.3.5 In-situ leaching

The fracture system is modeled as a 1d aquifer with high permeability (20 mobile cells with the numbers 1-20), each one connected to immobile cells (number 22-41, number 21 is reserved for the column´s discharge). The content of the immobile cells can only be transferred to the mobile cells by diffusion. The value for α is calculated from Eq. 101 assuming $D_e = 2 \cdot 10^{-10}$ m^2/s (range from $3 \cdot 10^{-10}$ to $2 \cdot 10^{-9}$ for ions in water, approximately one order of magnitude less for water in clays), $\theta_{im} = 0.15$, a = 0.1 m (thickness of the stagnant zone accompanying the fracture), and $f_{s \to 1} = 0.533$ (Table 17)

$$\alpha = \frac{D_e \theta_{im}}{(a f_{s \to 1})^2} = \frac{2 \cdot 10^{-10} \cdot 0.15}{(0.1 \cdot 0.533)^2} = 1.056 \cdot 10^{-8}$$

The fracture volume θ_m was set to 0.05, the pore volume θ_{im} to 0.15.

Already after 30 days the concentrations for the depicted elements U, S, Fe, and Al drop. Further in the simulation the decrease is much smaller (Fig. 75). At the end of the data record, at a fictitious time of 230 days, the concentration of the ground water is shown as a target value. However, to get down to this concentration, the simulation would have to be continued for many more years because of the slow diffusive transfer of contaminants from the immobile to the mobile cells.

Summing up the uranium concentrations for the time steps 1 to 20 gives the amount of uranium in the fractures (3.2 mmol). Because the pore volume is 3 times more than the fracture volume (0.15 compared to 0.05), the uranium concentration in the matrix is also 3 times higher (9.6 mmol). The sum of time steps 21 to 201 is the amount of uranium discharged from the matrix over a period of 180 days (0.298 mmol). This simple calculation shows that after 180 days only about 3.1 % of the total uranium left the matrix via diffusion. Because the process is almost linear, the total time for uranium removal can be estimated to about 16 years.

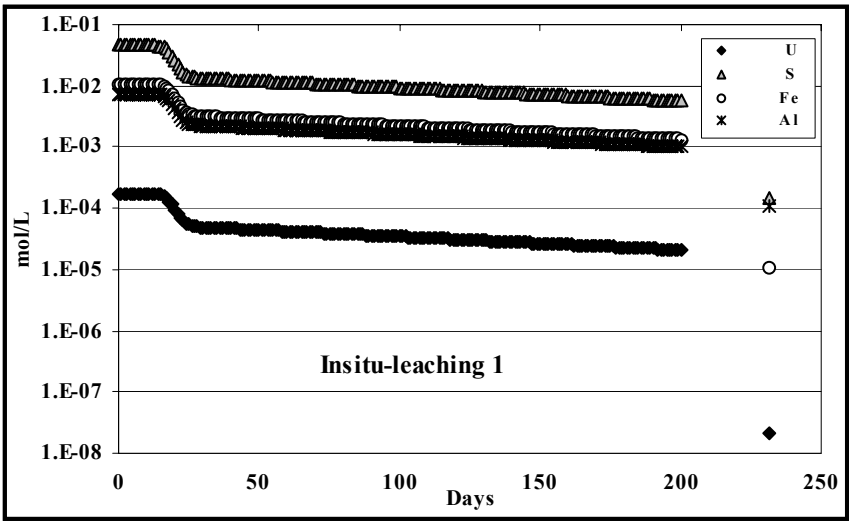

Fig. 75 Simulated concentration at the pumping well over a period of 200 days (fracture volume 0.05, pore volume 0.15, 10 cm of pore matrix connected to the fracture), points on the right side mark the target concentrations.

Changing the parameters as required by the exercise the following value for the exchange parameter results:

$$\alpha = \frac{D_e \theta_{im}}{(a f_{s\to 1})^2} = \frac{2 \cdot 10^{-10} \cdot 0.05}{(0.01 \cdot 0.533)^2} = 3.52 \cdot 10^{-7}$$

If this value is used for modeling together with the smaller value for the size of the connected matrix with 0.01 m, the discharge behavior looks completely different (Fig. 76) For instance the uranium concentration has dropped to the groundwater values already after 100 days, all uranium is removed.

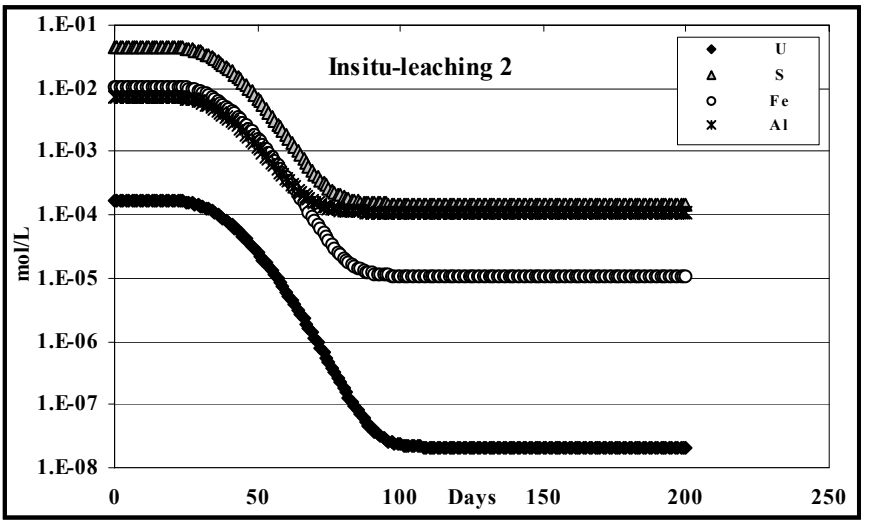

Fig. 76 Simulated concentration at the pumping well over a period of 200 days (fracture volume 0.05, pore volume 0.05, 1 cm of pore matrix connected to the fracture)

References

Abbott MB (1966) An introduction to the method of characteristics.-American Elsevier; New York

Allison JD, Brown DS, Novo-Gradac KJ (1991) MINTEQA2, A geochemical assessment database and test cases for environmental systems: Vers.3.0 user´s manual.-Report EPA / 600 / 3-91 / -21. Athens, GA: U S EPA

Alloway, Ayres (1996) Schadstoffe in der Umwelt.-Spektrum Akademischer Verlag; Heidelberg

Appelo CAJ, Postma D (1994) Geochemistry, groundwater and pollution.- Balkema; Rotterdam

Appelo CAJ, Beekman HE and Oosterbaan AWA (1984) Hydrochemistry of springs from dolomite reefs in the southern Alps of Northern Italy: International Association of Hydrology.- Scientific Publication 150: pp 125-138

Ball JW, Nordstrom DK (1991) User´s Manual for WATEQ4F -US Geological Survey Open-File Report pp 91-183

Bernhardt H, Berth P, Blomeyer KF, Eberle SH, Ernst W, Förstner U, Hamm A, Janicke W, Kandler J, Kanowski S, Kleiser HH, Koppe P, Pogenorth HJ, Reichert JK, Stehfest H (1984) NTA - Studie über die aquatische Verträglichkeit von Nitrilotriacetat (NTA).-Verlag Hans Richarz, Sankt Augustin

Besmann TM (1977) SOLGASMIX-PV, A computer program to calculate equilibrium relationships in complex chemical systems. ORNL/TM-5775

Bohn HL, McNeak BL, O´Connor GA (1979) Soil Chemistry.-Wiley-Interscience; New York

Bunzl K, Schmidt W, Sansoni B (1976) Kinetics of ion exchange in soil organic matter. IV Adsorption and desorption of Pb^{2+}, Cu^{2+}, Cd^{2+}, Zn^{2+} and Ca^{2+} by peat.-J Soil Sci., 17: 32-41; Oxford

Cash JR, Karp AH (1990) A Variable Order Runge-Kutta Method for Initial Value Problems with Rapidly Varying Right-Hand Sides: Transactions on Mathematical Software 16, 3: pp 201-222

Chukhlantsev VG (1956) Solubility products of arsenates.- Journal of Inorganic Chemistry (USSR) 1: pp 1975-1982

Davies CW (1938) The extent of dissociation of salts in water. VIII. An equation for the mean ionic activity coefficient of an electrolyte in water, and a revision of the dissociation constant of some sulfates.- Jour.Chem.Soc.: pp.2093-2098

Davies CW (1962) Ion Association.- Butterwoths, London: pp.190

Davis J, Kent DB (1990) Surface complexation modeling in aqueous geochemistry. In: Hochella M F, White A F (eds) Mineral-Water Interface Geochemistry.-Mineralogical Society of America, Reviews in Mineralogy 23, 5.; Washington D C

Debye P, Hückel E (1923) Zur Theorie der Elektrolyte.- Phys.Z.; 24: pp. 185-206

Drever JI (1997) The Geochemistry of natural waters. Surface and groundwater environments, 3rd edition.-Prentice Hall; New Jersey

DVWK (1990) Methodensammlung zur Auswertung und Darstellung von Grundwasserbeschaffenheitsdaten.- Verlag Paul Parey; 89

Dzombak DA, Morel FMM (1990) Surface complexation modeling - Hydrous ferric oxide.-John Wiley & Sons; New York

Emsley J (1992) The Elements, 2nd edition.-Oxford University Press; New York

Faure G (1991) Inorganic chemistry - a comprehensive textbook for geology students.-Macmillan Publishing Company New York . Collier Macmillan Canada Toronto - Maxwell Macmillan International New York - Oxford - Singapore - Sydney

Fehlberg E (1969) Klassische Runge-Kutta-Formeln fünfter und siebenter Ordnung mit Schrittweiten-Kontrolle: Computing 4: pp 93-106

Fuger J, Khodakhovskyi II, Sergeyeva EJ, Medvedey VA, Navratil JD (1992) The Chemical Thermodynamics of Actinide Ions and Compounds.-Part 12, IAEA; Vienna

Gaines GL, Thomas HC (1953) Adsorption studies on clay minerals. II A formulation of the thermodynamics of exchange adsorption: Journal of Chemical Physics, 21, pp 714-718

Gapon EN (1933) Theory of exchange adsorption [russisch].-J.Gen.Chem. (USSR), 3: pp 667-669

Garrels RM, Christ CL (1965) Solutions, Minerals and Equilibria.-Jones and Barlett Publishers; Boston [Neuauflage: 1990]

Gildseth W, Habenschuss A, Spedding FH (1972) Precision measurements of densities and thermal dilation of water between 5.deg. and 80.deg. J. Chem. Eng. Data, 17 (4): pp 402-409

Grenthe I, Fuger J, Konings RJM, Lemire RI, Muller AB, Nguyen-Trung C, Wanner H (1992) The Chemical Thermodynamics of Uranium.-NEA/OECD; Paris

Gueddari M, Mannin C, Perret D, Fritz B, Tardy Y (1983) Geochemistry of brines of the Chottel Jerid in southern Tunesia. Application of Pitzer´s equations.-Chemical Geology, 39: pp 165-178

Güntelberg E (1926) Untersuchungen über Ioneninteraktion.-Z. Phys. Chem. 123: pp 199-247

Harvie CE, Weare JH (1980) The prediction of mineral solubilities in natural waters. The Na-K-Mg-Ca-Cl-SO_4-H_2O system from zero to high concentrations at 25°C - Geochimica et Cosmochimica Acta, 44: pp 981-997

Hem JD (1985) Study and interpretation of the chemical characteristics of natural waters.-U S Geol. Surv. Water-Supply Paper 2254, 3rd ed.

Hollemann W, Wiberg E (1976) Lehrbuch der Anorganischen Chemie.-DeGruyter Verlag; Berlin

Hölting B (1996) Hydrogeologie.-5.Aufl., Enke

Johnson JW , Oelkers EH & Helgeson HC (1992) SUPCRT92: A software package for calculating the standard molal thermodynamic properties of minerals, gases, aqueous species, and reactions from 1 to 5000 bar and 0 to 1000 C - Computers and Geosciences 18: pp 899-947

Käss W (1984) Redoxmessungen im Grundwasser (II).-Dt. gewässerkdl. Mitt. 28: pp 25-27

Kharaka YK, Gunter WD, Aggarwal PK, Perkins EH, Debraal JD (1988) SOLMINEQ.88 - A Computer Program for Geochemical Modeling of Water-Rock Interactions.-Water-Resources Investigation Reports 88-4227, 420 S.

Kinzelbach W (1983) Analytische Lösungen der Schadstofftransportgleichung und ihre Anwendung auf Schadensfälle mit flüchtigen Chlorkohlenwasserstoffen.-Mitt. Inst. f. Wasserbau, Uni Stuttgart 54: pp 115-200

Kinzelbach W (1987) Numerische Methoden zur Modellierung des Transportes von Schadstoffen im Grundwasser.-Oldenbourg Verlag; München-Wien

Konikow LF, Bredehoeft JD (1978) Computer model of two-dimensional solute transport and dispersion in groundwater.-Techniques of Water-Resource Investigations, TWI 7-C2, U S Geol. Survey; Washington D C

Kovarik K (2000) Numerical models in groundwater pollution.-Springer; Berlin Heidelberg

Lau LK, Kaufman WJ, Todd DK (1959) Dispersion of a water tracer in radial laminar flow through homogenous porous media.-Hydraulic lab., University of California; Berkeley

Langmuir D (1997) Aqueous environmental geochemistry.-Prentice Hall; New Jersey

Meinrath G (1997) Neuere Erkenntnisse über geochemisch relevante Reaktionen des Urans. Wissenschaftliche Mitteilungen des Institutes für Geologie der TU Bergakademie Freiberg Bd.4:, pp 150

Merkel B (1992) Modellierung der Verwitterung carbonatischer Gesteine.-Berichte-Reports Geol.-Paläont. Inst. Univ. Kiel, Nr. 55

Merkel B, Sperling B (1996) Hydrogeochemische Stoffsysteme, Teil I - DVWK-Schriften, Bd. 110.; Komissionsvertrieb Wirtschafts- und Verlagsgesellschaft Gas und Wasser mbH, Bonn

Merkel B, Sperling B (1998) Hydrogeochemische Stoffsysteme, Teil II - DVWK-Schriften, Bd. 117.; Komissionsvertrieb Wirtschafts- und Verlagsgesellschaft Gas und Wasser mbH, Bonn

Nordstrom DK, Plummer LN, Wigley TML, Wolery TJ, Ball JW, Jenne EA, Bassett RL, Crerar DA, Florence TM, Fritz B, Hoffman M, Jr G R Holdren, Lafon GM, Mattigod SV, McDuff RE, Morel F, Reddy MM, Sposito G, Thrailkill J. (1979) Chemical Modeling of Aqueous Systems: A Comparison of Computerized Chemical Models for Equilibrium Calculations in Aqueous Systems. Am. Chem. Soc.: pp 857-892.

Nordstrom DK, Plummer LN, Langmuir D, Busenberg E, May HM, Jones BF, Parkhurst DL (1990) Revised chemical equilibrium data for major water-mineral reactions and their limitations.- In: Melchior DC, Bassett RL (eds) Chemical modeling of aqueous systems II. Columbus, OH, Am Chem Soc: pp 398-413.

Nordstrom DK, Munoz JL (1994) Geochemical Thermodynamics.- 2nd edition, Blackwell Scientific Publications

Nordstrom DK (1996) Trace metal speciation in natural waters: computational vs. analytical. Water, Air, Soil Poll 90: pp 257-267.

Nordstrom (2004) Modeling Low-temperature Geochemical Processes. Treatise on Geochemistry; Vol 5; pp. 37-72, Elsevier.

Parkhurst DL, Appelo CAJ (1999) User's guide to PHREEQC (Version 2) -- a computer program for speciation, batch-reaction, one-dimensional transport, and inverse geochemical calculations.- U S Geological Survey Water-Resources Investigations Report 99-4259: pp 312

Parkhurst DL (1995) User´s guide to PHREEQC - A computer program for speciation, reaction-path, advective-transport, and inverse geochemical calculations.- U S Geol.Survey Water Resources Inv. Rept. 95 - 4227

Parkhurst DL, Plummer LN, Thorstenson DC (1980) PHREEQE - A computer program for geochemical calculations.-Rev.U S Geol.Survey Water Resources Inv. Rept. 80 - 96

Pinder GF, Gray WG (1977) Finite element simulation in surface and subsurface hydrology.-Academic Press; New York

Pitzer KS (1973) Thermodynamics of electrolytes. I Theoretical basis and general equations.-Jour.of Physical Chemistry, 77: pp 268-277

Pitzer KS (1981) Chemistry and Geochemistry of Solutions at high T and P -In: RICKARD & WICKMANN, 295, V 13-14

Pitzer KS (ed) (1991) Activity coefficients in electrolyte solutions. 2nd edition, CRC Press, Boca Raton, pp 542.

Planer-Friedrich B, Armienta MA, Merkel BJ (2001) Origin of arsenic in the groundwater of the Rioverde basin, Mexico; Env Geol, 40, 10: pp.1290-1298

Plummer LN, Busenberg E (1982) The solubility of Calcite, Aragonite and Vaterite in CO_2-H_2O solutions between 0 and 90°C and an evaluation of the aqueous model for the system $CaCO_3$-CO_2-H_2O. Geochimica Cosmochimica Acta 46: pp 1011-1040

Plummer LN, Wigley TML & Parkhurst DL (1978) The kinetics of calcite dissolution in CO_2 -water systems at 5 to 60 C and 0.0 to 1.0 atm CO_2: American Journal of Science 278: pp 179-216

Plummer LN, Parkhurst DL, Fleming GW, Dunkle SA (1988) A computer program incorporating Pitzer´s equation for calculation of geochemical reactions in brines. U S Geol.Surv.Water Resour.Inv.Rep.88-4153

Pricket TA, Naymik TG, Lonnquist CG (1981) A „random walk“ solute transport model for selected groundwater quality evaluations. Illinois State Water Survey Bulletin 65

Robins RG (1985) The solubility of barium arsenates: Sherritt´s barium arsenate process.-Metall.Trans.B 16 B: pp 404-406

Rösler HJ, Lange H (1972) Geochemische Tabellen.- VEB Deutscher Verlag f. Grundstoffindustrie: 674 [Neuauflagen 1975, 1981]

Sauty JP (1980) An analysis of hydrodispersive transfer in aquifers. Water Resources. Res. 16, 1: pp 145-158

Scheffer F, Schachtschabel P (1982) Lehrbuch der Bodenkunde, 11.Aufl.-Enke Verlag; Stuttgart

Schnitzer M (1986) Binding of humic substances by soil mineral colloids. In: Interactions of soil Minerals With Natural Organics and Microbes. In: HUANG P M, SCHNITZER M (Eds).-Soil. Sci. Soc. Am. Publ. No. 17, Madison, WI

Sigg L, Stumm W (1994) Aquatische Chemie.-B G Teubner Verlag; Stuttgart

Silvester KS, Pitzer KS (1978) Thermodynamics of electrolytes. X. Enthalpy and the effect of temperature on the activity coefficients.-Jour. of Solution Chemistry, 7: pp 327-337

Sparks DL (1986) Soil Physical Chemistry.- CRC Press Inc., Boca Raton; FL

Stumm W, Morgan JJ (1996) Aquatic Chemistry, 3rd edition.-John Wiley & Sons; New York

Truesdell AH, Jones BF (1974) WATEQ, a computer program for calculating chemical equilibria of natural waters.-U S Geol. Survey J Research 2: pp 233-48

Umweltbundesamt (1988/89) Daten zur Umwelt.-Erich Schmidt Verlag; Berlin

Van Cappellen P, Wang Y (1996) Cycling of iron and manganese in surface sediments: American Journal of Science 296: pp 197-243

Van Gaans PFM (1989) A reconstructured, generalized and extended FORTRAN 77 Computer code and database format for the WATEQ aqueous chemical model for element speciation and mineral saturation, for the use on personal computers or mainframes.-Computers & Geosciences, 15, No.6.

Van Genuchten MTh (1985) A general approach for modeling solute transport in structured soils: IAH Memoirs.- 17: pp 513-526

Vanselow AP (1932) Equilibria of the base-exchange reactions of bentonies, permutites, soil colloids and zeolites.- Soil Sci. 33

Wedepohl KH (Hrsg.) (1978) Handbook of Geochemistry.- Vol.II/2; Springer, Berlin-Heidelberg-New York

Whitfield M (1975) An improved specific interaction model for seawater at 25°C and 1 atmosphere pressure.-Mar. Chemical, 3: pp 197-205

Whitfield M (1979) The Extension of Chemical Models for Seawater to include Trace Components at 24 Degrees C and 1 atm Pressure.-Geochmimica et Cosmochimica Acta, 39: pp 1545-1557

Wolery TJ (1992a) EQ 3/6, A software package for geochemical modeling of aqueous systems: Package overview and installation guide (Ver.7.0).-UCRL - MA - 110662 Pt I Lawrence; Livermore Natl. Lab

Wolery TJ (1992b) EQBNR, A computer program for geochemical aqueous speciation-solubility calculations: Theoretical manual, user´s guide, and related documentation (Ver.7.0).-UCRL - MA - 110662 Pt I Lawrence; Livermore Natl. Lab

Index